

AFFDL-TR-78-158

THE INFLUENCE OF FLEET VARIABILITY ON  
CRACK GROWTH TRACKING PROCEDURES FOR  
TRANSPORT/BOMBER AIRCRAFT

G. E. Lambert  
D. F. Bryan

Boeing Wichita Company  
A Division of The Boeing Company  
Wichita, Kansas 67210

November 1978

Final Report for Period 1 November 1976 - 1 June 1978

Approved for Public Release; Distribution Unlimited

Air Force Flight Dynamics Laboratory  
Air Force Wright Aeronautical Laboratories  
Air Force Systems Command  
Wright-Patterson Air Force Base, Ohio 45433

Best Available Copy

2006092/207

NOTICE

When Government drawings, specifications, or other data are used for any purpose other than in connection with a definitely related Government procurement operation, the United States Government thereby incurs no responsibility nor any obligation whatsoever; and the fact that the government may have formulated, furnished, or in any way supplied the said drawings, specifications, or other data, is not to be regarded by implication or otherwise as in any manner licensing the holder or any other person or corporation, or conveying any rights or permission to manufacture, use, or sell any patented invention that may in any way be related thereto.

This report has been reviewed by the Information Office (OI) and is releasable to the National Technical Information Service (NTIS). At NTIS, it will be available to the general public, including foreign nations.

This technical report has been reviewed and is approved for publication.

*TERRY D. GRAY*

---

Terry D. Gray  
Project Engineer

*Philip A. Parmley*

---

Philip A. Parmley, Chief  
Structural Integrity Branch

For the Commander

*Ralph L. Kuster, Jr.*

---

Ralph L. Kuster, Jr., Col., USAF  
Chief, Structural Mechanics Division

If your address has changed, if you wish to be removed from our mailing list, or if the addressee is no longer employed by your organization, please notify AFFDL/IFBE, W-PAFB, OH 45433 to help us maintain a current mailing list.

Copies of this report should not be returned unless return is required by security considerations, contractual obligations, or notice on a specific document.

REPORT DOCUMENTATION PAGE		READ INSTRUCTIONS BEFORE COMPLETING FORM										
1. REPORT NUMBER AFFDL-TR-78-158	2. GOVT ACCESSION NO.	3. RECIPIENT'S CATALOG NUMBER										
4. TITLE (and Subtitle) THE INFLUENCE OF FLEET VARIABILITY ON CRACK GROWTH TRACKING PROCEDURES FOR TRANSPORT/BOMBER AIRCRAFT		5. TYPE OF REPORT & PERIOD COVERED Final Technical Report November 1976 - 1 June 1978										
		6. PERFORMING ORG. REPORT NUMBER										
7. AUTHOR(s) G. E. Lambert D. F. Bryan		8. CONTRACT OR GRANT NUMBER(s)  F33615-76-C-3130										
9. PERFORMING ORGANIZATION NAME AND ADDRESS Boeing Wichita Company A Division of The Boeing Company Wichita, Kansas 67210		10. PROGRAM ELEMENT, PROJECT, TASK AREA & WORK UNIT NUMBERS  486U-02-25										
11. CONTROLLING OFFICE NAME AND ADDRESS Air Force Flight Dynamics Laboratory (FBE) Wright-Patterson Air Force Base Ohio 45433		12. REPORT DATE November 1978										
		13. NUMBER OF PAGES 198										
14. MONITORING AGENCY NAME & ADDRESS (if different from Controlling Office)		15. SECURITY CLASS. (of this report)  Unclassified										
		15a. DECLASSIFICATION/DOWNGRADING SCHEDULE										
16. DISTRIBUTION STATEMENT (of this Report)  Approved for Public Release; Distribution Unlimited												
17. DISTRIBUTION STATEMENT (of the abstract entered in Block 20, if different from Report)												
18. SUPPLEMENTARY NOTES												
19. KEY WORDS (Continue on reverse side if necessary and identify by block number)												
<table border="0"> <tr> <td>Crack Growth Tracking</td> <td>Spectrum Development</td> </tr> <tr> <td>Individual Aircraft Tracking</td> <td>Crack Growth Analysis</td> </tr> <tr> <td>Force Management</td> <td>Crack Growth Retardation</td> </tr> <tr> <td>Damage Tolerance</td> <td>Retardation Models</td> </tr> <tr> <td>Durability</td> <td>Data Acquisition Systems</td> </tr> </table>			Crack Growth Tracking	Spectrum Development	Individual Aircraft Tracking	Crack Growth Analysis	Force Management	Crack Growth Retardation	Damage Tolerance	Retardation Models	Durability	Data Acquisition Systems
Crack Growth Tracking	Spectrum Development											
Individual Aircraft Tracking	Crack Growth Analysis											
Force Management	Crack Growth Retardation											
Damage Tolerance	Retardation Models											
Durability	Data Acquisition Systems											
20. ABSTRACT (Continue on reverse side if necessary and identify by block number)												
<p>The purpose of this program is to provide generalized crack growth tracking procedures for transport/bomber aircraft. The study was composed of three major tasks, (1) an evaluation of the effects of usage parameters on crack growth, (2) the development of generalized tracking procedures and (3) an evaluation of the techniques for implementing the individual aircraft tracking program. The KC-135A tanker was selected as the baseline aircraft for this study. Approximately thirty tests were conducted to experimentally verify predictions made from analyses and to determine the crack growth rate characteristics of the specimen material. The results of the parametric and variability studies were used to develop analysis</p>												

Unclassified

SECURITY CLASSIFICATION OF THIS PAGE(When Data Entered)

schemes for predicting the effects of usage variations on crack growth. Four tracking procedures were evaluated: (1) pilot logs with the use of parametric crack growth rate data, (2) pilot logs with the use of parametric stress exceedance data, (3) the Mechanical Strain Recorder (MSR) and (4) the crack growth gauge. The implementation of each tracking procedure was evaluated by developing a cost model to study relative life cycle costs.

Unclassified

SECURITY CLASSIFICATION OF THIS PAGE(When Data Entered)

## FOREWORD

This report describes results of work performed by Boeing Wichita Company (BWC) under Air Force Contract F33615-76-C-3130, "The Influence of Fleet Variability on Crack Growth Tracking Procedures for Transport/Bomber Aircraft." The effort was sponsored by the Air Force Flight Dynamics Laboratory as part of the Advanced Metallic Structures - Advanced Development Program Project No. 4864. Mr. Terry D. Gray (AFFDL/FBE) served as technical monitor.

The program manager for BWC was Fred K. Fox. The BWC principal investigator was Mr. David F. Bryan. The major BWC contributor was Mr. Gordon E. Lambert.

This report covers work accomplished during the period 1 November 1976 to 1 June 1978.

This report was released by the authors in November 1978.

## TABLE OF CONTENTS

SECTION	PAGE
I	INTRODUCTION ..... 1
II	TASK I, EFFECT OF USAGE PARAMETERS ON CRACK GROWTH ..... 4
2.1	Transport/bomber – Baseline Aircraft ..... 4
2.2	Development of Stress Spectra ..... 4
2.2.1	Random Gust Environment ..... 8
2.2.2	Maneuver Environment ..... 11
2.2.3	Ground-Air-Ground Cycle (GAG) ..... 11
2.2.4	Stress Spectra Sequence Generation ..... 12
2.3	Analytical Crack Growth Procedures ..... 14
2.3.1	Crack Growth Retardation Models ..... 15
2.3.1.1	Wheeler Model ..... 15
2.3.1.2	Willenborg Model ..... 16
2.3.1.3	Willenborg/Gallagher Model ..... 18
2.3.2	Use of Crack Growth Rate Data ..... 20
2.4	Experimental Verification Test Procedures ..... 20
2.4.1	Alloy Selection ..... 20
2.4.2	Specimen Configuration ..... 20
2.4.3	Test Procedure ..... 22
2.4.3.1	Test Environment ..... 22
2.4.3.2	Application of Test Loads ..... 23
2.4.3.3	Instrumentation ..... 23
2.4.3.4	Crack Growth Monitoring ..... 23
2.5	Constant Amplitude Crack Growth Rate Tests ..... 23
2.5.1	Test Procedure ..... 23
2.5.2	Kmax Versus Crack Growth Rate (da/dn) Data ..... 24
2.6	Preliminary Study – Analyses and Tests to Select a Retardation Model ..... 24
2.6.1	Selection of Stress Spectra ..... 24
2.6.2	Crack Growth Analyses and Test Results ..... 29
2.7	Parametric Study ..... 32
2.7.1	Mission Usage and Loading Parameters ..... 33
2.7.2	Mission Segments Selected ..... 33
2.7.3	Analysis Locations ..... 34
2.7.4	Mission Segment Stress Spectra ..... 36
2.7.5	Parametric Crack Growth Predictions ..... 36
2.7.6	Parametric Crack Growth Rates ..... 39
2.7.7	Verification Test Results ..... 43
2.7.8	Parametric Study Results ..... 45
2.8	Variability Study ..... 45
2.8.1	Selected Mission Profiles ..... 46
2.8.2	Mission Stress Spectra ..... 46
2.8.3	Mission Crack Growth Predictions ..... 48
2.8.4	Effect of Mission Parameter Variations on Crack Growth ..... 54
2.8.4.1	Mission Mix ..... 60
2.8.5	Verification Test Results ..... 61
2.8.5.1	Determination of m Values and Retardation Factors ..... 67
2.8.6	Variability Study Results ..... 68

## TABLE OF CONTENTS (CONT'D)

SECTION	PAGE
III	TASK 2, DEVELOPMENT OF GENERALIZED TRACKING PROCEDURES ..... 70
3.1	Important Tracking Parameters ..... 70
3.2	Available Data Acquisition Systems ..... 70
3.2.1	Pilot Logs ..... 70
3.2.2	Multichannel Recorders ..... 71
3.2.3	Strain Recorders ..... 71
3.2.4	VGH Recorders ..... 71
3.2.5	Counting Accelerometers ..... 72
3.2.6	Crack Growth Gages ..... 72
3.3	Tracking Procedures Evaluated ..... 72
3.3.1	Procedure A, Pilot Logs and Parametric Crack Growth Rate Tables ..... 73
3.3.2	Procedure B, Pilot Logs and Parametric Stress Exceedance Tables ..... 74
3.3.3	Procedure C, Mechanical Strain Recorders (MSR) ..... 75
3.3.4	Procedure D, Crack Growth Gages ..... 75
3.3.5	Primary Data Acquisition Systems ..... 76
3.3.5.1	Pilot Log ..... 76
3.3.5.2	Mechanical Strain Recorder (MSR) ..... 78
3.3.5.3	Crack Growth Gage ..... 80
3.3.6	Analysis Schemes for Tracking ..... 81
3.3.6.1	Parametric Crack Growth Rate Method ..... 81
3.3.6.2	Parametric Stress Exceedance Method ..... 89
3.3.6.3	Mechanical Strain Recorder Method ..... 90
3.3.6.4	Crack Growth Gage Method ..... 93
3.3.7	Accuracy of Results ..... 93
3.3.7.1	Mission Analyses Versus Verification Test Results ..... 94
3.3.7.2	Total Mission Analysis Versus Crack Growth by Summation of Mission Segments ..... 94
3.3.7.3	Mechanical Strain Recorder ..... 94
3.3.7.4	Crack Growth Gage ..... 94
3.3.8	Advantages and Disadvantages of Tracking Procedures Studied ..... 97
3.3.9	Application of Results to Other Locations ..... 98
3.3.9.1	Control Points ..... 98
3.3.9.2	Tracking Parameter Data ..... 100
IV	TASK 3, IMPLEMENTATION OF TRACKING PROGRAM ..... 103
4.1	Relative Cost Study ..... 103
4.2	Technical Difficulties ..... 106
4.3	Optimum Tracking Scheme ..... 107
V	CONCLUSIONS ..... 108
APPENDIX A – RELATED PARAMETRIC ANALYSIS DATA	
1.	Mission Segment Stress Spectra ..... 109
2.	Mission Segment Crack Growth Curves ..... 109
APPENDIX B – RELATED VARIABILITY ANALYSIS DATA	
1.	Mission Stress Spectra ..... 143
2.	Mission Crack Growth Curves ..... 143

TABLE OF CONTENTS (CONT'D)

	PAGE
<b>APPENDIX C – RELATED TEST DATA</b>	
1. Mission Profiles and Test Spectra, Verification Tests of Variable Missions .....	185
2. Mission Crack Growth Curves Using Derived m Values Versus Test Results .....	185
<b>APPENDIX D – RELATED COST STUDY DATA</b>	
1. Relative Cost Study Data .....	193
<b>REFERENCES .....</b>	<b>198</b>

## LIST OF ILLUSTRATIONS

FIGURE		PAGE
1	Individual Airplane Tracking Program/Force Management Functions .....	2
2	Comparison of Measured and Specified Loads, C/KC-135 Aircraft .....	5
3	Variation in Fatigue Damage Rate with Type of Usage, C/KC-135 Fleet .....	6
4	Stress Analysis Flow Chart .....	7
5	Typical Wing Lower Surface GAG Cycle .....	12
6	Calculated Stress Exceedance Curve for a Typical Flight Segment from PSD Stress Program .....	13
7	Typical Mission Spectrum Representation .....	14
8	The Model of Wheeler .....	15
9	The Model of Willenborg .....	17
10	Center Crack Panel Specimen .....	21
11	Test Humidity Chamber and Test Specimen .....	22
12	Crack Growth Rate Data for 7075-T651, R = 0.8, 0.6 and 0 .....	25
13	Crack Growth Rate Data for 7075-T651, R = 0.7, 0.4 and -1.0 .....	26
14	Low Level Mission Profile and Spectrum .....	27
15	Benign Mission No. 1 Profile and Spectrum .....	28
16	Benign Mission No. 2 Profile and Spectrum .....	29
17	Test Results and Crack Growth Predictions, Preliminary Study .....	30
18	Test Results and Crack Growth Predictions, Repeated Tests .....	31
19	Analysis Life Versus Test Life, Preliminary Study .....	32
20	Analysis Locations .....	35
21	Time to Grow Crack from 0.25 to 0.35 Inches Used for Comparisons .....	37
22	Parametric Crack Growth Comparison, Wing .....	38
23	Parametric Crack Growth Comparison, Body .....	38
24	Parametric Crack Growth Comparison, Fin .....	39
25	Technique Used to Determine Crack Growth Rate .....	39
26	Analytical Crack Growth Rates, Wing .....	40
27	Analytical Crack Growth Rates, Body .....	41
28	Analytical Crack Growth Rates, Fin .....	42
29	Verification Test Spectra for Mission Segments .....	43
30	Verification Test Spectra for Mission Segment Spectra .....	44
31	Analysis Life Versus Test Life, Mission Segment Spectra .....	45
32	Variable Missions Matrix .....	47
33	Mission Spectrum Definition using Parametric Flight Segments .....	48
34	Variable Mission Analysis Results, Medium Takeoff Gross Weight, Wing .....	50
35	Variable Mission Crack Growth, Wing .....	51
36	Variable Mission Crack Growth, Body .....	52
37	Variable Mission Crack Growth, Fin .....	53
38	Variation in Crack Life with Altitude, Gross Weight and Duration, Wing 297 Kip Takeoff .....	55
39	Variation in Crack Life with Altitude, Gross Weight and Duration, Wing 230 Kip Takeoff .....	55
40	Variation in Crack Life with Altitude, Gross Weight and Duration, Fin 297 Kip Takeoff .....	56
41	Spectrum Derivation, Variation in Crack Life with Altitude, Gross Weight and Duration .....	56
42	Variation in Crack Life with Low Level Entry Gross Weight, Wing 297 Kip Takeoff .....	57

LIST OF ILLUSTRATIONS (CONT'D)

FIGURE		PAGE
43	Variation in Crack Life with Number of Touch and Go's, Wing, 230 and 170 KIP Takeoff .....	58
44	Verification Test Spectra, Mission 3A, Wing and Fin .....	63
45	Verification Test Results, Variable Missions 1A, 3A, and 3A-1, Wing .....	64
46	Verification Test Results, Variable Missions 1B, 2B, and 3B-1, Wing .....	64
47	Verification Test Results, Variable Missions 4B and 5B Wing .....	65
48	Verification Test Results, Variable Missions 3A and 3B, Fin .....	65
49	Analysis Life Versus Test Life, Variable Missions Spectra .....	66
50	Verification Test Results, Mission Mixes, Wing .....	66
51	Derived m values versus $F_{max}/\sqrt{Q}$ .....	68
52	Correlation between Linear Analysis and Test Results .....	69
53	Diagram of Tracking Procedure A .....	73
54	Diagram of Tracking Procedure B .....	74
55	Diagram of Tracking Procedure C .....	75
56	Diagram of Tracking Procedure D .....	76
57	C/KC-135 Pilot Log (AFTO 76 Form) .....	77
58	Change in Crack Growth Rate with Altitude, Wing .....	78
59	Mechanical Strain Recorder (MSR) .....	79
60	Crack Growth Gage .....	80
61	Analysis Scheme, Procedure A .....	81
62	Average Gross Weights and Flight Durations for Variable Missions .....	83
63	Comparison of Crack Growth by Total Mission Analysis and Summation of Mission Segments .....	84
64	Crack Life by Summation of Mission Segments and by Total Mission Analysis, Wing .....	84
65	Crack Life by Summation of Mission Segments and by Total Mission Analysis, Body .....	85
66	Crack Life by Summation of Mission Segments and by Total Mission Analysis, Fin .....	85
67	Comparison of Crack Growth by Mission Mix Analysis and Summation of Mission and Mission Segment Crack Growth Rates, Wing .....	86
68	Estimated Mission Mix Crack Growth .....	87
69	Individual Mission Crack Growth Rates to Predict Mission Mix Crack Growth Using Test Results .....	88
70	Analysis Scheme, Procedure B .....	89
71	Analysis Scheme, Procedure C .....	90
72	Composite Stress Exceedance Representation .....	91
73	Simplified MSR Analysis Scheme .....	92
74	Analysis Scheme, Procedure D .....	93
75	Crack Growth Gage Test Results, Wing, Mission 3A Spectra .....	95
76	Crack Growth Gage Test Results, Wing, Mission 3B Spectra .....	96
77	Crack Growth Gage Test Results, Gage Crack Length Versus Specimen Crack Length .....	97
78	Normalized Crack Growth Curves .....	99

LIST OF TABLES

TABLE		PAGE
1	C/KC-135 Turbulence Parameters .....	11
2	Constant Amplitude da/dn Tests Conducted .....	24
3	Parametric Analysis Matrix, Flight Conditions .....	33
4	Usage Parameters Affecting Crack Growth .....	34
5	Analytical Crack Growth with and without Critical Flight Segments .....	49
6	Effects of Significant Flight Segments on Crack Growth .....	54
7	Variation in Crack Life with Airspeed .....	58
8	Mission Parameter Variations, Usage Variation/Baseline, Life in Flight Hours .....	59
9	Mission Parameter Variations, Usage Variation/Baseline, Life in Flights .....	60
10	Random Ordering of Mission Mix No. 1 and No. 2 .....	61
11	Variable Missions Test Matrix .....	62
12	Derived Wheeler Shaping Exponent, m and Retardation Factor .....	67
13	Tracking Procedures – Advantages and Disadvantages .....	98
14	Relative Cost Study, Costs Considered .....	104
15	Relative Cost Study, Dollar Summary .....	105
16	Relative Cost .....	106

## SECTION I

### INTRODUCTION

The current Air Force structural integrity philosophy relies heavily on the use of damage tolerance design requirements defined in MIL-A-83444 to protect safety of flight structure from unexpected catastrophic failure. Damage tolerance is defined as the ability of the airframe to resist failure due to the presence of flaws, cracks or other damage for a specified period of unrepaired usage. The damage tolerance design requirements are based on the hypothesis that initial flaws exist in the structure, and that these flaws will grow during operational use, under the influence of repeated stress cycles, thermal, chemical or other environmental factors that vary with usage.

For compliance with the damage tolerance design requirements specified in MIL-A-83444, it is necessary to show analytically, with experimental verification, that initial flaws will not exceed specified growth limits which are dependent on the design concept, degree of inspectability and inspection interval established for each major component of the airframe.

The overall airplane structural integrity program requirements for the Air Force aircraft are defined in MIL-STD-1530A (USAF). A relatively new requirement is an individual airplane tracking program to predict the potential flaw growth in critical areas of each major airframe component. Requirements to develop parametric fatigue analysis methods have existed for some time but have primarily consisted of a cumulative damage concept to determine the expected time to crack initiation. With the new requirement, the potential flaw growth is monitored and compared with the growth limits specified in MIL-A-83444. Results from the individual airplane tracking program will be used by the Air Force when making force management decisions throughout the operational life of the airplane.

Operational fleets of aircraft frequently experience usage that is significantly different from that considered during design. Many aircraft in use today perform a multimission role which may be affected by zone of operation and strategic or tactical requirements. The various mission differences will affect the rate at which flaws will grow in the structure. Individual aircraft in the fleet may experience usage that is significantly more or less severe than the average for the fleet. Adjustments must, therefore, be made periodically to the initially predicted safe crack growth intervals for individual aircraft to account for the variations in actual usage. This information will be used by the Air Force to plan specific inspections, maintenance actions and possibly modification/replacements tasks throughout the service life of the particular fleet. To realistically track the potential flaw growth on individual aircraft, an analysis procedure for predicting crack growth as a function of usage, and a data acquisition system for recording the usage variations that significantly affect crack growth must be developed.

The objective of this study is to provide generalized tracking procedures applicable to transport/bomber aircraft. The scope of this study included:

- (1) The identification of the significant parameters that affect crack growth, and an evaluation of how these parameters may vary on a fleetwide basis
- (2) The investigation of the analysis techniques that will best predict the effects of usage change on crack growth
- (3) The identification of the data that must be recorded and an evaluation of how the data acquisition may be influenced by analysis techniques
- (4) A review of the recording devices available including advantages and disadvantages of each, and

(5) An evaluation of the techniques for organizing and implementing a fleet tracking program

Figure 1 is a block diagram (reproduced from Figure 3 of MIL-STD-1530A) showing the relationship between the individual airplane tracking program and the force management functions. The major elements of the tracking program addressed in this study are indicated by the cross-hatched areas in the figure.

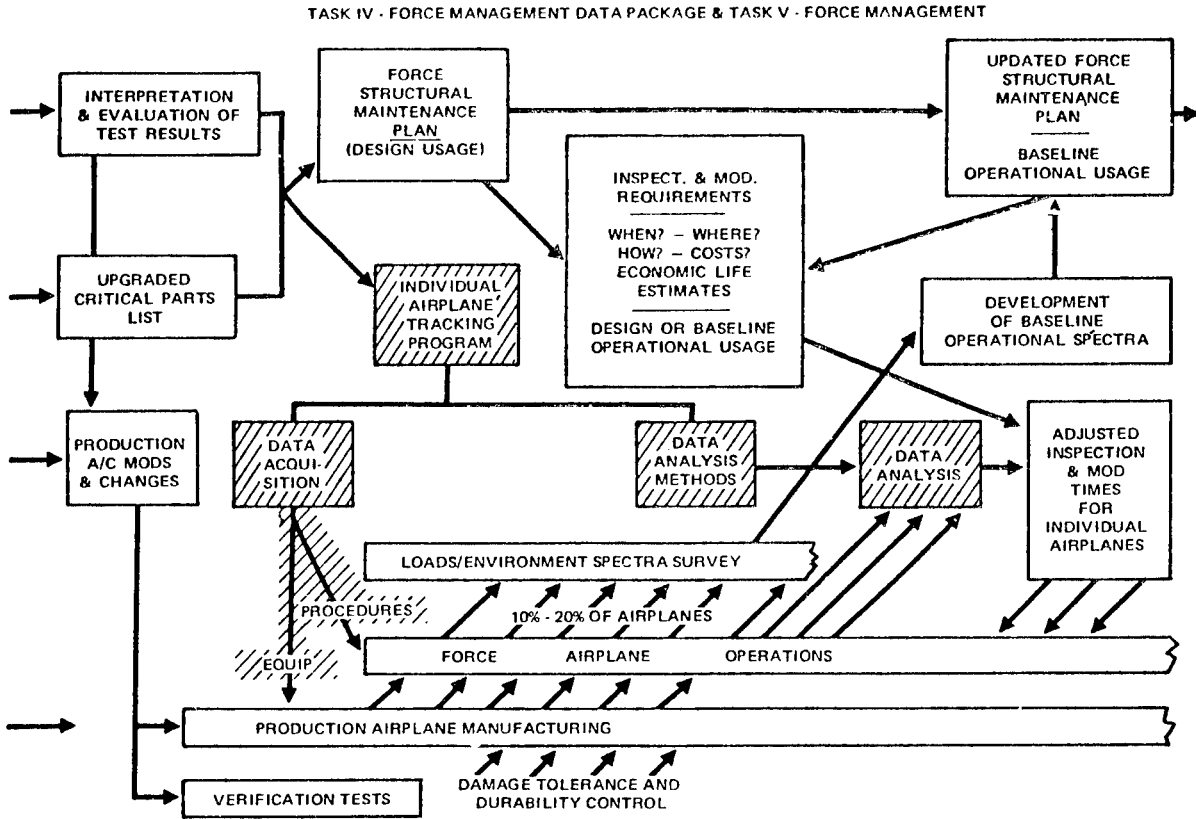


Figure 1. Individual Airplane Tracking Program/Force Management Functions

This study was composed of three major tasks:

- (1) An evaluation of the effects of aircraft usage and loading parameters on crack growth
- (2) The development of generalized tracking procedures for transport/bomber aircraft, and
- (3) An evaluation of the techniques for implementing the individual aircraft tracking program

The effects of usage variations on crack growth were evaluated analytically and verified experimentally.

The KC-135A tanker was selected as the baseline aircraft to study usage variations representing transport and bomber missions. Computer programs were used to generate sequenced stress spectra using stress exceedance data applicable to three fracture critical locations on the KC-135A aircraft; the wing lower surface, fuselage crown and the vertical fin rear spar.

Analytical crack growth calculations were made for selected mission segments to isolate and evaluate the effect of mission usage and loading parameters on crack propagation. Similar calculations were also made for selected mission profiles representative of actual and possible fleet usage variations to evaluate the effect of usage variability on crack propagation.

Approximately 20 missions and mission segment spectra were selected for experimental testing to verify crack propagation analyses using center cracked specimens.

The data accumulated from analyses and experimental verification tests were used to develop analysis schemes for predicting the effects of usage variations on crack growth.

Four different tracking procedures were developed and evaluated using present and future data acquisition systems. The implementation of each tracking procedure was evaluated by developing a cost model from which relative life cycle costs were estimated.

## SECTION II

### TASK 1, EFFECTS OF USAGE PARAMETERS ON CRACK GROWTH

The multimission role performed by transport/bomber aircraft results in wide variations in the usage of individual aircraft within a given fleet. This in turn causes variation in the number, magnitude and order of application of loads experienced by individual aircraft. For the baseline aircraft selected, analytical parametric studies were conducted to determine and isolate the effects of airplane usage and loading parameters on the rate of crack growth for three primary airframe structural locations. The mission segments selected for the parametric study were used to construct mission stress spectra which in turn were used to estimate the effect on crack growth caused by variations in the usage parameters most influential.

The results of the analytical parametric and variability studies were experimentally verified by subjecting test specimens to stress spectra representing variations which were found to be significant in the analytical studies.

#### 2.1 Transport/Bomber – Baseline Aircraft

The KC-135A tanker was selected as the baseline transport/bomber aircraft for this study. Among the more obvious reasons for selecting an in-service aircraft for this study was the availability of structural data already generated from durability and damage tolerance analyses and from full scale tests. Also, measured loads data from the operational fleet were available to update early estimates of airplane load history. For example, Figure 2 shows a comparison of the loads specified in MIL-A-8861A and loads measured on the KC-135 airplane during typical fleet operation. Note that the relative frequency scale is logarithmic. These curves show that the magnitude and frequency of the high and low loads experienced during actual operation were different from those specified for design. The difference in curve shape is important because the frequency and magnitude of high loads affect the amount of crack growth that will occur.

A large quantity of recorded loads data has been accumulated during actual operation of the KC-135 fleet. These data have proved valuable in developing representative loads spectra over a wide range of operating conditions.

There is a wide variation in fatigue damage with type of mission for the C/KC-135 fleet as shown in Figure 3. These damage values were calculated using actual C/KC-135 fleet usage profiles. Figure 3a shows damage per mission values varying as much as five to one; whereas, damage per flight hour varies by a factor of 12 (Figure 3b). These values should give some indication of the expected trend for crack propagation.

#### 2.2 Development of Stress Spectra

The most frequently used techniques for defining gust load (stress) spectra are based on either discrete or continuous random interpretations of the load inducing environment in which the aircraft is operated. Power Spectral Density (PSD) analysis methods are used to predict the loads due to continuous random disturbances. The discrete load method is simple to use and produces results quickly. However, there are often certain subtle effects of varying mission parameters which could be partially or totally masked when the discrete load concept is used.

The PSD analysis method is considered to be the most realistic and versatile method for predicting the number and magnitude of loads experienced during actual operation. This method allows a rational description of the random load inducing environment, as well as a method for defining the combined stresses at a given location in the structure due to multiple responses and multiple sources of load excitation. It was believed that the demands of this program warranted the use of the PSD method for deriving the basic random gusts loads spectra.

The loads due to maneuvers were computed separately using a measured KC-135 maneuver environment ( $\Delta n$  exceedances) and calculated steady-state loads. The gust and maneuver loads spectra were then combined to obtain the total loads spectra.

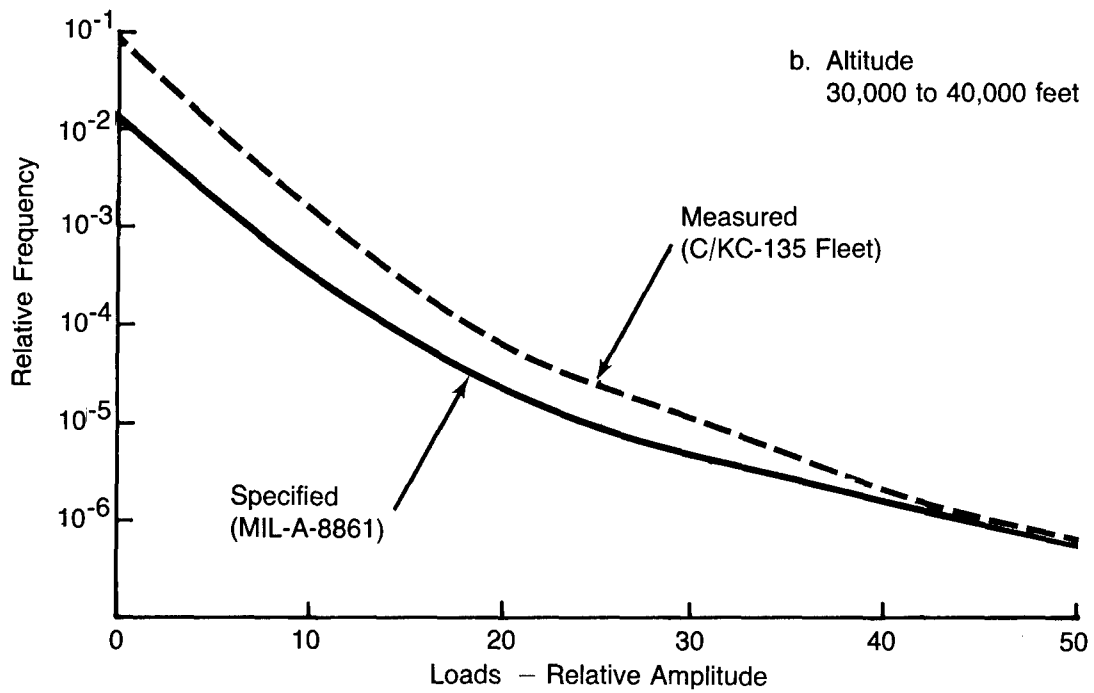
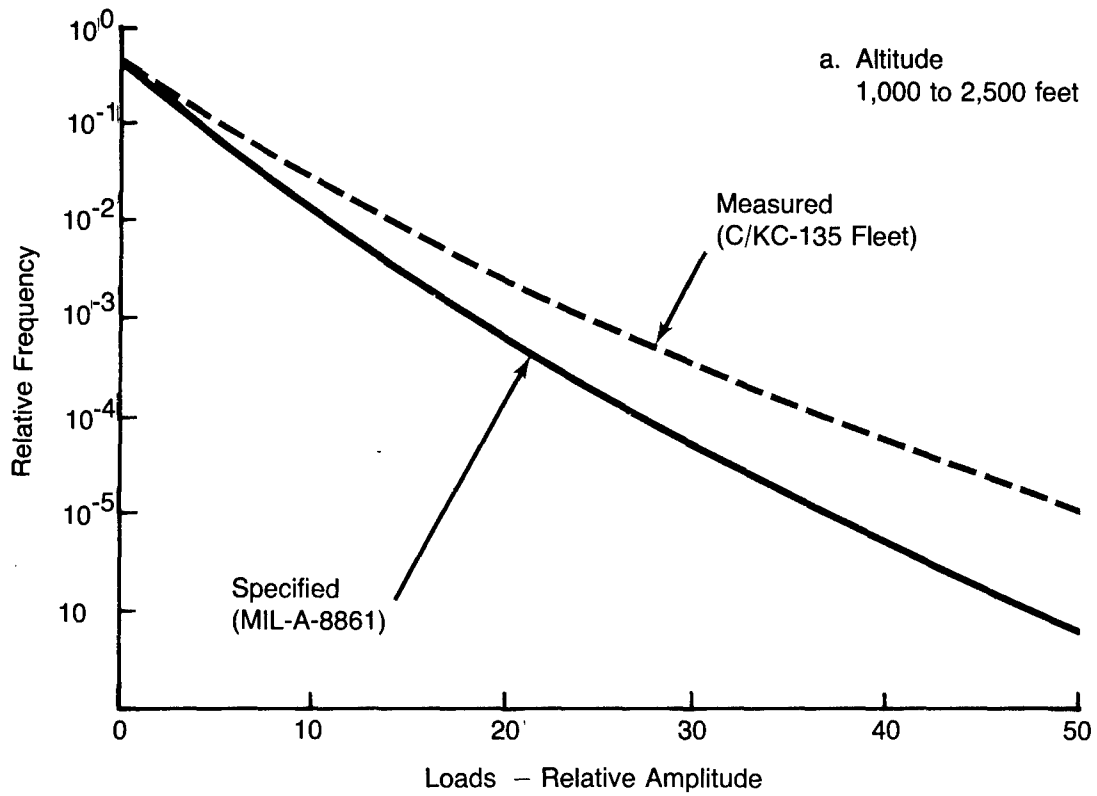


Figure 2. Comparison of Measured and Specified Loads, C/KC-135 Aircraft

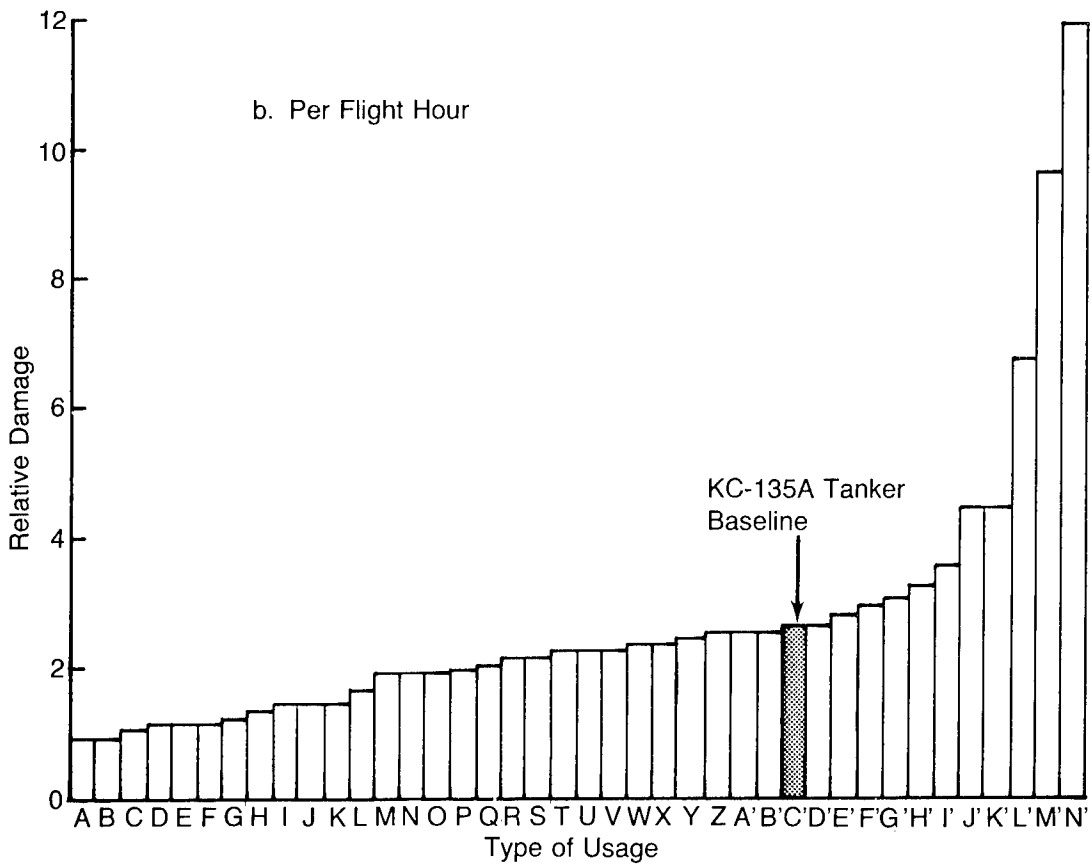
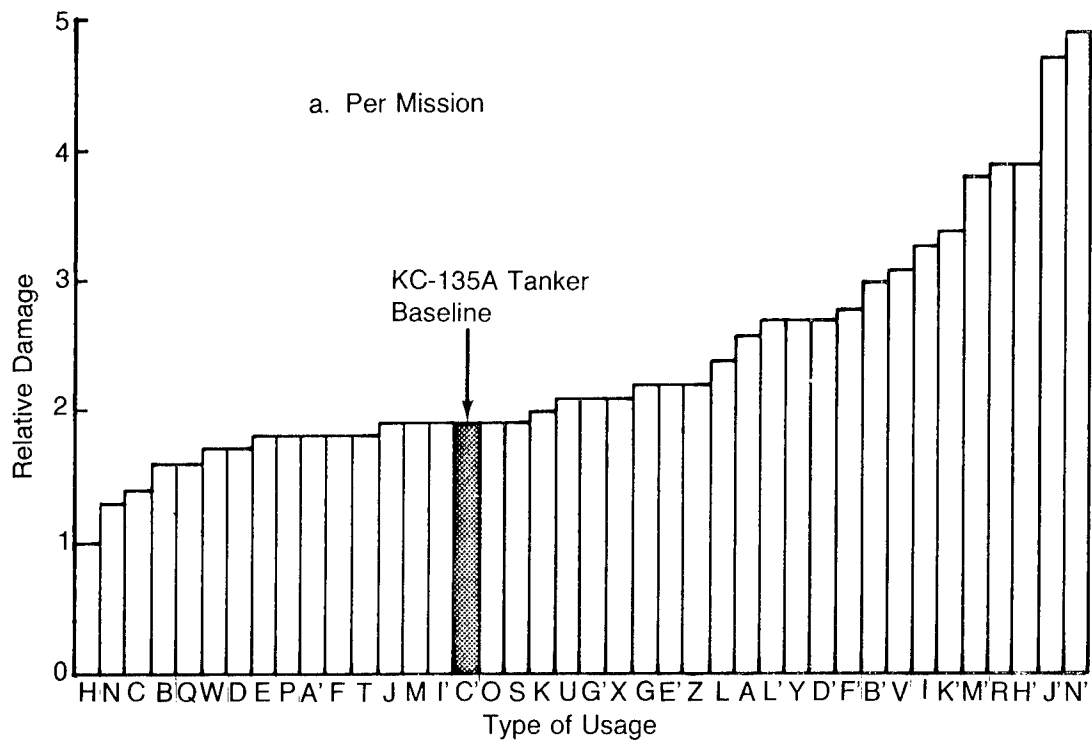


Figure 3. Variation in Fatigue Damage Rate with Type of Usage, C/KC-135 Fleet

An updated PSD analysis computer program for calculating KC-135 stress spectra (including maneuver loads), Reference 1, was available and was used in this study. The output from the computer program included stress exceedances of maximum, minimum and alternating stress and the 1g stress by mission segment. A flow diagram depicting the analysis steps is shown in Figure 4. More detailed discussions of techniques used in developing the stress spectra are given in the following sections.

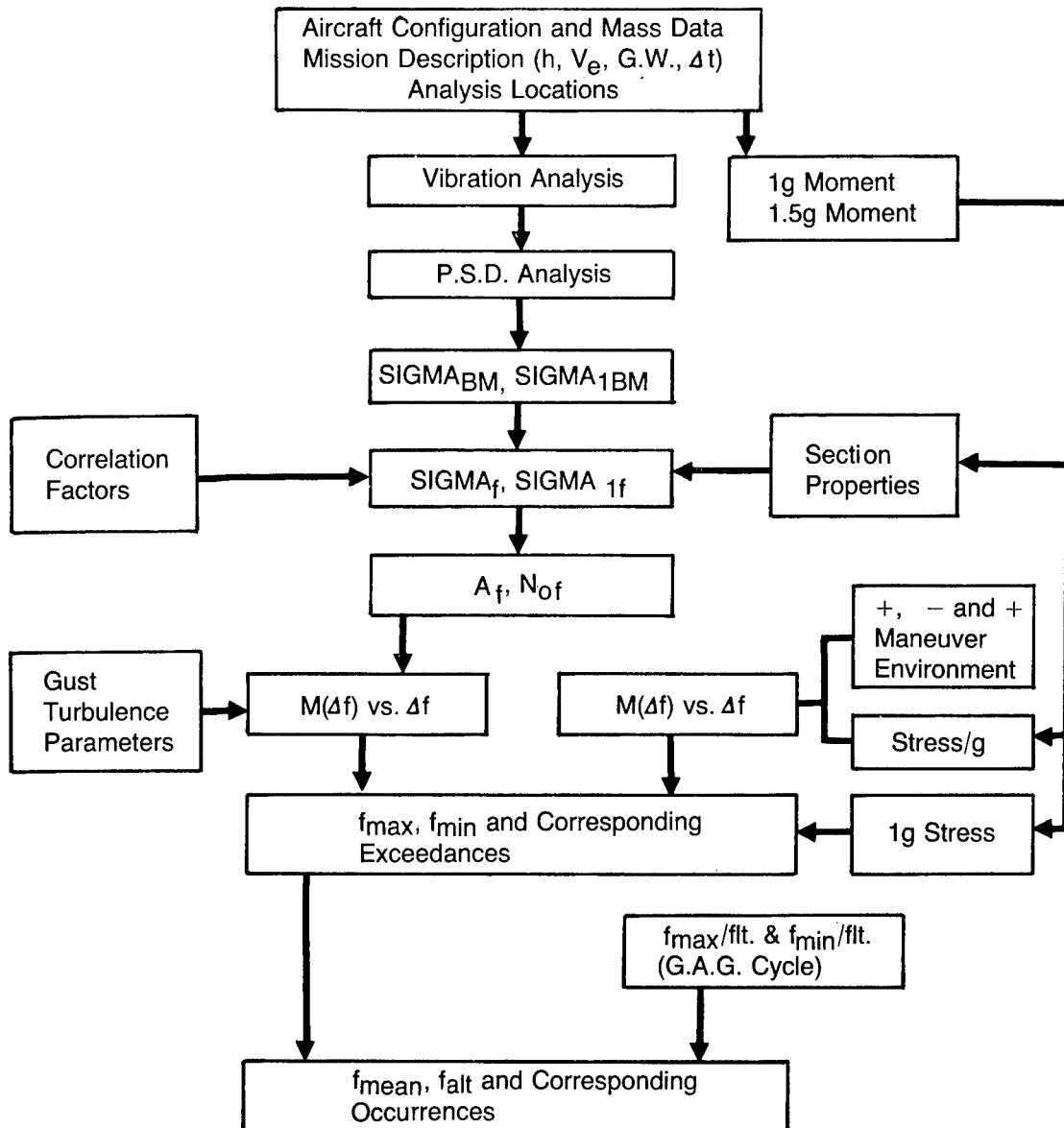


Figure 4. Stress Analysis Flow Chart

## 2.2.1 RANDOM GUST ENVIRONMENT

Power Spectral Density (PSD) analysis methods were used for calculating structural stress history due to random gust load environment. The load environment induced by atmospheric turbulence (hereafter called turbulence) was represented by a power spectral density function of the gust velocity and a probability distribution of root mean square (RMS) gust velocities. The von Karman Power Spectral Density Function was chosen to represent the power spectrum of the turbulence as defined in Reference 2. This is stated as:

$$\phi_j(\Omega) = \frac{\sigma_u^2 L}{\pi} \frac{1 + 8/3 (1.339L\Omega)^2}{[1 + (1.339L\Omega)^2]^{1.833}} \quad (1)$$

where,

- $\sigma_u$  = rms gust velocity, feet/second
- L = Characteristic wavelength of turbulence (Ref. 4)
- $\Omega$  = Reduced frequency, rad/foot

The probability density distribution of the RMS gust velocity is defined as:

$$f(\sigma_u) = \frac{P_1}{b_1} \sqrt{\frac{2}{\pi}} e^{-\sigma_u^2/2b_1^2} + \frac{P_2}{b_2} \sqrt{\frac{2}{\pi}} e^{-\sigma_u^2/2b_2^2} \quad (2)$$

where,

- $P_1$  = Fraction of flight time spent in normal turbulence
- $P_2$  = Fraction of flight time spent in severe turbulence
- $b_1$  = Intensity of normal turbulence
- $b_2$  = Intensity of severe turbulence

$\phi(\Omega)$  and  $f(\sigma_u)$  must be consistent and jointly represent the atmospheric turbulence.

The response power spectrum is related to the turbulence power spectrum through the frequency response function by:

$$\phi_o(\Omega) = |T(\Omega)|^2 \phi_j(\Omega) \quad (3)$$

where,

$\phi_o(\Omega)$  = The desired response power spectrum

$T(\Omega)$  = Frequency response function of the desired response

The root mean square of each response is obtained from its power spectrum by:

$$\sigma = \left| \int_0^{\infty} \phi_o(\Omega) d\Omega \right|^{1/2} \quad (4)$$

and the RMS response per unit RMS gust velocity is:

$$A = \frac{\sigma}{\sigma_u} \quad (5)$$

The characteristic frequency is obtained from:

$$N_o = \frac{\sigma_1}{\sigma} \quad (6)$$

where,

$$\sigma_1 = \frac{V}{2\pi} \left| \int_0^{\infty} \Omega^2 \phi_o(\Omega) d\Omega \right|^{1/2} \quad (7)$$

$V$  = Airplane velocity, feet/second

The vertical and lateral gust components are considered to be statistically independent random disturbances for the aircraft. This independence depends only upon randomness of the algebraic sign of the gusts and is true even though the vertical and lateral RMS values are correlated. Total response spectra caused by combined vertical and lateral gust components can be expressed as:

$$\phi_o(\Omega)_{\text{total}} = \phi_o(\Omega)_{\text{vertical}} + \phi_o(\Omega)_{\text{lateral}} \quad (8)$$

The corresponding total spectral response parameters for the combined vertical and lateral gust components are then:

$$A_T = \frac{1}{\sigma_u} (\sigma_V^2 + \sigma_L^2)^{1/2}$$

(9)

$$N_{OT} = \left( \frac{\sigma_{1V}^2 + \sigma_{1L}^2}{\sigma_V^2 + \sigma_L^2} \right)^{1/2}$$

Bending moment response parameters ( $\sigma_m$  and  $\sigma_{1m}$ ) were used with unit stress coefficients to determine the required stress response parameters ( $\sigma_f$  and  $\sigma_{1f}$ ) of a particular structural element using the following equations:

$$\sigma_f^2 = K_1^2 \sigma_{M_1}^2 + K_2^2 \sigma_{M_2}^2 + 2 K_1 K_2 \sigma_{M_{12}}^2$$

(10)

$$\sigma_{1f}^2 = K_1^2 \sigma_{1M_1}^2 + K_2^2 \sigma_{1M_2}^2 + 2 K_1 K_2 \sigma_{1M_{12}}^2$$

where,

$K_1$  &  $K_2$  = Unit stress coefficients for vertical and chord bending, respectively, PSI/In-Lb

$\sigma_{m_{12}}$  = Time phase coefficient between vertical and chordwise bending parameters

The response level exceedance rate is related to the response parameters, A and  $N_o$ , and the probability density distribution of RMS gust velocity  $f(\sigma_u)$  as follows:

$$M(Y) = N_o \int_0^{\infty} f(\sigma_u) e^{-Y^2/2A^2 \sigma_u^2} d\sigma_u$$

(11)

Substitution of  $f(\sigma_u)$  into the above equation leads to the following expression for response-exceedance rate:

$$\frac{M(Y)}{N_o} = P_1 e^{-Y/b_1 A} + P_2 e^{-Y/b_2 A}$$

(12)

where,

$M(Y)$  = Average cycles per second equal to or exceeding the load (stress) level, Y

Y = Incremental load (stress) level

$N_o$  = Characteristic frequency, CPS

A = RMS response for RMS turbulence velocity, (response units)/FPS

$P_1, P_2, b_1, b_2$  = Turbulence parameters

This equation, modified to account for any increment of time,  $\Delta t$ , was used to determine the incremental gust stress exceedances for each mission segment analysed in this study.

Turbulence parameters,  $P_1$ ,  $b_1$ ,  $P_2$  and  $b_2$ , were derived from generalized relationships between  $M(Y)/N_0$  and  $Y/A$ . These parameters were derived from center of gravity acceleration ( $\Delta n$ ) data using Equation (12) and theoretical values of  $A$  and  $N_0$  at the airplane cg for gross weight, velocity and altitude bands. The cg acceleration data used to derive the turbulence parameters were obtained from C-135A/B Fleet Load History Data, Reference 3. The turbulence parameters derived for ascent, cruise and descent as a function of altitude and for flaps retracted and extended are shown in Table 1. The vertical and lateral gust environments were assumed to be the same.

TABLE 1  
C/KC-135 TURBULENCE ENVIRONMENT

Ascent-Cruise-Descent, Flaps Up				
Altitude, Feet	$P_1$	$b_1$	$P_2$	$b_2$
500	.5884	3.7502	$2.307 \times 10^{-2}$	6.9945
1,750	.3973	3.5127	$1.795 \times 10^{-2}$	6.6932
3,750	.2497	2.9772	$8.906 \times 10^{-3}$	6.7181
7,500	.1636	2.7146	$4.832 \times 10^{-3}$	6.7559
15,000	.1273	2.4771	$2.992 \times 10^{-3}$	6.7286
25,000	.0949	2.4265	$2.169 \times 10^{-3}$	6.5198
35,000	.0779	2.3405	$1.192 \times 10^{-3}$	6.5786
45,000	.0475	2.3540	$7.379 \times 10^{-4}$	6.5146
Flaps Down				
	$P_1$	$b_1$	$P_2$	$b_2$
All Altitudes	.6363	3.5546	$2.221 \times 10^{-2}$	5.2408

## 2.2.2 MANEUVER ENVIRONMENT

The structural stress history due to the maneuver load environment was determined using cg acceleration ( $\Delta N$ ) data recorded as part of the C-135A/B aircraft flight loads program, Reference 4. These data and steady-state 1.0 g and 1.5 g loads computed for the required flight conditions were used to calculate stress exceedances for the maneuver environment.

For each flight condition analyzed, the gust and maneuver stress exceedance data were combined to obtain the total stress history.

## 2.2.3 GROUND-AIR-GROUND CYCLE (GAG)

A combination of flight and ground stresses defines the GAG cycle for most structural locations. A stress time history at a location on the lower wing surface is shown schematically in Figure 5 to illustrate the concept of the GAG cycle. The maximum compressive stress is the largest compressive stress that occurs before takeoff or after landing. The maximum tension stress is the largest tension stress that occurs while airborne. The opposite is true for the upper surface.

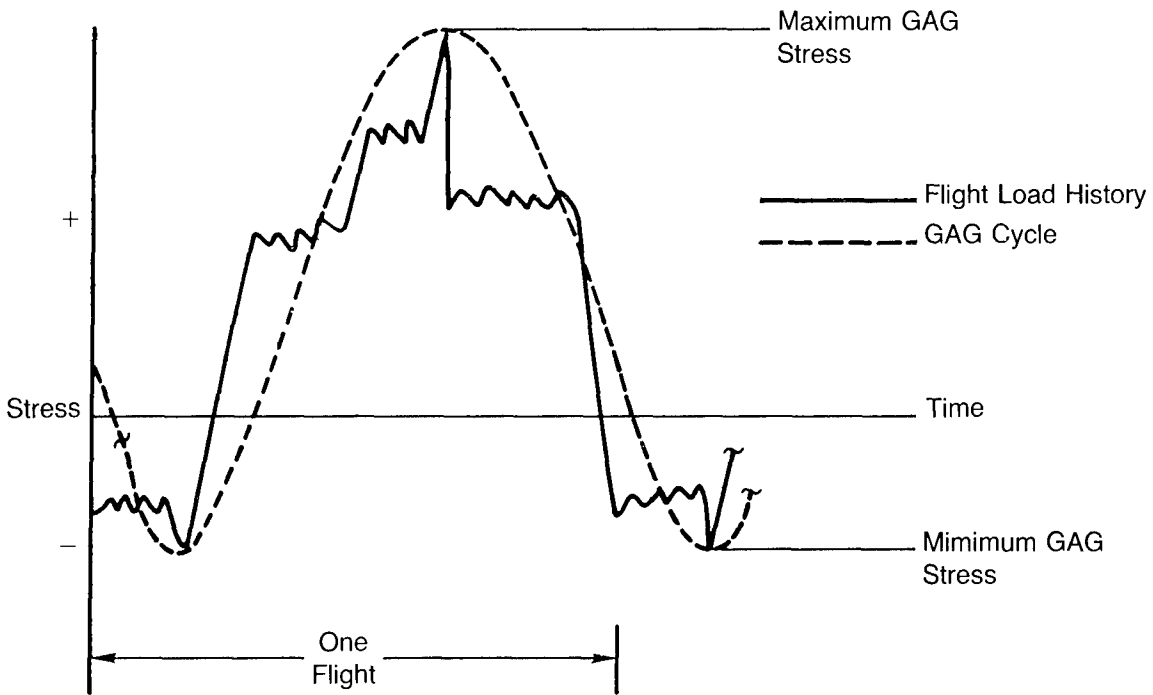


Figure 5. Typical Wing Lower Surface GAG Cycle

Similar cycles exist for other locations on the airframe. However, it is possible for the maximum and minimum stresses to occur during flight, i.e., on the body or stabilizer. The random interpretation of flight loads does not allow a separate consideration for a GAG cycle on the fin.

The minimum (or maximum) stress occurring during ground operation was defined as that stress corresponding to an incremental center of gravity acceleration of 0.2g during the takeoff ground roll with the engine thrust that causes the minimum (maximum) stress condition.

The maximum (or minimum) stresses occurring during flight operation were determined by generating a stress level exceedance rate curve and selecting the stress level expected to occur once per flight. In this study, the less frequent GAG stress cycles occurring once in 10,100 and 200 flights were also included in the stress spectra.

#### 2.2.4 STRESS SPECTRA SEQUENCE GENERATION

As discussed in the previous paragraphs, a PSD stress computer program was used to develop stress spectra in terms of cumulative cycles (exceedances) or alternating stress and 1g stress for each flight condition analyzed. For this study an alternating stress bandwidth of 0.50 KSI was used to define the exceedance values. These data were output on IBM cards for use in a sequence generator computer program. Typical output data are illustrated in Figure 6.

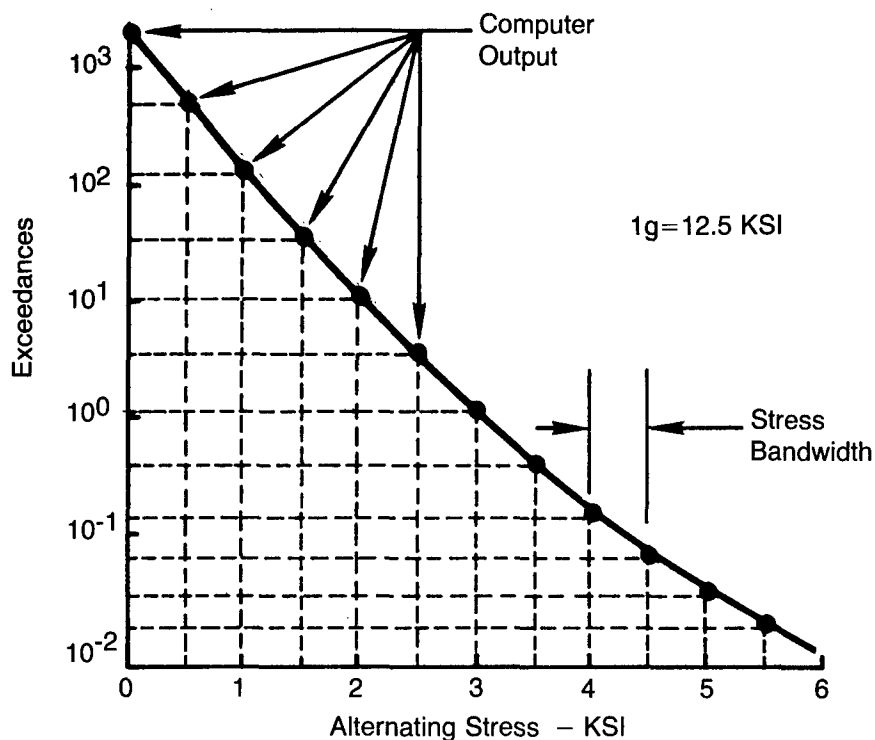


Figure 6. Calculated Stress Exceedance Curve for a Typical Flight Segment from PSD Stress Program

The sequence generator program, Reference 5, was primarily written to efficiently process a large volume of stress exceedance and 1g stress data by combining, scaling, truncating, editing and ordering the data as required to produce a stress spectrum for input into an analytical crack growth program or a test program. All mission and mission segment stress spectra were determined by this procedure.

Each mission segment stress spectrum was determined in the following manner:

- (1) A set of stress exceedance and 1g stress data corresponding to a number of flight segments was input into the sequence generator program
- (2) All stress exceedance data for analyses and tests were truncated at 1.0 KSI alternating and a bandwidth of 1.0 KSI was selected to define stress levels and occurrences
- (3) The program determined the stress and exceedance values for the selected stress bandwidth for each flight segment
- (4) The occurrences corresponding to the average bandwidth stress was determined and rounded to the nearest complete cycle
- (5) The stress occurrence data were then arranged in a Lo-Hi-Lo order of application
- (6) The 1g stress level was then used to determine the maximum and minimum stresses and the  $\beta$  ( $f_{max}/f_{min}$ ) ratios
- (7) The  $f_{max}$ , number of cycles and a  $\beta$  ratio were output on IBM cards for input into the crack growth program. An option allows output to be generated for use in defining a test loads control tape

The stress spectrum for a complete mission was determined in a similar manner. Each mission analyzed in this study was comprised of an assemblage of mission segment exceedance data. For a selected takeoff gross weight condition, the mission segment data needed to develop any number of different mission spectra were input into the sequence generator program as well as the GAG stress cycles associated with the takeoff and climb and other flight operations (e.g., touch and go). In this study, the primary GAG cycle was defined from the ground and/or climb portion of each mission. For the structural locations selected for this study this procedure proved satisfactory.

A mission spectrum was defined by specifying the segments which comprise the mission, applying a factor to account for the flight duration of each segment and ordering the segments in the proper sequence. Similar steps were carried out as described above to obtain an assemblage of Lo-Hi-Lo stress cycle segments. The GAG cycle(s) is placed in the spectrum by indicating the segment which is to be preceded by the GAG cycle(s). The final mission spectrum is a compilation of a GAG cycle(s) and a number of segment-by-segment Lo-Hi-Lo stress sequences as depicted in Figure 7. These data are output from the computer program on punched cards for direct input into the crack growth program.

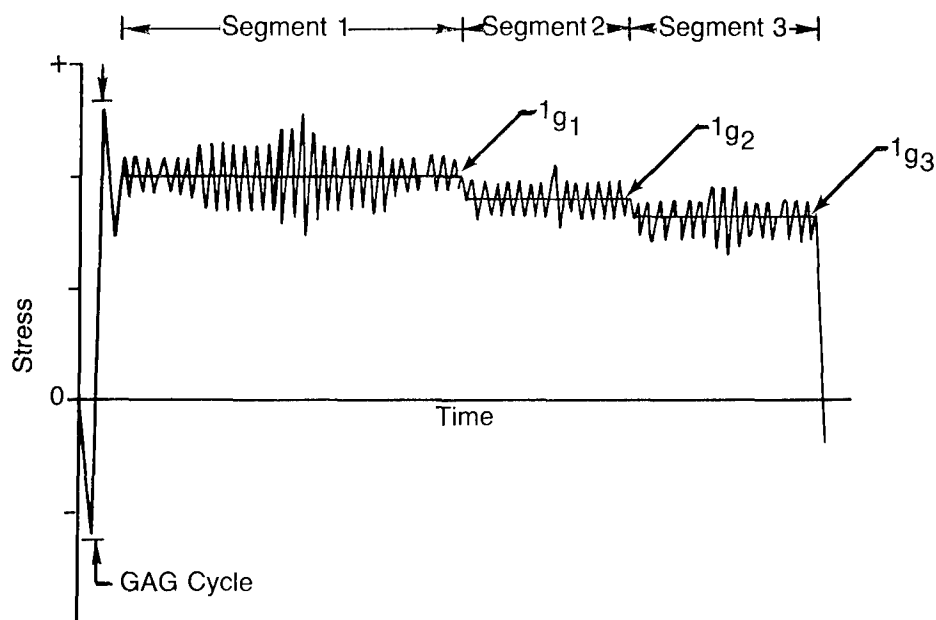


Figure 7. Typical Mission Spectrum Representation

### 2.3 Analytical Crack Growth Procedures

One of the earliest widely used crack growth retardation models was that proposed by Wheeler, Reference 6. To account for retardation following an overload, he introduced a retardation factor,  $\phi$ , which is a power function of the crack tip plastic zone size and the distance to the boundary of the plastic enclave caused by the overload. The power,  $m$ , of the retardation factor is determined experimentally. Crack growth rates following the overload are reduced by the factor  $\phi$  until the crack grows through the overload plastic enclave.

Another method was proposed by Willenborg, Engle and Wood, Reference 7, which is also based on the size of the plastic zone at the crack tip. This method does not require experimentally determined values, but instead, calculates the maximum stress intensity factor ( $K_{\max}$  required) necessary for the current crack tip plastic zone to reach the boundary of the plastic enclave caused by the preceding overload. An effective stress ratio,  $R$  effective, and an effective  $K$  range,  $\Delta K$  effective, are calculated based on the calculated  $K_{\max}$  required. These values are then used in a crack growth rate equation or table to determine the reduced crack growth rate. More recently, Gallagher reformatted the Willenborg Model in a stress intensity factor format, Reference 8.

The Wheeler, Willenborg and Willenborg/Gallagher Retardation Models were considered as candidates for the primary crack growth prediction method to be used in this study. A preliminary study was conducted using each method to predict crack growth for comparison with verification test results (Section 2.6). As a result, the Wheeler Retardation Model was chosen for the evaluation of the effects of usage parameters on crack growth.

### 2.3.1 CRACK GROWTH RETARDATION MODELS

The basic crack growth equation for which crack length is estimated by summing the incremental crack growth caused by each stress level in a spectrum is as follows:

$$a_k = a_0 + \sum_{i=1}^k (da/dn)_i \Delta n_i \quad (13)$$

where,

- $a_k$  = Final crack length
- $a_0$  = Initial crack length
- $da/dn_i$  = Crack growth rate for stress level  $i$ , based on constant amplitude tests  $K_{max}$  vs.  $da/dn$  data
- $\Delta n_i$  = Number of cycles of a given stress level  $i$
- $i$  = Given stress level in spectrum

This equation represents a linear crack growth, i.e., without retardation. Wheeler modifies the crack growth rate,  $da/dn$ , by a retardation factor,  $\phi$ , for each stress level in the spectrum. Willenborg uses an effective stress intensity and effective stress ratio to determine an effective crack growth rate,  $da/dn_{eff}$ . Gallagher modified the Willenborg approach by introducing a factor that modifies the effective stress intensity factor using a shut-off overload ratio. Descriptions of these models are provided in the following sections.

#### 2.3.1.1 Wheeler Model

The Wheeler Model accounts for retardation caused by peak loads in the spectrum by applying a retardation parameter,  $\phi$ , in the basic crack growth equation, such that:

$$a_k = a_0 + \sum_{i=1}^k \phi_i (da/dn)_i \Delta n_i \quad (14)$$

The retardation factor,  $\phi$ , accounts for effects on crack growth rate when peak tension stresses are followed by lower stress levels. This factor is based on the ratio of the current plastic zone size,  $r_{pi}$ , and the size of the plastic enclave formed at an overload,  $r_{po}$  (see Figure 8).

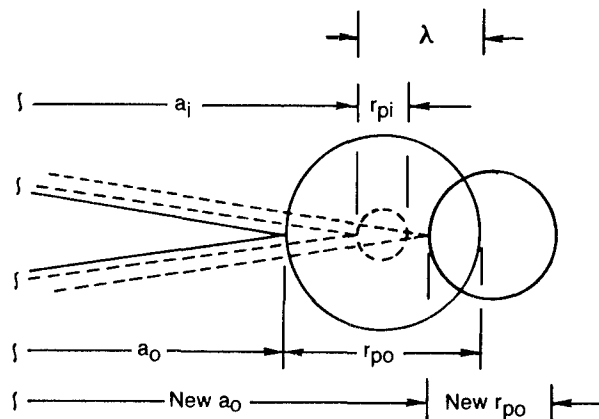


Figure 8. The Model of Wheeler

The overload or peak stress occurring at a crack length  $a_0$ , will cause a crack tip plastic zone of size:

$$r_{po} = \frac{K_0^2}{2\pi \sigma_{ys}^2} \quad (15)$$

where,

$K_0$  = Overload stress intensity

$\sigma_{ys}$  = Yield stress

When the crack has propagated further to length  $a_i$ , the current plastic zone size will be:

$$r_{pi} = \frac{K_i^2}{2\pi \sigma_{ys}^2} \quad (16)$$

where,

$K_i$  = Stress intensity for stress Level i

This plastic zone is still embedded in the plastic enclave of the overload which proceeds over a distance  $\lambda = a_0 + r_{po} - a_i$  in front of the current crack  $a_i$ . Wheeler assumes that the retardation factor  $\phi$  will be a power function of  $r_{pi}/\lambda$  which amounts to:

$$\phi_i = \left( \frac{r_{pi}}{a_0 + r_{po} - a_i} \right)^m \quad \begin{array}{l} \text{As long as} \\ a_i + r_{pi} < a_0 + r_{po} \end{array} \quad (17)$$

where,

$m$  = Shaping exponent

If  $a_i + r_{pi} \geq a_0 + r_{po}$  the crack has grown through the overload plastic zone, and the retardation factor,  $\phi$ , becomes 1.0 by definition. The power  $m$  in equation (17) has to be determined empirically to relate the amount of retardation required to bring the predicted crack growth into agreement with experimental test data. Determining this shaping exponent is, of course, the key drawback to using this method since it cannot be known in advance of testing.

### 2.3.1.2 Willenborg Model

The Willenborg Model also makes use of the plastic enclave formed by the overload to determine an effective crack growth rate,  $(da/dn)_{eff}$ , for use in the basic crack growth equation, such that:

$$a_k = a_0 + \sum_{i=1}^k (da/dn)_{eff i} \Delta n_i \quad (18)$$

The effective  $da/dn$  is determined by using a formulation based on the model shown in Figure 9.

The plastic enclave extends to:

$$a_p = a_0 + r_{po} \quad (19)$$

where  $a_p$  is the distance from the crack center to the boundary of the plastic enclave. Willenborg considered the stress intensity that would be required to produce a plastic zone, at the tip of the current crack length  $a_i$ , that would extend to the border of the plastic enclave (Figure 9). This can be expressed in equation form as follows:

$$a_i + r_{p req} = a_0 + r_{po}, \quad (20)$$

where  $r_{p req}$  is the plastic zone required to reach the boundary of the existing plastic enclave. The  $K_{max req}$  to achieve this, is given by:

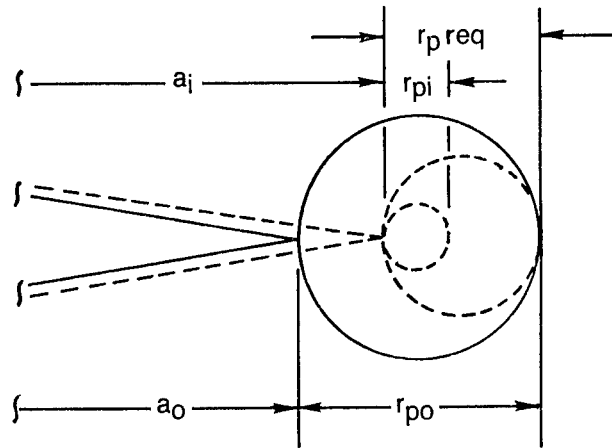


Figure 9. The Model of Willenborg

$$\frac{K_{max req}^2}{2\pi \sigma_{ys}^2} = a_0 + r_{po} - a_i \quad (21)$$

In the first cycle subsequent to the overload,  $a_i$  is still equal to  $a_0$ . Hence,  $K_{max req}$  would be equal to the stress intensity of the overload.

Willenborg made the further assumption that the  $K_{max i}$  actually occurring at the current crack  $a_i$ , would be effectively reduced by an amount  $K_{red}$ , given by:

$$K_{red} = K_{max req} - K_{max i} \quad (22)$$

The residual compressive stress caused by the overload reduces the effective stress at the crack tip. As implied by equation (22) the expected magnitude of the residual stress is given by:

$$\sigma_{red} = \frac{K_{max req}}{\sqrt{\pi a_i}} - \frac{K_{max i}}{\sqrt{\pi a_i}} \quad (23)$$

This means that both  $K_{max i}$  and  $K_{min i}$  for cycle  $i$  are reduced by an amount  $K_{red}$ . Hence, the effective stress intensity is given by:

$$K_{max eff i} = K_{max i} - K_{red} = 2K_{max i} - K_{max req} \quad (24)$$

$$K_{min eff i} = K_{min i} - K_{red} = K_{min i} + K_{max i req}$$

The stress cycle ratio then becomes:

$$R_{eff i} = \frac{K_{min eff i}}{K_{max eff i}} \quad (25)$$

The effective crack growth rate,  $(da/dn)_{eff i}$ , can then be determined by entering  $K_{max}$  versus  $da/dn$  constant amplitude curves for various  $R$  values with the effective values of  $K_{max}$  and  $R$ . An objection to this model is that the assumption regarding the residual compressive stresses is doubtful. Also, there is no parameter that can be adjusted easily to match test data.

### 2.3.1.3 Willenborg/Gallagher Model

It was observed by Gallagher that the Willenborg Model predicted retardation by depressing the effective stress ratio below that actually applied while leaving the stress intensity range intact as shown by:

$$\begin{aligned}\Delta K_{\text{eff}} &= K_{\text{max eff}} - K_{\text{min eff}} \\ &= (K_{\text{max}} - K_{\text{red}}) - (K_{\text{min}} - K_{\text{red}}) \\ &= \Delta K\end{aligned}\quad (26)$$

Since  $K_{\text{red}}$  decreases as the crack grows through the overload interaction zone, the Willenborg Model predicts that the maximum retardation will occur just after the overload and that the growth rate will return to unretarded value when the current interaction zone extends to the end of the overload interaction zone.

The use of a residual stress intensity factor concept suggests that the local or effective stress intensity factor which is sensed by the propagating crack be calculated from:

$$K_{\text{max eff}} = K_{\text{max}} - K_{\text{red}} \quad (27)$$

which is the same as equation (24) of the Willenborg formulation. The residual stress intensity factor,  $K_{\text{red}}$ , would in general be considered a function of many interacting variables, e.g.:

$$K_{\text{red}} = f(K_{\text{max}}^{\text{OL}}, K_{\text{min}}^{\text{OL}}, \text{NOL}, K_{\text{max}}, R, \sigma_{\text{ys}}, n, \dots) \quad (28)$$

Where,

$K_{\text{max}}^{\text{OL}}$  =  $K_{\text{max}}$  of overload

$K_{\text{min}}^{\text{OL}}$  =  $K_{\text{min}}$  of overload

$\text{NOL}$  = Number of overloads applied

$K_{\text{max}}$  =  $K_{\text{max}}$  of loads following overload

$R$  = Stress ratio of loads following overload

$\sigma_{\text{ys}}$  = Yield strength

$n$  = Number of cycles of  $K_{\text{max}}$

One test of any crack growth prediction model is its ability to predict the number of cycles of applied load to achieve a given crack length. The Willenborg Model as detailed by Gallagher takes a form identical to that of Equation (27) where the residual stress intensity factor  $K_{\text{red}}$  is defined by:

$$K_{\text{red}}^{\text{W}} = K_{\text{max}}^{\text{OL}} \left( 1 - \frac{\Delta a}{z_{\text{OL}}} \right)^{1/2} - K_{\text{max}} \quad (29)$$

Where,

$K_{\text{red}}^{\text{W}}$  = Willenborg reduced stress intensity factor

$\Delta a$  = Crack growth into overload interaction zone,  $z_{\text{OL}}$

$z_{\text{OL}}$  = Interaction zone

Following an overload,  $\Delta a$  is approximately zero and the reducing stress intensity factor is maximum. The assumption expressed by Equation (29) was shown to be in error by a comparison of measured and calculated affected zones. Measured data showed that a finite number of cycles were required to propagate the crack through the overload affected crack length. It has also been shown that cracks grow after single overload applications where  $K_{\max}^{\text{OL}}/K_{\max} \geq 2.0$ , the condition that the Willenborg Model predicts zero crack tip effective stress intensity factors.

Gallagher suggested that  $K_{\text{red}}$  may actually be proportional to the Willenborg  $K_{\text{red}}^{\text{W}}$  expressed in Equation (29) such that:

$$K_{\text{red}} = \phi_{\text{F}} K_{\text{red}}^{\text{W}} \quad (30)$$

Where,

$K_{\text{red}}^{\text{W}}$  = Willenborg  $K_{\text{red}}$  of Equation (29)

$\phi_{\text{F}}$  = Gallagher proportionality factor

The proportionality factor  $\phi_{\text{F}}$  was defined in the following manner. One boundary might be the "shutoff" overload to maximum load ratio ( $K_{\max}^{\text{OL}}/K_{\max}$ ) that produces no crack growth. This value can be determined by tests. It was assumed that the shutoff overload level develops a local  $K_{\max}$  condition such that no growth is induced. Since the fatigue threshold stress intensity factor maximum ( $K_{\max\text{TH}}$ ) is approximately constant for negative stress ratios, the maximum local stress intensity factor ( $K_{\max\text{eff}}$ ) is set equal to  $K_{\max\text{TH}}$  for zero tension loading ( $R=0$ ). Using equations (29) and (30)  $K_{\max\text{eff}}$  can be expressed as:

$$K_{\max\text{eff}} = K_{\max} - \phi_{\text{F}} \left[ K_{\max}^{\text{OL}} \left( 1 - \frac{\Delta a}{z_{\text{OL}}} \right)^{1/2} - K_{\max} \right] \quad (31)$$

Immediately following the shutoff overload ( $K_{\max}$ ) which produces no growth,  $\Delta a = 0$  and  $K_{\max\text{eff}} = K_{\max\text{TH}}$  and Equation (31) can be solved for  $\phi_{\text{F}}$  as:

$$\phi_{\text{F}} = \frac{K_{\max} - K_{\max\text{TH}}}{K_{\max}^{\text{OL}} - K_{\max}} \quad (32)$$

In a more familiar form,  $\phi_{\text{F}}$  is:

$$\phi_{\text{F}} = \frac{1 - \frac{K_{\max\text{TH}}}{K_{\max}}}{\frac{K_{\max}^{\text{OL}}}{K_{\max}} - 1} \quad (33)$$

Tests have shown that the overload ratio  $K_{\max}^{\text{OL}}/K_{\max}$  varies from about 2.3 to 2.5 for aluminum.

Section 2.6 presents the results of a preliminary study to select one of the retardation models discussed above to be used as the primary model for making crack growth predictions in this study. A crack growth computer program, Reference 9, was used for all crack growth predictions and the user has the option to select any of the retardation models discussed above.

### 2.3.2 USE OF CRACK GROWTH RATE DATA

Crack growth rate (da/dn) data used in crack growth predictions are usually stored in or input into a crack growth computer program in a table look-up or equation form. The most accurate method is to store or input the actual test data points in table look-up form for the actual test stress ratios. This allows a complete da/dn curve to be utilized, from the threshold end to the failure end. This approach requires more computer time than the approach using an equation, but it has been shown that a simple mathematical expression will not accurately represent test da/dn data over a large range of  $K_{max}$  and R values. In this study, therefore, the crack growth program (independent of retardation model selection) made use of the table look-up method. The da/dn data were in the form of  $K_{max}$  versus  $d2a/dn$  for various values of R which were derived from a series of constant amplitude tests to define the crack growth rate characteristics of the test material. The results of these tests are discussed in Section 2.5.

## 2.4 Experimental Verification Test Procedures

The results of analytical studies performed as part of this study were experimentally verified by subjecting test specimens to selected usage variation conditions. A total of 24 specimens were tested to verify the validity of crack growth predictions. These tests consisted of; (1) preliminary tests of selected stress spectra to aid in selection of the primary retardation model that would be used to make the crack growth predictions in this study, (2) tests of mission segment spectra and (3) tests of total variable mission spectra. In addition, eight specimens were fabricated from the same sheet of material as the verification test specimens for the purpose of performing constant amplitude crack growth rate tests to provide baseline da/dn data for use in analytical crack growth analyses.

The program test plan was submitted in Reference 10 and subsequently approved by the Air Force monitor. Alloy and specimen selection and the test procedures which include the test environment, application of test loads, instrumentation and crack growth monitoring are summarized in the following sections.

### 2.4.1 ALLOY SELECTION

The aluminum alloy 7075-T651 bare plate was selected as the analysis and test alloy because of its general availability, common usage in aircraft and the existence of relevant materials property data. The fracture properties of this alloy are also well characterized by available fracture mechanics techniques. The experimental verification test and da/dn specimens were all fabricated from a single sheet of material of dimensions 48 x 144 x .26 inches.

### 2.4.2 SPECIMEN CONFIGURATION

A center crack panel specimen design was selected for the experimental verification and constant amplitude crack growth rate tests because it is simple, symmetrical, typical of actual flaws in airplanes, and has a widely accepted solution for stress intensity factor K including a width correction factor, i.e., as indicated by:

$$K = \sigma \sqrt{\pi a \sec \frac{\pi a}{W}} \quad (34)$$

Where,

- $\sigma$  = Stress
- $a$  = Half crack length
- $w$  = Specimen width

A sketch of the specimen is shown in Figure 10. Specimen dimensions were chosen to provide a width which would avoid large free edge effects during peak loads. An EDM notch was used as a crack starter. The specimens were 24 inches in length and 8 inches in width.

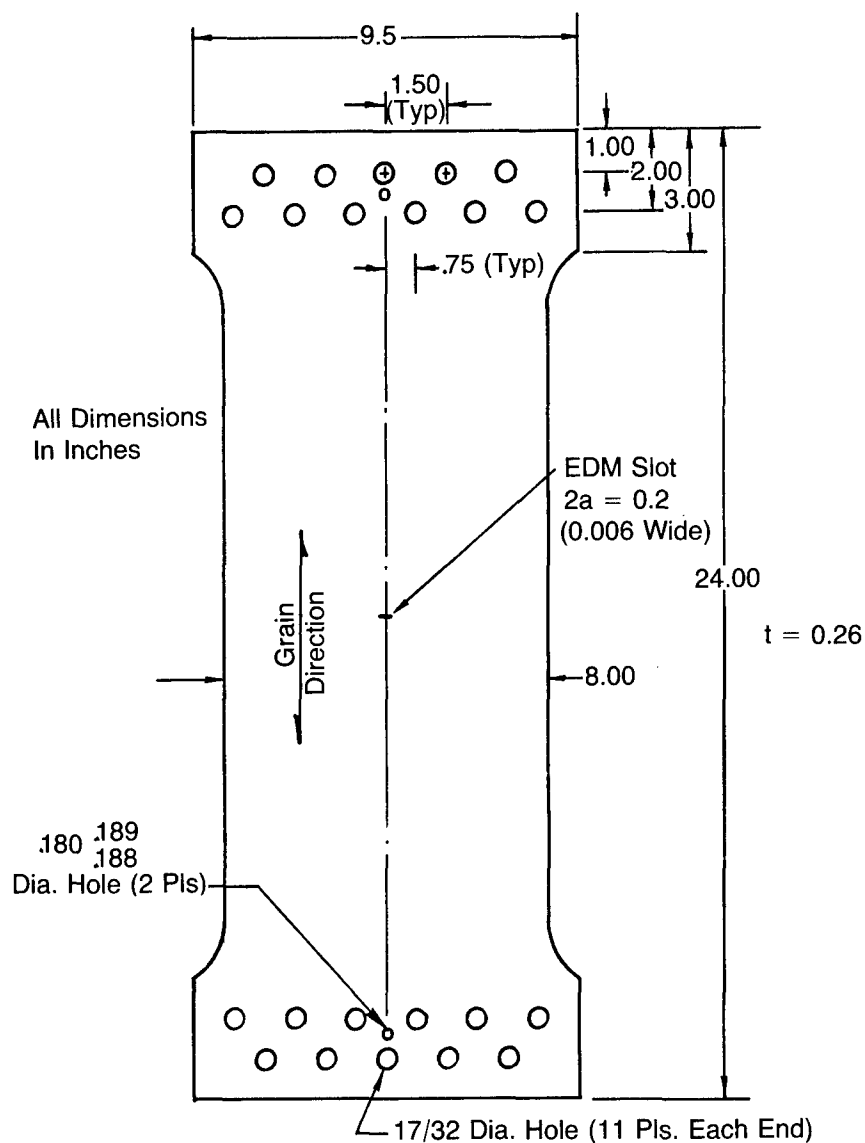


Figure 10. Center Crack Panel Specimen

To resist buckling under compressive loads edge type buckling restraints were used. These restraints consisted of heavy maple blocks backed up with steel structure and with two sheets of teflon between the restraints and the specimen.

Grips were designed to hold the specimen by friction. The ends of the specimens were sandblasted to provide better gripping. Alignment holes in the specimen and grips permitted alignment of the load line and the specimen centerline to within 0.020 inch.

### 2.4.3 TEST PROCEDURE

The baseline constant amplitude  $da/dn$  tests were conducted first. Next, a limited number of tests were conducted with a few selected spectra to aid in the selection of an analytical crack growth model to be used in this study. Following those tests, the verification tests of mission segment spectra were performed (parametric study) followed by the verification tests of variable mission spectra (variability study).

#### 2.4.3.1 Test Environment

Three levels of relative humidity were considered for the test environment; room air, dry air and humid air. The use of room air with uncontrolled humidity would introduce the unknown effect of variable humidity in the tests, while the dry air would not be representative of the actual aircraft environment. Humid air more closely represents actual aircraft environment than does dry or laboratory air. Therefore, all baseline  $da/dn$  and experimental verification tests were conducted in a controlled 95 percent or higher relative humidity environment by passing room air through a water bath and into a chamber surrounding the test section of the specimen. Most industry testing is done today in humid air which permits correlation with other data. A photograph of the humidity chamber and test specimen is shown in Figure 11.



Figure 11. Test Humidity Chamber and Test Specimen

#### 2.4.3.2 Application of Test Loads

The baseline  $da/dn$  and experimental verification tests were conducted in a 200,000-pound capacity MTS servo-hydraulic test machine. This machine was fully automated utilizing a Digital Equipment Corporation (DEC) PDP 11/05 mini-computer as a central processor. The PDP 11/05 has 16,384 words of 16 bit core memory capacity and upgraded to include a dual drive magnetic tape cassette utilized as a mass storage device. A programmable hardware segment generator for increased speed of operation and a basic language capability for greater programming efficiency are also provided. This language and the large core memory allowed definition of up to 600 discrete load blocks within the program proper. Essentially unlimited complexity and length of spectra could be defined for testing.

The load sequences generated by the sequence generator program, Section 2.2.4, were reformatted onto punched paper tape. The load sequence data was read into the PDP 11/05 via the paper tape reader terminal and was stored on the MTS system's cassette tapes for input into test operating programs as required for test execution. The load control program was written to require the input of mean load, maximum load, minimum load, frequency and the number of quarter cycles to be input to describe the sequence.

The constant amplitude tests were run at a rate of 10 Hz. The verification tests were performed at a rate of approximately 5 Hz.

Prior to each test, the programmed voltage inputs were remotely applied to obtain a trace of the loads on an X-Y recorder for checking the input load spectrum. Accuracy of load control with the test system was checked and it was verified that loads were applied with an accuracy of at least 0.25 percent of full-scale up to frequencies of 10 Hz.

To accomplish testing in a reasonable length of time, all analytical stresses (loads) determined for use in the parametric and variability analyses and tests were increased by a factor of 1.275.

#### 2.4.3.3 Instrumentation

Specimens which were tested early in the program were instrumented with strain gages to verify that the required stresses were being produced by the programmed loads and to check stress distributions in the specimens. As the program progressed, a few additional specimens were instrumented to check loads from time to time.

#### 2.4.3.4 Crack Growth Monitoring

The principal item to be measured during the constant amplitude and verification tests was crack length. Direct measurements of the crack length offer a reliable way of achieving the desired accuracy. It was intended that measurements be made using a camera system consisting of a 2-1/4 inch Hasselblad camera Model 500 ELM with remote electronic shutter trigger to be used in conjunction with 0.005-inch grids etched on one side of the specimen to record crack growth automatically. However, due to poor quality photographs this method was not used. As a result, crack growth measurements were obtained with a 50-power Gaetner measuring microscope. Side measurements were conveniently made at small increments of crack growth on both sides of the specimen and an average crack length determined.

### 2.5 Constant Amplitude Crack Growth Rate Tests

Crack growth rate ( $da/dn$ ) tests were performed as part of this study to obtain the crack growth rate characteristics of the 7075-T651 material used in fabrication of the verification test specimens. The results from these tests were reduced to a tabular form for input into a digital IBM computer crack growth program, Reference 9.

#### 2.5.1 TEST PROCEDURE

Eight specimens were selected for testing to obtain  $da/dn$  data for a range of R values from 0.8 to -1.0 at maximum gross area stresses varying from 5.0 to 12.0 KSI as summarized in Table 2.

TABLE 2.  
CONSTANT AMPLITUDE  $da/dn$  TESTS CONDUCTED

Test No.	R	$\sigma_{max}$	Cycles Applied	Spec. No.
1	0.8	11.5	2,745,000	FV-7
2	0.4	6.7	931,000	FV-16
3	0	5.8	760,000	FV-19
4	-1.0	5.8	580,000	FV-13
5	-1.0	4.8	862,000	FV-29
6	0.6	7.7	1,654,000	FV-22
7	0	5.3	800,000	FV-25
8	0.7	6.7*	4,126,000	FV-1

\*Load changed several times to increase growth rate

Test loads were selected to provide crack growth over a large range of K values. Due to the high toughness of the test material ( $K_C = 66.4 \text{ KSI} \sqrt{\text{in}}$ ), which contributed to slow crack growth, two of the tests required that the loads be increased to increase crack growth. Once crack growth commenced in each specimen, the test loads were unchanged during the test.

Crack length measurements were made at short intervals such that a nearly even distribution of  $da/dn$  versus  $K_{max}$  was obtained over a  $2a$  crack length range of approximately 0.30 to 2.0 inches. The following limits were observed: For  $2a$  lengths up to 0.80 inch, readings were taken at intervals such that  $\Delta 2a$  was less than 0.04 inch. For  $2a$  lengths between 0.80 and 2.0 inches, readings were taken at intervals such that  $\Delta 2a$  was less than 0.08 inch.

### 2.5.2 $K_{max}$ VERSUS CRACK GROWTH RATE ( $d2a/dn$ )

The results of the constant amplitude crack growth tests are shown in Figures 13 and 14. The maximum stress intensity factor,  $K_{max}$ , was computed using Equation (34) for each crack length reading taken during each test. The average  $K_{max}$  for each increment of crack growth was determined and the corresponding crack growth rate,  $\Delta 2a/\Delta n$  computed. These data are shown for R values of 0.8, 0.6 and zero in Figure 12 and R values of 0.7, 0.4 and -1.0 in Figure 13. The curve representing a best fit through each data set is shown with the data at the low crack growth rate end smoothly extrapolated to an assumed minimum  $K_{max}$  threshold of 1.0. The upper portion of each curve was smoothly extrapolated to the measured  $K_C$  value for the test material ( $66.4 \text{ KSI} \sqrt{\text{in}}$ ). A table look-up method and logarithmic interpolation subroutine in the analytic crack growth program retrieved this data for use in the crack growth process.

## 2.6 Preliminary Study – Analyses and Tests to Select a Retardation Model

Limited analyses and testing were conducted to aid in the selection of an analytical crack growth model to be used in performing the parametric and variability studies. Prior to performing these studies, discussed in Sections 2.7 and 2.8, three mission profiles of varying severity were used to define five different spectra for the wing lower surface. Crack growth predictions were made using the Wheeler, Willenborg and the Willenborg/Gallagher retardation models discussed in Section 2.3.1. These predictions were then compared to test results of the five spectra.

### 2.6.1 SELECTION OF STRESS SPECTRA

The three mission profiles were selected to represent a wide range of usage in order to give a wide variation in spectrum stress severity and content. The profiles were arbitrarily selected to represent severe, average and benign usages which produced significant differences in crack life and retardation effects. The stress spectrum for each profile was developed by using mission segment flight spectra derived as part of the parametric study, Section 2.7. The three missions were identified as a low level mission and a benign mission Numbers 1 and 2. A sketch of the mission profiles and the wing stress spectra used in analyses and testing is shown in Figures 14, 15 and 16.

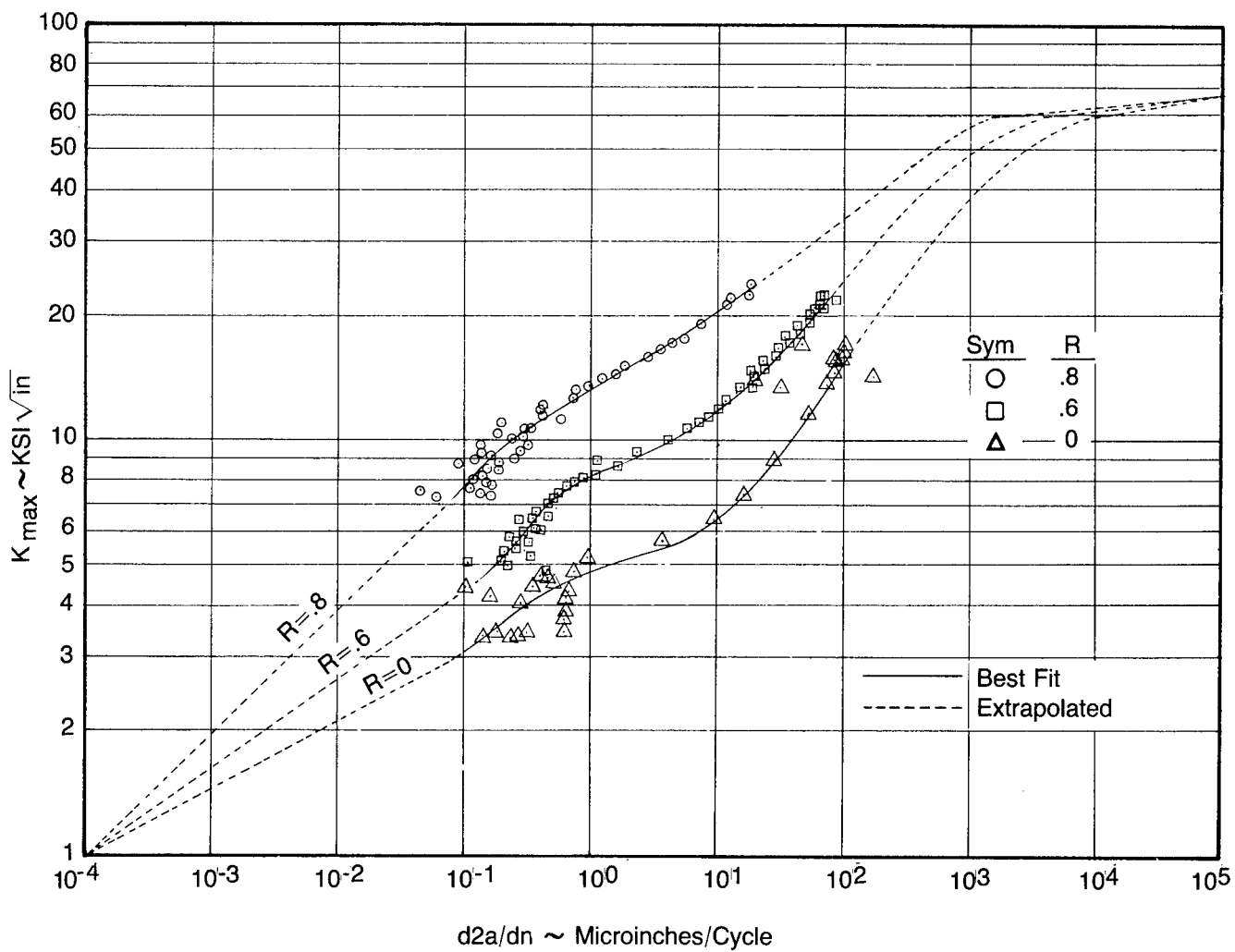


Figure 12. Crack Growth Rate Data for 7075-T651, R=0.8, 0.6 and 0

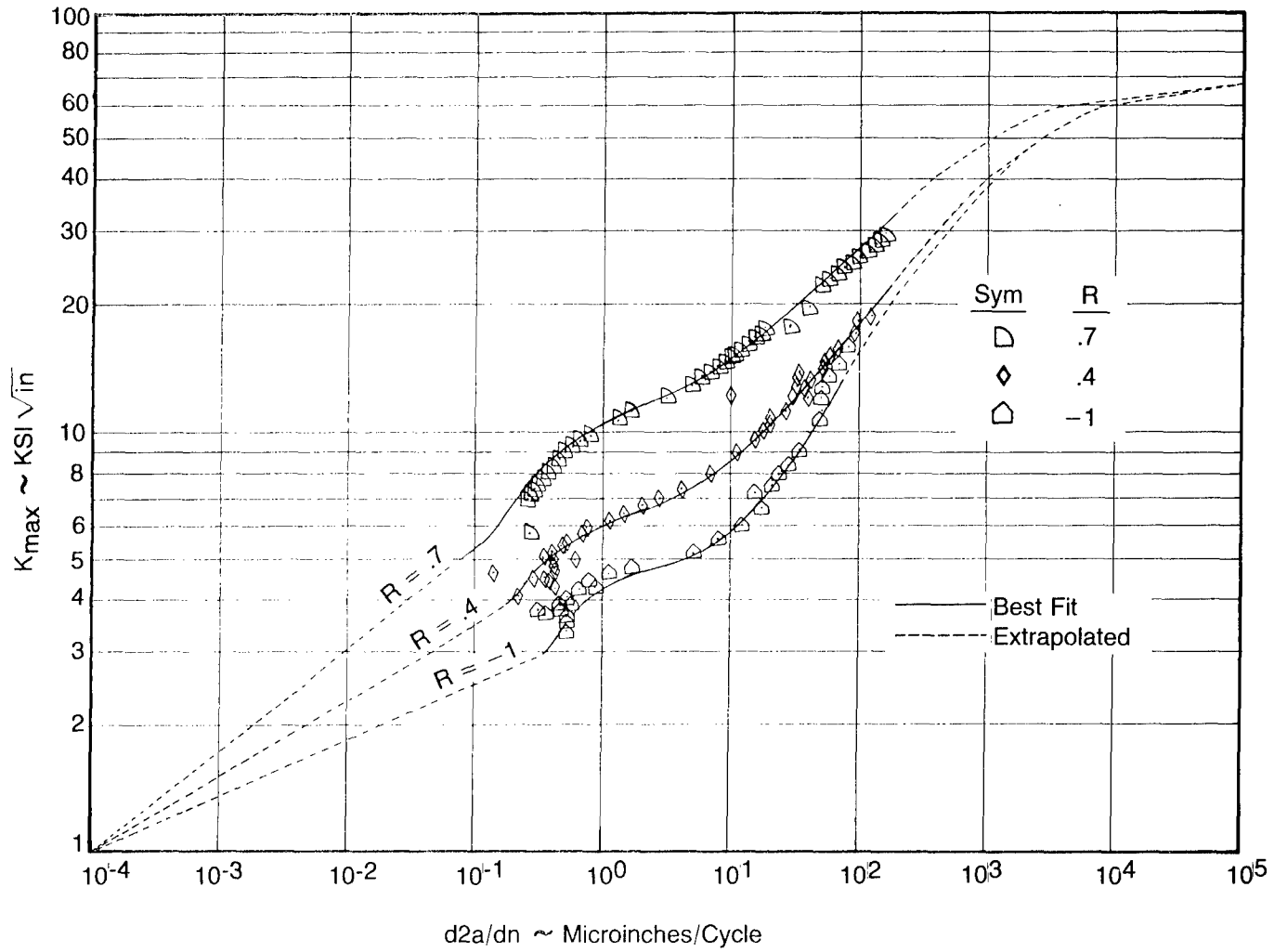


Figure 13. Crack Growth Rate Data for 7075-T651, R = 0.7, 0.4 and -1.0

Figure 14 shows the low level mission profile and wing stress spectrum. This mission consists of a takeoff at maximum gross weight (297 KIPS), one hour of cruise, two hours of low level flight and four touch and go segments. The test and analysis spectrum shown was determined for the entire flight and was used to form two variations of this spectrum. The additional two spectra were representative of the low level segment only (as noted in Figure 14) and a spectrum consisting of the mission spectrum without the low level segment. The mission is considered to be a severe spectrum consisting of 1391 stress cycles, 1003 of which are low level, and has a peak stress of 26.0 KSI per flight. Only wing stress spectra were used in the preliminary study to select a delay model.

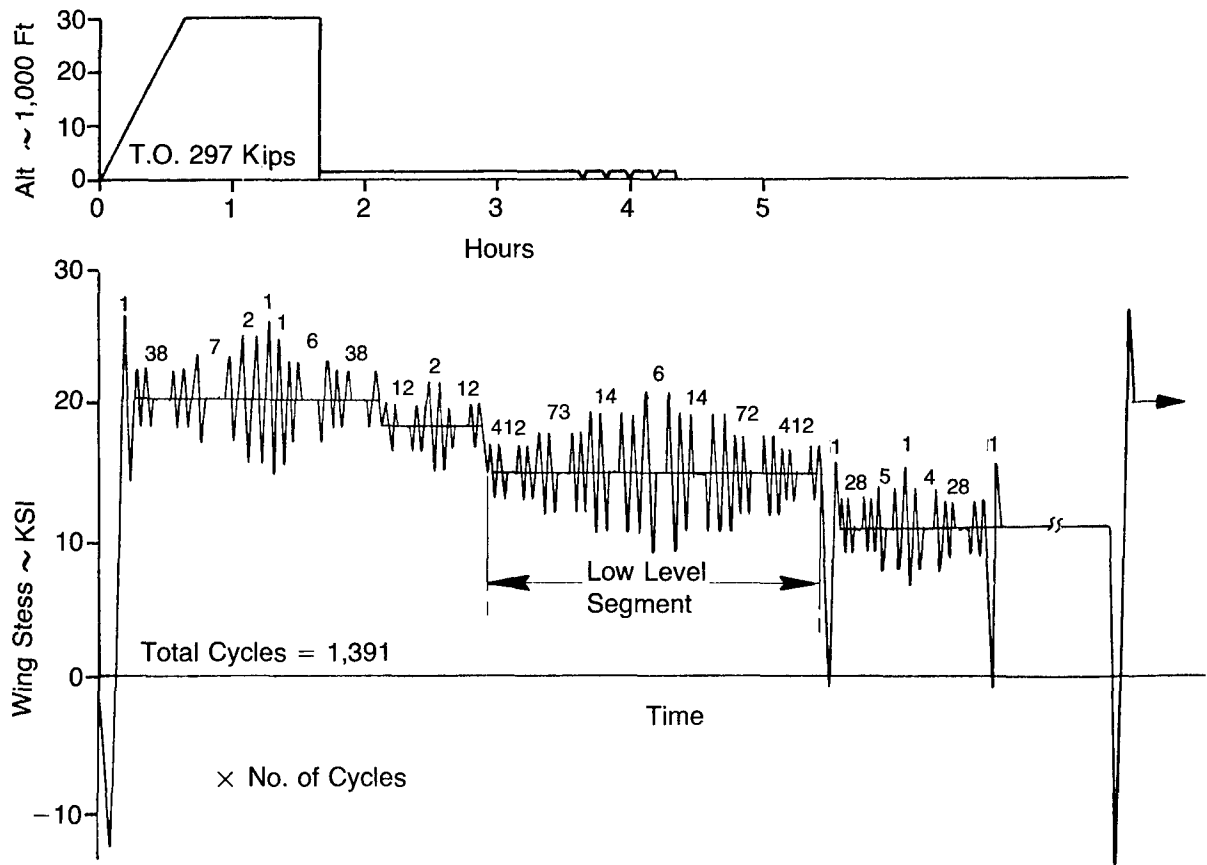


Figure 14. Low Level Mission Profile and Spectrum

The Benign Mission No. 1 (Figure 15) has a takeoff gross weight of 260 KIPS and includes three hours of cruise followed by one touch and go segment. The spectrum contains 175 stress cycles and a peak stress of 21.5 KSI once per flight.

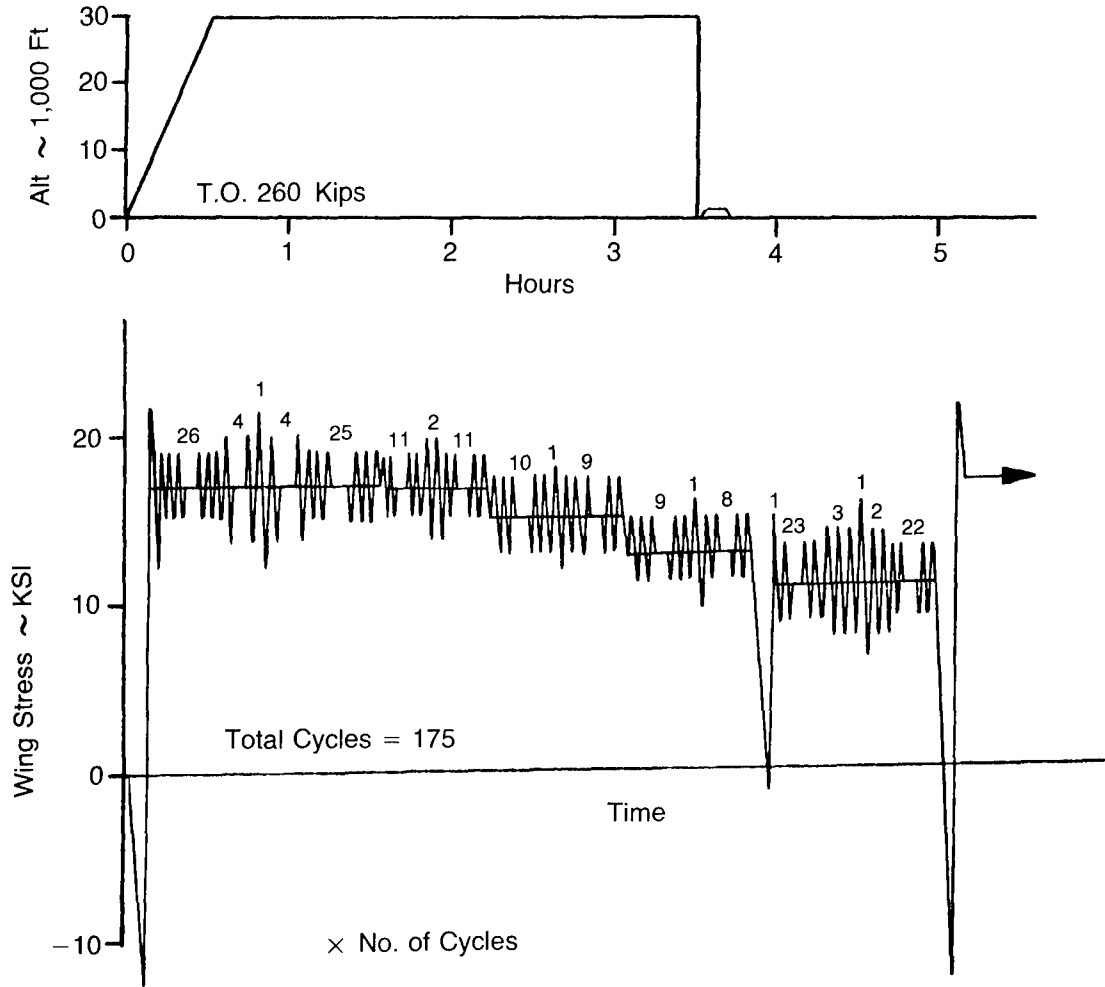


Figure 15. Benign Mission No. 1 Profile and Spectrum

The third mission, Benign Mission No. 2, was selected to represent the least severe form of usage and to enable evaluation of both extremes of the usage spectrum. This mission, Figure 16, has a takeoff gross weight of 170 kips and includes one hour of cruise. The spectrum consists of 31 cycles and a peak stress of 12.5 KSI once per flight.

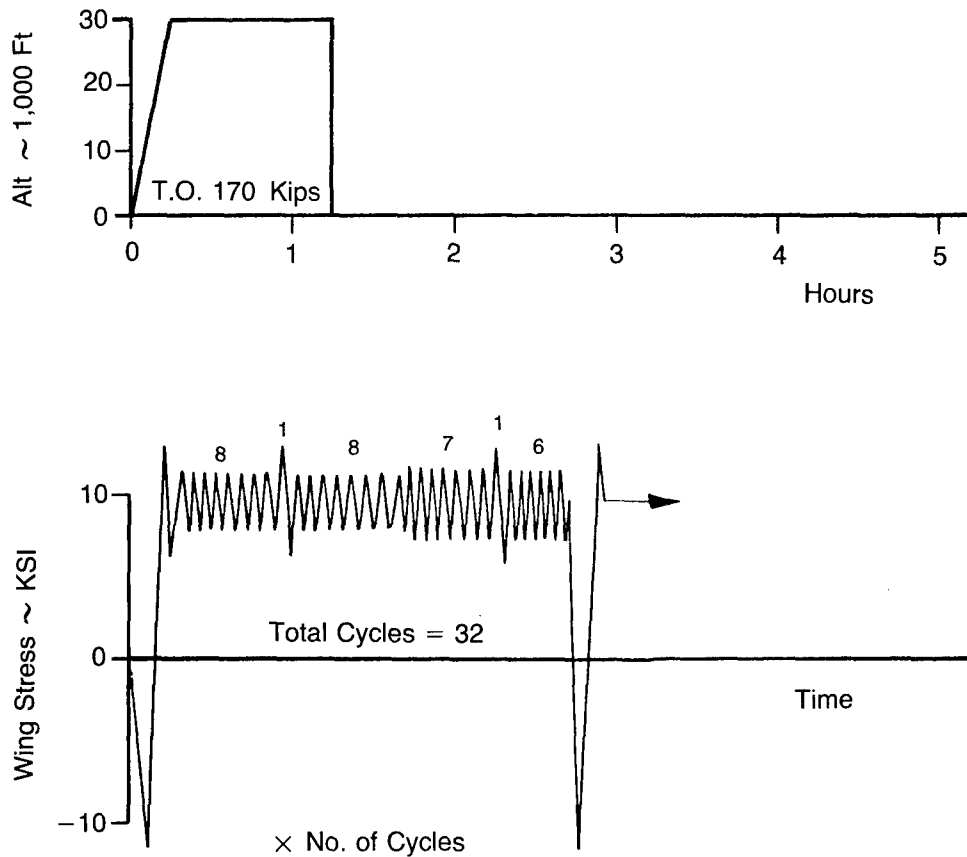


Figure 16. Benign Mission No. 2 Profile and Spectrum

## 2.6.2 CRACK GROWTH ANALYSES AND TEST RESULTS

The results of the preliminary crack growth analyses and tests are shown in Figures 17, 18 and 19. Figure 17 shows the results of the five tests with a comparison of predicted crack growth using the Wheeler Retardation Model with a shaping exponent,  $m$ , of 0.90. This analysis proved to have the best overall agreement with test results. A comparison with analyses using other delay models and different Wheeler shaping exponents is shown in Figure 19.

The tests showed that the low level segment spectrum alone was the most severe. The low level mission (including the low level segment) had about 2.5 times more life than the low level segment alone. Deleting the segment from the low level mission spectrum only produced about 1.3 times more life than the complete mission. The Benign Missions 1 and 2 produced about 2.3 and 11.2 times more life, respectively, than the low level mission.

The tests of the low level mission and the low level mission with the low level stresses deleted showed that deletion of the low level segment stresses appeared to have much less effect on crack life than predicted by analysis (note diamond versus circle symbols in Figure 17). The test results indicated that the reduction in life due to the low level segment was about 35 percent while analysis indicated 70 percent reduction. These surprising results led to a decision to repeat these tests. Results of these repeated tests are shown in Figure 18. The results were similar; however, the low level segment only reduced life by about 20 percent which was less than before. Even though the low level segment was very severe, as shown in Figure 17, the peak load delay effects in the mission on the low level segment stresses are significant and could not be predicted by any of the delay models except by using a large shaping exponent with the Wheeler Retardation Model.

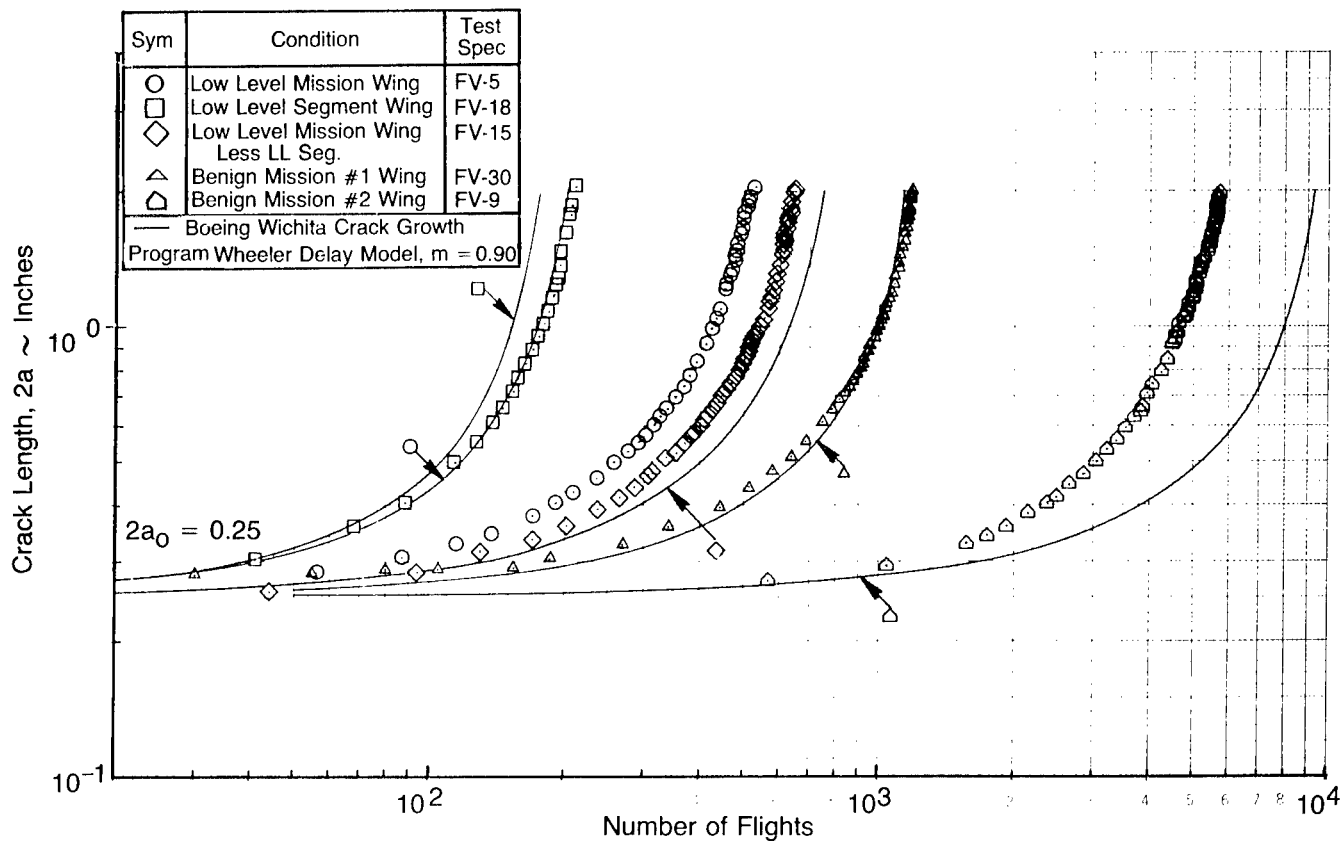


Figure 17. Test Results and Crack Growth Predictions, Preliminary Study

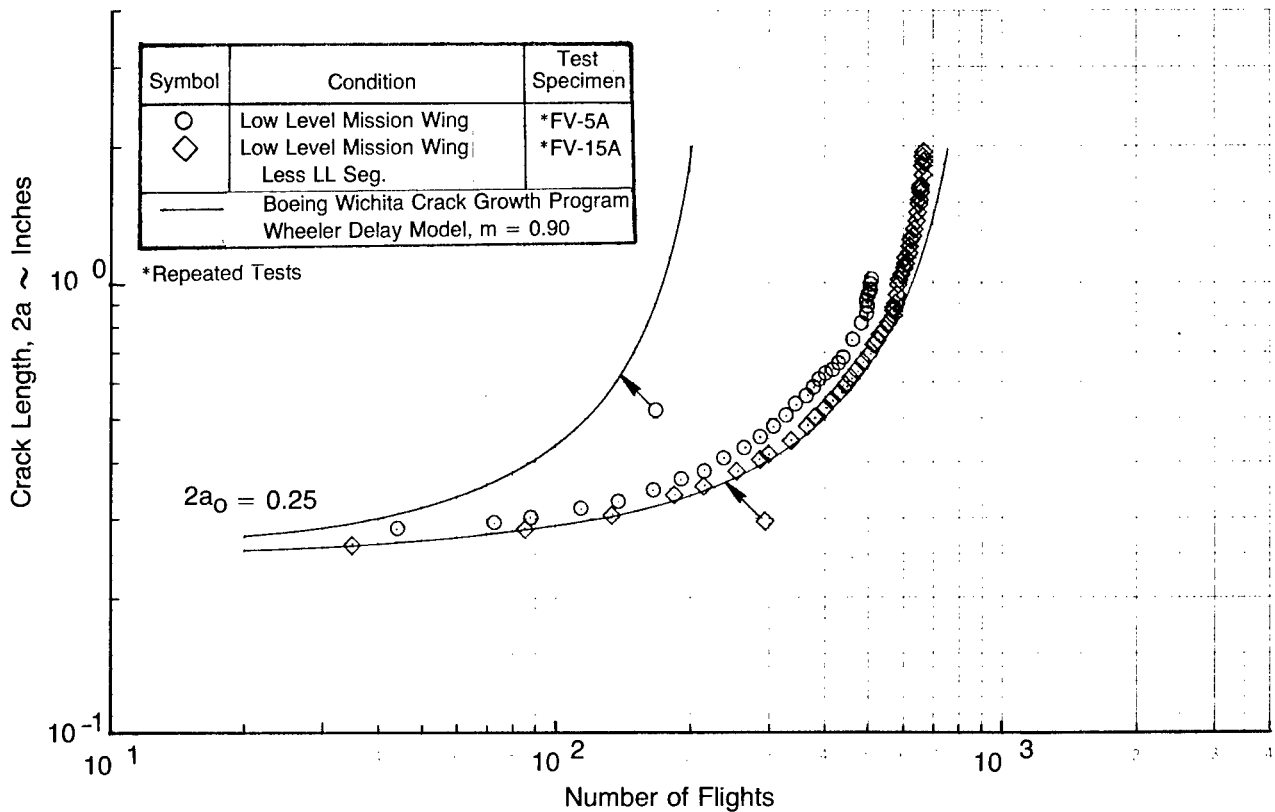


Figure 18. Test Results and Crack Growth Predictions, Repeated Tests

A comparison of test results and crack growth predictions using the various retardation models is shown in Figure 19. This figure is a plot of analysis life versus test life for crack growth from 0.25 to 0.35 inches. Crack growth predictions shown in Figure 19 were made using the Wheeler, Willenborg and Willenborg/Gallagher Retardation Models. Crack growth predictions using the Wheeler Model with a shaping exponent,  $m$ , equal to zero (no retardation) and for an  $m$  value of 2.2 (found to match test results for the low level mission) are shown for comparison of extreme crack growth predictions. The trends relative to spectrum severity were found to be the same for all delay models and none of the retardation models could consistently predict test crack growth for all spectra. However, the variation in crack growth predictions using a no-retardation analysis and a Wheeler Model analysis with an  $m$  equal to 2.2 is significant. The preliminary study indicated that spectrum severity and the amount of retardation are related and that the amount of retardation increases with spectrum severity. The results show that the Willenborg/Gallagher Model, using an overload ratio of 2.5 for aluminum, produces similar results as the Wheeler delay model using an  $m$  of 0.90 and produced the best overall correlation with test. Since the Wheeler Model is the easiest to adjust to correlate with test results, it was selected to perform the parametric and variability studies. A value of  $m = 0.90$  was judged to give the best overall analysis versus test comparison.

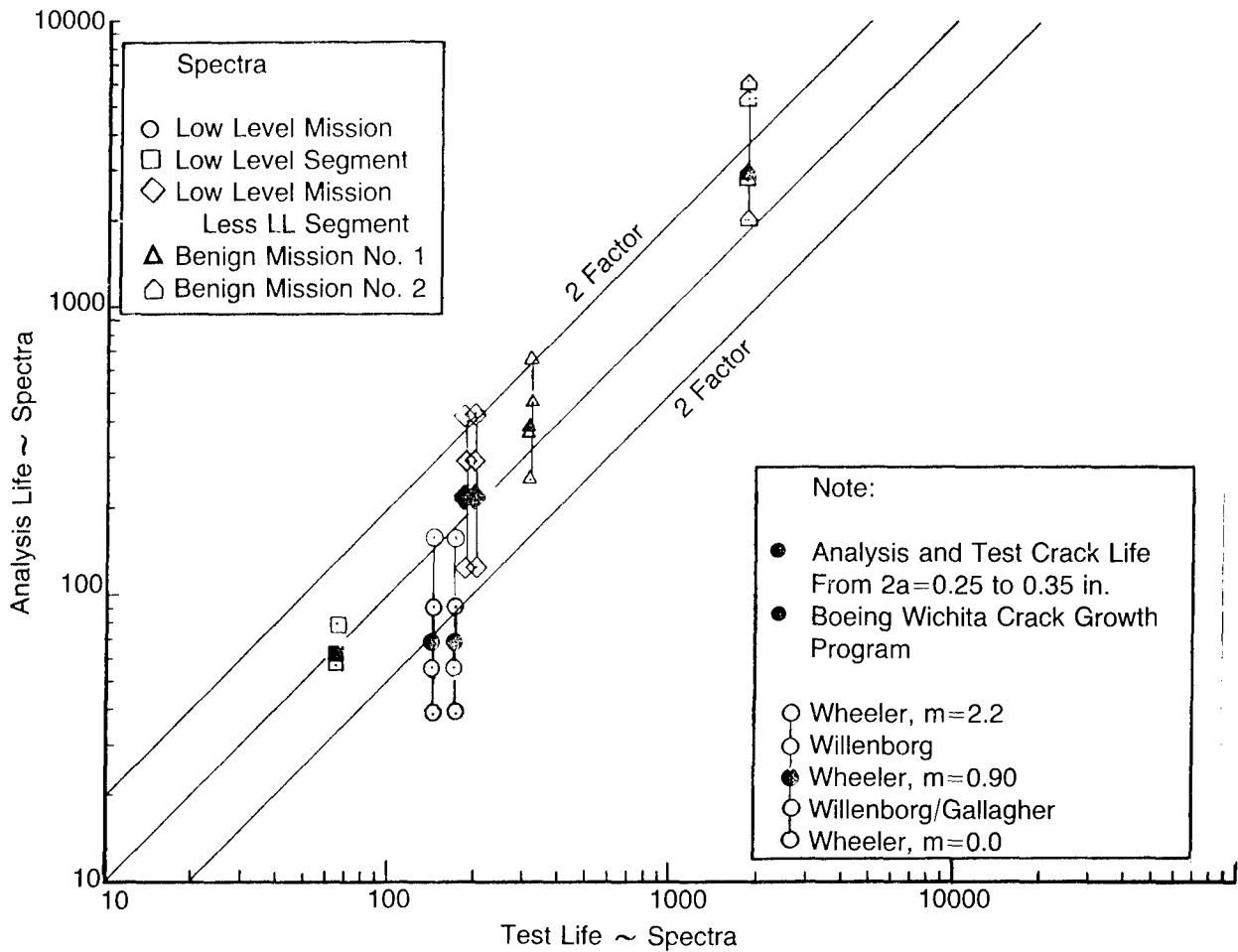


Figure 19. Analysis Life Versus Test Life, Preliminary Study

It was evident from the preliminary study results that the selection of a retardation model, and, in the case of Wheeler, a shaping exponent, is highly dependent on usage severity or spectrum content. Each aircraft and its usage must be studied in order to make this selection.

### 2.7 Parametric Study

A parametric study was conducted to determine and study the effects of significant mission usage and loading parameters on the rate of crack growth for selected airframe locations. The results of this study were used to demonstrate the use of parametric crack growth rates in calculating the potential crack growth in individual aircraft as a function of actual usage.

The general approach in this study was to select a matrix of parametric flight segments that adequately define the range of usage and loading parameters of the baseline aircraft. The stress spectra were then developed in terms of cumulative cycles of stress amplitude exceedances per flight segment. These exceedances were defined for a given unit of flight time. The stress exceedances were then converted to a stress sequence of Lo-Hi-Lo order for simplicity. These data were used in a crack growth analysis program to compute crack growth for each segment. Crack growth rates were then determined. The results of the parametric analysis were used to identify those parameters that most effect crack growth.

## 2.7.1 MISSION USAGE AND LOADING PARAMETERS

The KC-135A Tanker (baseline aircraft) is a cargo class airplane in accordance with the classifications defined in MIL-A-8861A. The C/KC-135 fleet is divided into 37 different model designated series which fly basically different mission profiles. Flight length varies from less than one hour for some missions to over 15 hours for others. The usage rate in terms of flight hours per year ranges from 240 to over 2000 hours per airplane.

Generally, the C/KC-135 fleet flies the entire cruise portion of the mission at high altitude; however, some of the special purpose aircraft have a mission segment at low altitude. Several of the C/KC-135 aircraft are also equipped for on-load refueling similar to bomber usage. Therefore, stress spectra representative of both transport and bomber aircraft were derived for this aircraft. Typical usage parameters investigated were climb, cruise, refuel on-load, low level, pattern and touch and go flight conditions.

Since the C/KC-135 fleet accomplishes a variety of mission assignments, there is a considerable variation in loading parameters such as gross weight, speed and altitude. These parameters along with the variation in airplane center of gravity location due to normal fuel sequencing procedures for the baseline airplane were evaluated in this study.

Changes due to airplane configuration (e.g. engines, cargo and equipment) were not included because past damage analyses had indicated little difference in damage accumulation for the KC-135A and C-135B configurations. The effect of changes in configuration of crack growth is discussed further in Section 3.1.

## 2.7.2 MISSION SEGMENTS SELECTED

Mission segments selected for the parametric study were defined by reviewing individual C/KC-135 aircraft usage forms (AFTO Form 76) which are presently being used to monitor fatigue damage on the C/KC-135 fleet. These forms were used to generate a coded listing, generally in the form of an edited tape, which comprises the flight-by-flight usage parameters for each airplane by serial number. A preliminary review of these data led to the selection of approximately 70 different flight conditions to adequately study and isolate those parameters which are the most significant in predicting crack growth in primary airframe structure. The parametric flight segments were selected such that they could be used to build a matrix of operational mission profiles for use in the variability study discussed in Section 2.8. Table 3 shows a summary of the parametric conditions selected. This table shows the

TABLE 3  
PARAMETRIC ANALYSIS MATRIX, FLIGHT CONDITIONS

Gross Weight Kips	Flight Conditions				
	Climb (T.O. GW) 	Low Level	Cruise 	Refuel	Pattern 
297	X		X		
280		X	X	X	
260	X	X	X		
240		X	X		
230	X				
220		X	X	X	
200	X	X	X		X
180		X	X		X
170	X				
160			X	X	X
140			X		X

 6 Phases Per Climb (Flaps Down 1st Phase)

 5,000, 10,000 and 30,000 feet

 Flaps Down, Touch & Go

flight condition and the corresponding gross weights analyzed. Cruise was analyzed for three altitudes; 5,000, 10,000 and 30,000 feet. The condition noted as pattern represents flying low altitude with flaps extended and includes touch and go landing operations.

A typical operating speed was used for each flight condition. During the variability study, the low level flight conditions were analyzed for one additional speed to study the effects of speed on crack growth.

### 2.7.3 ANALYSIS LOCATIONS

Several locations on the baseline airplane were used to evaluate the difference in sensitivity to similar usage parameters. Table 4 shows usage parameters judged to have a significant effect on crack growth in the various airplane components. This table indicates that each component is affected by most of the usage parameters. Therefore, it was considered prudent to select one analysis location from each major section of the airplane, i.e., wing, fuselage and empennage. The actual locations selected for study are shown in Figure 20.

TABLE 4  
USAGE PARAMETERS AFFECTING CRACK GROWTH

Usage Parameters		KC-135 Aircraft Component				
		Wing		Fuselage	Fin	Stabilizer
		Upper	Lower			
Loading or Configuration	Gross Weight	X	X	X		X
	Speed		X	X	X	X
	Altitude		X	X	X	X
	Center-Of-Gravity	X	X	X		X
	Weight Distribution	X	X	X		X
Mission	Climb	X	X	X	X	X
	Cruise		X	X	X	X
	Low Level		X	X	X	X
	Landing	X	X	X		
	Cabin Pressure	(Center Wing) X		X		

Stresses representative of these locations were used for all of the Task 1 analyses and tests.

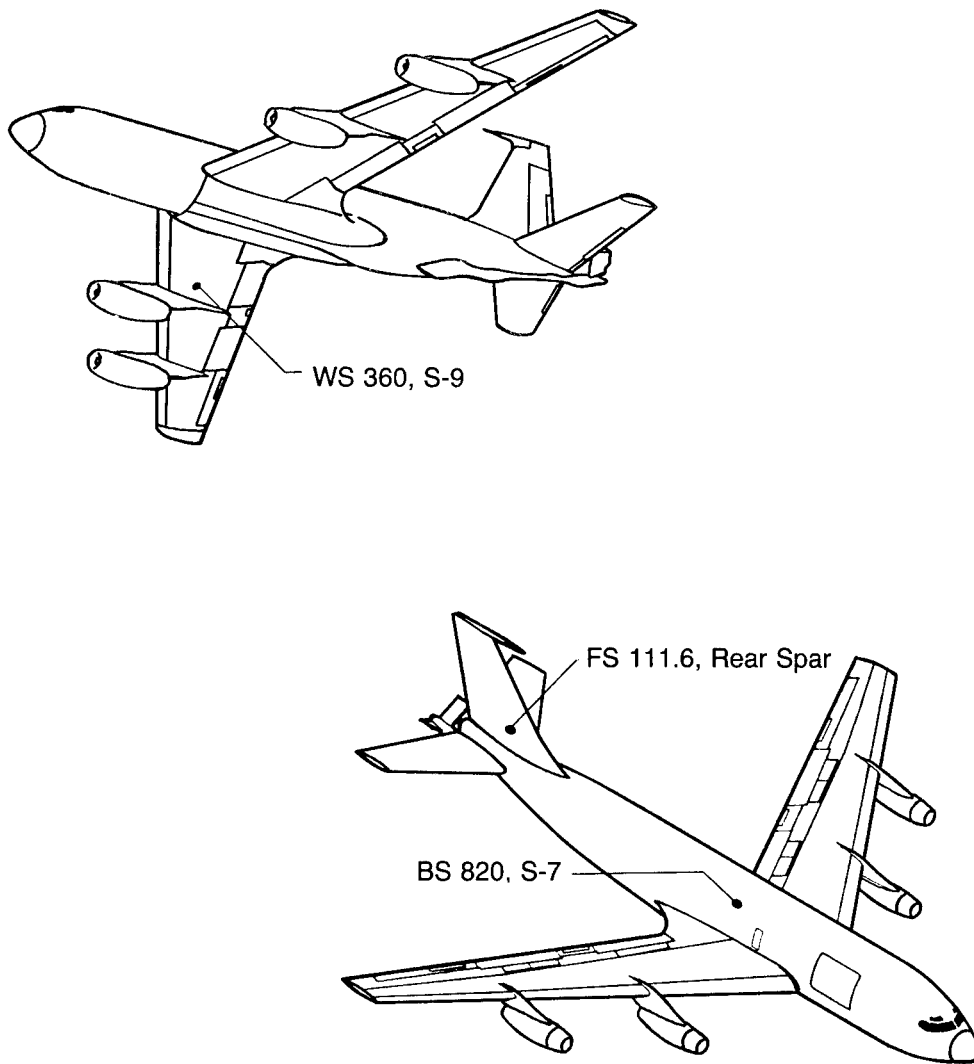


Figure 20. Analysis Locations

## 2.7.4 MISSION SEGMENT STRESS SPECTRA

A PSD stress/damage and a stress sequence generator computer program were used to generate mission segment stress spectra. These programs and the analysis methods used were discussed in Section 2.2. The PSD load responses and steady-state loads at the analysis locations used in the PSD stress/damage program were available from past and current analyses performed on the C/KC-135 aircraft.

A stress spectrum was determined for each of the flight conditions shown in Table 3. Climb conditions were defined for five takeoff gross weights ranging from 170 to 297 kips and from zero to 40,000 feet. Each climb consisted of six separate flight segments for altitude bands of zero to 1,000, 1,000 to 5,000, 5,000 to 10,000, 10,000 to 20,000, 20,000 to 30,000 and 30,000 to 40,000 feet. This permitted the determination of a climb spectrum to any of the altitudes noted. The climb speeds were determined per Air Force Technical Order based on normal rated thrust and altitude. The GAG cycle, as discussed in Section 2.2.3, was included in the climb spectrum and was identified as the cycle comprised of the peak stress occurring during the climb phase and the ground stress (or minimum stress). The peak stresses occurring less frequent, e.g., the stresses occurring once in 10, 100 and 200 flights, were also included in the climb spectra.

The low level spectra were derived for a gross weight range of 280 to 180 Kips for an altitude of 500 feet and speed of 280 KIAS.

Cruise spectra were developed for gross weight conditions from 140 Kips to a maximum gross weight of 297 Kips. Cruise speeds were also 280 KEAS. Cruise altitudes of 5,000, 10,000 and 30,000 feet were selected for analyses.

Refueling spectra were derived for fuel on-load conditions only for the gross weights noted in Table 3. Each refuel segment corresponded to a transfer of 20 Kips of fuel. At an altitude of 30,000 feet and a speed of 282 KEAS.

The low level, cruise and refuel spectra were defined for a one-hour flight duration.

The spectra developed for pattern operations were defined in two ways. Spectra were developed for flight segments representing one-hour flight duration at 1,000 feet with flaps extended and spectra for touch and go operations which include a go around segment of 0.13 hour duration with the GAG cycle associated with touch-and-go included. This GAG cycle consisted of the peak stress resulting from the go around portion at 1,000 feet with flaps extended and the ground stress occurring during touchdown. The speed used for pattern operations was 175 KEAS. The gross weight range analyzed was 200 Kips to 140 Kips.

A tabulation of the mission segment stress spectra for the three selected structural analysis locations is shown in Appendix A.

## 2.7.5 PARAMETRIC CRACK GROWTH PREDICTIONS

Crack growth analyses were performed using each of the mission segment spectra generated for the three structural locations. The Wheeler Retardation Model with a shaping exponent,  $m$ , of 0.9 was used to perform the crack growth analyses based on the results of the preliminary crack growth study presented in Section 2.6. The Wheeler Retardation Model was discussed in Section 2.3.1.1. The crack growth curves obtained from the analysis are presented in Appendix A. Since so many crack growth curves were generated in this analysis it was not convenient to compare these curves directly. Therefore, the method used to numerically characterize the results and make comparisons was to compare the number of hours or flights ( $\Delta N$ ) to grow a crack from 0.25 to 0.35 inches. The parameter  $\Delta N$  was used to summarize all crack growth predictions and test data presented in this program and is shown schematically in Figure 21.

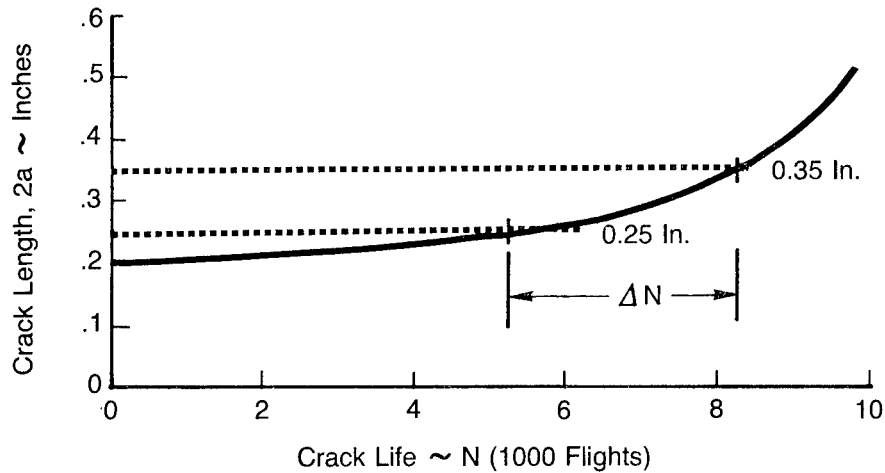


Figure 21. Time to Grow Crack from 0.25 to 0.35 Inches Used for Comparisons

A comparison of the parametric crack growth analyses is shown in Figures 22, 23 and 24 for the wing, body and fin, respectively. These figures show the crack life,  $\Delta N$ , to grow the crack from 0.25 to 0.35 inches over a low to high gross weight range for the various mission segments. As noted in the figures, the crack life for the climb and touch and go flight segments is in terms of the number of climb or touch and go segments while the crack life for all other flight segments (low level, cruise and pattern) is in terms of flight hours. The results show that crack growth for the wing and body locations analyzed are greatly influenced by gross weight and altitude.

The crack growth for the fin, Figure 24, shows that crack growth is primarily influenced by altitude. The dynamic lateral responses of the fin with flaps up and operating cruise speeds are relatively insensitive to changes in gross weight. However, when the airplane is operating at the lower speeds with flaps extended, the electronic yaw damper becomes active due to instability and causes the lateral responses to become sensitive to gross weight. This is shown by the data in Figure 24. The climb crack growth is also influenced by the time to climb to altitude which varies with gross weight.

The available retardation models investigated in this study appear to be a source of additional conservatism when dealing with missions experiencing severe stress environments. The test and analysis results shown in Figures 17 and 18 indicate that a common retardation factor will not adequately predict crack growth for all spectrum severities and content. As shown in Figure 19 the low level segment actually contributed much less to crack growth than predicted by any of the crack growth models.

Those flight conditions that most influence crack growth can be identified in Figures 22, 23 and 24. It is important to note that the climb and touch and go segments do include GAG cycles (wing and body) and will therefore realize more retardation during crack growth than the other parametric conditions.

The parametric analysis showed that for the baseline aircraft, crack growth at all locations was sensitive to changes in altitude; the wing and body locations were very sensitive to gross weight changes.

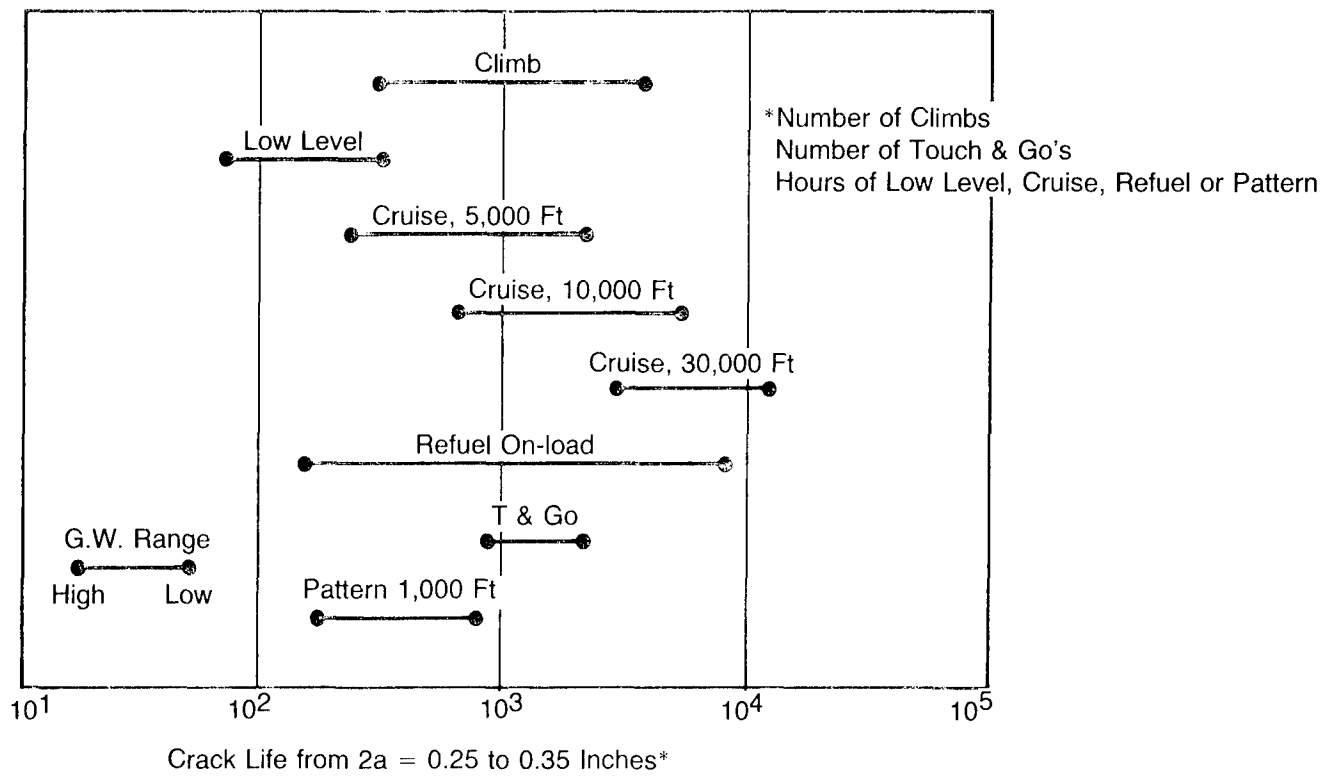


Figure 22. Parametric Crack Growth Comparison, Wing

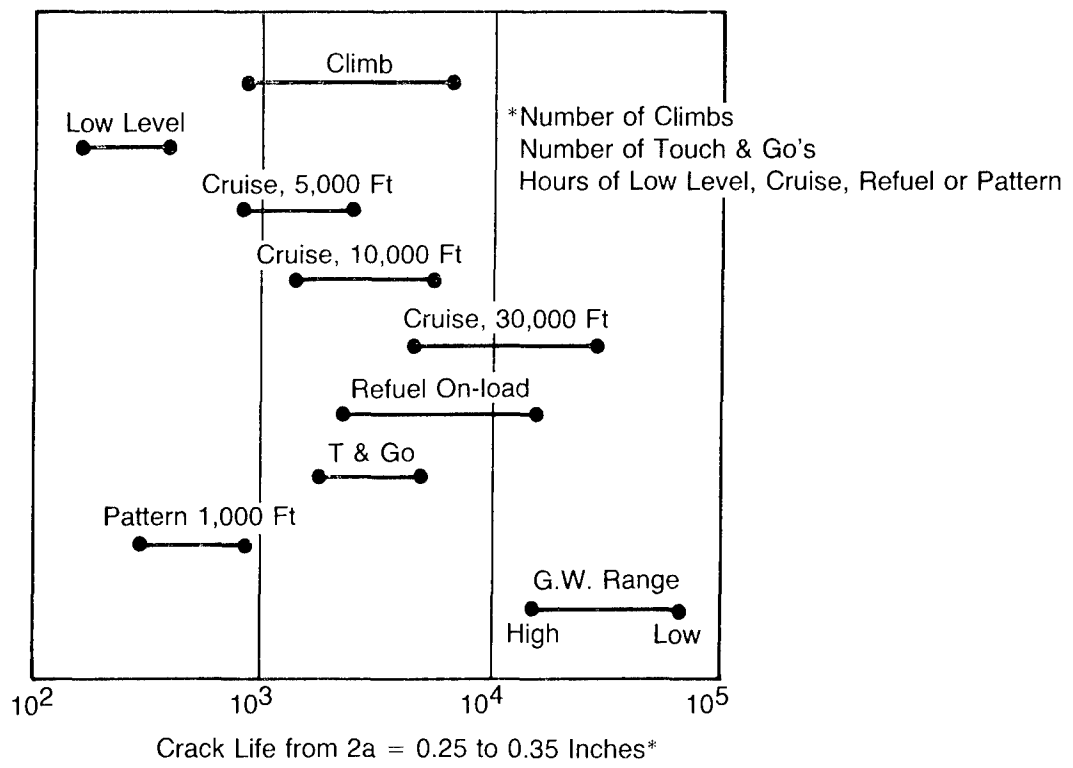


Figure 23. Parametric Crack Growth Comparison, Body

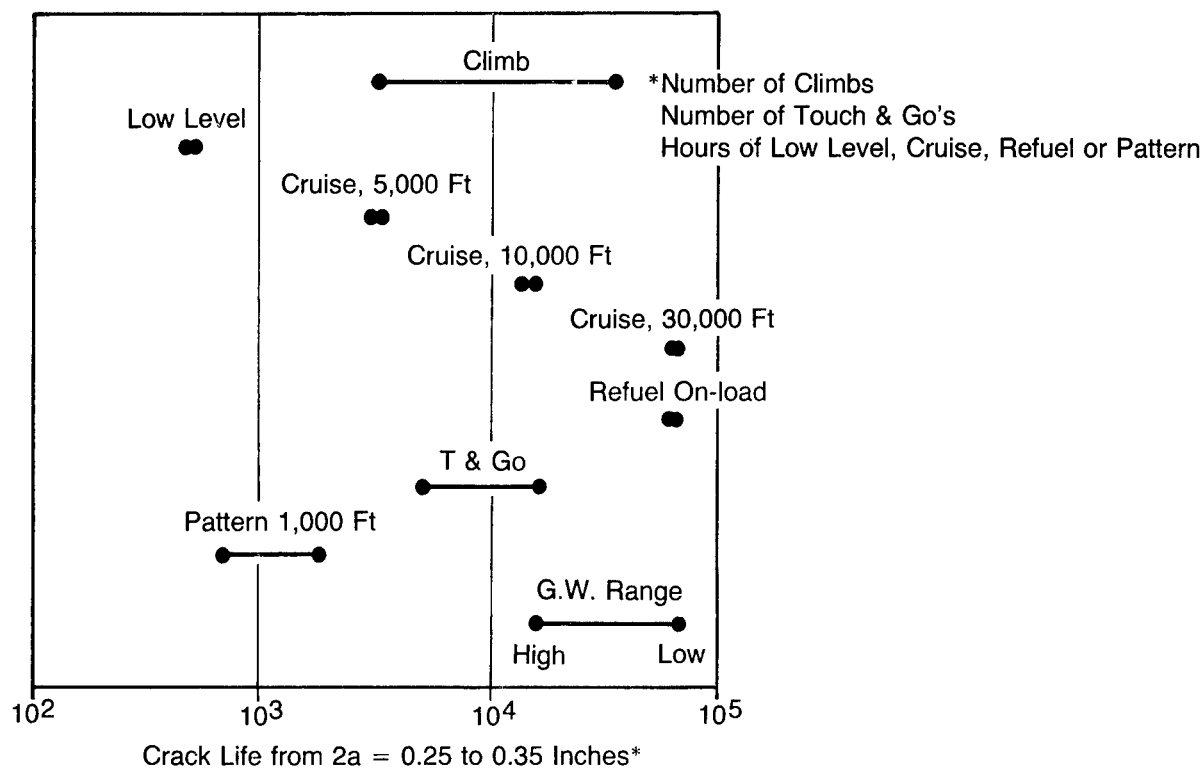


Figure 24. Parametric Crack Growth Comparison, Fin

### 2.7.6 PARAMETRIC CRACK GROWTH RATES

As a means of demonstrating the use of the summation of mission segment crack growth to predict potential crack growth in individual aircraft, mission segment crack growth rates were calculated from the parametric analytical crack growth curves presented in Appendix A. These rates were determined from the crack growth analyses data by determining  $\Delta 2a$  and  $\Delta N$  values at various values of crack length,  $2a$ , as depicted in Figure 25. These rates are shown in Figures 26, 27 and 28 for the wing, body and fin, respectively. The rates are shown as a function of crack length,  $2a$ , and gross weight for each flight condition analyzed.

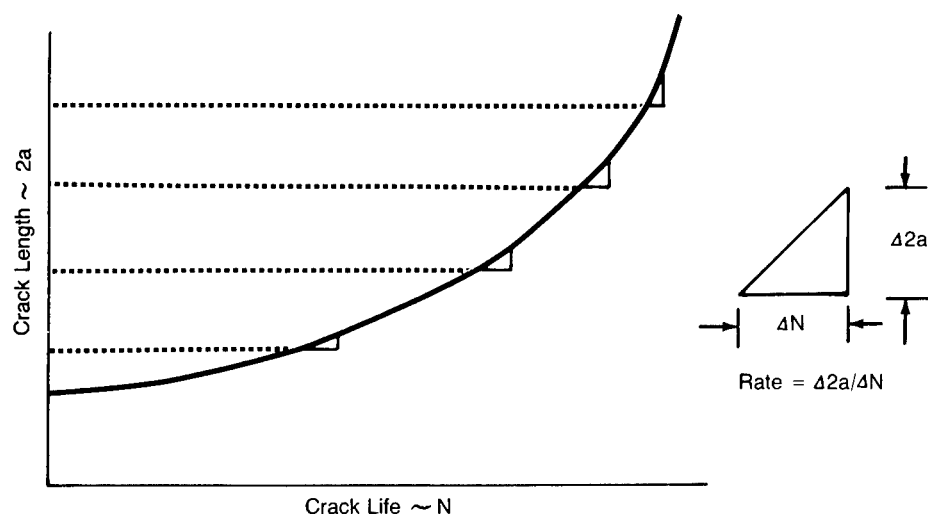


Figure 25. Technique Used to Determine Crack Growth Rate Data

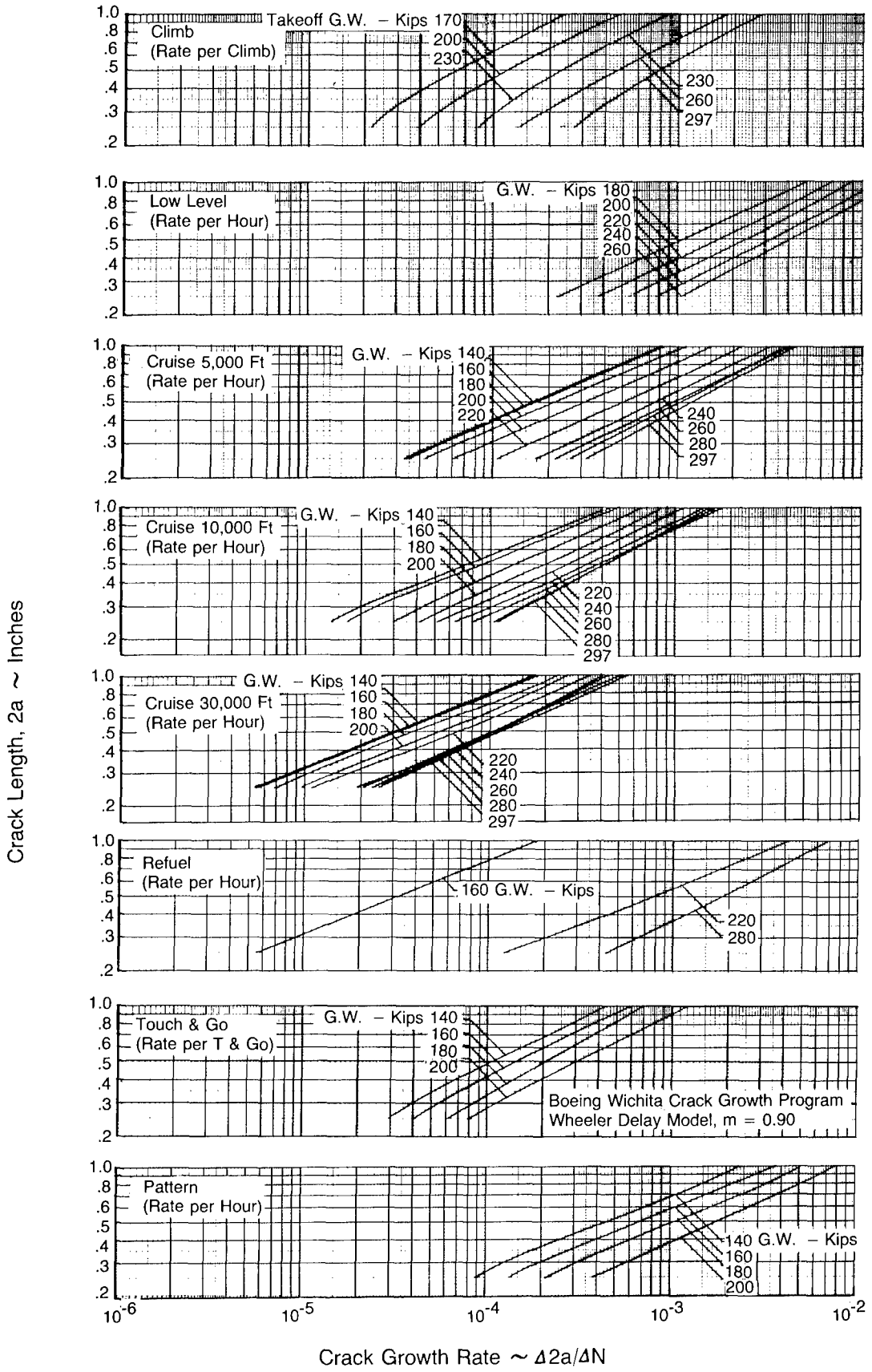
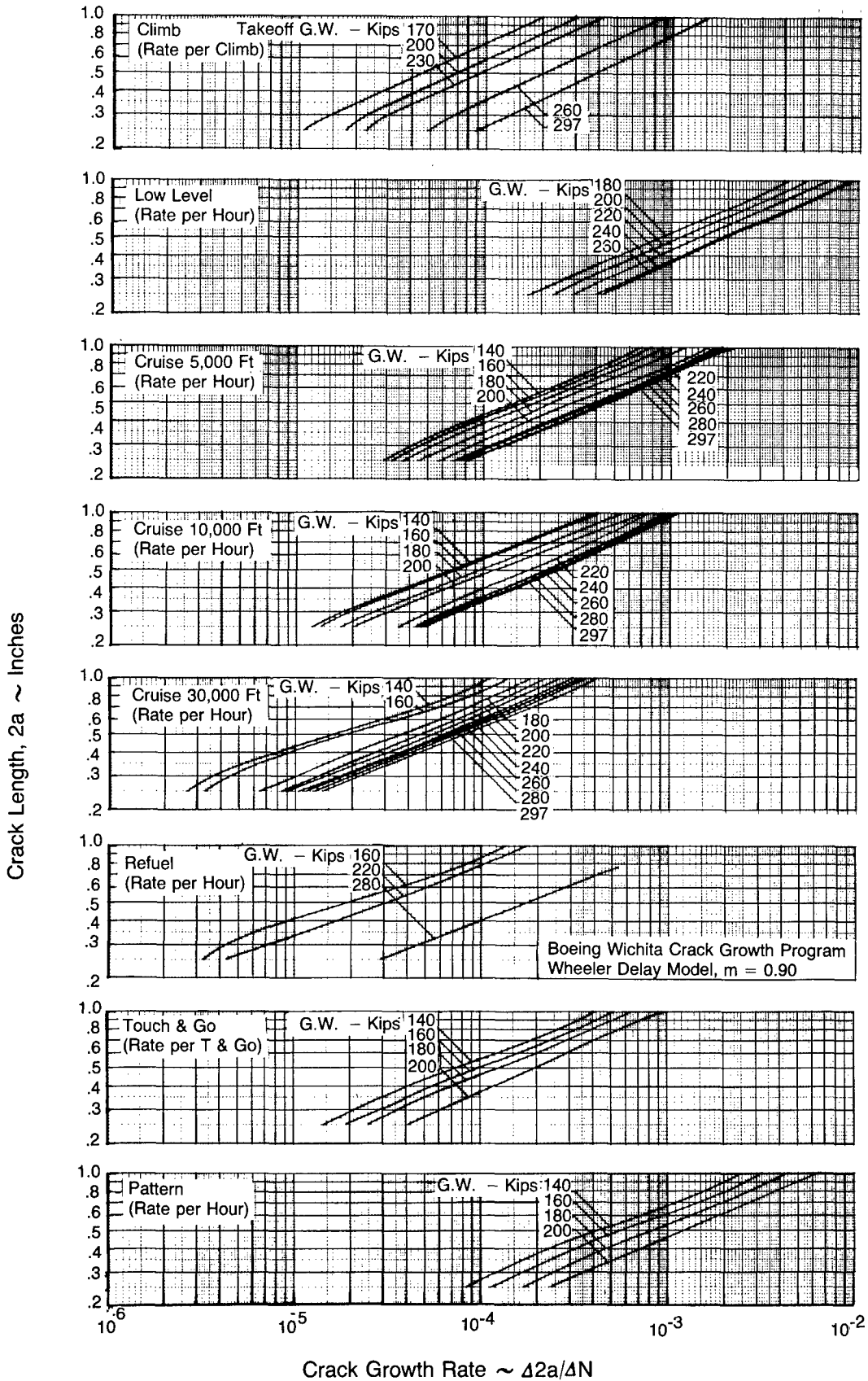


Figure 26. Analytical Crack Growth Rates, Wing



Crack Length, 2a ~ Inches

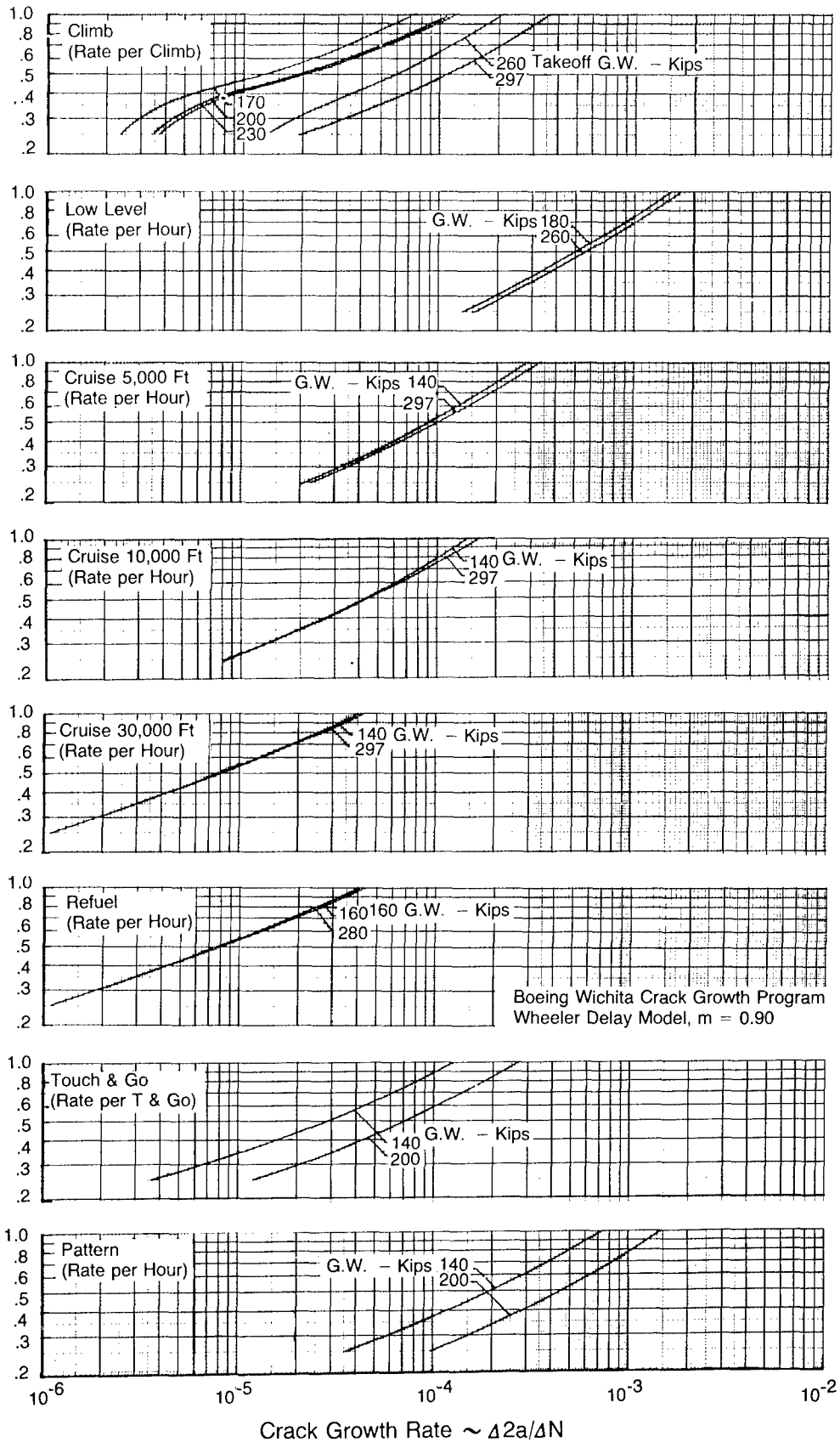


Figure 28. Analytical Crack Growth Rates, Fin

The straight line characteristic shown on logarithmic plots indicates that these data can be easily used in a tabular or equation form in a data format scheme that may be devised for a fleet tracking program. These data were used to develop a tracking analysis scheme which will be discussed in Section 3.

### 2.7.7 VERIFICATION TEST RESULTS

Experimental verification tests were run of four selected mission segment spectra to verify the analysis methods selected. Only four were selected for mission segment testing so that the majority of remaining tests could be conducted for verification of the mission spectra developed for the variability crack growth analyses. The four parametric flight conditions selected for testing were:

- Climb segment, takeoff 297 Kips, wing
- Climb segment, takeoff 170 Kips, wing
- Touch and go segment, 200 Kips, wing
- Climb segment, takeoff 297 Kips, fin

A schematic drawing of the stress spectrum for each of the four flight segments selected for verification testing is shown in Figure 29. The number of cycles applied of each stress level is indicated in the figure. The spectra for

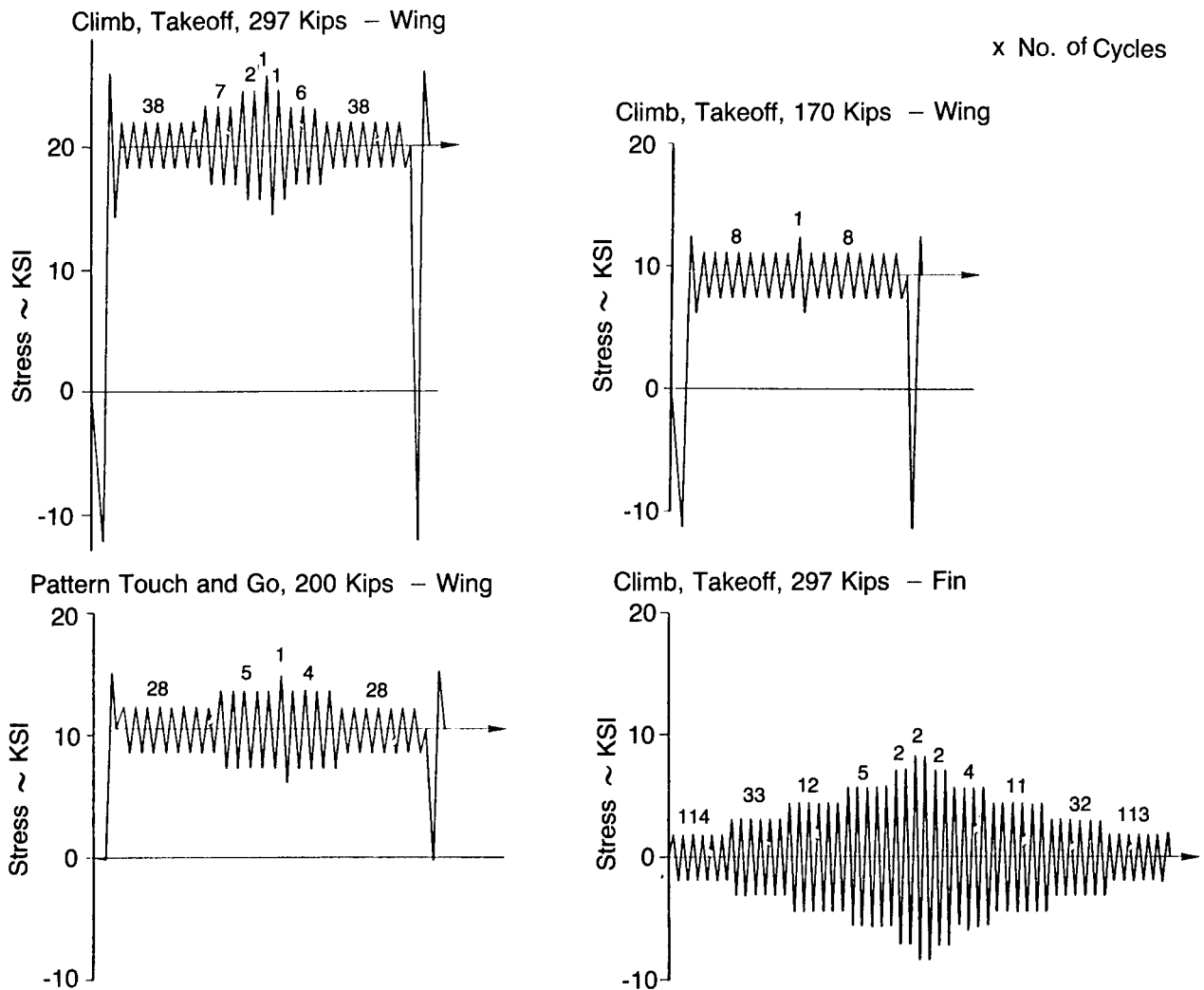


Figure 29. Verification Test Spectra for Mission Segments

the two climb segments for the wing indicate the variation in the magnitude of stresses and the number of cycles between the high and low takeoff gross weight conditions. This was the primary reason for the selection of these two spectra. The maximum stress experienced once per flight varies from 26.0 KSI for the high takeoff gross weight condition to 12.5 KSI for the low takeoff gross weight condition. The pattern with touch and go is more severe than the low gross weight climb condition as shown by higher stress levels and a greater number of stress cycles. The peak stress experienced during go-around was 15.0 KSI.

The fin segment spectrum was selected for test verification since the fin experiences a somewhat different spectrum than either the wing or body, i.e., the fin spectrum has a mean stress of zero ( $R = -1.0$ ) and there is no identifiable ground-air-ground cycle. The maximum stress experienced by the fin during the climb segment was about 9.5 KSI.

The results of the experimental verification testing of mission segments are shown in Figure 30. Shown in this figure is a comparison of test results and analytical crack growth predictions using the Wheeler Retardation Model with a shaping exponent,  $m$ , of 0.90. The results showed about a factor of ten between the high and low takeoff gross weight climb segments for the wing. The fin climb segment spectrum for the maximum takeoff gross weight was no more severe than the low takeoff gross weight condition on the wing. Figure 31 shows a comparison of the time to grow the crack from 0.25 to 0.35 inch as predicted by analysis and test. The results of the verification test indicated that mission segment analyses using the Wheeler Retardation Model with a shaping exponent,  $m$ , of 0.90 agreed well with test results.

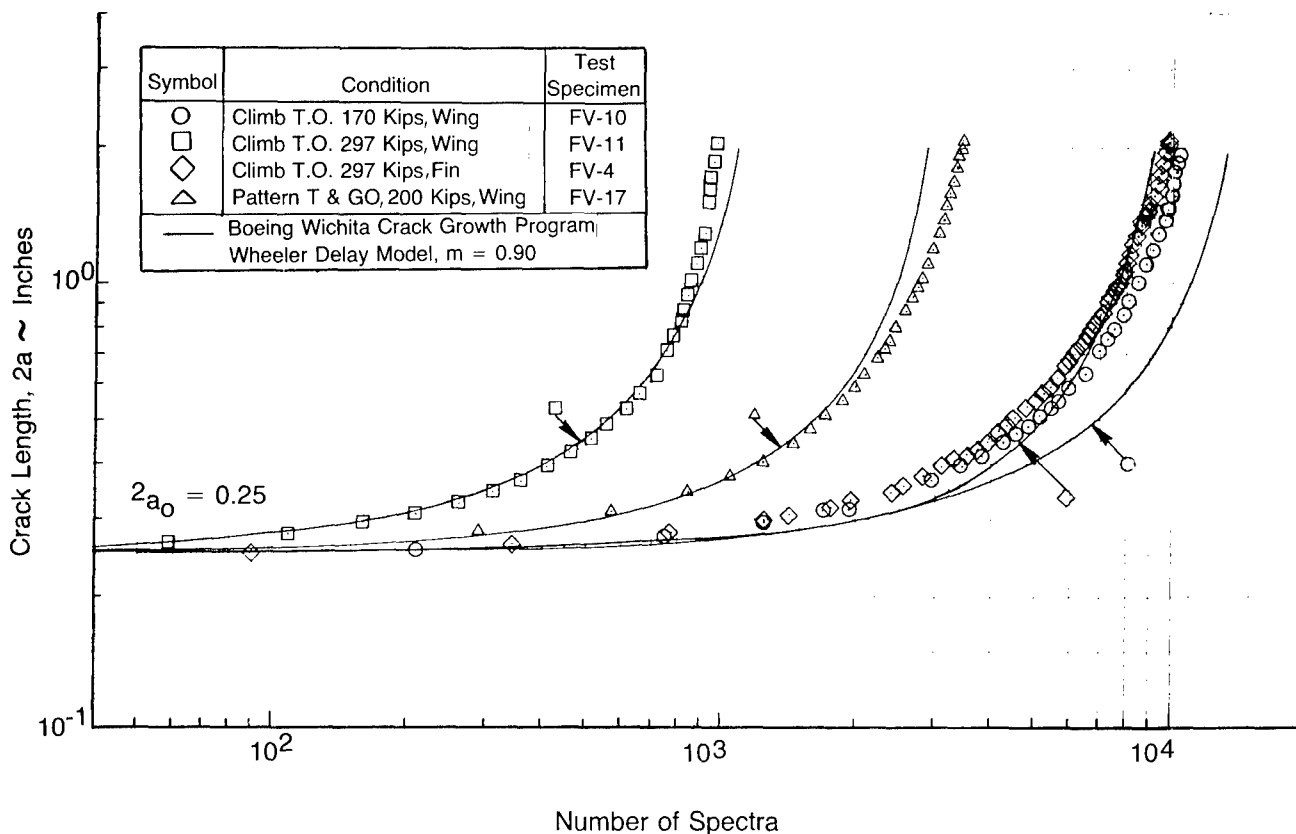


Figure 30. Verification Test Results For Mission Segment Spectra

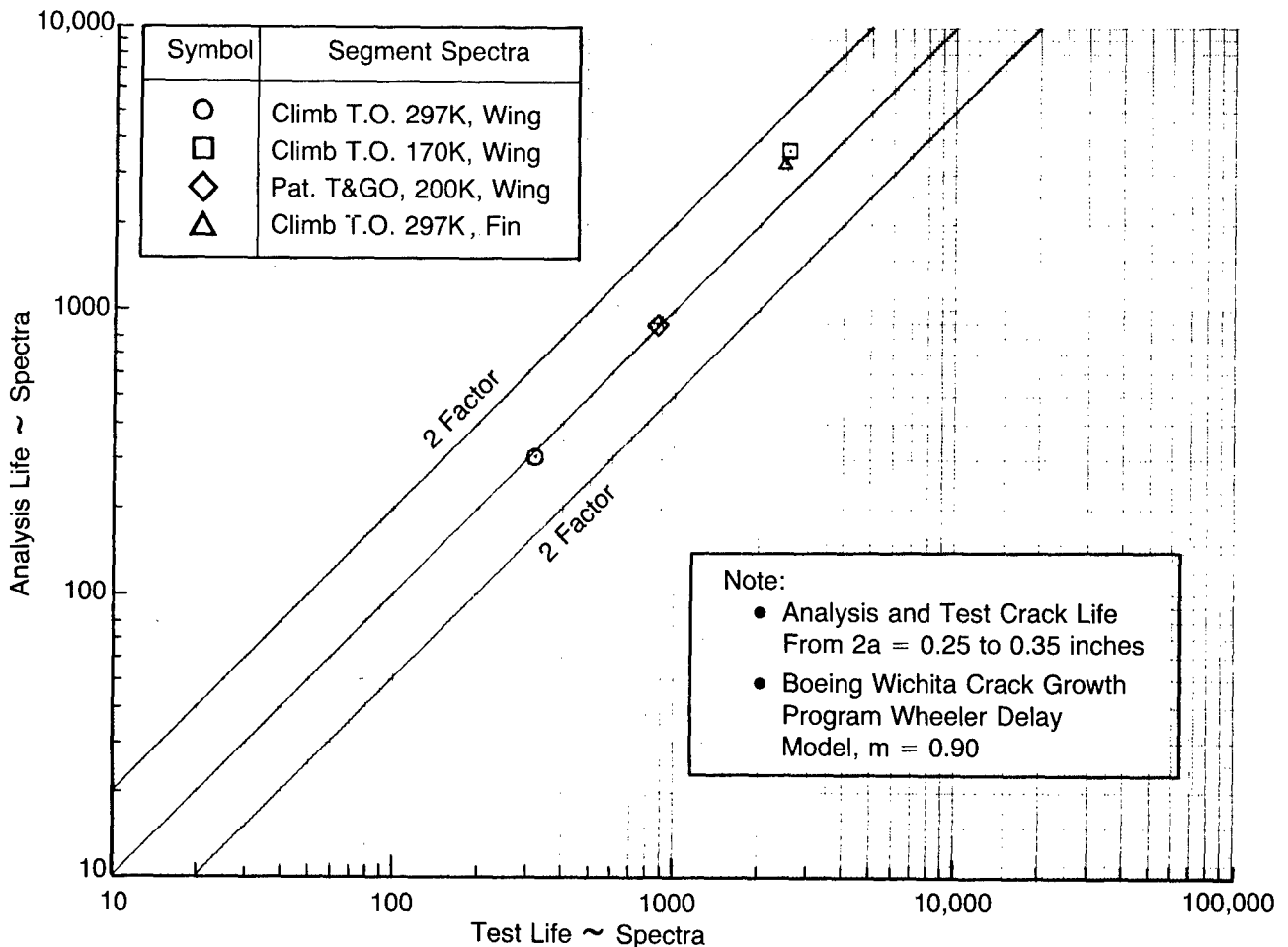


Figure 31. Analysis Life Versus Test Life, Mission Segment Spectra

## 2.7.8 PARAMETRIC STUDY RESULTS

During the parametric study, crack growth rates were determined for the wing, body and fin analysis locations. These rates were used to demonstrate the use of parametric crack growth in calculating mission crack growth based on actual usage. The mission segment stress spectra provided the data base needed to develop mission spectra used in the variability study.

The mission segment crack growth predictions showed that altitude and gross weight had a significant effect on crack growth rate for the wing and body locations. The fin location was primarily affected by altitude only but showed some variation in crack growth rate with gross weight for flaps extended low speed operations (pattern).

The mission segment verification tests showed that the selected analysis methods predicted test results well.

## 2.8 Variability Study

The usage parameters most influential on crack growth rate are expected to vary between individual aircraft within a particular fleet. The variability study was conducted to evaluate the effect on crack growth caused by the expected variations in these usage parameters.

Existing usage data for the baseline aircraft were used to define the different parametric flight segments that were analyzed during the parametric study. These flight segments formed the necessary matrix of flight segments to develop stress spectra for mission profiles representative of transport/bomber aircraft.

Several studies were conducted as part of the variability study to determine the effect of various individual mission segments and the variation in selected usage parameters on crack growth. The general approach used to determine the effect of various individual mission segments on crack growth was to delete from a mission spectrum a selected flight segment(s) that was considered to contribute significantly to crack growth. As an example, the low level segment of a bomber mission was deleted. A comparison of the crack growth that occurs in this mission with that of the baseline mission indicated the effects of the low level segment. This process was repeated for other flight segments for a matrix of different flight profiles for several takeoff gross weight conditions.

For specific types of flight segments (cruise, low level, pattern, etc.), variations in flight duration, gross weight, altitude, airspeed and the number of touch and go's were evaluated for several takeoff gross weight conditions to determine the influence on crack growth. The selection of a mission matrix, development of stress spectra, crack growth analyses and verification test results are presented in the following sections.

### 2.8.1 SELECTED MISSION PROFILES

The mission profiles selected for the variability study were defined from existing C/KC-135 usage data and based on typical flight profiles that might be flown if the baseline aircraft were a bomber. The variable missions matrix selected for study consisted of missions of various types defined for three different takeoff gross weights as shown in Figure 32. This matrix includes a significant variation in takeoff gross weight, e.g., from a maximum takeoff gross weight of 297 kips to a low takeoff gross weight of 170 kips. These missions include mission segments considered to be most influential on crack growth such as refuel, low level, touch and go and pattern flying. Mission flight lengths varied from about six hours for the high takeoff gross weight missions to about three hours for the low takeoff gross weight missions.

Mission identification numbers were assigned to each of the missions shown in Figure 32 with a brief description of each directly below the profile sketches. All reference to mission spectra, crack growth predictions or test results pertaining to the mission matrix will be by mission identification number.

Studies to investigate the effects of flight duration, gross weight, altitude, number of touch and go's, etc., were accomplished by varying mission content as required. These studies will be discussed in Section 2.8.4.

### 2.8.2 MISSION STRESS SPECTRA

Mission stress spectra for the variable missions shown in Figure 32 were developed from the stress exceedance data generated for the parametric flight segments. These data were all generated for one-hour flight durations except climb and touch and go segments which included the appropriate time increments. Since the parametric flight segments were defined for 20-kip increments of gross weight (Table 3) each mission was segmented into 20-kip bands such that the average gross weight of each segment could be identified as one of the parametric conditions. The stress exceedance data for each mission segment were factored to account for the amount of flight time to burn the amount of fuel associated with each band, i.e., the time associated with each segment is the time to burn 20 kips or a fraction thereof. An illustration of this is shown in Figure 33. This analysis method eliminated the need to interpolate between parametric flight segments.

For each takeoff gross weight condition in the mission matrix, Figure 32, the parametric stress exceedance data needed to define each mission segment were input into the sequence generator program. The user then specifies the flight segments and sequence and the program assembles the total mission spectrum with the appropriate segment time included. A discussion of the computer programs and the analysis methods used to generate the mission spectra are presented in Section 2.2

The stress spectra derived for each mission identified in Figure 32 for the wing, body and fin analysis locations are presented in tabular form in Appendix B.

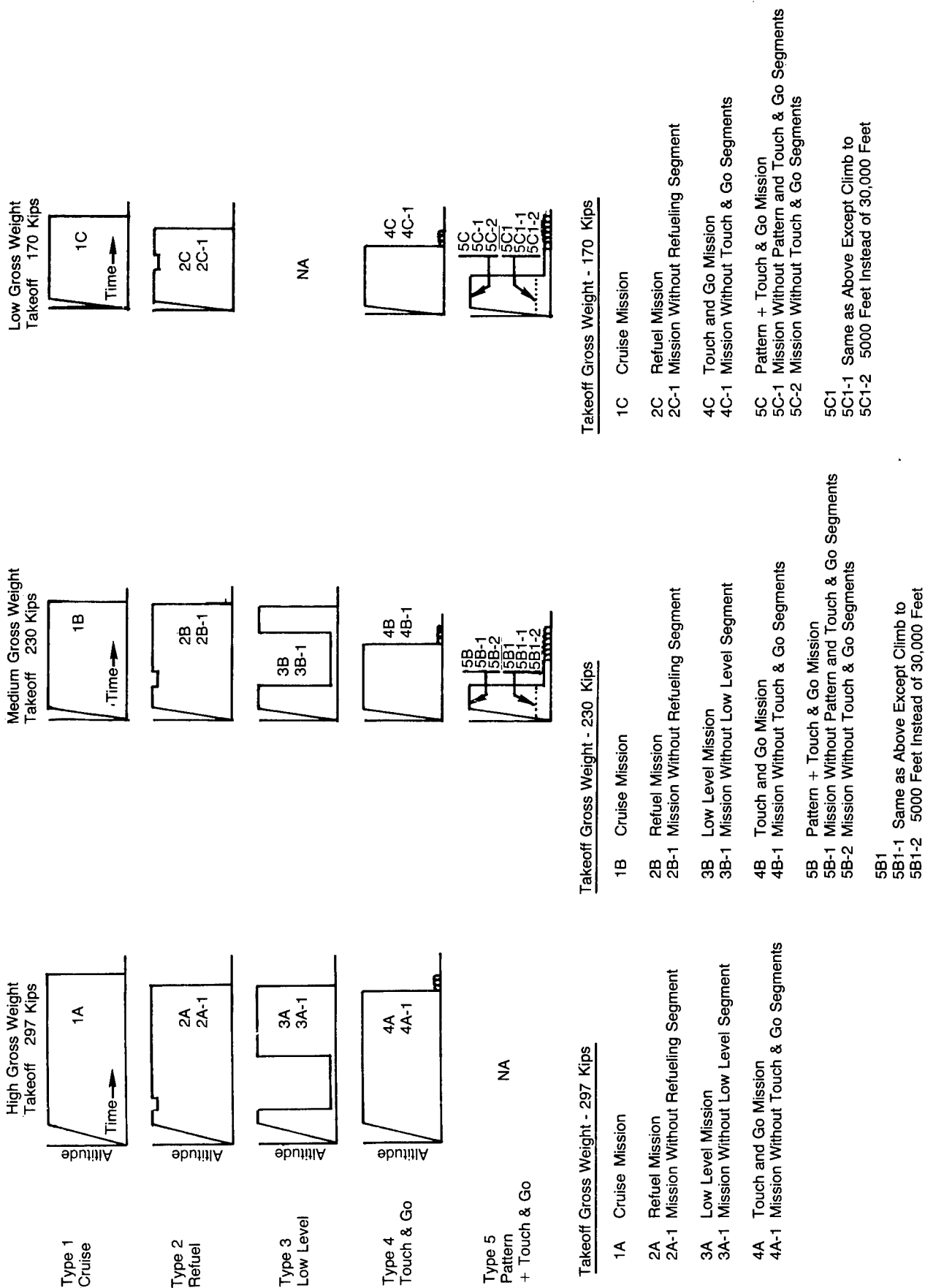


Figure 32. Variable Missions Matrix

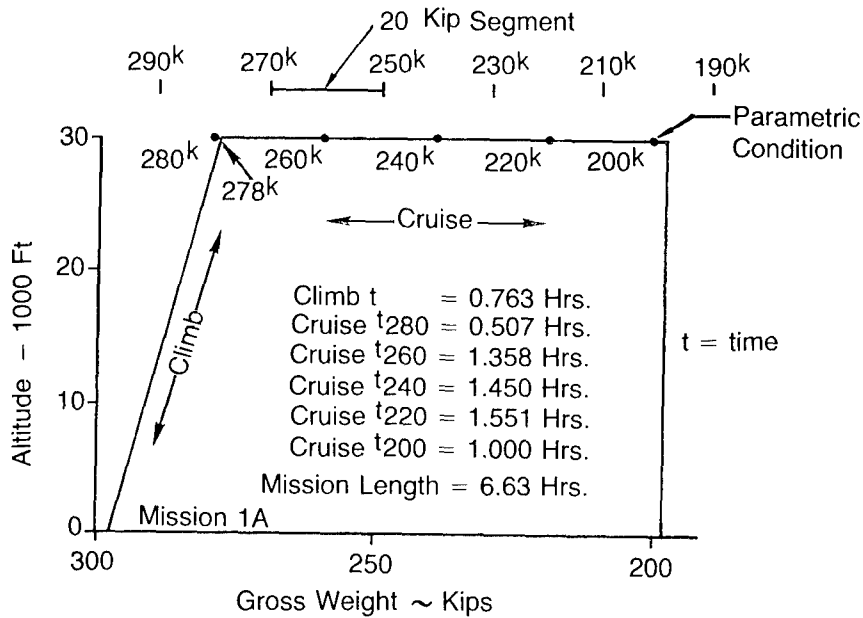


Figure 33. Mission Spectrum Definition Using Parametric Flight Segments

### 2.8.3 MISSION CRACK GROWTH PREDICTIONS

Crack growth analyses were performed using the mission spectra developed for the mission profiles shown in Figure 32 for the wing, body and fin structural locations. These analyses were performed using the Wheeler Retardation Model with a shaping exponent,  $m$ , of 0.90. Plots of the predicted crack growth for the variable missions are presented in Appendix B.

To examine the influence of various individual mission segments on crack growth, crack growth analyses were made with the mission segment under investigation deleted from the total mission spectrum. A comparison of crack growth before and after deletion of the segment shows the effects of that segment on crack growth. Since the crack growth analyses were too numerous to compare crack growth curves directly, a comparison was made by comparing the number of flight or flight hours to grow a crack from 0.25 to 0.35 inch. Table 5 shows a tabulation of these data for the wing, body and fin analysis locations. Refer to Figure 32 for a description of the variable missions.

For added visibility of the effects of various mission segments on crack growth rate, the data in Table 5 was plotted in bar chart form as illustrated in Figure 34. This figure shows the results of the crack growth analyses for the medium takeoff gross weight missions for the wing analysis location. The number of flights of each mission required to grow a crack from 0.25 to 0.35 inch is shown in the left-hand part of this figure; the mission profiles are shown to the right. The dark bars show the crack life for each complete mission spectrum; the cross hatched bars represent the crack life for the mission spectrum without the particular flight segment under investigation. The open bars identified as 5B-2 and 5B1-2 represent the life of missions 5B and 5B1 without the touch and go's but do include the low altitude pattern prior to the touch and go's. Comparing the dark bars to the cross hatched or open bars for a given mission shows the impact of refueling, low level, touch and go and pattern operations on crack growth.

The results of the mission crack growth predictions for the three takeoff gross weight conditions for the wing, body and fin analysis locations are shown in Figures 35, 36 and 37, respectively. These figures clearly show the significant effects of takeoff gross weight, refueling and low level operations. Table 6 shows a comparison of relative life values which indicate the effect of some of the individual flight segments on crack growth as predicted by the variable mission crack growth analyses results shown in Figures 35, 36 and 37. This figure shows that the low takeoff gross weight condition has 9 times the crack life of the high takeoff gross weight condition. The effects of refuel, low level, touch and go and pattern flight segments are also shown based on the intermediate takeoff gross weight missions.

TABLE 5  
ANALYTICAL CRACK GROWTH WITH AND WITHOUT CRITICAL FLIGHT SEGMENTS  
(See Figure 32 For Mission Description)

Variable Mission	Takeoff G.W. Kips	Crack Life From 2a = 0.25 to 0.35 In.					
		Wing		Body		Fin	
		Flights	Flight Hours	Flights	Flight Hours	Flights	Flight Hours
1A	297	238	1,578	543	3,600	2,352	15,594
2A	297	138	807	500	2,925	2,383	13,941
2A-1	297	221	1,182	553	2,959	2,396	12,818
3A	297	42	244	88	512	221	1,286
3A-1	297	277	1,058	692	2,643	2,454	9,374
4A	297	183	1,102	358	2,155	1,133	6,821
4A-1	297	242	1,362	571	3,215	2,389	13,450
1B	230	728	3,196	1,588	6,971	9,980	43,812
2B	230	436	1,875	1,392	5,986	9,998	42,991
2B-1	230	691	2,626	1,470	5,586	10,404	39,535
3B	230	123	523	239	1,016	259	1,101
3B-1	230	885	1,991	2,388	5,373	12,415	27,934
4B	230	321	1,053	960	3,149	1,751	5,743
4B-1	230	787	2,274	1,887	5,453	11,817	34,151
5B	230	102	309	265	803	464	1,406
5B-1	230	918	1,148	2,548	3,185	14,467	18,084
5B-2	230	173	389	366	824	667	1,501
5B1	230	92	277	184	554	402	1,210
5B1-1	230	387	476	905	1,113	2,268	2,790
5B1-2	230	141	314	246	549	547	1,220
1C	170	2,177	7,336	2,846	9,591	13,443	45,303
2C	170	2,260	6,803	3,372	10,150	13,800	41,538
2C-1	170	2,369	5,946	3,598	9,031	14,241	35,745
4C	170	762	2,210	1,529	4,434	3,897	11,301
4C-1	170	2,361	5,926	3,677	9,229	14,257	35,785
5C	170	289	951	524	1,724	1,236	4,066
5C-1	170	2,854	4,310	4,161	6,283	17,019	25,699
5C-2	170	671	1,684	886	2,224	1,693	4,249
5C1	170	253	805	400	1,272	827	2,630
5C1-1	170	1,243	1,740	1,693	2,370	2,303	3,224
5C1-2	170	500	1,200	627	1,505	1,010	2,424

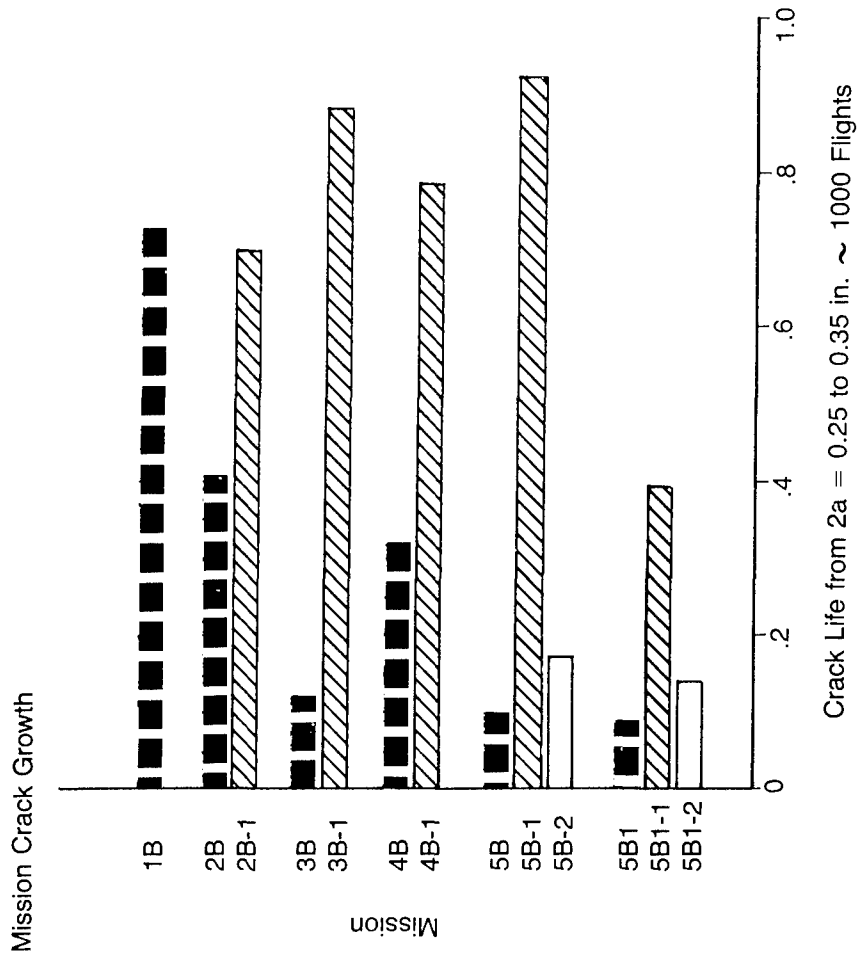
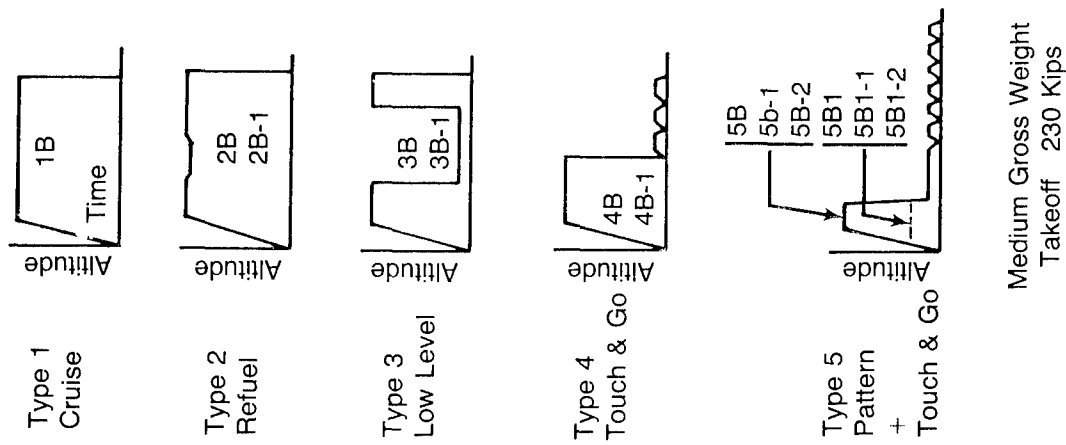


Figure 34. Variable Mission Analysis Results, Medium Takeoff Gross Weight, Wing

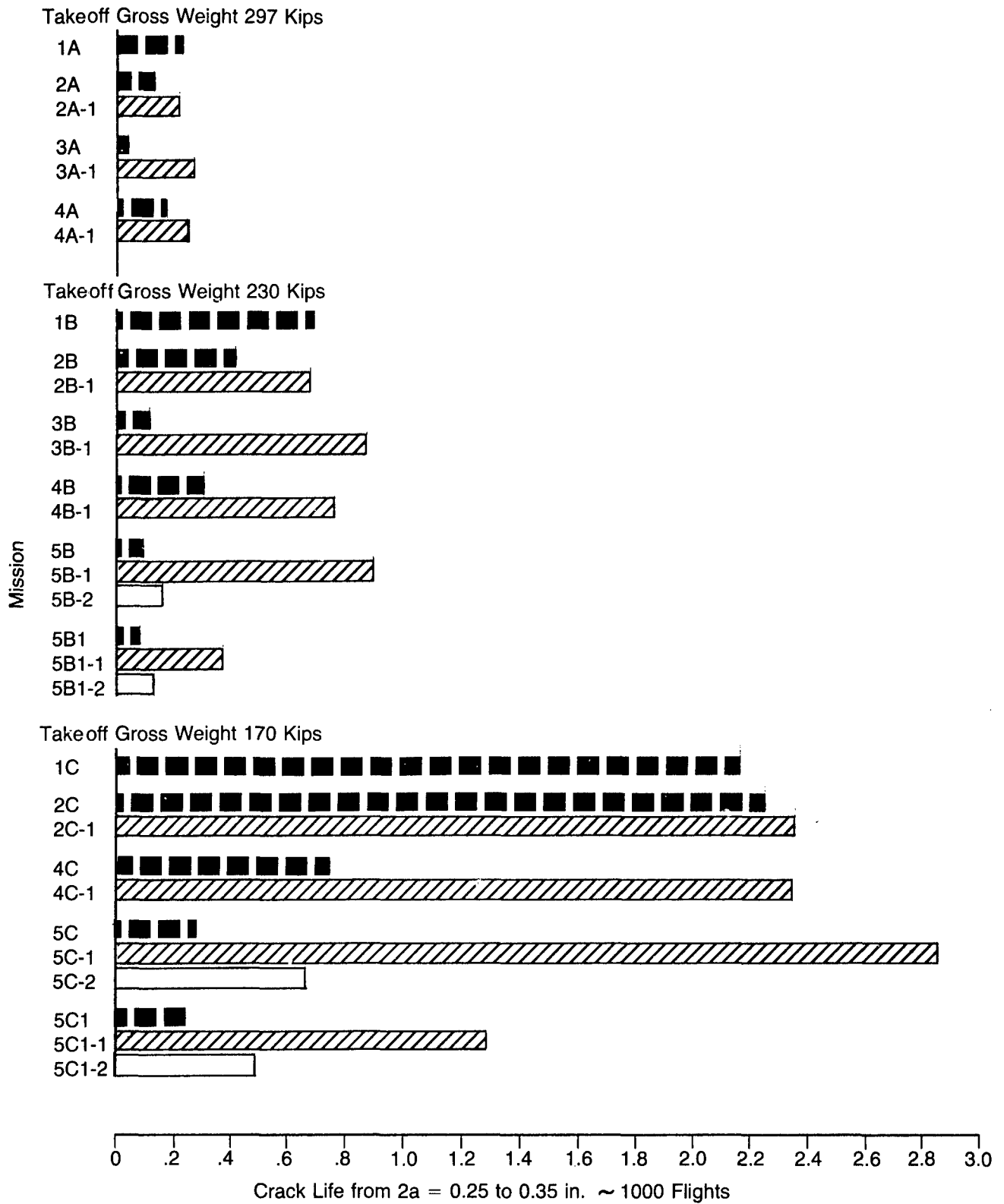


Figure 35. Variable Mission Crack Growth, Wing

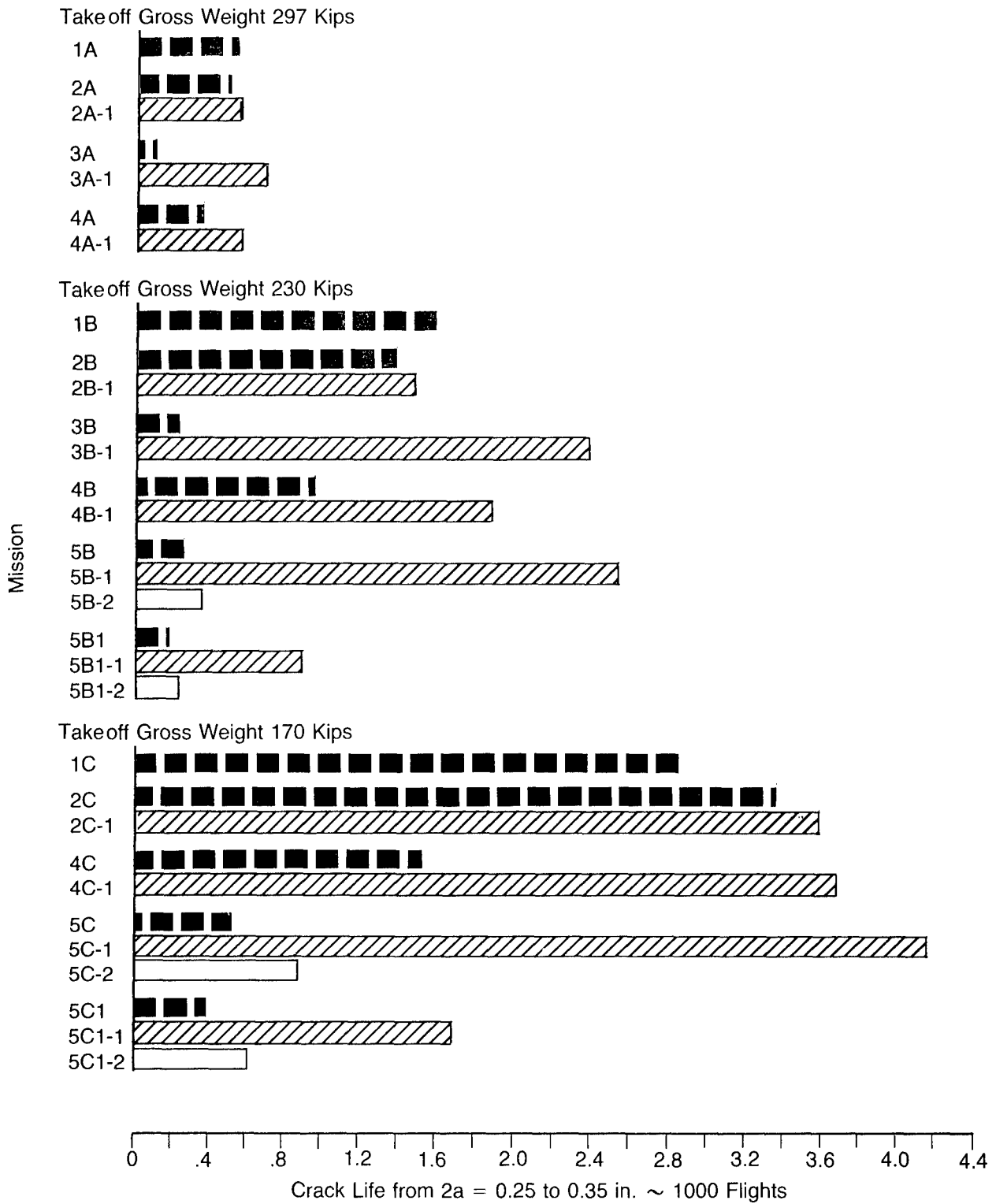
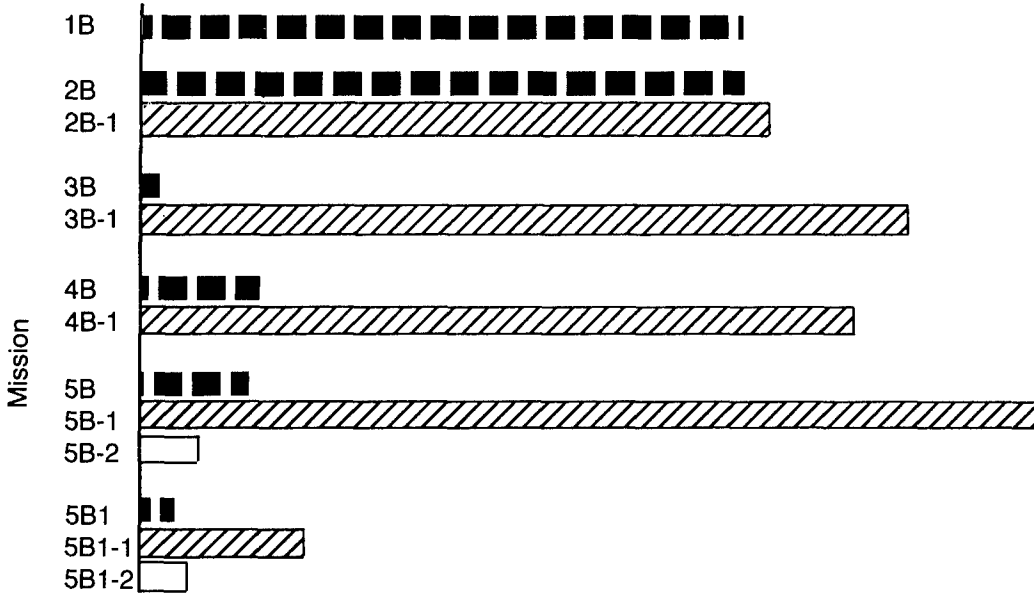


Figure 36. Variable Mission Crack Growth, Body

Take off Gross Weight 297 Kips



Takeoff Gross Weight 230 Kips



Takeoff Gross Weight 170 Kips

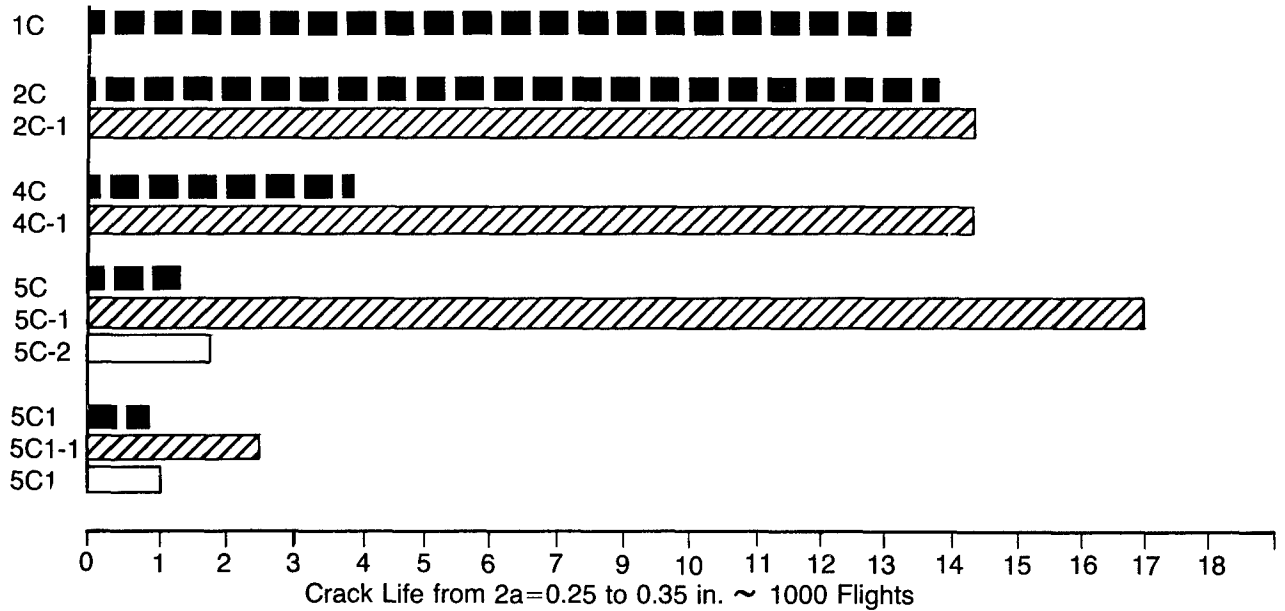


Figure 37. Variable Mission Crack Growth, Fin

TABLE 6  
EFFECTS OF SIGNIFICANT FLIGHT SEGMENTS ON CRACK GROWTH

Effects of Flight Condition	Missions Ratioed	Relative Life*		
		Wing	Body	Fin
Takeoff Gross Weight	1C/1A	9.1	5.2	5.7
Refuel	2B/1B	.60	.88	1.0
Low Level	3B/1B	.17	.15	.03
Touch & Go	4B/1B	.44	.60	.18
Pattern+ Touch & Go	5B/1B	.14	.17	.05

\*Based on Flights

#### 2.8.4 EFFECT OF MISSION PARAMETER VARIATIONS ON CRACK GROWTH

##### Effects of Altitude, Gross Weight and Duration

Analyses were performed to provide greater visibility of the variation in crack life with altitude, gross weight and flight duration. Figures 38, 39 and 40 show the results of these analyses for takeoff gross weights of 297 and 230 kips for the wing and 297 kips for the fin. Crack life in flight hours and number of flights from 2a equal to 0.25 to 0.35 inch are shown in the upper and lower charts, respectively. The spectra for these analyses were developed by inputting the parametric stress exceedance data for each climb condition, which was comprised of six segments so that a climb segment could be defined to different altitudes, and the stress data for the appropriate altitudes and gross weights into the sequence generator program. The flight duration for each parametric flight segment was also input. A stress spectrum was then developed for a flight consisting of a takeoff condition, climb to the specified altitude and cruise for a specified time. The gross weight variation with time is also shown.

The crack growth analyses were conducted by making several runs for each altitude by deleting gross weight segments from the spectrum as illustrated in Figure 41. Each curve of Figures 38, 39 and 40 represents a mission consisting of a takeoff and climb to the altitude noted followed by a cruise of different durations. These curves show significant variations in crack life with altitude and gross weight. The lower chart shows that crack life in terms of the number of flights is reduced as the duration of the cruise segment is increased. Conversely, the upper chart shows crack life in terms of flight hours increases as the duration of the cruise segment increases. These figures clearly show that the majority of crack growth occurs during the early portions of the flight where stresses are the highest. Also shown is the difference in life comparisons based on flight hours and flights since the increase in crack growth rate per flight diminishes with flight duration, which, while predicting less flights produces more flight hours.

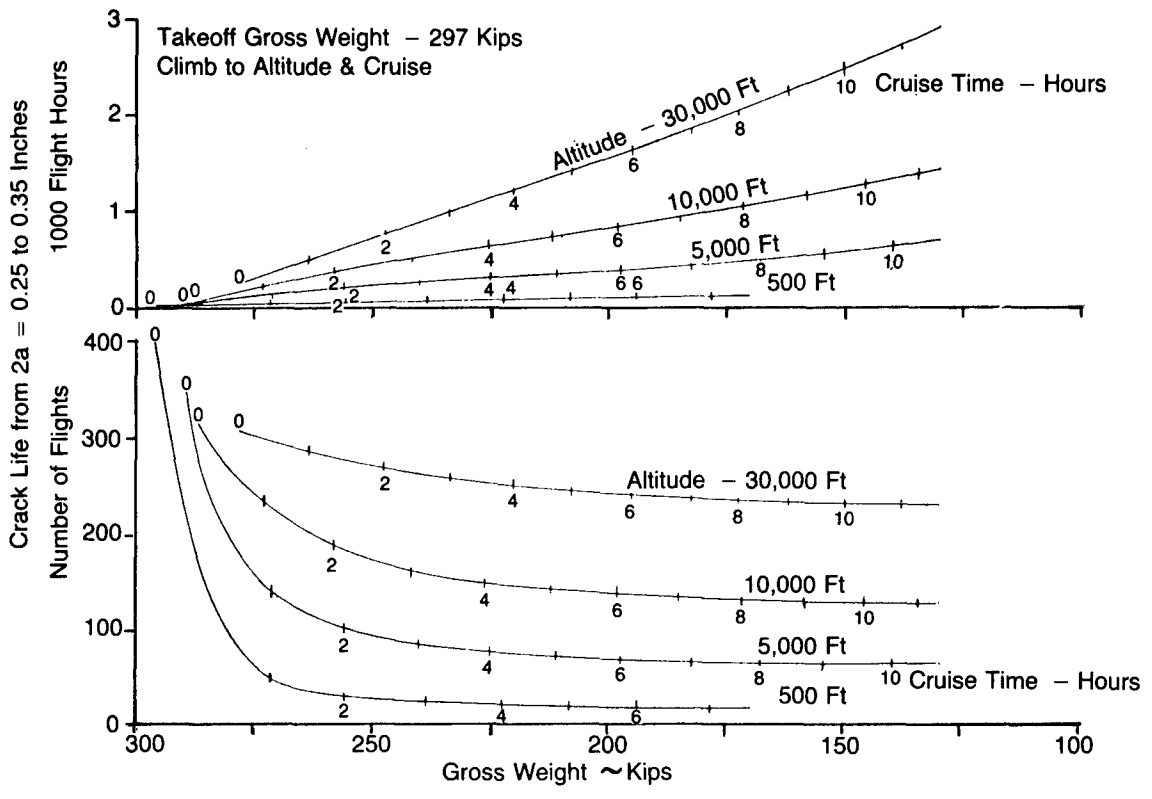


Figure 38. Variation in Crack Life with Altitude, Gross Weight and Duration, Wing, 297 Kip Takeoff

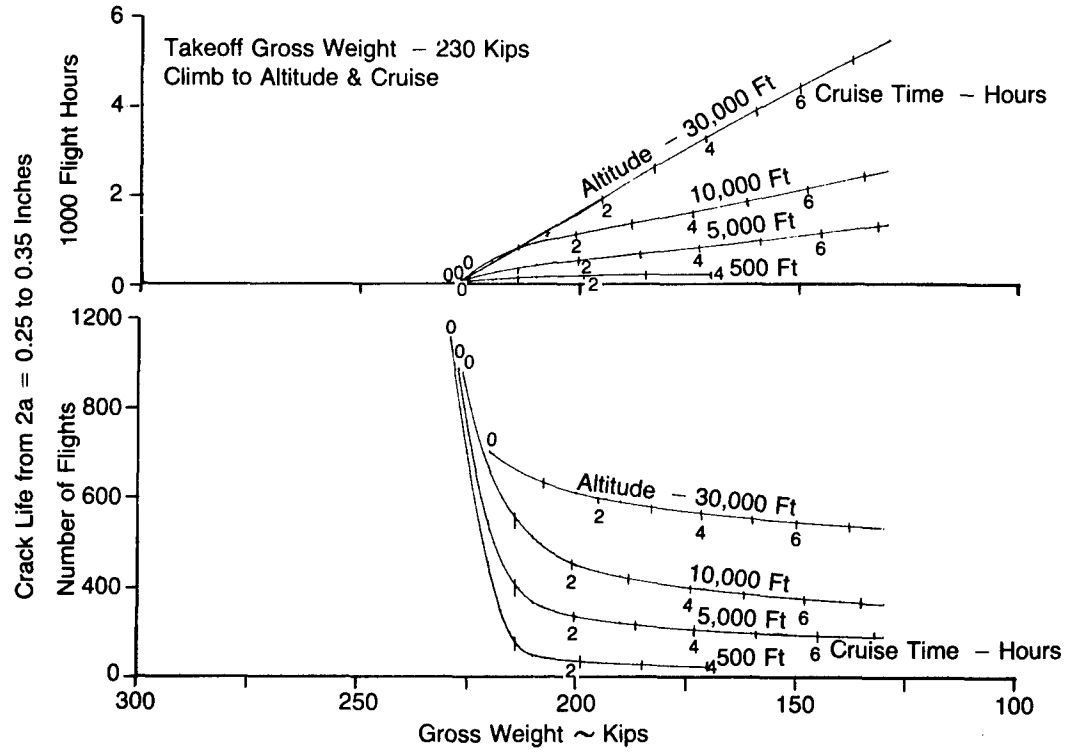


Figure 39. Variation in Crack Life with Altitude, Gross Weight and Duration, Wing, 230 Kip Takeoff

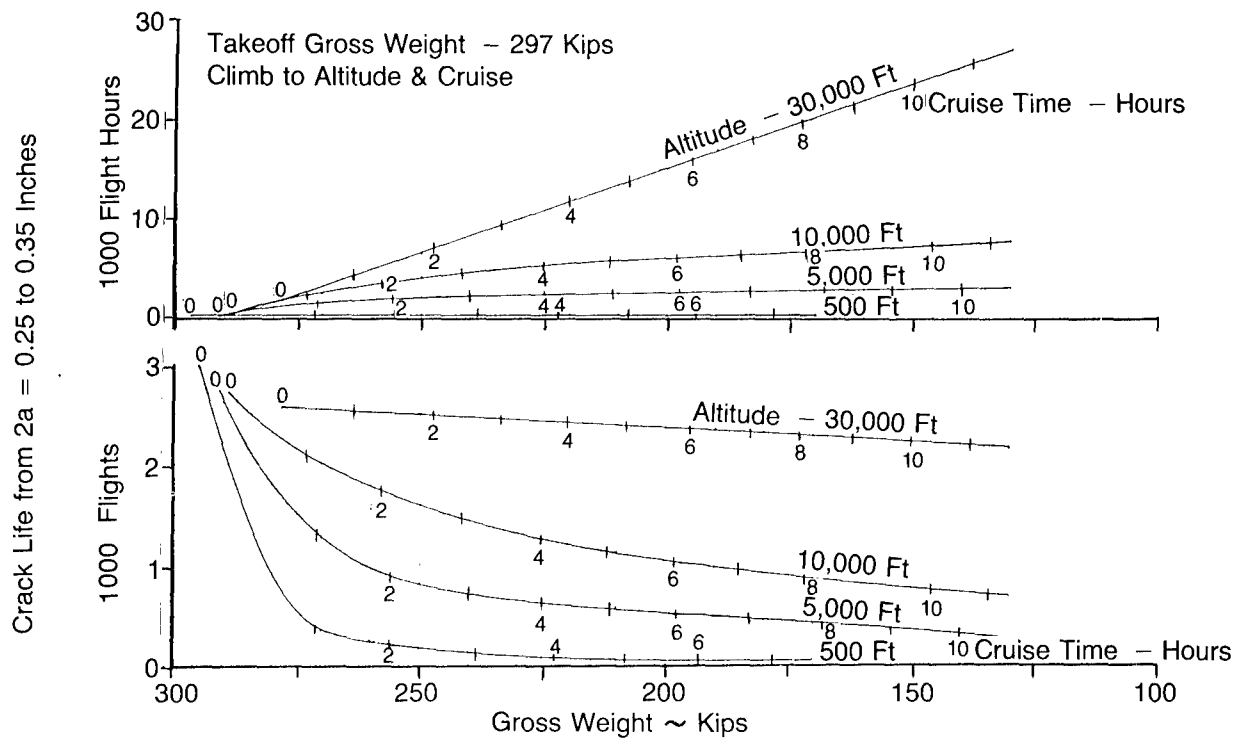


Figure 40. Variation in Crack Life with Altitude, Gross Weight and Duration, Fin, 297 Kip Takeoff

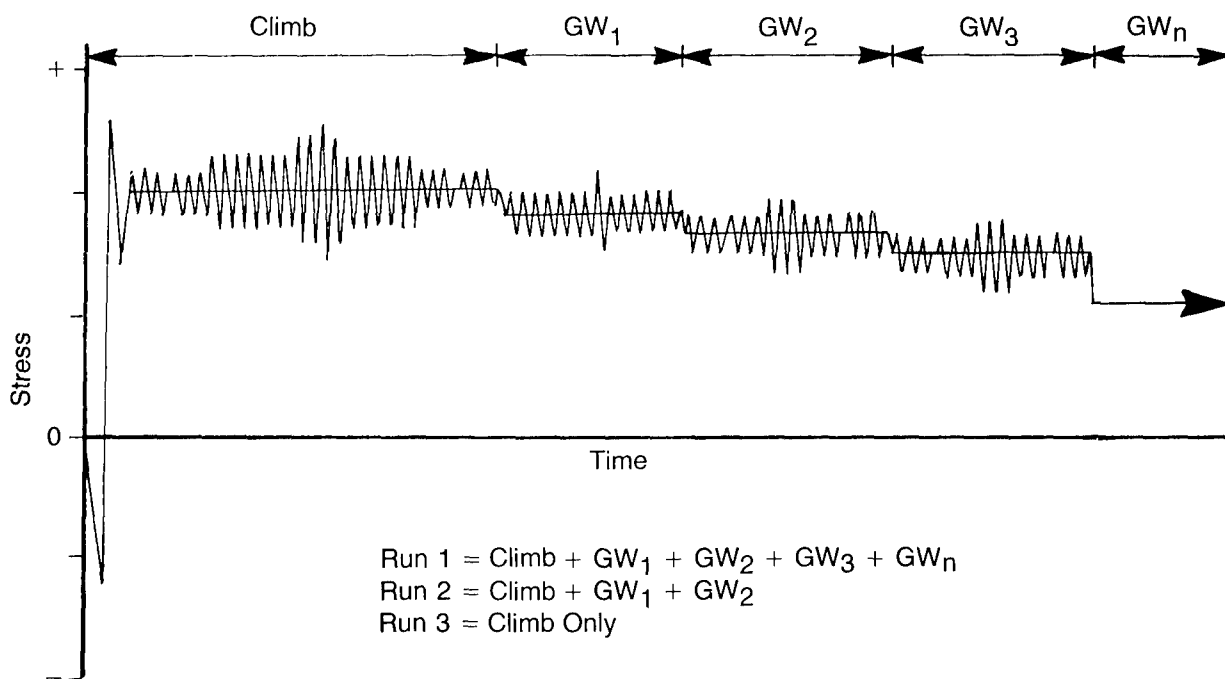


Figure 41. Spectrum Derivation, Variation in Crack Life with Altitude, Gross Weight and Duration

Effects of Low Level Entry Gross Weight

The variation in crack life with low level entry gross weight is shown in Figure 42 for a 297-kip takeoff gross weight. This figure shows the variation in crack life following takeoff and climb to 30,000 feet, then cruising at 30,000 feet for different flight durations prior to entering low level flight. The crack growth analyses were made in the same manner as for the previous figures. Again, a significant variation in crack life is seen with low level entry gross weight.

Effects of Touch and Go's

Figure 43 shows the variation in crack life with the number of touch and go flight segments. This figure shows the results for a 230- and 170-kip takeoff gross weight. Each curve represents a climb to 5,000 feet with a comparison made between a flight which cruises at 5,000 feet for one hour prior to the touch and go operations and a flight which descends immediately for touch and go operations. These curves show a significant variation in crack life with the number of touch and go's. A 5,000-foot cruise segment prior to touch and go operations affected crack life significantly; however, the addition of the cruise segment prior to the touch and go landings appeared to have a retarding effect on subsequent crack growth.

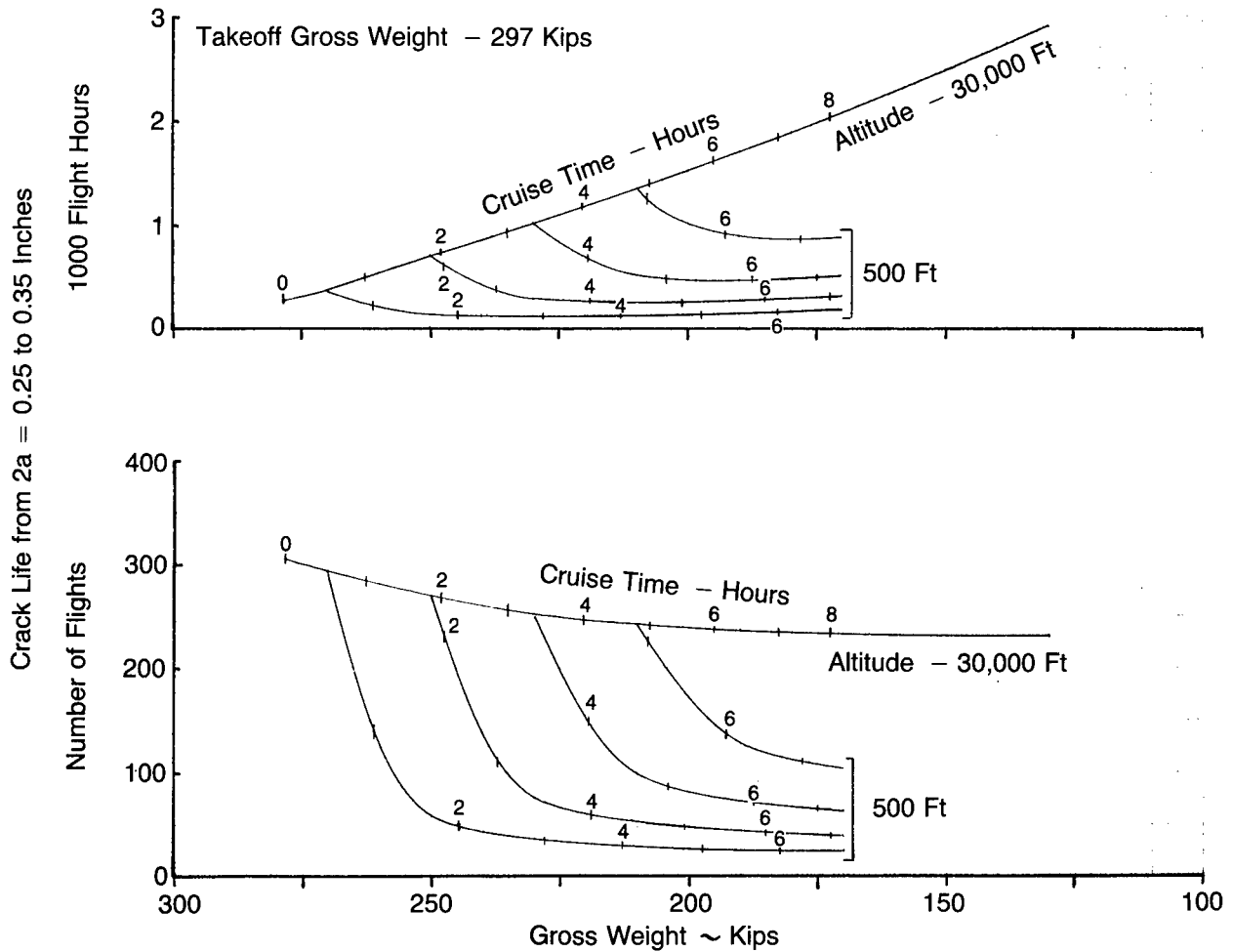


Figure 42. Variation in Crack Life with Low Level Entry Gross Weight, Wing, 297 Kip Takeoff

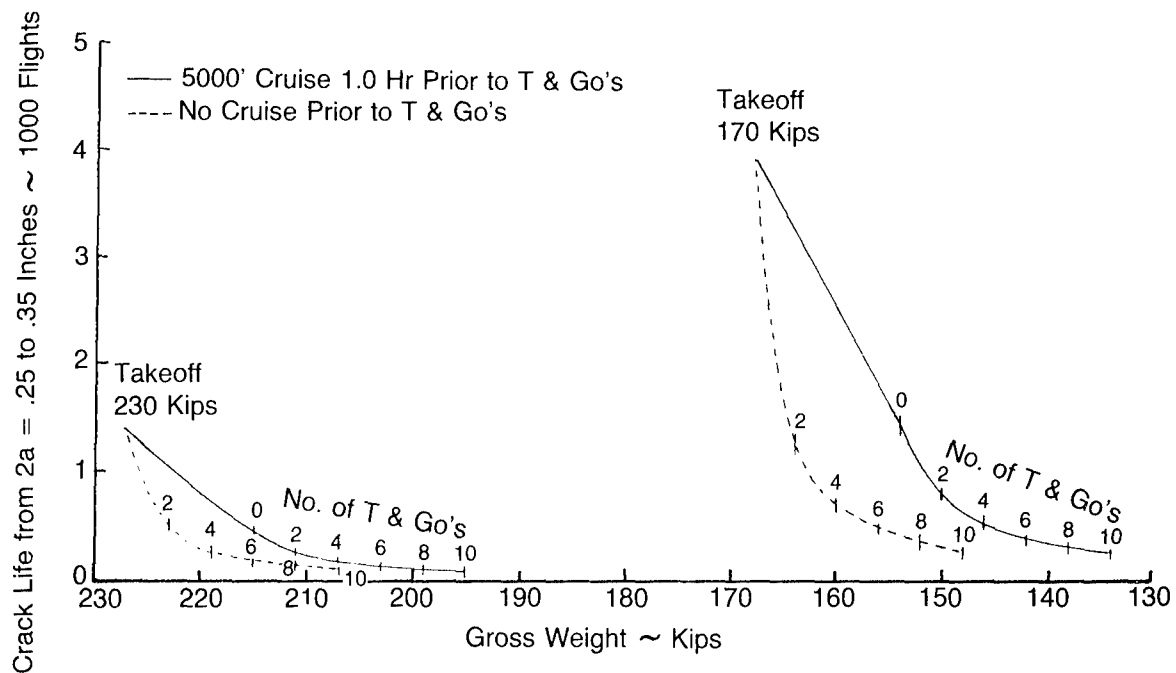


Figure 43. Variation in Crack Life with Number of Touch and Go's, Wing, 230 and 170 Kip Takeoff

Effects of Speed

A study to evaluate the effect of speed variations on crack growth was conducted for the wing analysis location. Low level missions 3A and 3B, which were high and medium takeoff gross weight missions, respectively, were used to determine the effect of increasing the speed during the low level portion from 280 to 350 KEAS. Two cases were examined; first, the speed was increased with the flight duration unchanged; and, second, the speed was increased keeping the distance flown the same. The results, Table 7, showed that the higher speed produces more crack growth for both the same duration and same distance; however, the effect of speed was considerably greater for the same duration condition. The influence of the higher speed in reducing crack life is greater at the lower than at the higher takeoff gross weights.

TABLE 7  
VARIATION IN CRACK LIFE WITH AIRSPEED

Speed	Life at 350 KEAS/ Life at 280 KEAS			
	Same Duration		Same Distance	
	3A	3B	3A	3B
280	1.0	1.0	1.0	1.0
350	0.77	0.70	0.97	0.83

Results

The results of crack growth predictions for the variable missions and mission parameter variations were used to define the effect on crack growth caused by the expected variation in selected usage parameters. A summary of these results is shown in Table 8 based on life in flight hours and in Table 9 based on life in flights. Each table shows the ratio of the parameter variation life to baseline life. Mission 1B (Figure 32) was selected as the baseline for these comparisons. Also shown is a ratio of the parameter variation life/baseline life to depict the range of variation in crack life for the particular parameters investigated.

TABLE 8  
MISSION PARAMETER VARIATIONS, USAGE  
VARIATION/BASELINE, LIFE IN FLIGHT HOURS

Description	Usage Variation/Baseline <sup>1</sup>		
	Wing	Body	Fin
Severe, Mission 3A, HI T.O. W/LL, 280 KTS Benign, Mission 1C, LO T.O.+Cruise	.076 ] 2.300 ] 30.3	.073 ] 1.38 ] 18.8	.029 ] 1.03 ] 35.7
Gross Wt., HI, Mission 1A, HI T.O.+Cruise <sup>2</sup> Gross Wt.,LO, Mission 1C, LO T.O.+Cruise	.30 ] 2.30 ] 7.7	.36 ] 1.38 ] 3.8	.20 ] 1.03 ] 5.2
Airspeed, Mission 3A, HI T.O., LL 280 KTS Airspeed, Mission 3A, HI T.O., LL 350 KTS Airspeed, Mission 3B, Med. T.O., LL 280 KTS Airspeed, Mission 3B, Med. T.O., LL 350 KTS	.076 ] .055 ] 1.38 .16 ] .11 ] 1.45	.073 - .15 -	.029 - .025 -
Altitude, Mission 1A, HI T.O., 30000' CR Altitude, Mission 3A, HI T.O., 500' LL Altitude, Mission 1B, Med. T.O., 30000' CR Altitude, Mission 3B, Med. T.O., 500' LL	.49 ] .076 ] 6.4 1.0 ] .16 ] 6.3	.52 ] .073 ] 7.1 1.0 ] .15 ] 6.7	.36 ] .029 ] 12.4 1.0 ] .025 ] 40.0
Duration, HI T.O., Cruise 1 Hr. 30000' Duration, HI T.O., Cruise 12 Hr. 30000' Duration, Med. T.O., Cruise 1 Hr. 30000' Duration, Med. T.O., Cruise 8 Hr. 30000' Duration, HI T.O., Cruise 1 Hr. 500' Duration, HI T.O., Cruise 8 Hr. 500' Duration, Med. T.O., Cruise 1 Hr. 500' Duration, Med. T.O., Cruise 4 Hr. 500'	.15 ] .91 ] 6.1 .36 ] 1.72 ] 4.8 .014 ] .041 ] 2.9 .035 ] .065 ] 1.9	- - - - - - - -	.101 ] .62 ] 6.1 - - .009 ] .010 ] 1.1 - -
Pattern, Med. T.O., Cruise+1 T&GO Pattern, Med. T.O., Cruise+4 T&GO Pattern, Med. T.O., Cruise+10 T&GO	.16 ] .11 ] .57 .091 ]	- - -	- - -

<sup>2</sup> Flight Time of 1A Reduced to Agree with 1C

<sup>1</sup> Baseline, Mission 1B, Med. T.O.+Cruise, Life from 0.25 to 0.35 In.  
(Ratio Based on Flight Hrs.)

{ Wing - 3,196 Hrs.  
  Body - 6,971 Hrs.  
  Fin - 43,812 Hrs.

TABLE 9  
MISSION PARAMETER VARIATIONS, USAGE  
VARIATION/BASELINE, LIFE IN FLIGHTS

Description	Usage Variation/Baseline <span style="font-size: 0.8em;">▶</span> 1		
	Wing	Body	Fin
Severe, Mission 3A, HI T.O. W/LL, 280 KTS Benign, Mission 1C, LO T.O.+Cruise	.058 ] 51.6 2.99 ]	.056 ] 32.0 1.79 ]	.022 ] 61.2 1.35 ]
Gross Wt., HI, Mission 1A, HI T.O.+Cruise <span style="font-size: 0.8em;">▶</span> 2 Gross Wt., LO, Mission 1C, LO T.O.+Cruise	.37 ] 8.1 2.99 ]	.45 ] 4.0 1.79 ]	.25 ] 5.4 1.35 ]
Airspeed, Mission 3A, HI T.O., LL 280 KTS Airspeed, Mission 3A, HI T.O., LL 350 KTS Airspeed, Mission 3B, Med. T.O., LL 280 KTS Airspeed, Mission 3B, Med. T.O., LL 350 KTS	.058 ] 1.41 .041 ] .17 ] 1.42 .12 ]	.056 - .15 -	.022 - .026 -
Altitude, Mission 1A, HI T.O., 30000' CR Altitude, Mission 3A, HI T.O., 500' LL Altitude, Mission 1B, Med. T.O., 30000' CR Altitude, Mission 3B, Med. T.O., 500' LL	.33 ] 5.7 .058 ] 1.0 ] 5.9 .17 ]	.34 ] 6.1 .056 ] 1.0 ] 6.7 .15 ]	.24 ] 10.9 .022 ] 1.0 ] 38.5 .026 ]
Duration, HI T.O., Cruise 1 Hr. 30000' Duration, HI T.O., Cruise 12 Hr. 30000' Duration, Med. T.O., Cruise 1 Hr. 30000' Duration, Med. T.O., Cruise 8 Hr. 30000' Duration, HI T.O., Cruise 1 Hr. 500' Duration, HI T.O., Cruise 8 Hr. 500' Duration, Med. T.O., Cruise 1 Hr. 500' Duration, Med. T.O., Cruise 4 Hr. 500'	.38 ] .84 .32 ] 1.14 ] .81 .92 ] .060 ] .38 .023 ] .15 ] .47 .070 ]	- - - - - - - -	.25 ] .84 .21 ] - - .038 ] .16 .0059 ] - -
Pattern, Med. T.O., Cruise+1 T&GO Pattern, Med. T.O., Cruise+4 T&GO Pattern, Med. T.O., Cruise+10 T&GO	.46 ] .28 .25 ] .13 ]	- - -	- - -

▶ 2 Flight Time of 1A Reduced to Agree with 1C

▶ 1 Baseline, Mission 1B, Med. T.O.+Cruise, Life from 0.25 to 0.35 ln.  
(Ratio Based on Flights.)

{ Wing - 728 Flts.  
Body - 1,588 Flts.  
Fin - 9,980 Flts.

#### 2.8.4.1 Mission Mix

Two multiple mission mixes were defined to study both analytically and experimentally the effect of different airplane usages on crack life. Each mission mix was comprised of three missions each. Mission Mix No. 1 was comprised Missions 1B, 2B and 4B (See Figure 32) and was randomly ordered in a mission mix of 26 percent of 1B, 18 percent of 2B and 56 percent of 4B as shown in Table 10. Mission Mix No. 2 was the same except Mission 4B was replaced with Mission 3A to increase the severity of the mix. The analysis as well as the test results of the two mixes is presented in the next section.

TABLE 10  
RANDOM ORDERING OF MISSION MIX NO. 1 AND 2

Order No.	Mission								
1	4B, 3A	11	1B	21	4B, 3A	31	4B, 3A	41	1B
2	4B, 3A	12	4B, 3A	22	1B	32	4B, 3A	42	1B
3	1B	13	4B, 3A	23	4B, 3A	33	4B, 3A	43	4B, 3A
4	1B	14	4B, 3A	24	4B, 3A	34	4B, 3A	44	1B
5	1B	15	4B, 3A	25	2B	35	4B, 3A	45	4B, 3A
6	4B, 3A	16	1B	26	2B	36	2B	46	2B
7	4B, 3A	17	4B, 3A	27	1B	37	2B	47	2B
8	2B	18	2B	28	4B, 3A	38	4B, 3A	48	4B, 3A
9	4B, 3A	19	1B	29	4B, 3A	39	1B	49	4B, 3A
10	4B, 3A	20	2B	30	4B, 3A	40	1B	50	4B, 3A

Note: Mission Mix No. 1 Includes Missions 1B, 2B and 4B  
 Mission Mix No. 2 Includes Missions 1B, 2B and 3A  
 Mission Mix Frequency is 26% (1B), 18% (2B) and 56% (4B, 3A)

### 2.8.5 VERIFICATION TEST RESULTS

Experimental verification tests were run using thirteen different complete mission spectra selected to verify analysis results. These spectra consisted of nine wing and two fin mission spectra and two mission mixes consisting of three wing mission spectra each. A summary of the variable missions test matrix is shown in Table 11. A sketch of the mission profile and of the applied stress spectrum for each variable mission test is shown in Appendix C. An example of a typical mission profile and applied stress spectrum for the wing and fin locations is shown in Figure 44. This figure shows the order of applied stresses which consists of an applied GAG cycle first (wing location) followed by the Lo-Hi-Lo representation of alternating stresses operating about a constant 1g stress level for each segment. Changes in the 1g stress levels represent the different mission segments which comprise the spectrum. The low amplitude stress cycles ( $\Delta f = 1.5$  KSI) shown in the fin spectra were included in analyses but were deleted for testing since analyses showed these cycles cause negligible crack growth. This truncation resulted in a fin spectrum containing 1540 cycles.

#### Correlation Between Analyses and Tests

The results of the experimental verification tests of variable missions are shown in Figures 45 through 49. The crack growth analyses for each spectrum tested were made using the Wheeler Retardation Model with a shaping exponent,  $m$ , of 0.90. Figures 45, 46 and 47 show the results of the nine-wing mission spectra tests and Figure 48 shows the results of the two-fin mission spectra tests. A comparison of test to analysis results, Figure 49 shows good agreement, with the exception of Missions 3A and 3B wing spectra tests which show the analysis results to be conservative by factors of two to three. Missions 3A and 3B are representative of flights with low level segments for different takeoff gross weights. Spectra 3A-1 and 3B-1 are the same as 3A and 3B, respectively, except the low level segment stresses were deleted.

TABLE 11  
VARIABLE MISSIONS TEST MATRIX

Mission Number	Analysis Location	Takeoff G.W.	Description	Cycles per Spectrum
1A	Wing	297	Cruise Mission	221
3A	↑ ↓	297	Low Level Mission	1243
3A-1		297	Mission W/O LL Segment	150
1B		230	Cruise Mission	107
2B		230	Refuel Mission	224
3B	↑ ↓	230	Low Level Mission	865
3B-1		230	Mission W/O LL Segment	63
4B		230	Touch & Go Mission	235
5B	Wing	230	Pattern + T & Go Mission	235
3A	Fin	297	Low Level Mission	1543
3B	Fin	230	Low Level Mission	1411
Mix #1	Wing	230	26% (1B), 18% (2B), 56% (4B)	Avg. 200
Mix #2	Wing	Variable	26% (1B), 18% (2B), 56% (3A)	Avg. 764

The inability of the selected crack growth retardation model to predict the crack growth for the missions with low level segments was not entirely unexpected since the preliminary study, Section 2.6, had shown similar results. None of the retardation models (Figure 19) could consistently predict test crack growth for all spectra but the Wheeler Retardation Model with an  $m$  of 0.90 gave the best overall results. It is evident that a particular usage must be studied in order to select the best retardation model. If a significant variation in usage parameters (spectrum content) must be considered, a means to account for variations in retardation must be established regardless of the model selected.

#### Mission Mix Tests

Verification tests were performed of two different mission mixes comprised of three missions each. The mission mix frequency and random ordering of missions within Mix No. 1 and Mix No. 2 were shown in Table 10. For simplicity, each mix was identical except that Mission 3A replaced Mission 4B in Mix No. 2 to increase the severity of the mix. The test and predicted crack growth analysis results are shown in Figure 50. The analysis results show good agreement for the benign mission mix but showed the analysis to be conservative by more than a factor of two for the more severe mix. These results are consistent with the Missions 3A and 3A-1 test and analysis results which showed the analyses predicted more crack growth from the low level segment than was indicated from test results.

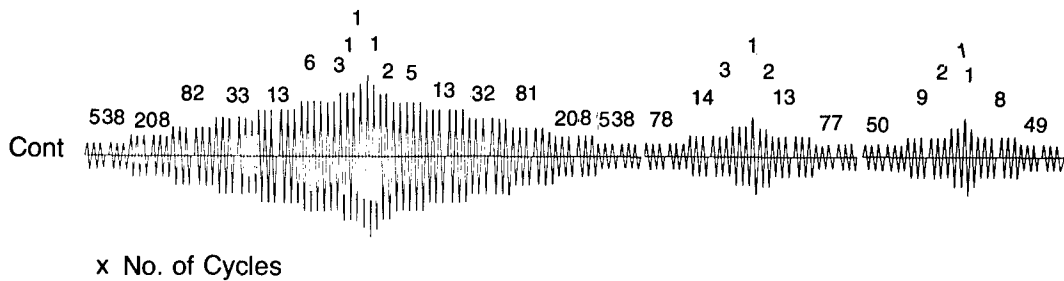
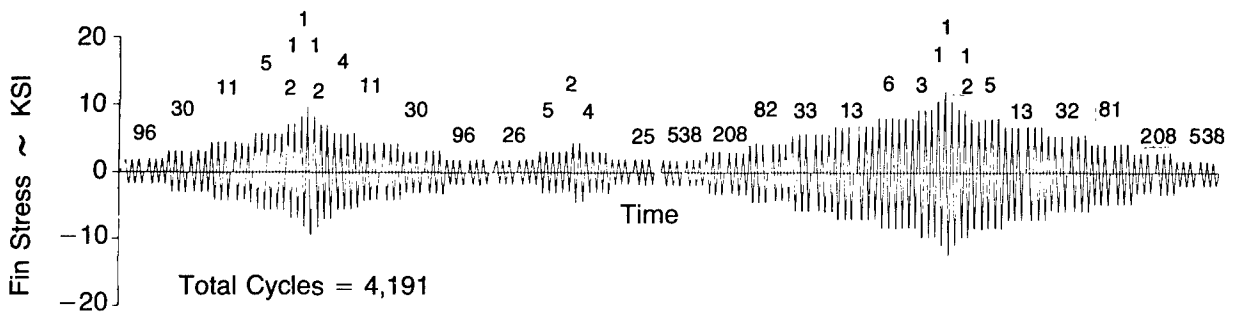
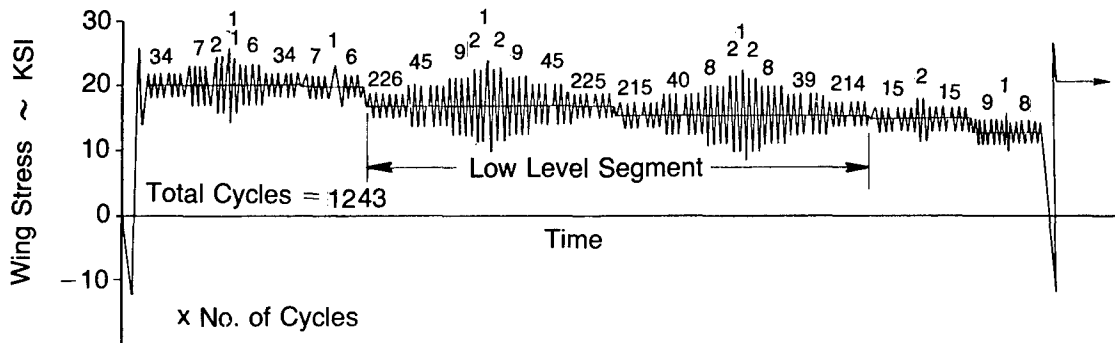
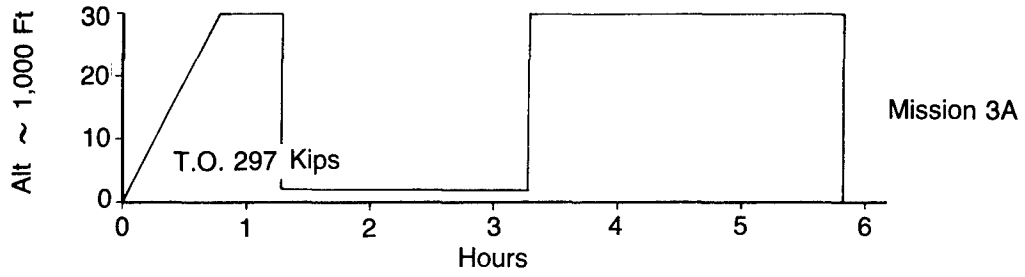


Figure 44. Verification Test Spectra, Mission 3A, Wing and Fin

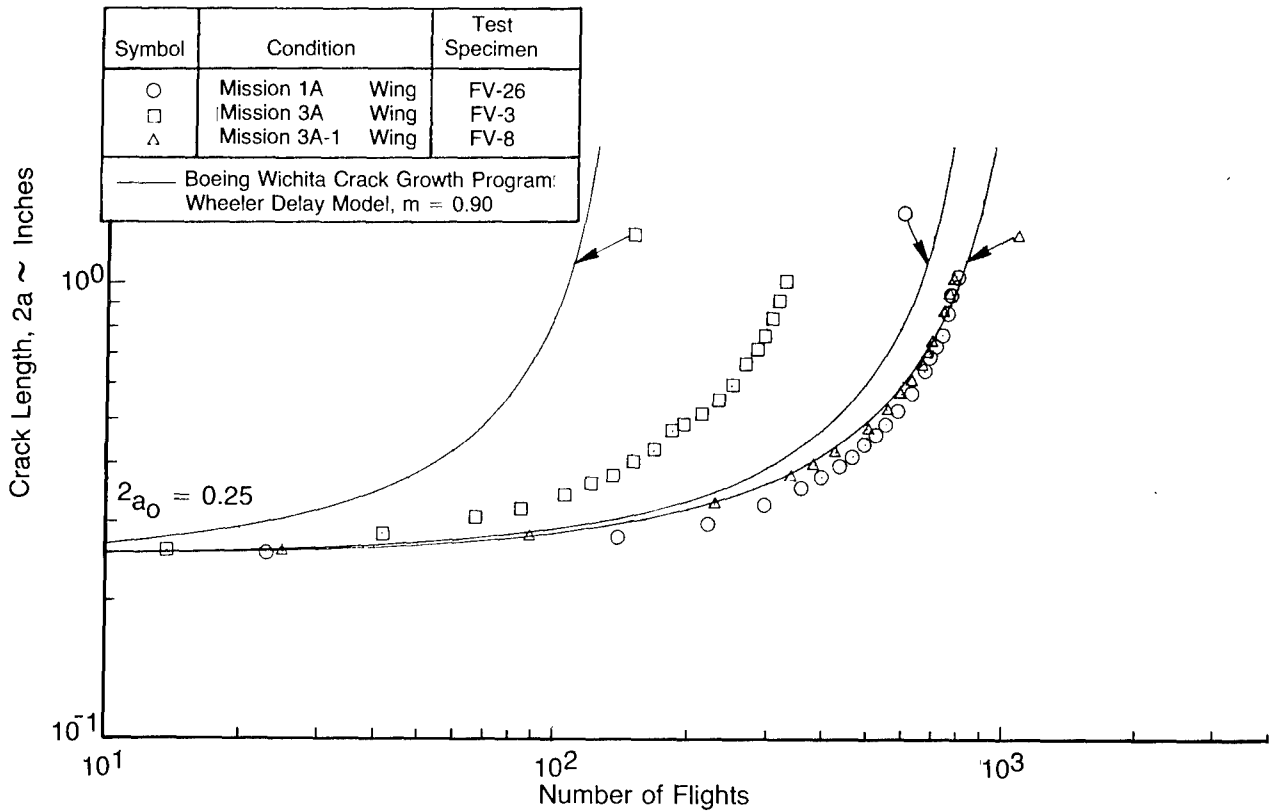


Figure 45. Verification Test Results, Variable Missions 1A, 3A and 3A-1, Wing

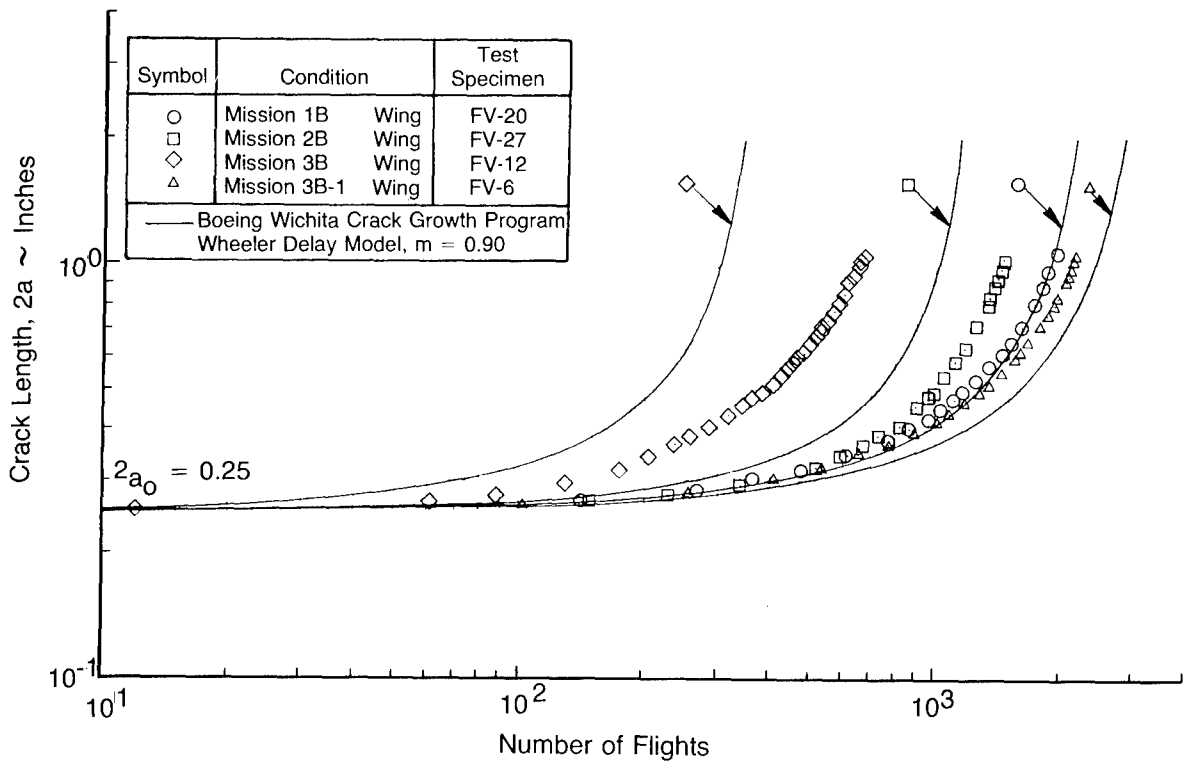


Figure 46. Verification Test Results, Variable Missions 1B, 2B, 3B and 3B-1, Wing

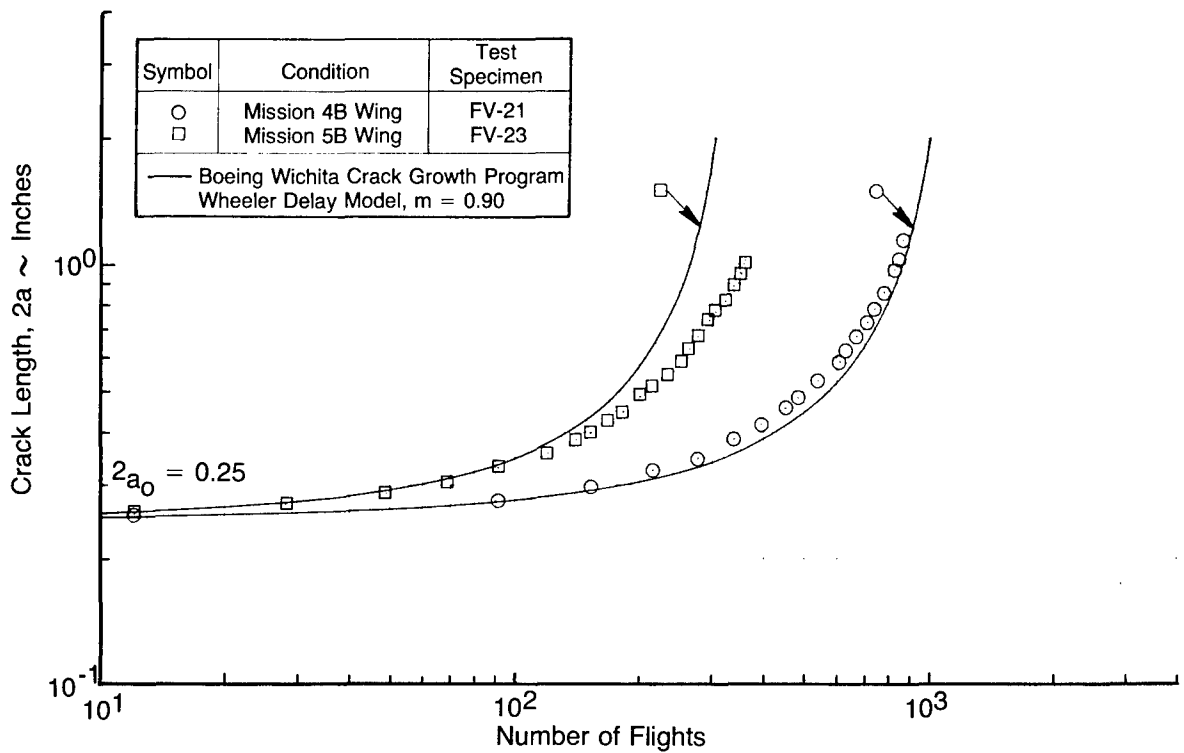


Figure 47. Verification Test Results, Variable Missions 4B and 5B, Wing

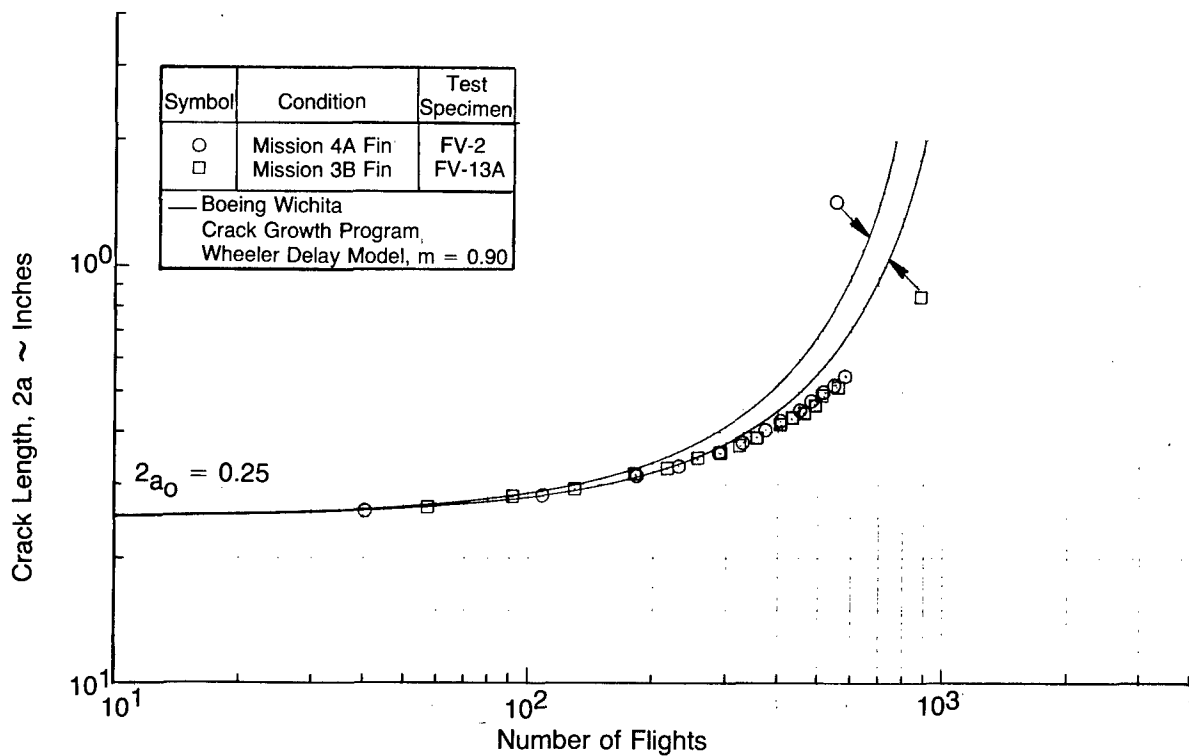


Figure 48. Verification Test Results, Variable Missions 3A and 3B, Fin

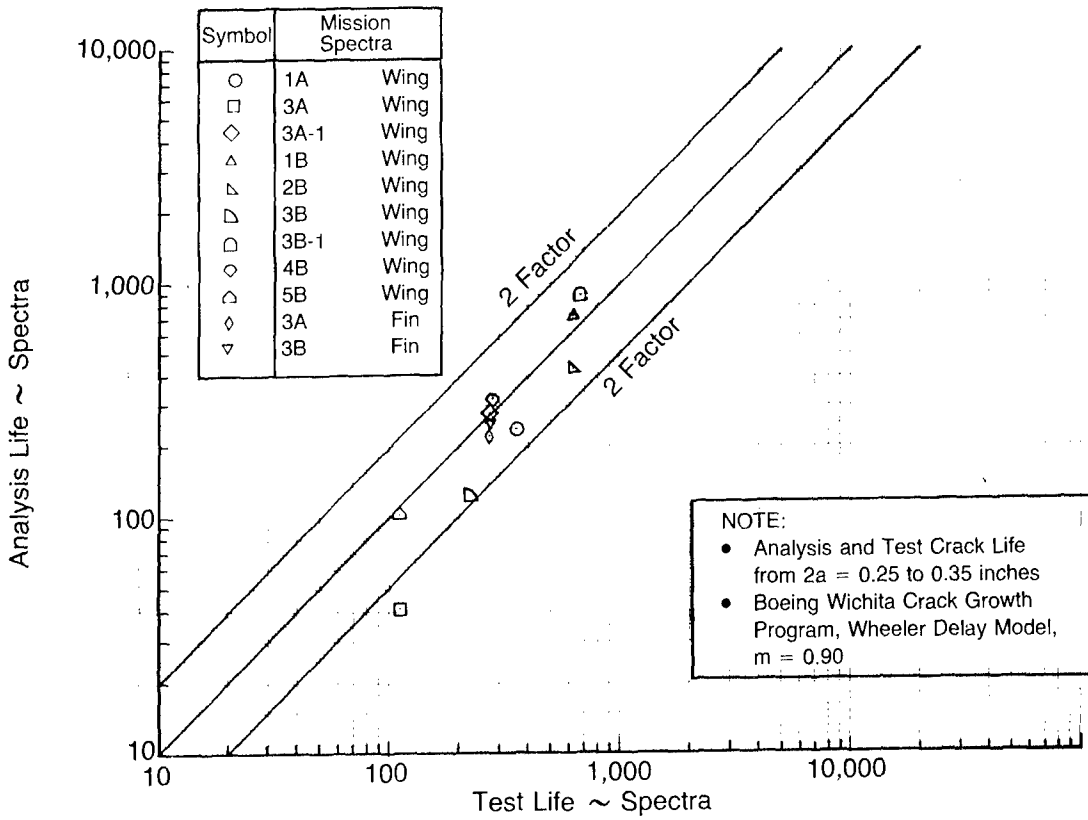


Figure 49. Analysis Life Versus Test Life, Variable Missions Spectra

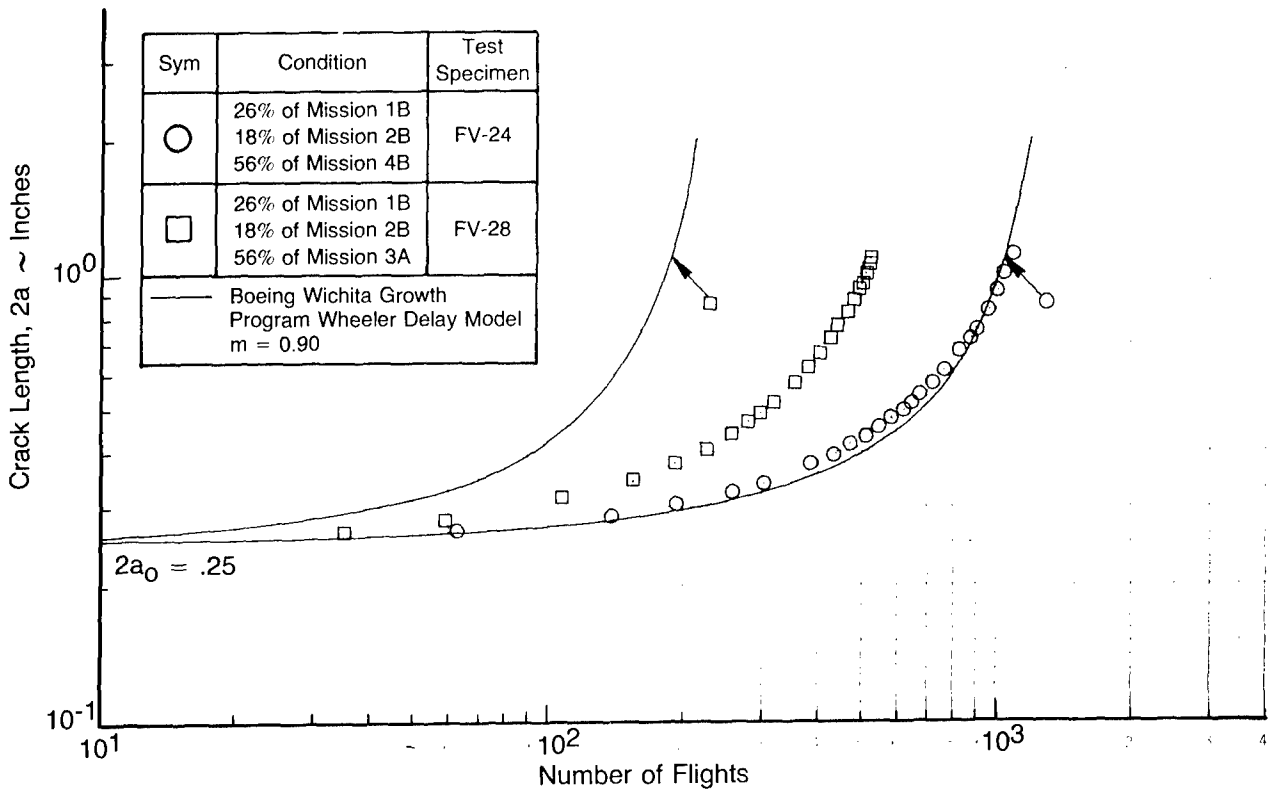


Figure 50. Verification Test Results, Mission Mixes, Wing

### 2.8.5.1 Determination of m Values and Retardation Factors

The Wheeler shaping exponent, m, was determined for each variable mission and mission segment spectrum that was subjected to experimental verification testing. The values of m were determined by trial and error by using different values of m until a good correlation between prediction and test results was obtained. A tabulation of the mission and mission segment tests, peak stress for each spectrum, the number of flights to grow the crack from 0.25 to 0.35 inch (linear analysis and test), the ratio of test to linear analysis, and the derived Wheeler shaping exponent, m, is shown in Table 12. This table was constructed to examine the relationship between peak stress, actual retardation, and the derived shaping exponent, m.

TABLE 12  
DERIVED WHEELER SHAPING EXPONENT, m, AND RETARDATION FACTOR

Condition	Specimen	Peak Spectrum Stress KSI	Flights from 0.25 to 0.35 in.		Retardation Factor Test/Analysis	Derived Wheeler Shaping Exponent m
			Analysis, m=0	Test		
<u>Variable Missions</u>						
1A, Wing	FV-26	26.0	180	355	1.97	2.0
3A	FV-3	26.0	28	114	4.07	3.0
3A-1	FV-8	26.0	215	283	1.32	0.9
1B	FV-20	18.5	525	635	1.21	0.6
2B	FV-27	18.5	340	613	1.80	1.9
3B	FV-12	18.5	80	214	2.68	2.0
3B-1	FV-6	18.5	655	660	1.01	0.1
4B	FV-21	18.5	210	279	1.33	0.6
5B	FV-23	18.5	67	112	1.67	1.0
3A, Fin	FV-2	12.1	110	272	2.47	1.2
3B, Fin	FV-13A	12.1	127	270	2.13	1.0
<u>Mission Segments</u>						
CL, T.O. 297, Wing	FV-11	26.0	245	320	1.31	0.9
CL, T.O. 170, Wing	FV-10	12.5	2440	2602	1.07	0.2
Pat. T&Go, 200, Wing	FV-17	15.2	800	903	1.13	0.9
CL, T.O. 297, Fin	FV-4	8.3	2260	2381	1.05	0.2

A comparison of the predicted crack growth using the derived values of m and test results is presented in Appendix C. The values of m were determined by matching the crack growth from 2a equal to 0.25 to 0.35 inch.

Previous studies, Reference 11, have found that both stress and flaw shape have an effect on the shaping exponent, m. The flaw shape parameter, Q, is equal to 1.0 for a through crack; therefore, the effects of Q on the derived values of m in this study were on through-the-thickness. It was also observed that stress intensity,  $K_I$ , is proportional to stress and inversely proportional to  $\sqrt{Q}$ .

It is evident, therefore, that a correlation exists between m and  $F_{\max}/\sqrt{Q}$ . Figure 51 shows a comparison of the derived m values from this study versus  $F_{\max}/\sqrt{Q}$ , where Q equals 1.0. The range of values obtained from Reference 11 is superimposed on this plot. As indicated in the Reference 11 study, there is a large scatter in m with

$F_{max}/\sqrt{Q}$ . The use of an average  $m$  value as a function of the peak spectrum stress may produce satisfactory overall correlation between analysis and test results. This method might work well for complete mission spectra but prove unsatisfactory to apply to crack growth predictions for individual mission flight segments. Our analyses, however, were made using a constant  $m$  value of 0.90 for the parametric and variability studies with analyses versus test results falling, for the most part, within a factor of plus or minus 2.0. See Figure 49.

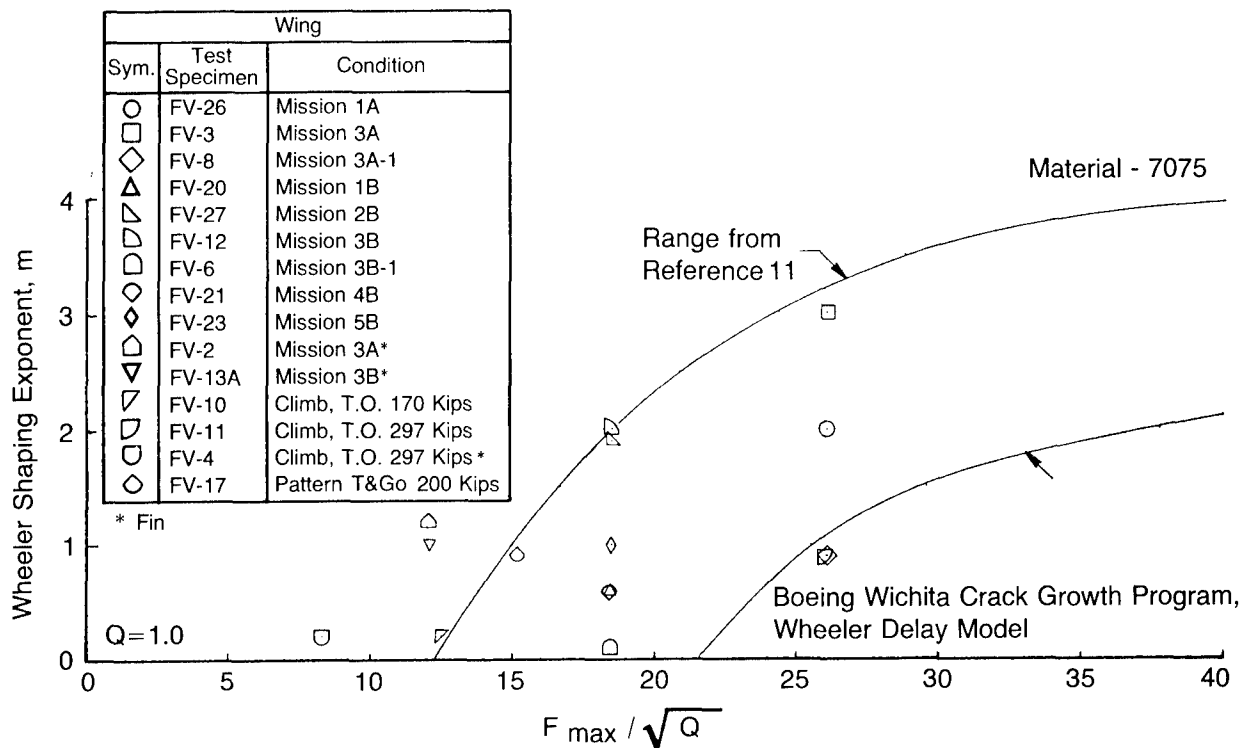


Figure 51. Derived  $m$  Values Versus  $F_{max}/\sqrt{Q}$

Another comparison was made to show the relationship between retardation and spectrum characteristics. Figure 52 shows a plot of the actual retardation (test life/linear analysis life) versus linear analysis life. The linear analysis life serves as a measure of the spectrum severity which cannot be characterized by the  $F_{max}/\sqrt{Q}$  ratio alone. This figure indicates that there exists a relationship between the actual retardation and the linear analysis prediction. Similar curves might be developed of mission crack growth rate as a function of crack length versus an average retardation factor – a factor that might prove useful in a fleet tracking program.

## 2.8.6 VARIABILITY STUDY RESULTS

The variability crack growth analyses showed significant variations in crack growth with mission parameter variations. Changes in gross weight and altitude were the two most significant usage parameters producing variations in crack life by factors of 8 and 6 times, respectively, for the wing analysis location and 5 to 38 times, respectively, for the fin. Total variation in crack life from the most severe to most benign spectrum analyzed was greater than a factor of 30 at all locations analyzed.

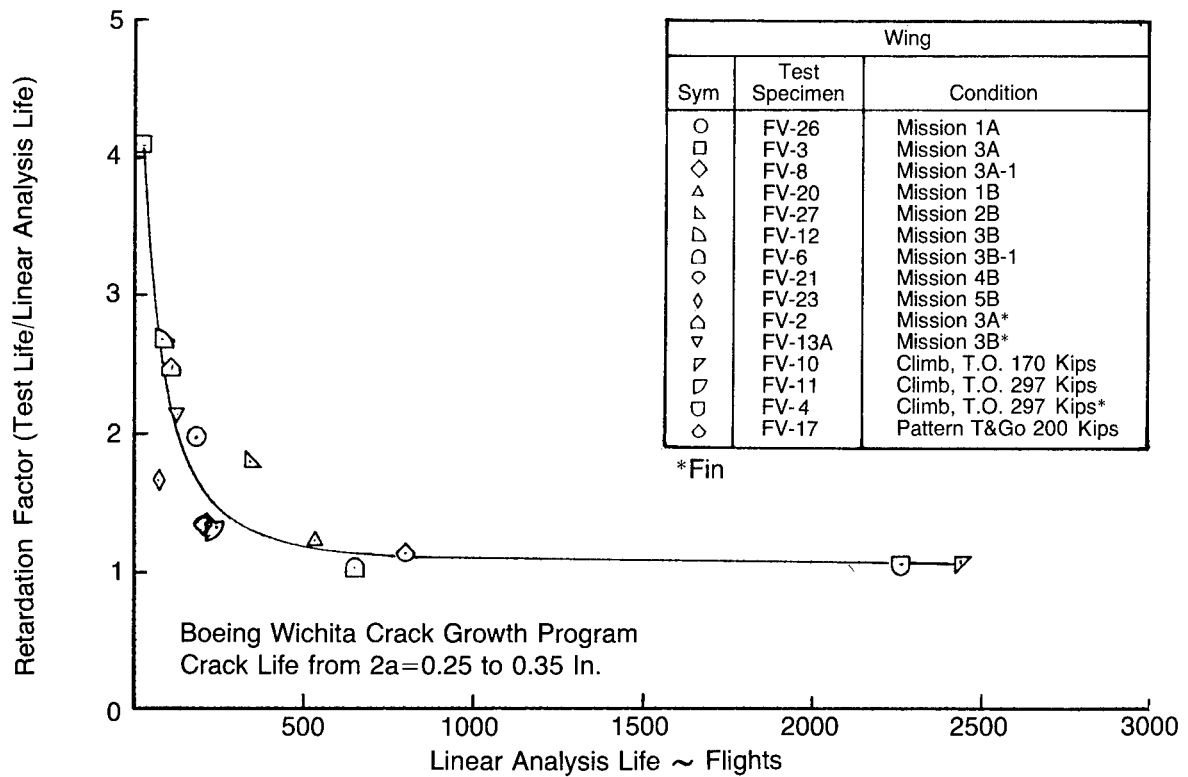


Figure 52. Correlation Between Linear Analysis and Test Results

Experimental verification test results clearly indicated that a means to account for retardation as a function of spectrum content should be defined for fleets which show a large variation in usage. The selection of a retardation model and/or a means to adjust crack growth for retardation is dependent on fleet variability and spectrum content. Using the Wheeler Retardation Model with a shaping exponent,  $m$ , of 0.90 will predict crack growth for typical C/KC-135 flight profiles within a  $\pm 1.5$  factor on test life. For bomber type operations consisting of low level flight, factors as high as three between test and analysis were encountered for the most severe flights.

The variability study provided predicted crack growth data which was used to define the important tracking parameters and was used as a base for comparing crack growth predictions using the mission segment crack growth rates determined during the parametric study. These subjects are discussed in Section 3.

### SECTION III

#### TASK 2, DEVELOPMENT OF GENERALIZED TRACKING PROCEDURES

The results of the parametric and variability studies of Task 1 were used to develop procedures for tracking crack growth applicable to transport/bomber aircraft. The primary objective of Task 2 was to identify the important tracking parameters based on the studies in Task 1, identify the available data acquisition systems that could be used in a crack growth tracking program and to develop generalized tracking procedures. The following sections will address these subjects.

#### 3.1 Important Tracking Parameters

The important usage and loading parameters must be identified for any fleet aircraft for which a tracking program is to be developed. This is necessary to select the optimum type of data acquisition systems and compatible analysis methods to incorporate into the tracking program.

The most important tracking parameters that must be evaluated and accounted for in the development of a transport/bomber tracking program are:

- Gross weight
- Altitude
- Flight duration
- Airspeed

The two most important parameters, which are the changes in airplane gross weight and the altitude at which the airplane operates, were found to effect crack growth rate by factors of 6 to 8 times for the wing while variations in altitude effected the fin crack growth rate by as much as 38 times. The crack growth rate per flight, while increasing with flight duration, eventually reaches a point when additional flight duration produces little or no crack growth. Conversely, this implies that the crack growth rate per flight hour is greatly reduced with flight duration in most cases.

Changes in airspeed had a lesser effect on crack growth than gross weight and altitude showing about 1.5 times more crack growth for a 25 percent increase in airspeed at low altitude.

Even though a study of configuration was not made in this program, it is considered that this parameter may be important for some fleet aircraft and must be evaluated so that if significant effects on crack growth occur they can be accounted for.

#### 3.2 Available Data Acquisition Systems

The recorded data required to support a crack growth tracking program depends on the selected analysis technique. The compatibility between analysis procedures and available data acquisition systems must be thoroughly evaluated. There are a number of systems currently available or in the development stage for recording information required for a crack growth tracking program. Some of these systems are discussed in the following sections.

##### 3.2.1 PILOT LOGS

The pilot log is a widely used form of acquiring operational data on a flight-by-flight basis. The information obtained on a pilot log generally includes all of the pertinent data necessary to define the entire flight profile consisting of gross weight, altitude, flight duration, airspeed, takeoff and landing data, etc. The pilot log provides an inexpensive means to acquire a lot of flight statistics. However, the discipline needed to assure an accurately completed form for all flights on all aircraft is sometimes lacking.

### 3.2.2 MULTICHANNEL RECORDERS

The multichannel recorder is generally a digital system that has the capability of recording airplane loading in sequence. It also can record strains directly at a selected location or locations. This recorder has the additional capability of recording flight parameters in terms of airspeed, altitude, multidirectional accelerations, angle of attack, flight control system, and control positions. The use of magnetic tape cassettes in these recorders have proven effective in reducing the cost of data reduction.

Some of the disadvantages of the system are that a transfer function is needed to determine stress levels at the critical locations on the aircraft; also, the system is expensive, making it costly to install on all aircraft in a fleet.

### 3.2.3 STRAIN RECORDERS

Strain recorders can be categorized as strain exceedance or strain cycle sequential recorders. The exceedance type recorder may be either an electrical or electromechanical system. The electrical type makes use of a bonded electrical strain gage as a transducer coupled to a signal conditioner which converts strain levels and amplitudes into peaks. The electromechanical type has a transducer which converts a mechanical displacement into an electrical signal which is then similarly converted into peaks. A counter is used to provide window readouts of exceedances at the desired stress levels.

One advantage of this system is its nominal cost. Also, a knowledge of flight parameters (airspeed, altitude, gross weight and accelerations) are not required, since the data can be used directly to perform crack growth calculations.

Disadvantages are that only one location can be monitored with each system requiring either additional systems per aircraft or development of transfer functions for locations not monitored directly. Also, this system involves the human element in reading and recording data from the counter. In addition, there is no provision for this system to provide information such as CG acceleration data to update environmental data. Other types of recorders must be used to provide this information.

The sequential type recorder may be either an electrical, electromechanical or purely mechanical type system. The first two types are the same as the exceedance recorder systems. The mechanical type (scratch gage) records displacement as an inscription on a metallic record, either disc or tape. This record is removed from the airplane periodically and reduced manually or with special transcriber equipment.

This system has the same advantages of the exceedance recorders with the added advantage of being able to evaluate the effect of load sequence on life. This data may also be reduced into strain exceedance data.

Disadvantages are the same for the exceedance type, i.e., acceleration data cannot be developed from the strain sequential recorders. More than one recorder would probably be required per aircraft or transfer functions must be defined.

### 3.2.4 VGH RECORDERS

The VGH recorder system includes a computer recorder, a sealed tape magazine and a servo-accelerometer which is mounted near the airplane CG. The computer converts differential and static pressure, sensed from the aircraft pitot-static system, to the corresponding pre-set intervals of indicated airspeed and pressure altitude before recording them. The system also continually monitors the vertical acceleration and records acceleration peaks in counters with preset acceleration levels.

The elapsed time and the indicated airspeed and pressure altitude codes are stored by the computer-recorder. If either the altitude or airspeed interval changes, an acceleration counter reaches its capacity or a certain elapsed time completes its cycle, the contents of all acceleration counters, the elapsed time, the airspeed and altitude interval code is transferred to a tape. After a transfer of data the process is repeated for another interval.

An advantage of the VGH system is the capability to record acceleration counts at prescribed airspeed and altitude ranges, which allows calculations of stress levels in terms of VGH data and gross weight. Also, the potential of human error in the collection and reduction of data is absent since magnetic recording tapes are used.

Disadvantages are that a transfer function is required to estimate stresses, symmetrical and unsymmetrical maneuvers cannot be separated, the system does not account for all acceleration directions, the control surface positions are not recorded and gross weights must be determined from takeoff and landing gross weight along with fuel burn rates.

The VGH recorder is generally used as a supplementary data source with its primary application being to record CG accelerations in preset speed and altitude bands.

### 3.2.5 COUNTING ACCELEROMETERS

This system is a simple, compact, inexpensive device that measures and records normal accelerations ( $\Delta n$ ) only. The counting accelerometer consists of a counting indicator which will record at preset intervals and a load sensitive transducer. The transducer transmits electrical signals produced by normal accelerations to the counting indicator which records acceleration exceedances. Successive peaks must be separated by a minimum load factor to be counted. The accelerometer is tuned to be insensitive to loads introduced by shock or vibrations.

The advantages of the accelerometer are low cost which makes it feasible to instrument all aircraft and it is easy to detect changes in usage.

Disadvantages are that the accelerometer will not supply data for airspeed, altitude, gross weight, etc. Transfer functions are required for other locations since recorded data is for the airplane CG. There is the expected human error in reading and transferring the data from the counter to paper.

### 3.2.6 CRACK GROWTH GAGES

The crack growth gage is a small, precracked metal element mounted on aircraft structure where it experiences the same displacement-time-environmental history as does the host structure. The concept behind the crack growth gage is that the crack in the gage grows in a manner relatable to assumed initial cracks in the structure. A transfer function must be developed to relate the structural and gage crack growth. Crack growth in the gage can then be conveniently measured during service and related to an assumed crack growth in the structure.

An advantage is that the gage is small and inexpensive so numerous gages could be installed on each airplane. However, the crack growth gage is in the development stage at present and its feasibility must be proven as an operational tracking device. Its overall simplicity makes the crack growth gage very attractive as a future tracking concept.

## 3.3 Tracking Procedures Evaluated

Four tracking procedures applicable to transport/bomber aircraft were selected for evaluation in this program. Two of the procedures utilize parametric analysis methods, the other two use mechanical recording devices. Procedures A and B are dependent on pilot logs for the primary data acquisition. Procedure A utilizes a parametric crack growth method while B utilizes parametric stress exceedance data. Procedure C is a strain recording system which uses the Mechanical Strain Recorder (MSR). Procedure D makes use of a gage that records crack growth directly. A detailed description of the tracking procedures, primary data acquisition systems, analysis schemes and accuracy is presented in the following sections.

### 3.3.1 PROCEDURE A, PILOT LOGS AND PARAMETRIC CRACK GROWTH RATE TABLES

Tracking Procedure A requires pilot logs to define individual airplane usage on a flight-by-flight basis. Tables of parametric crack growth rate as a function of crack length are compiled to cover all mission segments. These tabular values would then be stored in the monitoring program. A flow diagram of tracking Procedure A is shown in Figure 53.

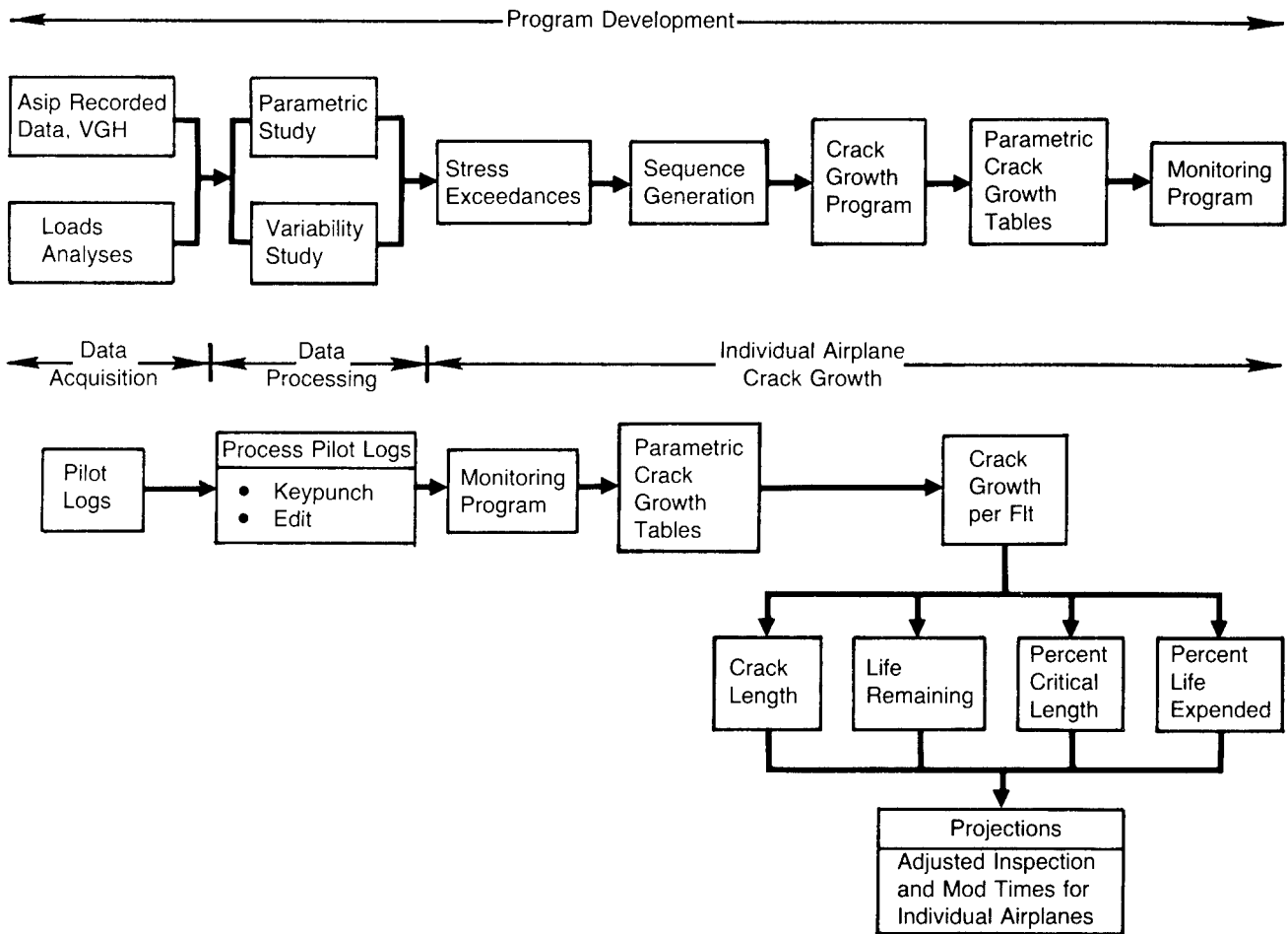


Figure 53. Diagram of Tracking Procedure A

The development of the tracking program will consist of parametric and variability studies to define the usage parameters required to predict crack growth. The crack growth data from the parametric analysis will then be used to develop crack growth rate tables which in turn will be used to calculate and accumulate incremental crack growth from the various mission segments.

The primary form of data acquisition, the pilot log, will be processed and edited to provide the mission profile information on pertinent usage parameters for each flight. This information will be fed into the monitoring program which contains the parametized crack growth data. The pilot log data is processed to define a number of individual flight segments which can be assembled to describe the mission. The incremental crack lengths for each mission segment are determined and accumulated to give total mission crack growth and crack length after each flight. Output from the monitoring program can be expressed in various forms that can be used to make projections and establish and adjust inspection and modification intervals for each critical location monitored.

### 3.3.2 PROCEDURE B, PILOT LOGS AND PARAMETRIC STRESS EXCEEDANCE TABLES

Tracking Procedure B is a variation of Procedure A. This scheme also requires a pilot log to define individual airplane usage on a flight-by-flight basis. Parametric stress exceedance tables are compiled to cover all mission segments. These tables would then be stored in the monitoring program. A diagram of this procedure is shown in Figure 54.

Development of the Procedure B tracking program would consist of parametric and variability studies to define the tracking parameters. Stress exceedance data generated during the parametric study will be tabulated in a form that will enable development of a stress spectrum for the entire mission. This procedure has certain advantage over Procedure A, i.e., provides additional flexibility in placement of peak loads, allows selecting the order of loading within the spectrum and accounts for peak load retardation on each flight segment.

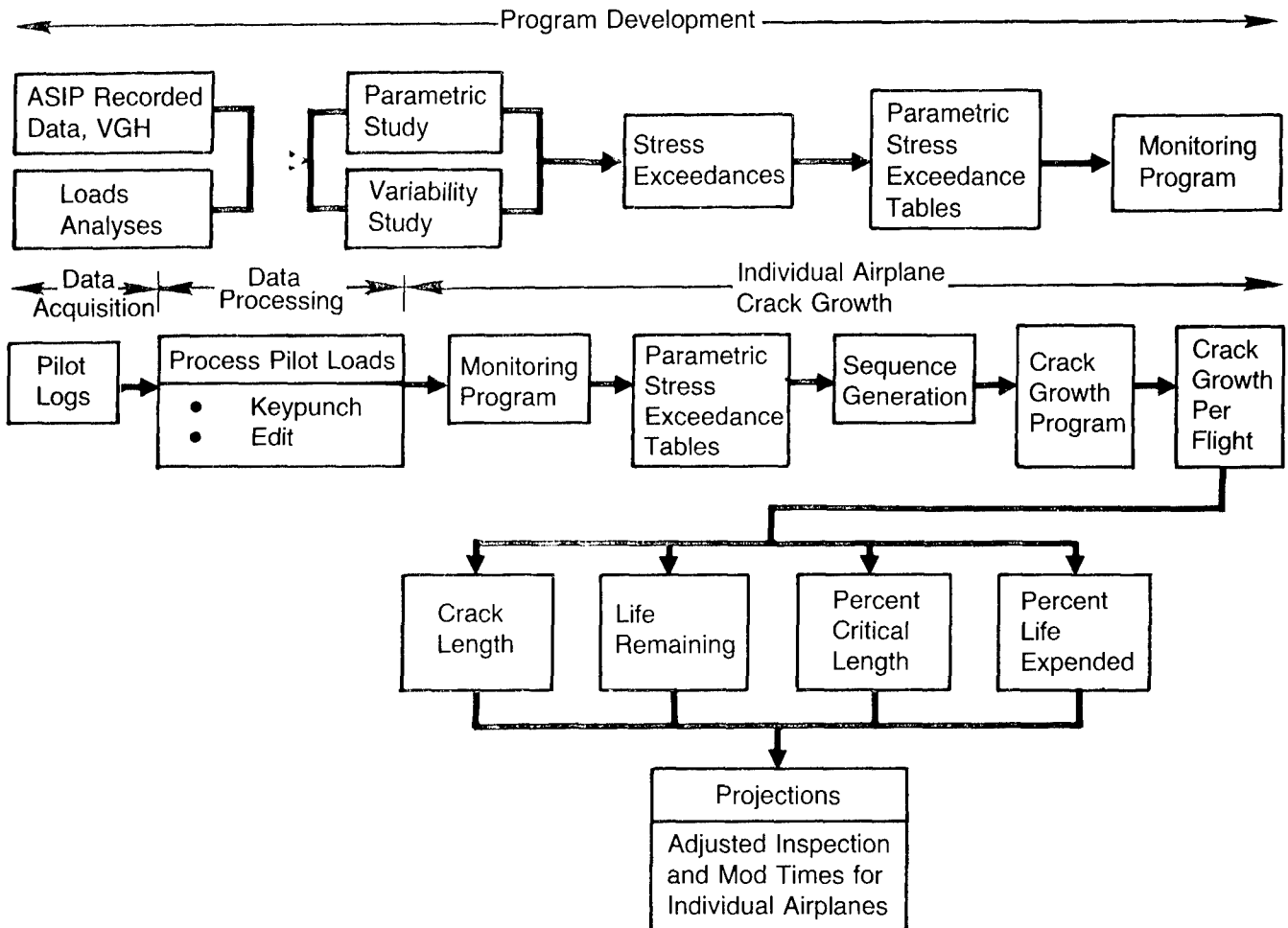


Figure 54. Diagram Of Tracking Procedure B

The primary form of data acquisition is the pilot log which is used to define each flight as an assemblage of individual flight segments. Once the pilot log data has been processed and flight segments defined, the monitoring program containing the paramatized stress exceedance data is used to define a composite stress spectrum. A block or cycle-by-cycle crack growth analysis is then performed to determine mission crack growth and total crack length after each flight. Output from the monitoring program is expressed in a form useful in making force management decisions.

### 3.3.3 PROCEDURE C, MECHANICAL STRAIN RECORDERS (MSR)

Tracking Procedure C is diagrammed in Figure 55. This procedure will require instrumentation of each airplane with strain recording equipment and development of a monitoring program that will process the recorded data.

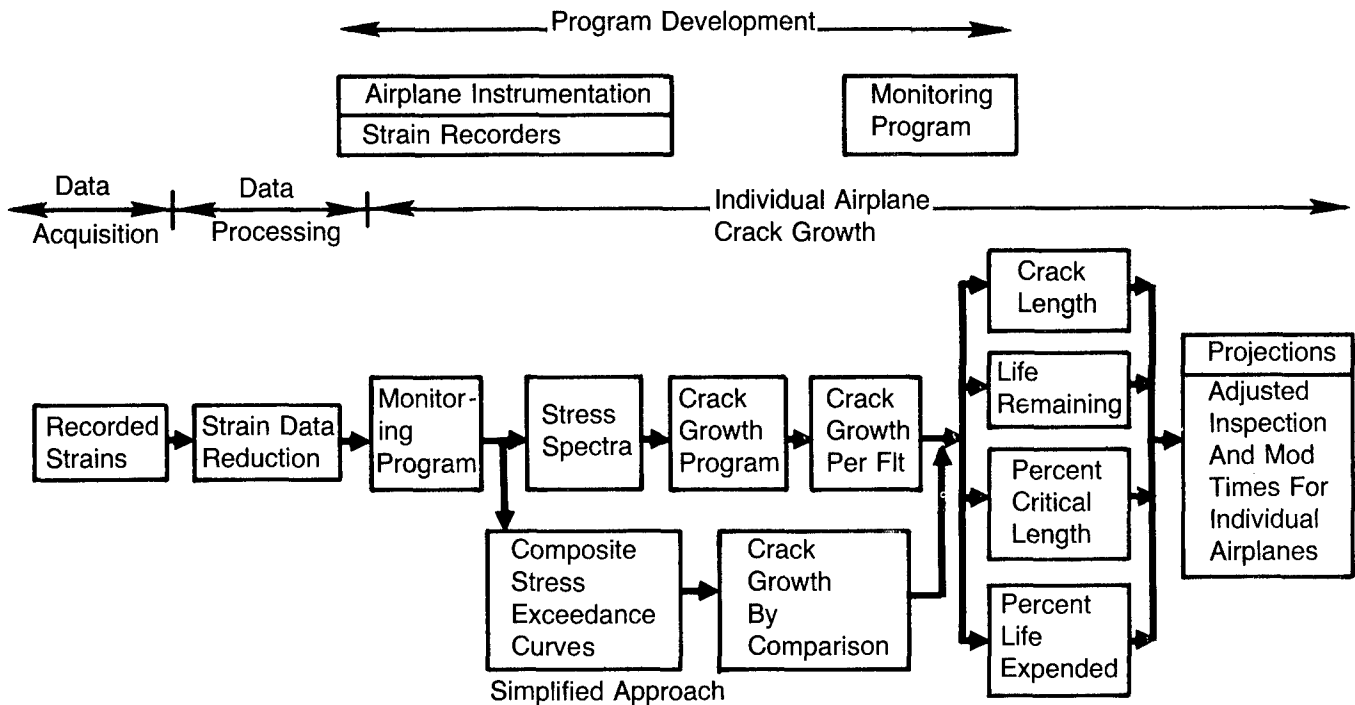


Figure 55. Diagram of Tracking Procedure C

The primary data acquisition, the mechanical strain recorder (MSR), will produce measured strain data on individual aircraft. These recorded data will be reduced to a form suitable for input into the monitoring program. The monitoring program will then further process the data to construct a stress spectrum for input into a block or cycle-by-cycle crack growth analysis to determine mission incremental crack growth and accumulated crack length after each flight. Output will be used to make projections and establish and adjust inspection and modification intervals for each critical structural location.

A limited study was performed to investigate a simplified approach using the strain recorded data which would eliminate the cycle-by-cycle crack growth analyses as part of the tracking program. This approach, shown in Figure 55, consists of reducing the strain (stress) data into a composite maximum stress exceedance curve for the usage period. These data will then be compared to a stress exceedance analysis model which represents the variability in fleet usage. This is done by superimposing the recorded data, normalized to the usage model time period, onto the usage model, then using a scheme to determine its relative severity and corresponding crack growth for the period. This approach will be discussed further in Section 3.3.6.

### 3.3.4 PROCEDURE D, CRACK GROWTH GAGES

Tracking Procedure D requires instrumentation of each airplane with crack growth gages and development of a monitoring program to process the recorded data. This procedure is diagrammed in Figure 56.

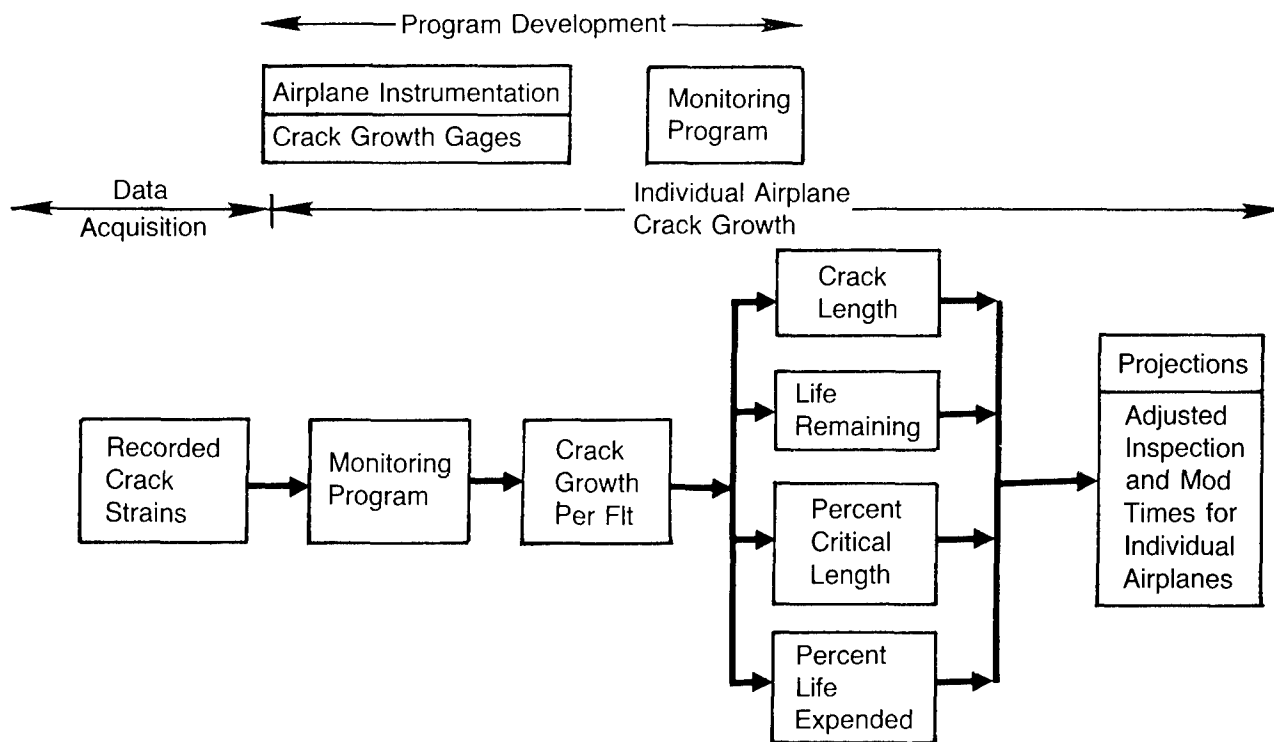


Figure 56. Diagram of Tracking Procedure D

The primary data acquisition, the crack growth gage, will provide program input data from periodic measurements of crack length. These data will then be accumulated and input into the monitoring program which will calculate structure crack length by application of appropriate transfer functions. Output will be formulated for use in force management decisions.

### 3.3.5 PRIMARY DATA ACQUISITION SYSTEMS

The primary data acquisition systems required for the four tracking procedures studies are the pilot log, mechanical strain recorder and crack growth gage. Each of these data acquisition systems will be discussed more fully in the following sections.

#### 3.3.5.1 Pilot Log

The pilot log, used for Procedures A and B, is a commonly used method of data acquisition and is presently being used in fleet damage monitoring programs on the B-52, C/KC-135, E-3A, C-141 and C-5 fleets. This method makes use of an Air Force Technical Order (AFTO) form or "Aircraft Structural Assessment Data" form which is used to determine the type and severity of usage that each aircraft undergoes in the performance of operational or training missions.

Air Force flight crews are responsible for filling out the forms and it is imperative that the forms are completed accurately and submitted for every flight. The flight log format is generally proposed by the Contractor and coordinated with the Air Force for concurrence with the format and related instructions. It is the responsibility of the using command to print and distribute these forms. It is important that the pilot logs be simple to fill out but include all pertinent information about each flight needed for fleet tracking.

Completed flight logs are collected and mailed to a processing location for reviewing and editing. Processing of the forms is normally accomplished by a combination of manual review and computer or edit programs. The key punched data is reformatted by the edit programs and put on tape (or disk) for input into the computer monitoring program. This program processes the flight log data with the data in the computer program to produce the tracking information needed to examine usage and/or make force management decisions.

Figure 57 shows the pilot log presently being used for tracking fatigue damage on the C/KC-135 aircraft. The format of this log is quite different from those used by other fleet airplanes (i.e., C-5, B-52, etc.) but contains roughly the same information about a flight.

135 AIRCRAFT STRUCTURAL ASSESSMENT DATA				1. AIRCRAFT SERIAL NUMBER				2. DEPARTURE BASE (CAO IDENT)				3. DATE FLIGHT ORIGINATED			REPORTS CONTROL SYMBOL		
7. OPERATIONAL PHASE				4. AIRCRAFT FLIGHT HOURS AT TAKEOFF				5. TAKEOFF WEIGHTS IN POUNDS						6. FLIGHT DURATION			
CLIMB	CRUISE	FUEL ON LOAD	FUEL OFF LOAD	DESCENT	TRAFFIC PATTERN	8. CLOCK TIME (Z)	9. ALTITUDE IN FEET	10. GROSS		10. CARGO		10. FUEL		HRS	MIN		
								0	0	0	0	0	0			0	0
START OF PHASE								11. INDICATED AIRSPEED IN KNOTS		12. RESERVE FUEL		14. NUMBER OF LANDING					
										FULL		EMPTY		T AND S		FULL STOP	
							00			00						2	
							00			00						3	
							00			00						4	
							00			00						5	
							00			00						6	
							00			00						7	
							00			00						8	
							00			00						9	
							00			00						10	
							00			00						11	
							00			00						12	
							00			00						13	
							00			00						14	
ENTER CLOCK TIME, FUEL WT. AND TOTAL LANDINGS AT END OF MISSION THIS ROW								00				FINAL LANDING		0		1	
TOTAL LANDINGS																	
15. REMARKS																	
16. PRINTED NAME AND RANK OF AIRCRAFT COMMANDER								17. PRINTED NAME AND RANK OF CREW MEMBER COMPLETING FORM				DUTY AT BASE		DUTY PHONE (AUTOVON)			

AFTO FORM 76 JAN 75

PREVIOUS EDITION IS OBSOLETE

Figure 57. C/KC-135 Pilot Log (AFTO 76 Form)

The pertinent information presently collected on the AFTO 76 form is needed to track crack growth and is indicated on the form. Each mission phase is identified by noting the type of operational phase, and the clock time, altitude, fuel weight, and airspeed at the start of each phase. Reserve fuel and the number of landings associated with traffic pattern operations are also noted. The clock time and fuel weight at the end of mission completes the form.

An important criteria that must be established for each pilot log is a definition of what constitutes an entry on the pilot log form. Obviously, changes of operational phases (i.e., climb, cruise, low level, etc.) must be entered. However, the effects of changes in gross weight, speed or altitude on crack growth needs to be determined so that as few entries as possible to the log will be required. Figure 58 shows an example of the change in mission crack

growth rate as a function of changes in altitude. This figure indicates little change in crack growth rate above 10,000 feet, but significant changes below 10,000 feet. Therefore, fewer pilot log entries need to be made with changes in cruise altitude above 10,000 feet. Changes in speed and other appropriate usage parameters must also be examined.

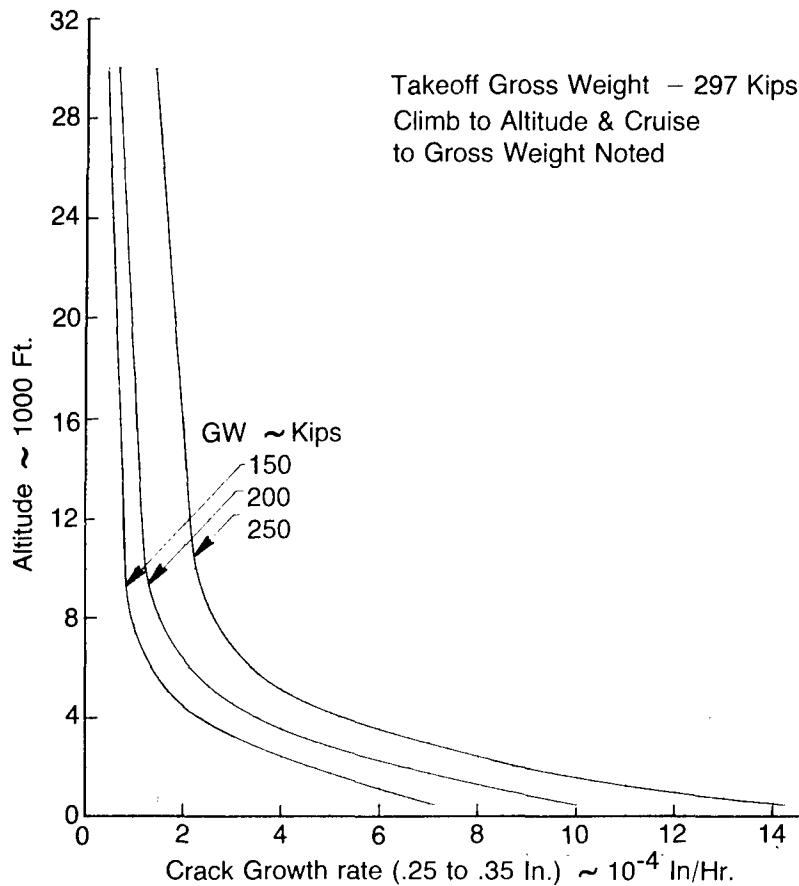


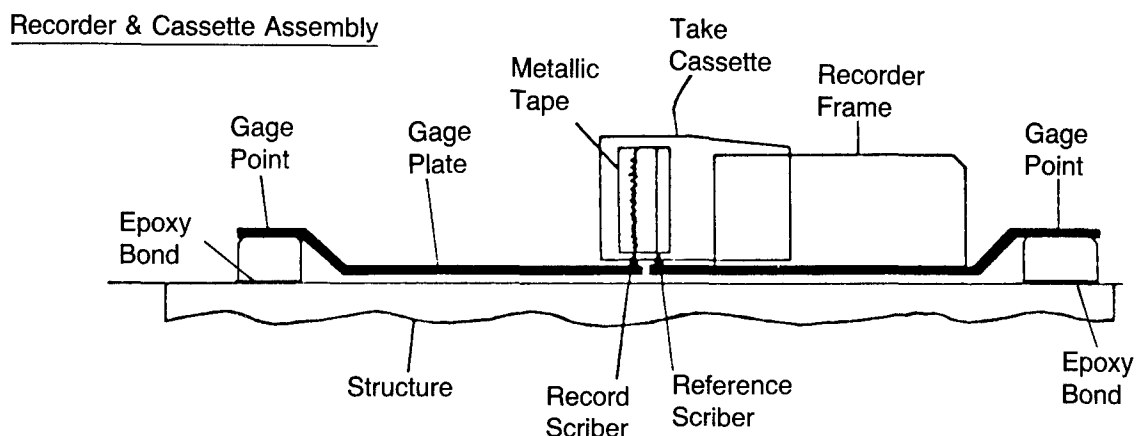
Figure 58. Change in Crack Growth Rate with Altitude, Wing

The primary objective of any data acquisition system is to obtain a high percentage of usable data. A history of today's tracking programs shows that many flights are not recorded on a pilot log or many of the logs are not properly or accurately filled out. It is imperative that the pilot log form be completed accurately for every flight for the tracking program to meet its objectives. Consequently, continued crew training and motivation are required.

### 3.3.5.2 Mechanical Strain Recorder (MSR)

The mechanical strain recorder, used for Procedure C, is a sequential strain history recorder which records strain as a trace on a removable metallic tape cassette for each flight. The recorder is a self-contained nonelectrical device needing no additional recorders transducers onboard the aircraft. A sketch of the recorder and cassette assembly and a typical MSR strain trace is shown in Figure 59. The MSR is attached to gage plates which are physically attached to the aircraft by two epoxy-bonded mounting blocks. As the structure experiences loads due to maneuvers or gusts in flight, the resulting strain (or metal elongation) is transmitted to the recorder through the gage plates. The relative movement of the gage plates (in either direction) is transmitted to an unidirectional spring clutch drive mechanism in the recorder housing. This action advances the tape in one direction so that separation of

successive strain peaks is possible. A diamond stylus is mechanically linked to each strain plate such that both dynamic "sawtooth" trace and a reference or baseline trace is generated. All strain cycle measurements are taken from the reference trace. A typical MSR trace is shown in Figure 59.



Typical MSR Trace

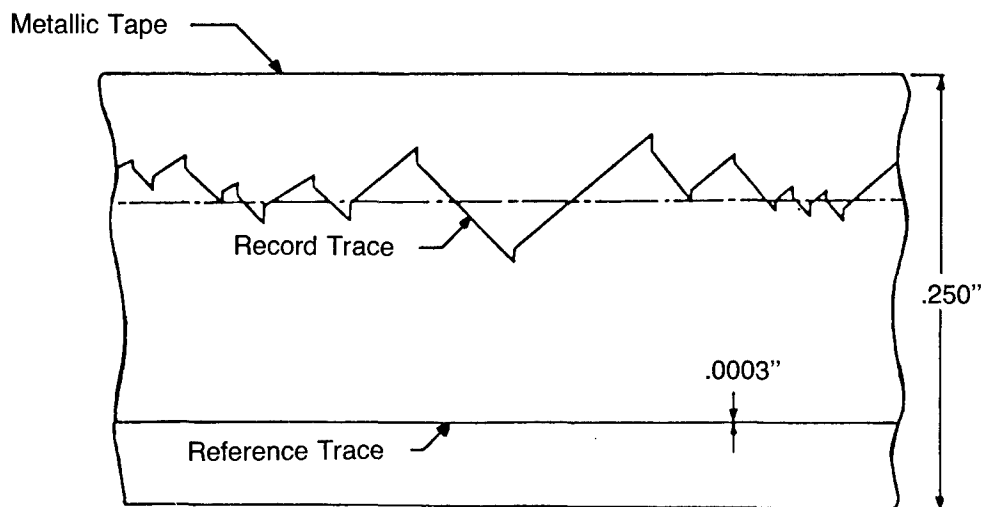


Figure 59. Mechanical Strain Recorder (MSR)

The trace can be reviewed manually but automatic data reduction is accomplished using a data transcriber unit which outputs sequential peak-valley data on computer compatible magnetic tape. This data can then be transformed into a strain exceedance format if desired. A practical method must be developed to convert the MSR strain output into absolute stress.

The MSR is an operational device but has not been utilized as that on a force wide basis. Even though it is inexpensive as compared to other strain recording devices and provides an accurate strain history, tape replacement and data reduction costs are high for a large fleet monitoring several locations per airplane. Crack growth can be predicted from MSR data alone; however, knowledge of flight parameters is needed to understand changes in usage.

### 3.3.5.3 Crack Growth Gage

The crack growth gage, used in procedure D, is a small, precracked element mounted on aircraft structure to experience the same displacement-time-environmental history as the structure. Since this system responds to the actual strain history of the airplane, the crack in the gage grows in a relatable manner to assumed cracks in the structure. Figure 60 shows a sketch of the crack growth gage mounted on a piece of structure.

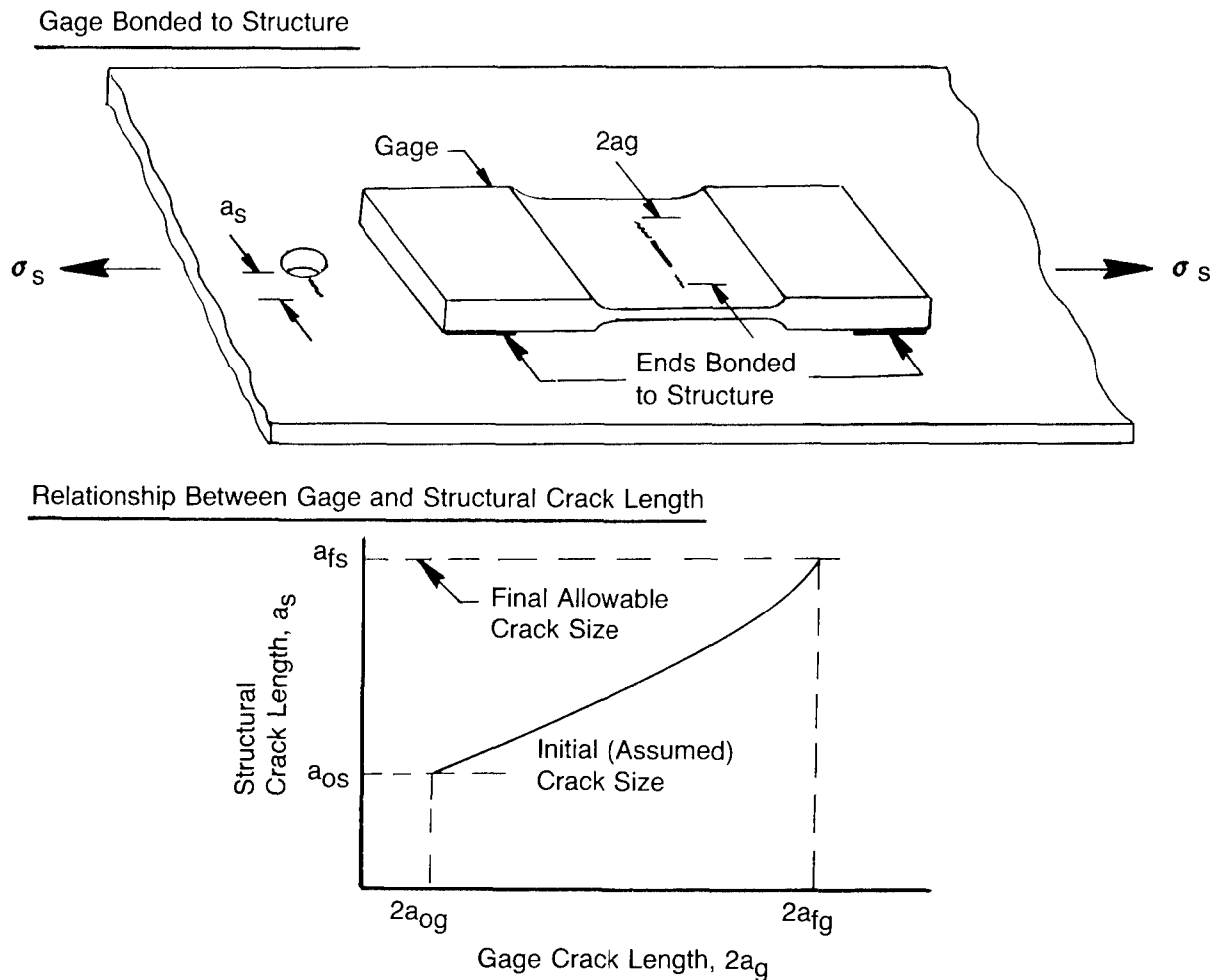


Figure 60. Crack Growth Gage

One characteristic of the gage is that it may be designed to effectively amplify crack growth rate. The lower plot, Figure 60, depicts the relationship between gage and structure crack length. Crack growth in the gage must be periodically measured during service for an indication of crack growth in the structure by applying a transfer function to the gage crack length.

The crack growth gage is in a developmental stage at the present time but may prove to be a feasible means to track crack growth as a future tracking program. Its overall simplicity makes the gage attractive as a tracking concept. A knowledge of flight parameters is needed, as with the MSR, to understand changes in crack growth rate for different usages.

### 3.3.6 ANALYSIS SCHEMES FOR TRACKING

Each of the four tracking procedures considered in this study requires a somewhat different analysis scheme. Procedures A and B both use analytical methods based on results of parametric studies. One uses parametric crack growth data; the other uses parametric stress exceedance data. Procedure C requires an analysis scheme to process the recorded MSR strain data to produce stress spectra for crack growth analyses. An alternate (simplified) approach might be used to compare measured MSR data to an analytical model to predict crack growth, thus, eliminating a crack growth analysis as part of the tracking program. Procedure D requires a scheme to review the gage readings, apply the appropriate transfer functions and present the data. The analysis schemes applicable to each of the tracking procedures and a demonstration of the use of parametric analyses results to predict potential crack growth will be discussed in the following sections.

#### 3.3.6.1 Parametric Crack Growth Rate Method

##### Basic Approach

The analysis scheme used for tracking Procedure A is depicted in Figure 61. The pilot log is the primary means of data acquisition. The pilot log is processed to determine the values of the usage parameter for each individual flight profile. Each mission is then divided into a number of operational phases such as climb, cruise, low level, etc.

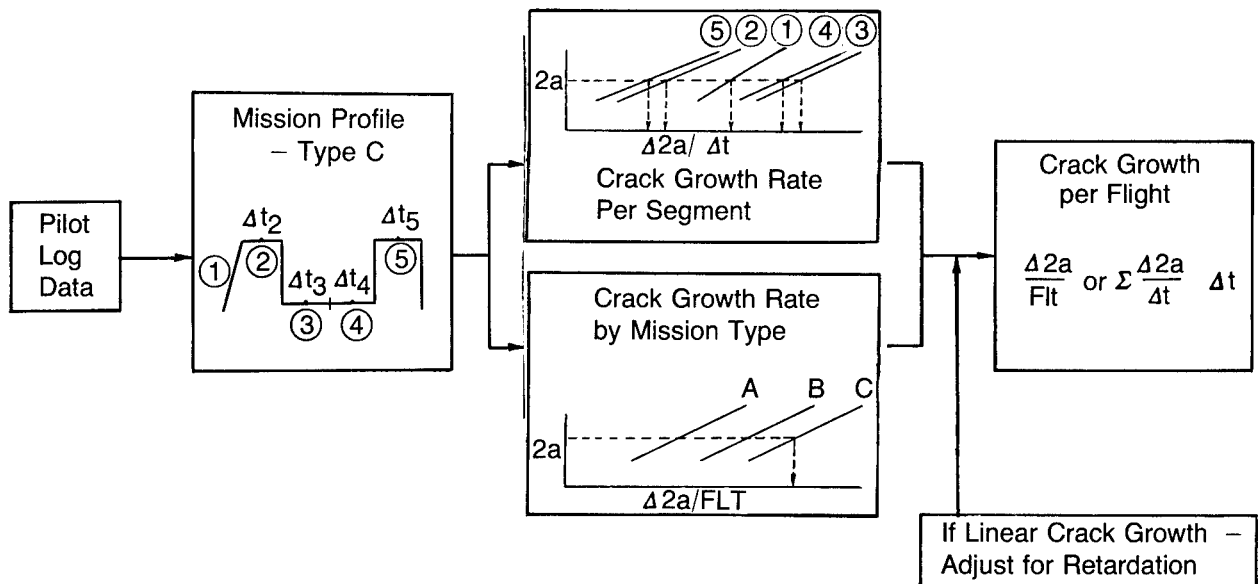


Figure 61. Analysis Scheme, Procedure A

Each operational phase is an assemblage of one or more flight segments having specific boundaries of gross weight, speed, altitude and/or other mission parameters as appropriate. These segments serve as building blocks for describing any mission. Knowing the crack length at the beginning of each flight the crack growth rate for each mission segment is determined. These crack growth rates are multiplied by flight duration,  $\Delta t$ , and accumulated. The summation of crack growth per segment yields the crack growth per flight. The resulting incremental crack growth for the flight is added to the crack length at the beginning of the flight to determine the current crack length.

##### Alternate Approach

An alternate approach to using mission segment crack growth rates is to determine total mission crack growth for different mission types. This method might be appropriate if the variation in fleet usage is minimal and/or if all of the missions flown can be defined. Crack growth rates are then calculated for these missions. Mission crack growth

is then determined by using the mission description defined by the pilot log and a mission categorization scheme to identify the appropriate crack growth rate as a function of the crack length at the beginning of the flight.

### Method

The results of the parametric and variability studies, Sections 2.7 and 2.8, will now be used to demonstrate the use of the parametric crack growth method to compute crack growth for typical transport/bomber type missions. The crack growth rates calculated during the parametric study were presented in Figures 26, 27 and 28 for the wing, body and fin locations, respectively. These rates were used to predict crack growth for each variable mission shown in Figure 32. The procedure used was to (1) select the parametric mission segments applicable to each mission profile by gross weight, (2) multiply the rates by the appropriate flight durations, (3) sum the crack growth rates as a function of crack length,  $2a$ , and (4) grow the crack by summing the crack growth for an appropriate increment of flights. The average gross weights and flight durations for each flight segment for the variable missions of Figure 32 are shown in Figure 62.

### Crack Growth By Summation Of Mission Segments

A mission crack growth calculation using the mission segment crack growth rates is depicted in Figure 63. This figure shows a comparison of crack length,  $2a$ , versus crack growth rate and crack life based on a summation of mission segments and on a cycle-by-cycle crack growth analysis (total mission analysis). Crack growth rates for each mission segment adjusted for flight duration are shown (upper plot) and the summation compared to the crack growth rate obtained from the total mission analysis. The crack growth rate obtained by summing the segments and an appropriate increment of flights was used to compute mission crack growth (lower plot) which is compared to a cycle-by-cycle analysis. Note that the summation of mission segments is very close (within 15 percent) to the total mission analysis.

A summary of the mission crack growth calculations for all variable missions by the summation of mission segment crack growth is shown in Figures 64, 65 and 66. These figures show a comparison of crack life from  $2a$  equal to 0.25 to 0.35 inch by the summation of mission segments versus total mission analysis. All of the analyses were conducted using the Wheeler Retardation Model with a shaping exponent,  $m$ , of 0.90. The results showed that for the wing analysis location, crack growth could be predicted within an average of about 12 percent of the total mission analysis. The body and fin results were within 20 and 8 percent of total mission analysis results, respectively. Crack growth predictions made using the summation of mission segments were conservative relative to the total mission approach.

### Approach Applied to Mission Mixes

The parametric crack growth method was also used to calculate crack growth for a typical mix of transport/bomber type missions. Mission Mix No. 2 (Section 2.8.4.1), comprised of a cruise mission (1B), a refueling mission (2B) and a low level mission (3A), was used to illustrate these calculations as depicted in Figure 67. As was illustrated in Figure 63, mission segment crack growth rates were summed to obtain mission crack growth rates. The mission crack growth rates, based on both the summation of mission segments and total mission analysis, were summed to obtain a mission mix rate based on the frequency noted and compared to results of a mission mix analyses (upper plot). Crack growth was then compared based on the summation of mission segments, total mission analysis and by mission mix analysis (lower plot). The calculation of crack growth using the total mission analysis and the mission mix analysis gave practically identical answers. This will be further illustrated with test results later. The crack growth based on summation of mission segments is shown to be approximately 15 percent conservative compared to the mission mix analysis.

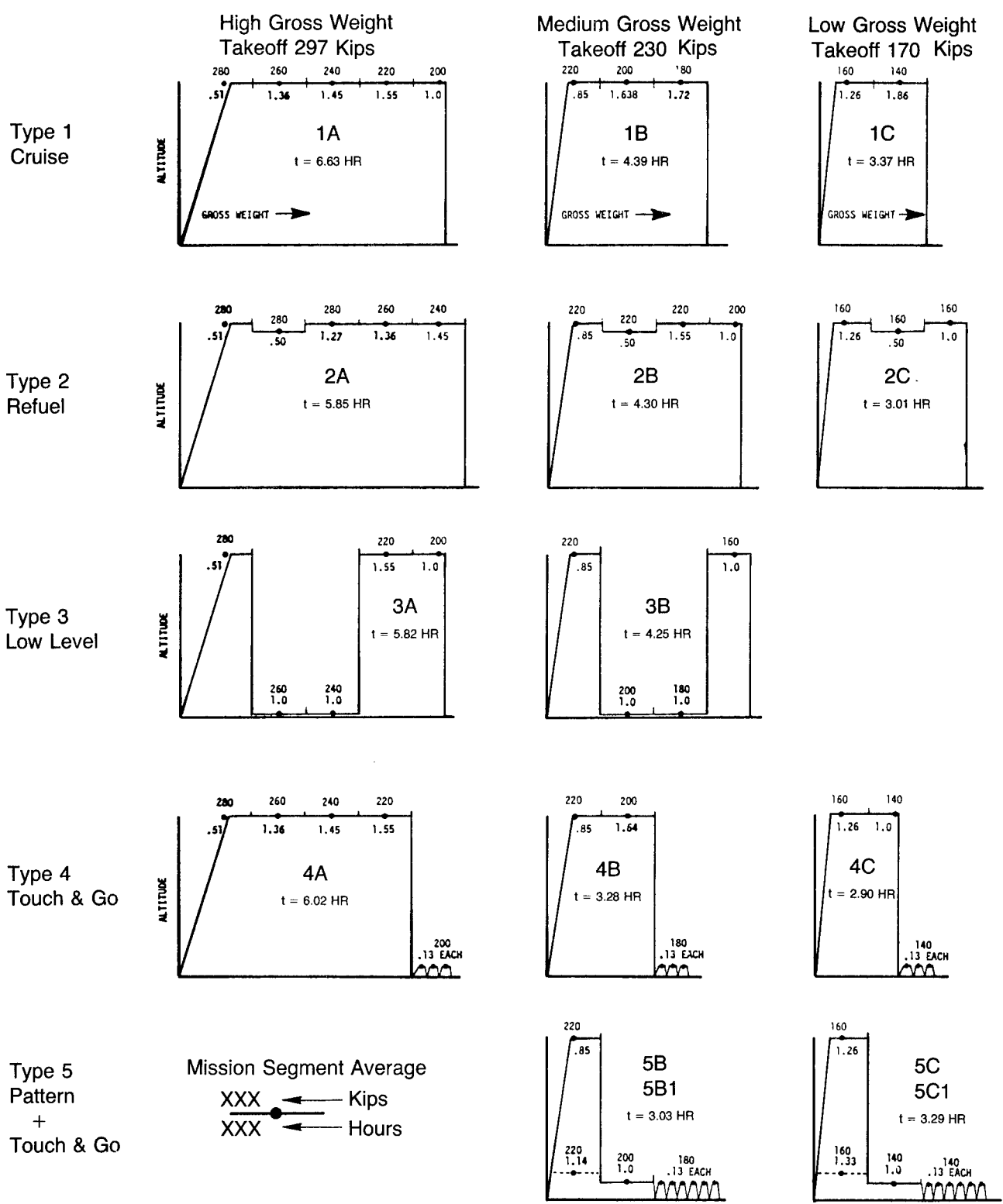


Figure 62. Average Gross Weights and Flight Durations for Variable Missions

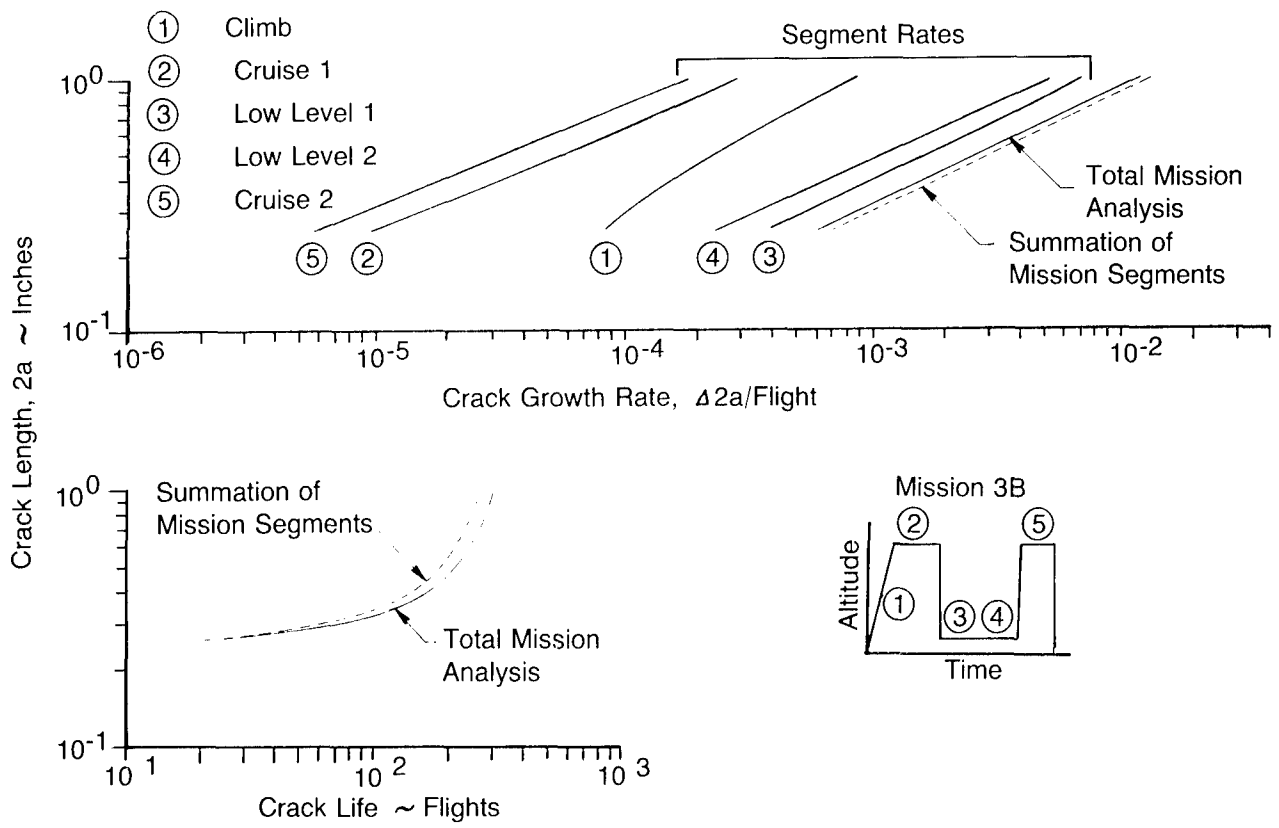


Figure 63. Comparison of Crack Growth By Total Mission Analysis and Summation of Mission Segments, Wing

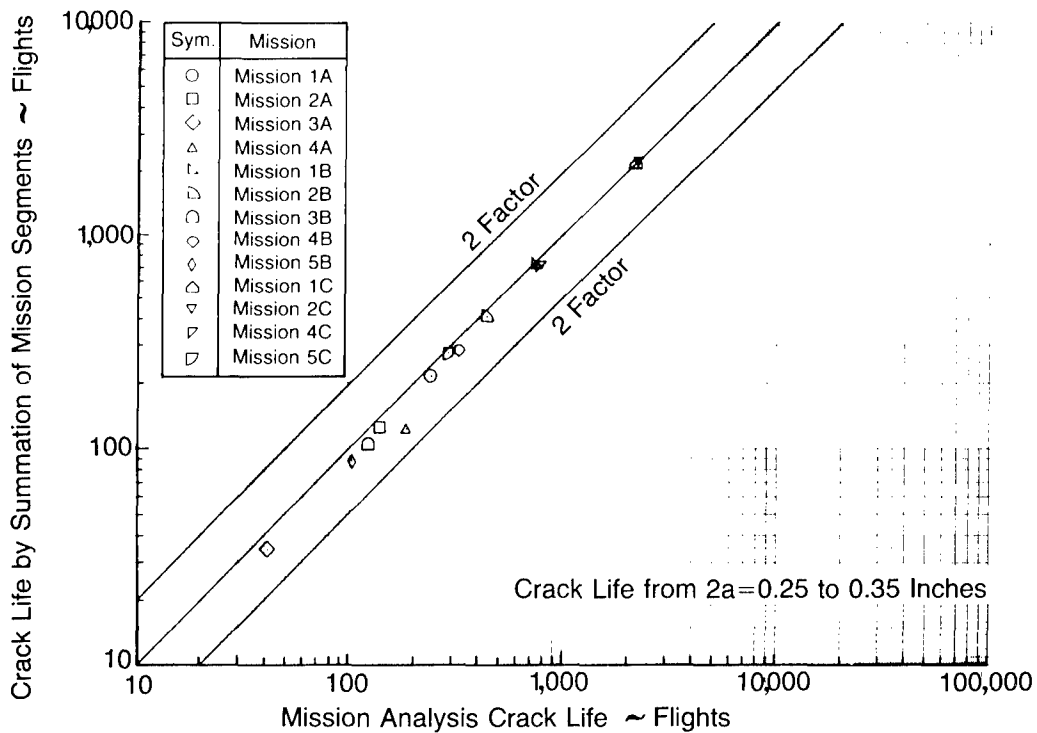


Figure 64. Crack Life by Summation of Mission Segments and by Total Mission Analysis, Wing

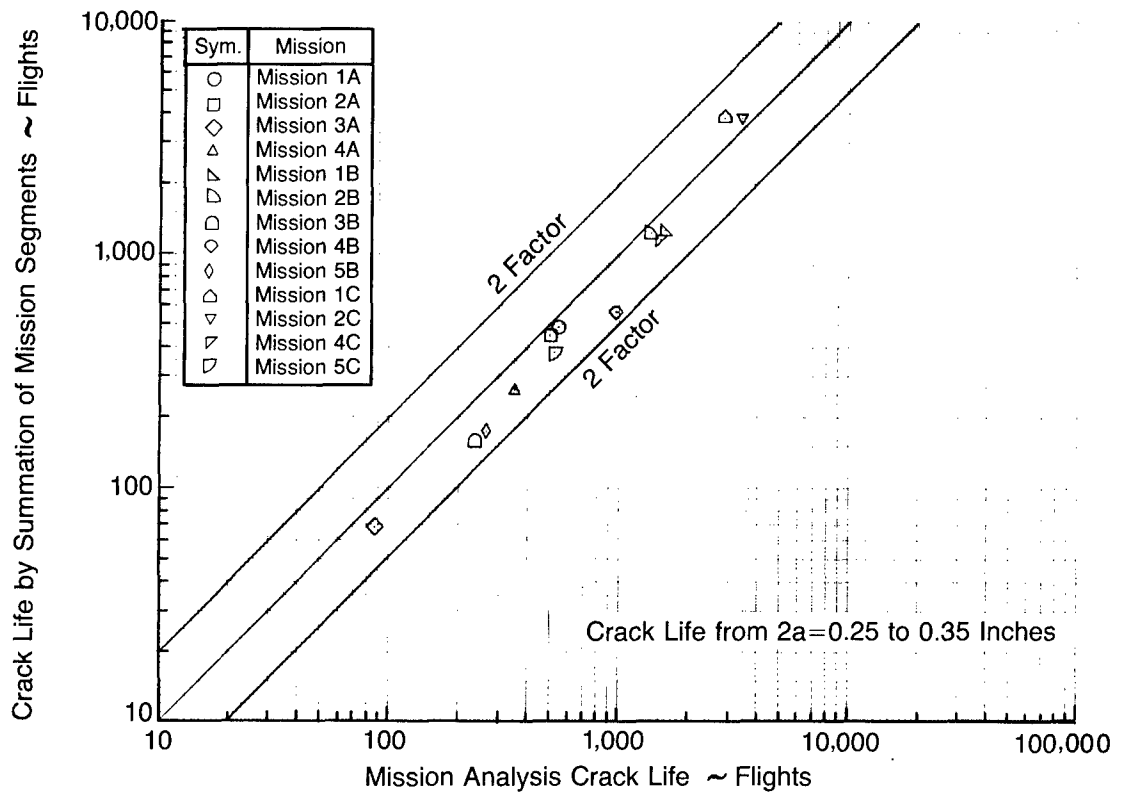


Figure 65. Crack Life by Summation of Mission Segments and by Total Mission Analysis, Body

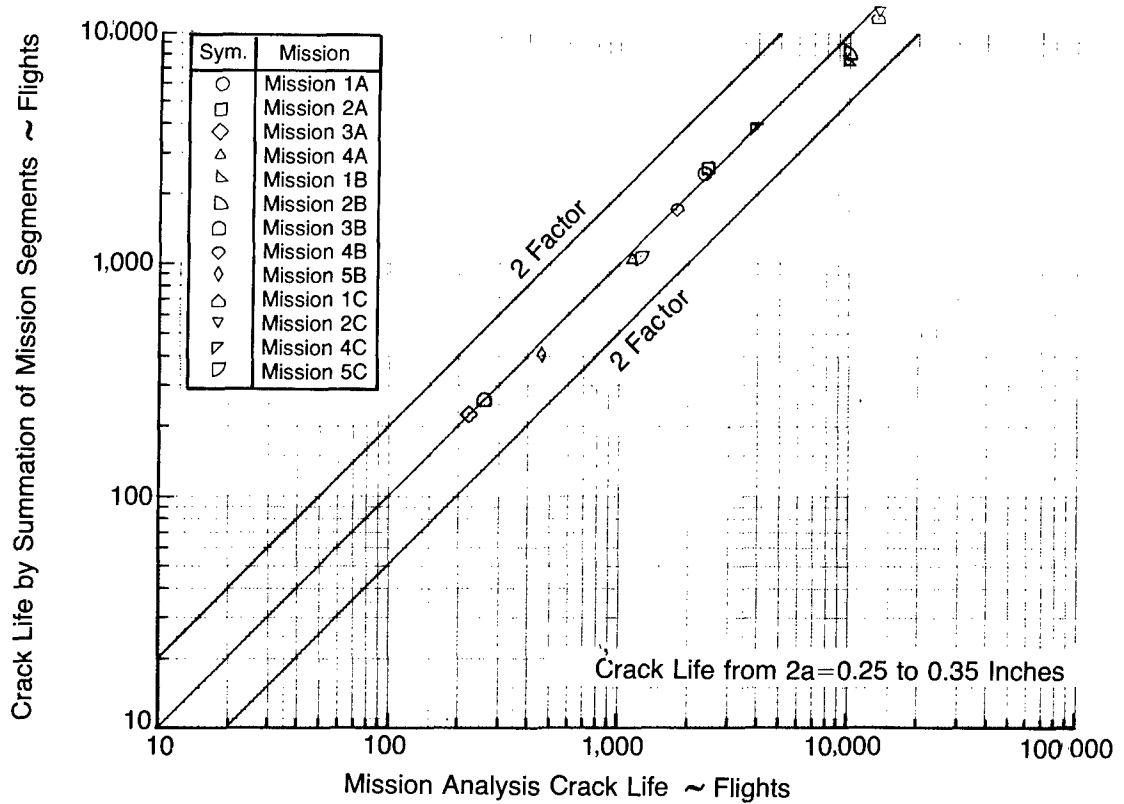


Figure 66. Crack Life by Summation of Mission Segments and by Total Mission Analysis, Fin

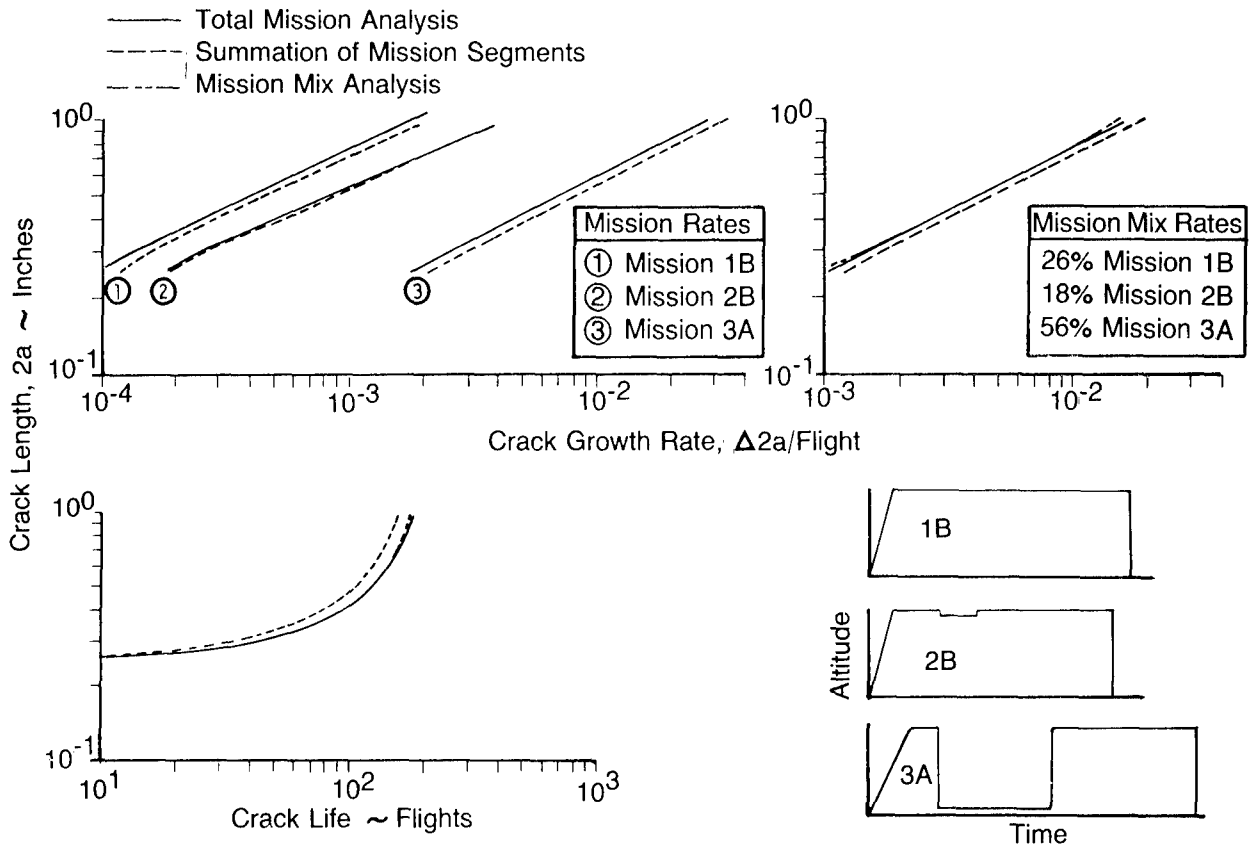


Figure 67. Comparison of Crack Growth by Mission Mix Analysis and Summation of Mission and Mission Segment Crack Growth Rates, Wing

An illustration of the predicted crack growth for Mission Mix No. 2 based on flight-by-flight crack growth analysis and based on the summation of individual mission crack growth rates, is shown in Figure 68. The dash line in the upper plot shows the change in crack growth rate on a flight-by-flight basis. A summation of frequency times individual mission crack growth rates as a function of crack length,  $2a$ , is shown by the solid line. The lower plot shows a comparison of the predicted crack growth using the rates in the upper figure.

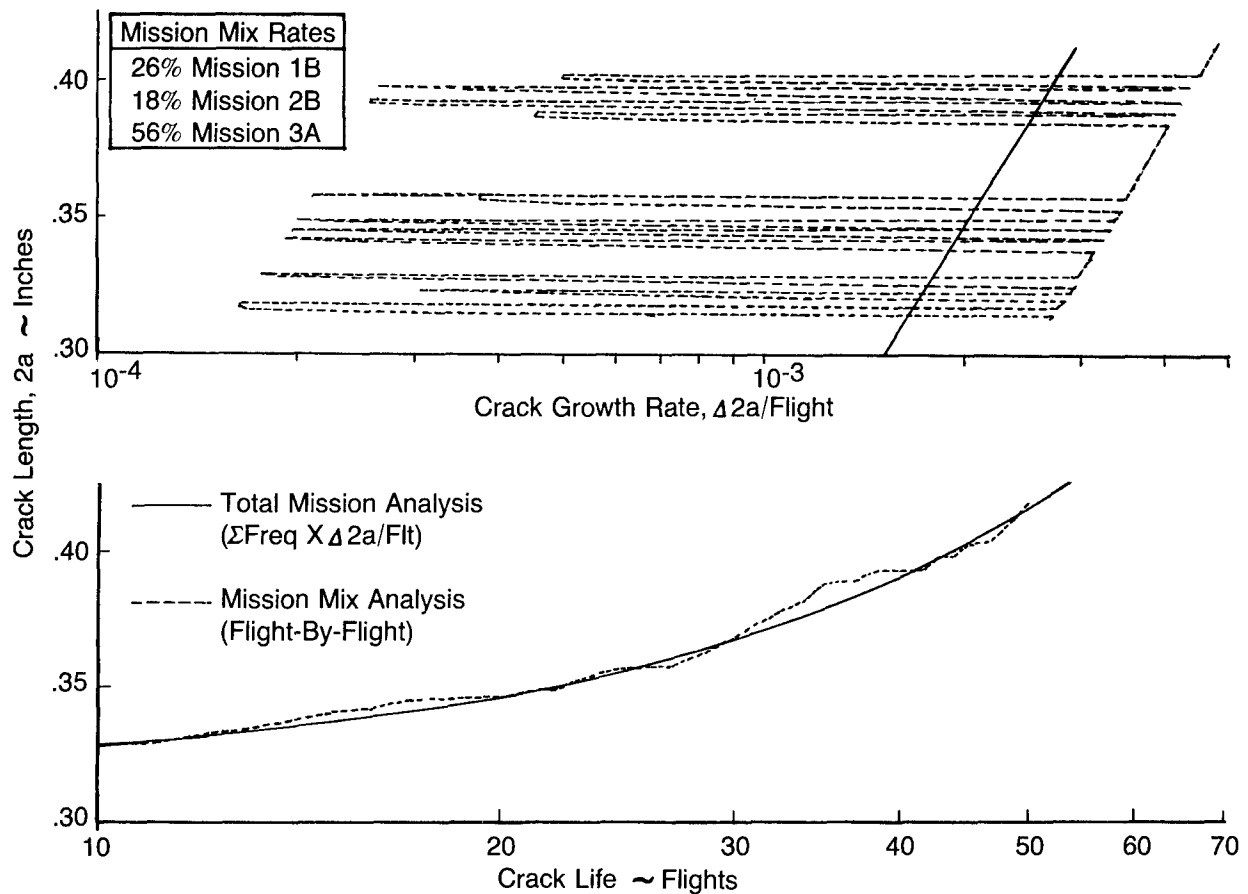


Figure 68. Estimated Mission Mix Crack Growth

The predicted crack growth illustrated in Figure 68 shows that if a particular usage consisting of a mission mix is known and the crack growth rates for each of the missions within the mix are known, an accurate estimate of the mission mix crack growth can be determined without a flight-by-flight analysis.

#### Test Verification

The use of individual mission crack growth to predict mission mix crack growth was verified from test results. The results of the verification tests of the two mission mixes discussed in Section 2.8.5 were compared to crack growth predictions using the crack growth rates determined from the individual tests of the missions that comprise each mix. The two mixes were comprised of variable missions 3A, 1B, 2B and 4B. Figure 69 shows the results of comparisons made. The crack growth predicted by test for the four missions is shown in the uppermost plot. These data were used to determine the mission crack growth rates shown in the second plot. The third plot shows the mission mix crack growth rates which were determined by summing the product of the mission crack growth rates and the frequency for each mix as a function of crack length,  $2a$ . These rates were then used to predict mission mix crack growth which is compared to test results in the last plot. Results were within eight percent.

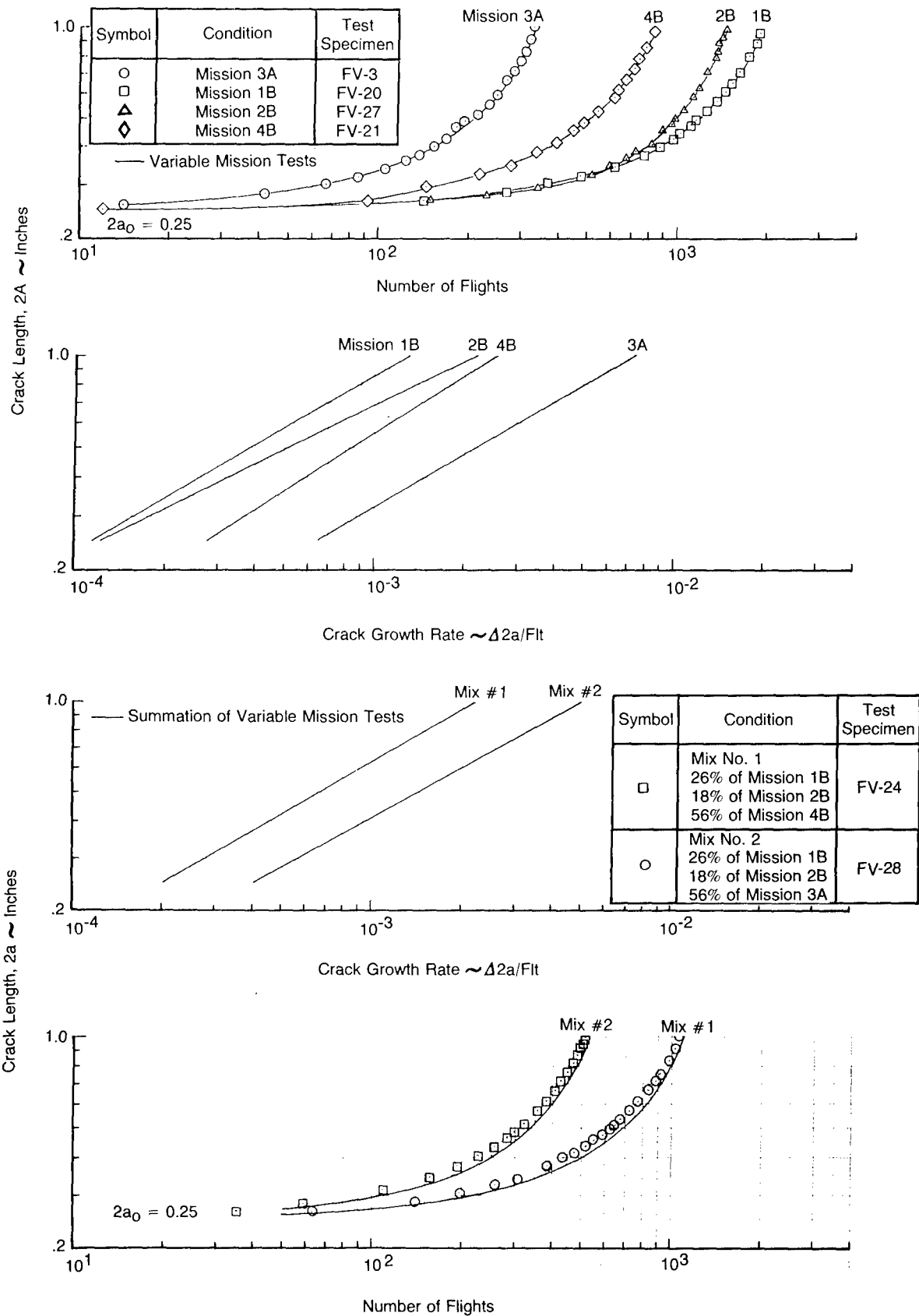


Figure 69. Individual Mission Crack Growth Rates to Predict Mission Mix Crack Growth Using Test Results

The results of these comparisons show that mission mix crack growth can be accurately predicted from individual mission crack growth rate data. Test results indicate that the accumulated effects of retardation from the summation of individual mission crack growth is nearly the same as the retardation produced by the mission mix spectrum.

The parametric crack growth method, such as that demonstrated in this study, appears to be an excellent method for predicting potential crack growth in transport/bomber fleet aircraft.

The usage blocks which describe the specific gross weight, speed and altitude conditions (flight segments) for which unit crack growth rates are determined, should be sized, so that recorded data from the Loads/Environment Spectra Survey (L/ESS) Program can be utilized as means to update the crack growth rate data used in the IAT Program. The L/ESS system will be installed on 10 to 20 percent of a fleet as part of the Aircraft Structural Integrity Program (ASIP) for the purpose of monitoring stresses experienced in actual service at specified structural locations (monitored locations). When sufficient L/ESS data has been accumulated or convergence in the data has been achieved for the selected usage blocks, these data should be interfaced with the analyses that support the IAT Program for the purpose of updating the crack growth rate data.

### 3.3.6.2 Parametric Stress Exceedance Method

The analysis scheme used for Tracking Procedure B is depicted in Figure 70. The pilot log, as with Procedure A, is the primary means of data acquisition. Procedure B is similar to Procedure A except that mission segment data used as building blocks for describing any mission is in the form of stress exceedance data rather than crack growth rates. Knowing the mission usage parameters described on the pilot log, the mission is divided into flight segments and an assemblage of sequenced stress exceedance data is defined. These data are adjusted for flight duration and used to define the complete stress spectrum for the mission. This spectrum is then used to calculate mission crack growth.

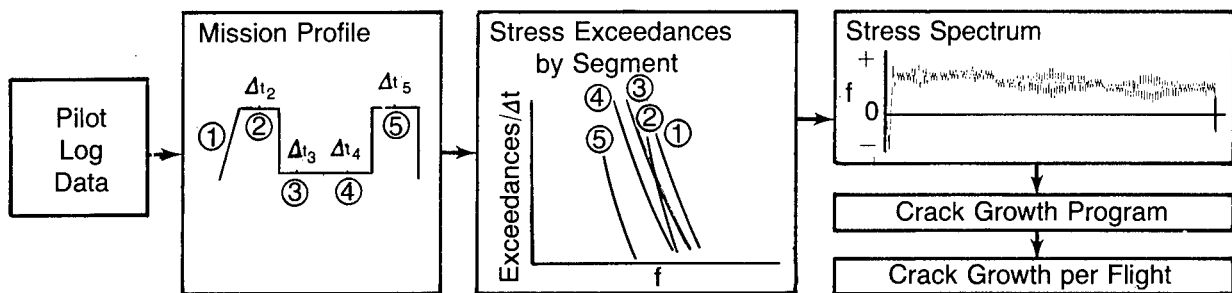


Figure 70. Analysis Scheme, Procedure B

In this analysis scheme, a routine similar to the sequence generator program, Section 2.2.4, must be incorporated in the tracking program to convert the stress exceedance data into a specified sequence of stress occurrences. In addition, the analysis methods selected for calculating crack growth including the retardation model and the appropriate crack growth rate data (either in equation or tabular form) must be programmed.

The crack growth results using this scheme would be comparable to the total mission analysis crack growth predictions of the previous section. The advantage of this scheme is that this method will allow proper load sequencing and the retardation of crack growth in all mission segments as a result of the peak spectrum stress.

Procedure B, as with Procedure A, should utilize the recorded data from the L/ESS Program to systematically update the parametric data (stress exceedance tables) used in the IAT Program.

### 3.3.6.3 Mechanical Strain Recorder Method

The analysis scheme used for tracking Procedure C is depicted in Figure 71. The Mechanical Strain Recorder (MSR) is the principal means of data acquisition. The MSR data, which is recorded on a metallic tape, must be processed to transform the strain data into a form for input into the computer tracking program. These data can then be reduced into several forms, i.e., a sequence of cycle-by-cycle stresses per flight, blocks of cycles of the same stress amplitudes or accumulated to define a composite stress exceedance curve for a specified usage period. The first two forms of data presentation are used with an analytical crack growth model to predict mission crack growth. A routine to transform the recorded data into either a cycle-by-cycle or blocks of cycles type of stress spectrum for crack growth analysis must be programmed. The latter form of data presentation, e.g., a composite stress exceedance data format, would be compared to analyses representative of various severities of usage to identify crack growth for the usage period. This approach can be called a simplified approach because a flight spectrum does not have to be defined nor does a crack growth analysis have to be performed. The following paragraphs will discuss this approach.

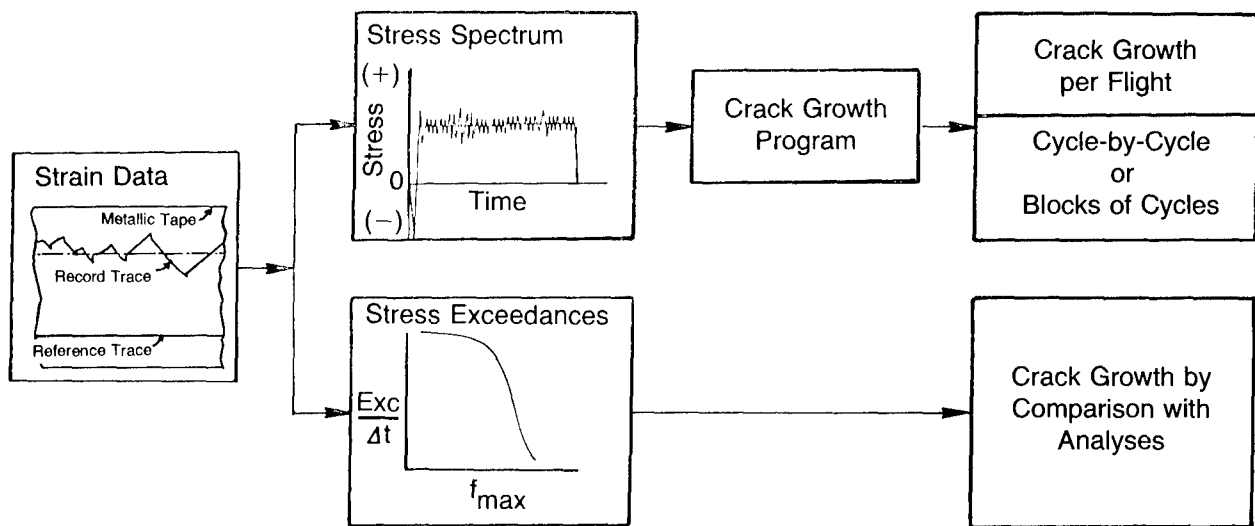


Figure 71. Analysis Scheme, Procedure C

#### Simplified MSR Approach

A simplified MSR or usage model approach has been proposed for the F-16, Reference 12, to reduce tracking costs while still delivering an adequate level of accuracy. In the simplified MSR approach, a number of stress exceedance curves must be defined to represent a usage model that describes the range in expected variations in fleet usage. For each usage model a flight-by-flight stress history would be generated and a crack growth analysis conducted. The MSR data for a current usage period would be reduced to a composite stress exceedance format. In theory, the usage model providing the closest match to the actual recorded data would be a measure of the usage severity and its associated crack growth curve would be used to predict the crack growth increment for the usage period.

To develop the usage model for the simplified approach, a mission matrix similar to that defined for the variability study (Figure 32) must be defined. From this matrix, a set of exceedance curves representing the variation in fleet usage is developed. Figure 72 shows the development of the stress spectrum for a mission consisting of low level operation. The mission profile is divided into five segments representative of climb, cruise and low level. Each of these segments represents a specific gross weight, speed and altitude at a constant 1g stress level. The calculated stress exceedance curves for each mission segment are shown in the lower right-hand portion of Figure 72. These data are used to define the stress spectrum (upper right) used for crack growth calculations and also used to derive the composite stress exceedance curve for the entire flight (lower left). A set of composite stress exceedance curves and associated crack growth could similarly be constructed for a number of mission profiles which encompass the expected usage variations in the fleet.

Stress Exceedance Representation:

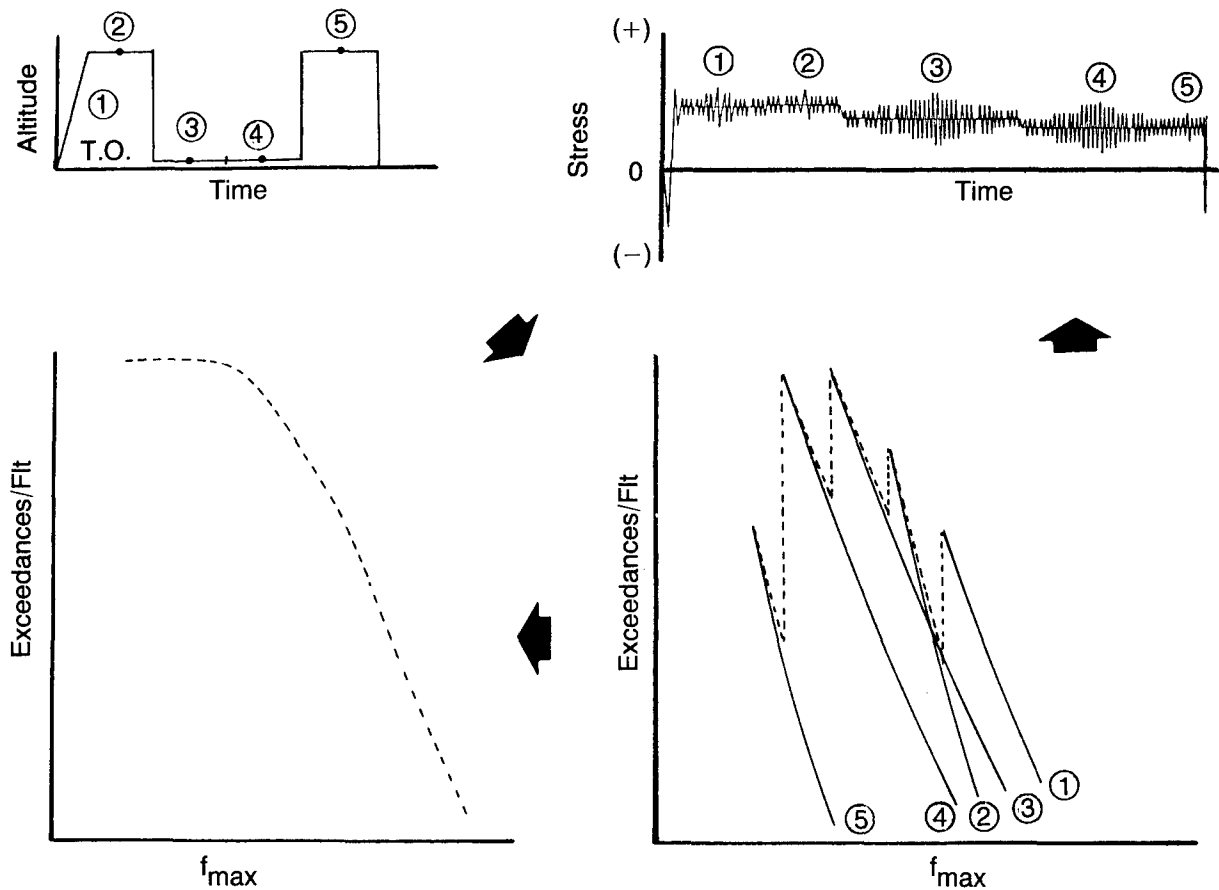


Figure 72. Composite Stress Exceedance Representation

The simplified MSR analysis scheme is shown in Figure 73. Composite exceedance curves are defined for severe and benign usages for several takeoff gross weights. A distinction is also made for long versus short flight durations. Each curve represents the stress history for a selected number of usage flight hours, i.e., 100 hours. These curves must cover the complete range of usage variations. As shown in the chart, the stress exceedance data, or usage model, varies considerably with takeoff gross weight, spectrum severity and mission duration. The curves shown were derived from data used in the variability study of Task 1 of this study. The associated crack growth curves (long flight duration only) are shown in the lower right-hand portion of the figure.

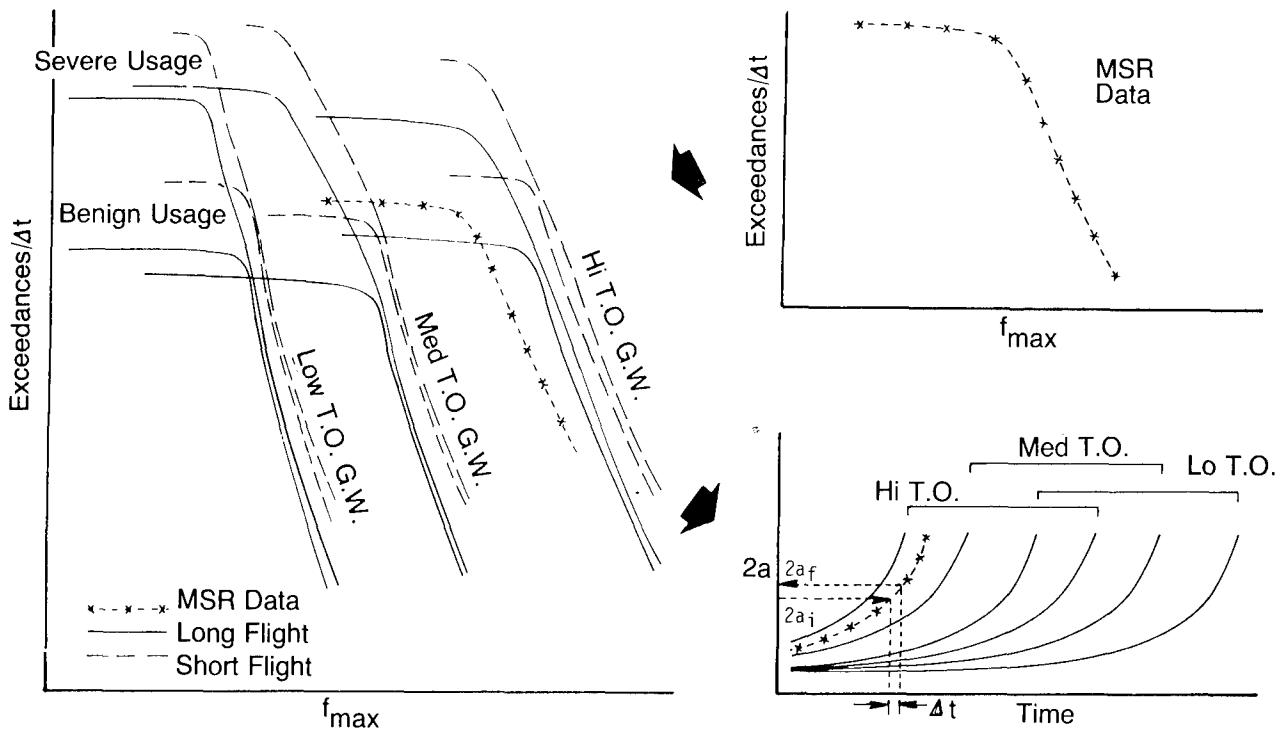


Figure 73. Simplified MSR Analysis Scheme

The data recorded by the MSR is reduced in the form of a composite stress exceedance curve for a given usage period. These data are then normalized to agree with the analysis usage period time. The MSR data is then superimposed onto the analysis usage model and a scheme is used to identify the usage severity and the associated crack growth increment using the crack length at the beginning of the period as depicted in the figure.

The simplified MSR approach, as depicted in Figure 73, may be significantly more involved for a transport/bomber aircraft than for a fighter aircraft. For the transport/bomber this approach may actually be "complex" depending on the variation in fleet usage that might have to be considered. The transport/bomber aircraft experiences much greater variations in gross weight, flight duration and mission activities than does the fighter aircraft. This means that the stress exceedance data which comprises the usage model can be much more complex.

From the investigation conducted of the simplified MSR approach, it was shown that a scheme to identify crack growth by superimposing the MSR data onto the usage model might be complicated. It was also observed that for each of the takeoff conditions, an exceedance curve representative of different usage severities and flight durations can produce the same incremental crack growth. Also, activity during the latter portion of a flight, which may affect crack growth, is masked in the composite exceedance curve and hard to identify. The use of the simplified MSR approach as a transport/bomber tracking method must be studied further to identify less complicated analysis models (i.e. based on predicted usage) and/or better identify the usage parameters which will permit the prediction of crack growth by comparison. The approach must be verified by analyses and test results.

Regardless of the manner in which the MSR data is used, i.e., cycle-by-cycle crack growth or simplified MSR approach, having aircraft with L/ESS instrumentation will allow periodic checks between the two sources of recorded data. Also, when significant or perhaps unexpected changes in stress history occur, some form of pilots log would be helpful in identifying the attendant usage change.

### 3.3.6.4 Crack Growth Gage Method

The analysis scheme associated with Tracking Procedure D may well be the least complicated of any of the procedures studied and is depicted in Figure 74. The crack growth gage provides a direct method for assessing crack growth and the rates of crack growth as a function of usage. All of the normal data reduction required when other instrumentation systems are used to determine potential crack growth is eliminated when the crack growth gage is used.

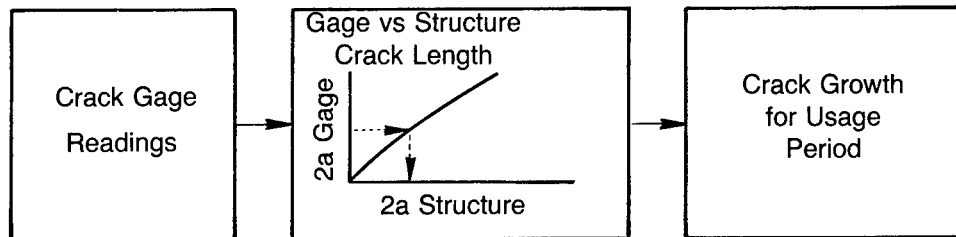


Figure 74. Analysis Scheme, Procedure D

Use of the crack growth gage requires that a relationship be defined between the observed crack length in the attached gage and another defect located elsewhere in the structure. This relationship should be relatively insensitive to stress history when both the gage and structural member experience the same loading. Calculation schemes can be developed to relate gage crack length to the predicted crack growth behavior at distant structural locations. Periodic readings of the gage will give the accumulative crack growth. The difference in readings from one period to another indicates crack growth rate.

A potential drawback of the crack growth gage is that it provides a limited amount of information if major usage changes are not adequately sensed by the aircraft's crack growth gages. Aircraft with the Loads/Environment Spectra Survey (L/ESS) instrumentation will allow periodic cross correlation between the data accumulated from the two sources. Also, the use of pilot logs to obtain a knowledge of flight parameters is still advisable to understand changes in crack growth rate due to usage changes.

### 3.3.7 ACCURACY OF RESULTS

An important aspect in the development of any tracking program is the accuracy attainable. Depending on the tracking program selected, the tracking data may be taken directly from recorded data, i.e., from the MSR or crack growth gage, or from predicted stresses based on information obtained from a pilots log.

The latter method depends on accurate information from the pilot's log about each mission flown by an aircraft being used in the best state-of-the-art analysis methods to predict potential crack growth. The analysis methods used must be verified by tests and provide adequate reliability in predicting crack retardation as a function of spectrum content.

Tracking methods which use recording devices to obtain tracking information depend on a high percentage of data being recovered and on appropriate transfer functions and analysis methods to transform the data into meaningful tracking information. Considering all of the differences between various tracking procedures, quantifying the accuracy of one method relative to another is difficult. However, the accuracy attainable using the analysis methods selected for this study will be addressed in the following sections.

### 3.3.7.1 Mission Analyses Versus Verification Test Results

Crack growth predictions made during the parametric and variability studies of Task 1 were verified by tests. Preliminary analyses and tests were first performed to select an analytical crack growth model to be used in this study. It was evident from the results of these analyses and tests, Figure 19, that none of analysis models examined could consistently predict crack growth for all spectra. The Wheeler Retardation Model with a shaping exponent,  $m$ , of 0.90 seemed to produce the best overall predictions and was selected for this study.

Experimental verification tests of mission spectra, Figure 49, indicated a scatter in test life to predicted life to vary, for the most part, from .75 to 2.71 for the mission spectra tested. From these results it is evident that depending on fleet usage variability, some more advanced retardation models should be used to make crack growth predictions. This study did show that for the typical type of missions flown by the KC-135A tanker (baseline aircraft), crack growth predictions could be made within a  $\pm 1.5$  factor of test life using the selected analysis model. The KC-135A usage does not include the low level missions typical of bomber operations. The use of linear crack growth analyses (no retardation) with properly defined retardation factors applied based on usage and defined by tests, could presumably produce the same accuracy as using a retardation model. However, more testing may be necessary to develop the retardation factors.

### 3.3.7.2 Total Mission Analysis Versus Crack Growth by Summation of Mission Segments

Estimates of mission crack growth were made using the mission profiles developed during the variability study (Section 2.8) and the segment crack growth rates derived during the parametric study (Section 2.7). The results of these analyses were presented in Figures 64, 65 and 66 for the wing, body and fin analysis locations, respectively. A comparison of the crack growth predictions using a summation of mission segment crack growth rates (Tracking Procedure A) with total mission spectra analysis (Tracking Procedure B) showed that, on the average, the predicted life using mission segments was conservative by 12, 20 and 8 percent for the wing, body and fin locations, respectively. In all cases it would be expected that crack growth by summation of mission segments would be conservative relative to total mission spectra analyses since the retardation resulting from peak loads cannot be accounted for in all mission segment crack growth rate values. It is emphasized again that accuracy in predicting crack growth will vary with the variability in fleet usages and the analysis methods selected to account for retardation as a function of spectrum content.

The use of linear (nonretarded) crack growth analyses to derive mission segment crack growth rates will produce the same crack life predictions for either a summation of segments or total mission analysis. The results can then be adjusted for retardation.

### 3.3.7.3 Mechanical Strain Recorders

This study did not provide a rational means of quantitatively evaluating the accuracy of the MSR relative to the other tracking procedures. However, assuming consistent recovery of a high percentage of usable strain data, it is believed the MSR procedure will, at the present time, produce the most accurate estimates of crack growth of any of the systems investigated.

### 3.3.7.4 Crack Growth Gage

As part of the present study, several Boeing designed crack growth gages were installed on ten verification test specimens to obtain crack growth gage response data to typical transport/bomber usage variations. The test instrumentation, procedures and test results for this contracted work are presented in Reference 13.

Typical results of the verification tests conducted with crack growth gages installed are shown in Figures 75 and 76. Eight gages were installed on each specimen as shown in the figures. Only the gage readings for the gages at the top of the specimens are shown in these illustrations. Figures 75 and 76 show the crack growth gage and specimen readings for tests of wing spectra for Missions 3A and 3B, respectively. The repeatability of the gage responses was good but a difference in response was seen from one side of the specimen to the other due to bending effects. The most significant observation seen from all the tests conducted was that the relationship between gage and specimen crack growth was highly dependent on spectrum content as illustrated in Figure 77. Additional development of the Boeing crack growth gage is needed before this gage can be considered a viable data acquisition device.

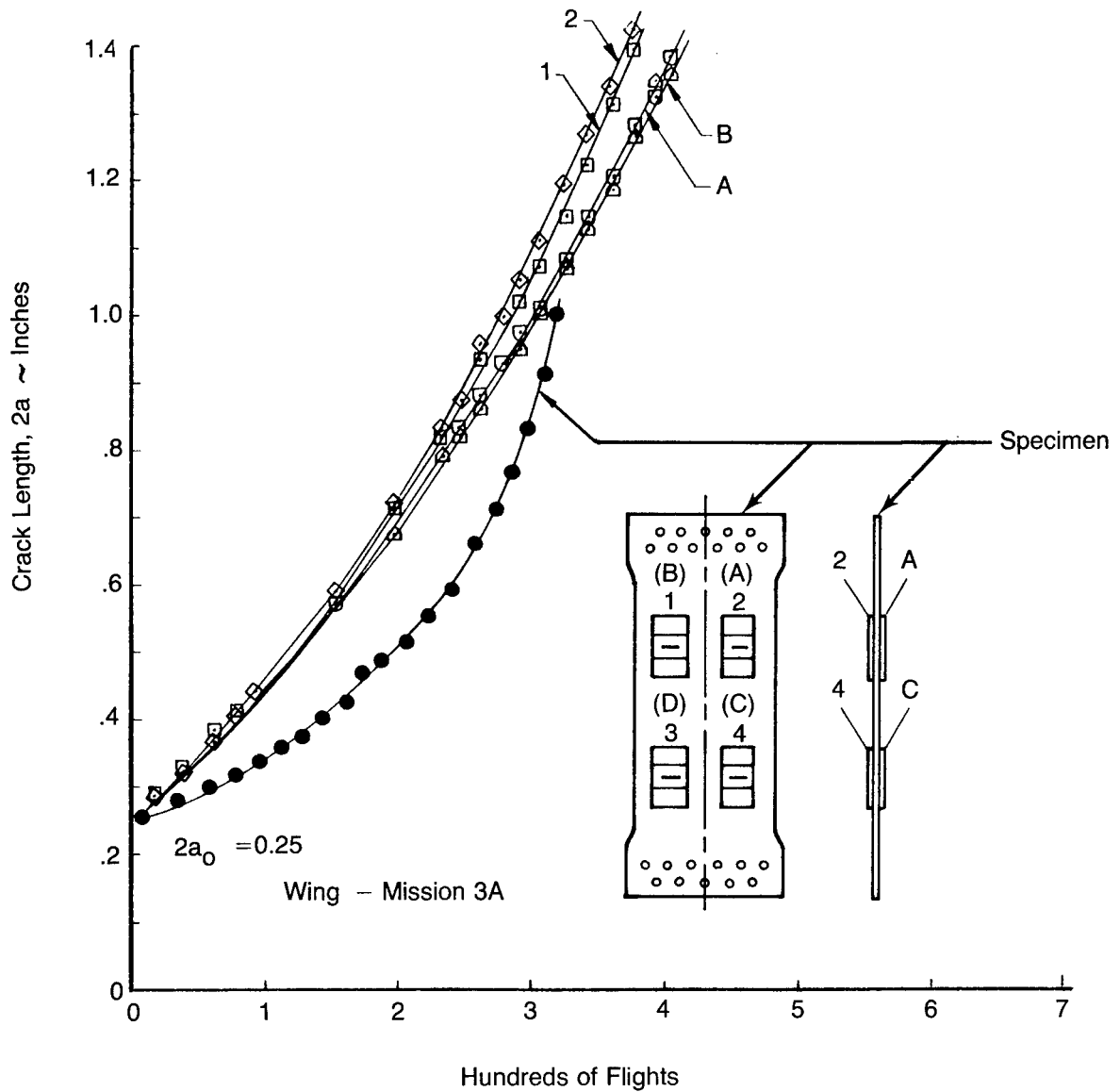


Figure 75. Crack Growth Gage Test Results, Wing, Mission 3A Spectra

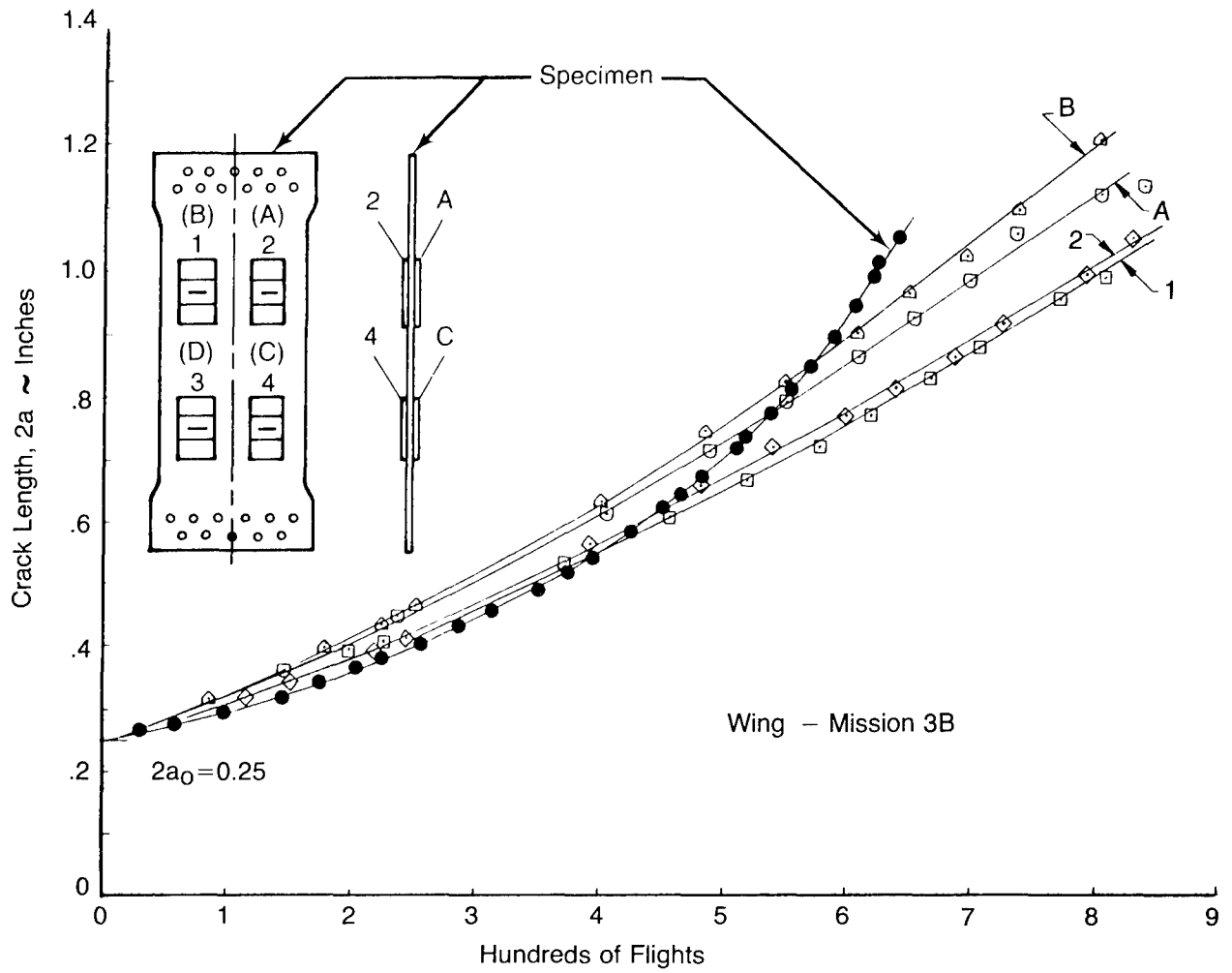


Figure 76. Crack Gage Test Results, Wing, Mission 3B Spectra

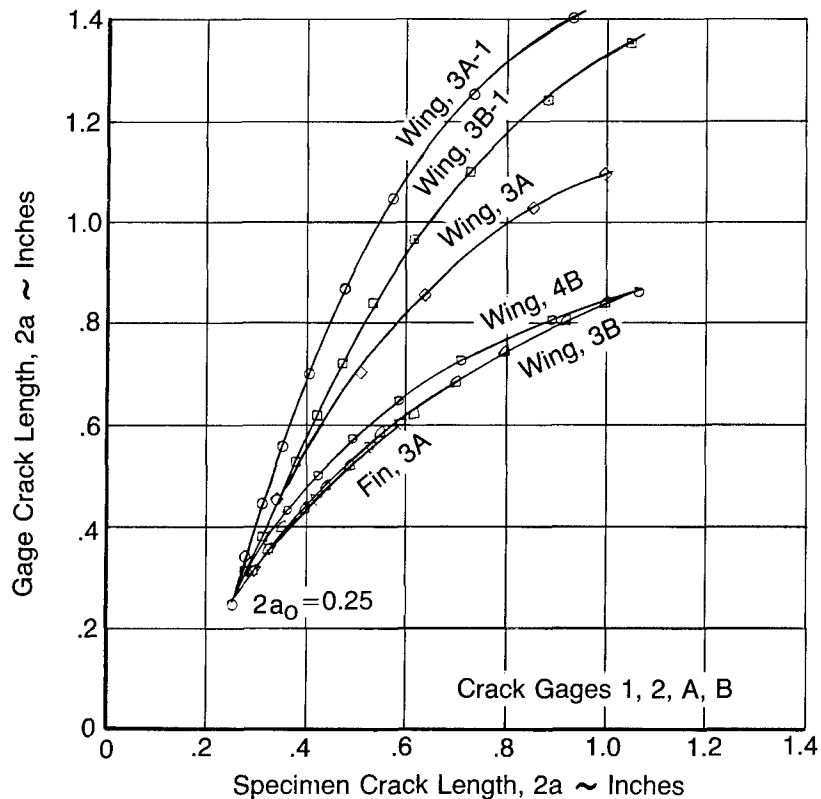


Figure 77. Crack Growth Gage Test Results, Gage Crack Length Versus Specimen Crack Length

### 3.3.8 ADVANTAGES AND DISADVANTAGES OF TRACKING PROCEDURES STUDIED

There are advantages and disadvantages inherent with any tracking procedure to be implemented in the fleet. Some of the advantages and disadvantages relative to accuracy and/or complexity of each of the tracking procedures studies are summarized in Table 13.

Procedure A, which uses the pilot log and parametric crack growth rates, is a simple method and is an extension of current tracking programs. However, this method uses predicted stresses and does not rigidly account for sequencing or delay effects relative to the placement of the peak stresses and retardation carry-over from segment-to-segment or flight-to-flight.

Procedure B, which uses the pilot log and parametric stress exceedance data, does allow for sequencing but uses predicted stresses and requires that a crack growth calculation be made for each flight.

Procedure C, which incorporates the mechanical strain recorder (MSR), will account for real stresses, sequencing and peak loads. Major disadvantages include the extensive instrumentation, data reduction and the crack growth analyses using a cycle-by-cycle or blocks of cycles approach. If a simplified MSR approach were possible, then the crack growth analyses are eliminated but the effects of sequencing and peak loads are no longer accounted for.

Procedure D, which utilizes the crack growth gage, like the MSR, responds to the real environment, so essentially experiences representative stresses, delay, sequencing and peak loads. Correlation between gage and

structure crack growth must be established, however. Testing of a Boeing designed crack growth gage as part of this contract indicated that more development was needed before a satisfactory gage-to-structure relationship which is independent of spectrum content can be defined.

TABLE 13.  
TRACKING PROCEDURES – ADVANTAGES AND DISADVANTAGES

Tracking Procedure	Advantages	Disadvantages
A	<ul style="list-style-type: none"> <li>– Simple</li> <li>– Extension of Current Monitoring Techniques</li> </ul>	<ul style="list-style-type: none"> <li>– Uses Predicted Stresses (Avg)</li> <li>– No Real Sequencing</li> <li>– No Real Delay</li> </ul>
B	<ul style="list-style-type: none"> <li>– Allows for Sequencing</li> </ul>	<ul style="list-style-type: none"> <li>– Uses Predicted Stresses (Avg)</li> <li>– Crack Growth Analysis Required After Each Flight</li> </ul>
C	<ul style="list-style-type: none"> <li>– Real Stresses</li> <li>– Allows for Sequencing</li> <li>– Effect of Peak Loads included</li> </ul>	<ul style="list-style-type: none"> <li>– Extensive Instrumentation</li> <li>– Extensive Data Reduction</li> <li>– Crack Growth Analysis Required After Each Flight</li> </ul>
D	<ul style="list-style-type: none"> <li>– Responds to Real Stresses</li> <li>– Real Delay Included</li> <li>– Real Environment</li> <li>– Allows for Effects of Sequencing</li> <li>– Allows for Effects of Peak Loads</li> </ul>	<ul style="list-style-type: none"> <li>– Correlation Between Gage and Structure Must Be Determined</li> <li>– More Development Needed</li> </ul>

### 3.3.9 APPLICATION OF RESULTS TO AIRCRAFT TRACKING

The purpose of tracking crack growth is to provide a rational basis for the inspection, modification and/or retirement of inservice aircraft. Economic limits are associated with the time to repair or modify an aircraft, while safety limit are associated with actions to prevent a catastrophic failure of an aircraft. Inspection intervals are associated with either the economic or safety limit. The following paragraphs discuss critical locations and derivation of tracking information needed to make force management decisions.

#### 3.3.9.1 Control Points

The generalized tracking procedures and associated analysis schemes considered in this study are applicable to all major structural locations. Regardless of the procedure implemented, a control point, or structural location selected as the site for monitoring, should be identified. Preferably, if critical details exist on each major component, a control point for each component should be selected. If stress spectrum content varies significantly within a given component, more than one control point will be needed.

The critical locations or details on each major component are identified by considering structural geometry, test results and/or Durability and Damage Tolerance Analysis (DADTA) studies. The time to Economic Repair Limit (ERL) and safety limit are then determined for each of the critical details based on a selected baseline usage. The number of critical areas that can be monitored using tracking data generated at a single control point depends on

deriving the appropriate transfer functions that will account for differences in (1) crack growth limits associated with the force structural maintenance plan, (2) structural geometry, (3) stress history and (4) the individual aircraft usage. It is obvious that small variations in these variables will contribute to more accurate crack growth predictions for a fleet of airplanes.

Normalized crack growth curves may be used to help identify or select control points and the locations that can best be related to a single control point. Figure 78 is an illustration of the wing lower surface of the baseline airplane and the normalized crack growth curves for two structural locations, one inboard, the other outboard of the production break. Each location might be selected as a control point. The normalized crack growth curves show the relationship between crack length and life. For any particular set or group of structural locations to be considered compatible with a given control point, normalized crack growth curves should show little variation with changes in usage between that of the control point and details to be monitored by the control point. The example curves shown in Figure 78 show significant variations between the two locations but little variation due to small changes in detail geometry and/or spectrum differences at each control point location. The normalized crack growth curve can be used to establish the percent life expended (economic or safety) at each control point and related details.

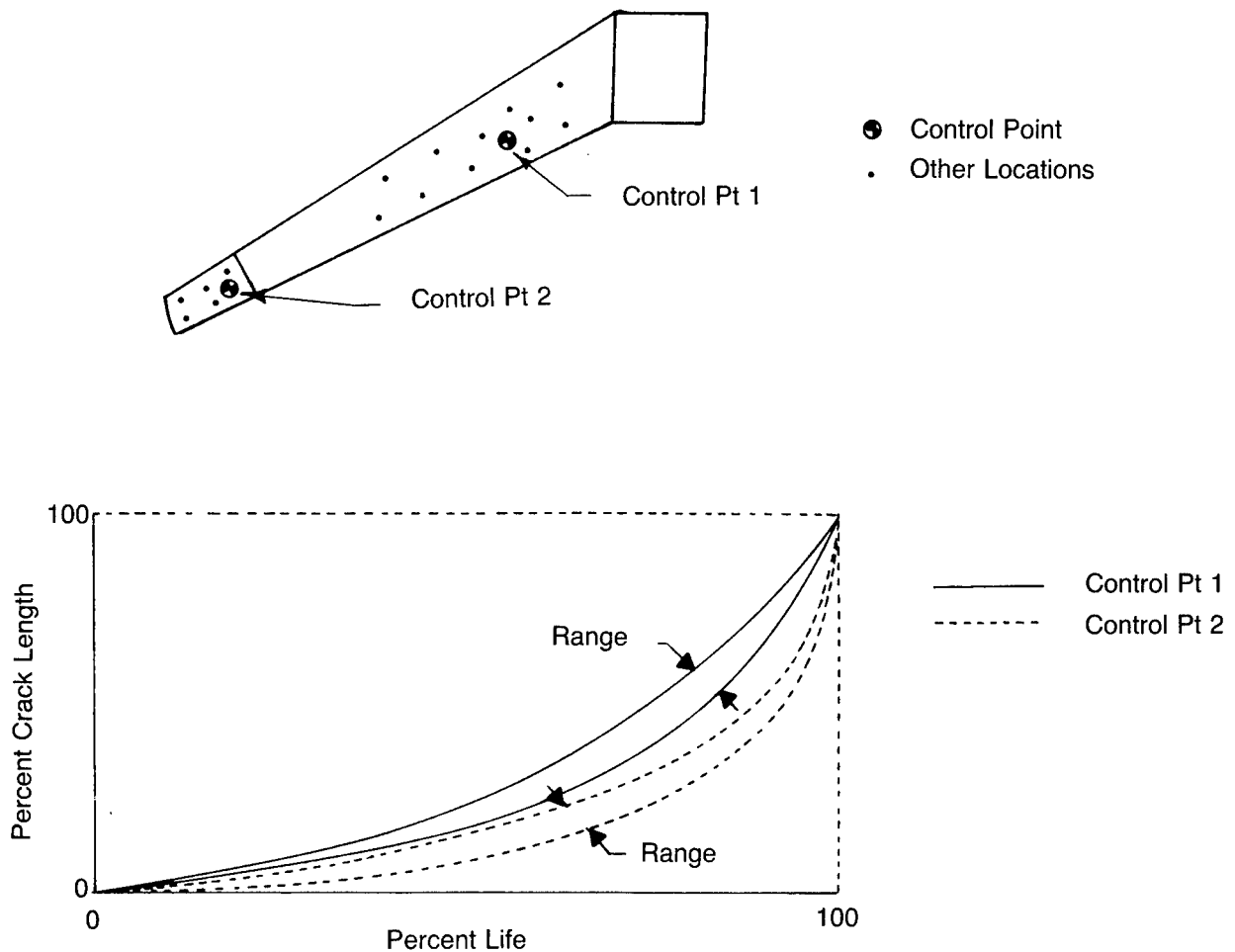
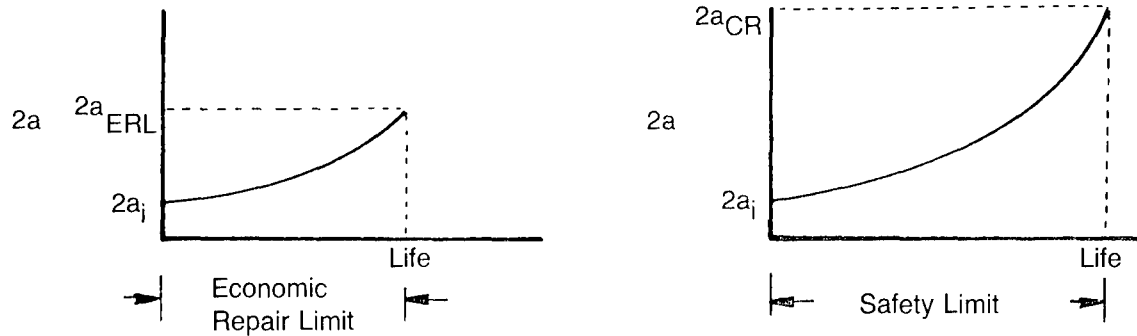


Figure 78. Normalized Crack Growth Curves

### 3.3.9.2 Derivation of Tracking Data for Force Management

#### Crack Length Definitions

Crack length and predicted life remaining until economic repair limit and safety limit should be monitored at each control point and related location. The economic and safety limits to be determined for each detail are illustrated below. The initial crack length,  $2a_i$ , for the economic repair limit might consist of an initial flaw size of 0.01

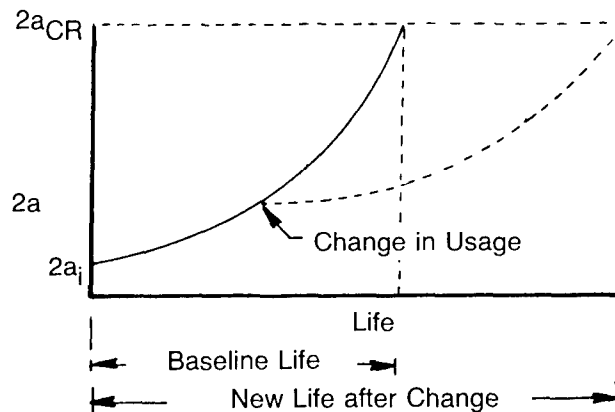


inch plus hole diameter and the final crack length,  $2a_{ERL}$ , might be 0.03 inch plus hole diameter. Similarly, the safety limit might be defined for a flaw growth from initial length of 0.05 inch to failure. The assumptions used in the crack growth analyses of each type of limit will vary. For instance, the environment and/or initial crack length for safety calculations might be more severe than for economic repair limits. For the case where a crack gage serves as the primary data acquisition device, use of different atmospheric environments may not be necessary since the measured data would already contain actual environmental effects.

#### Changes in Usage

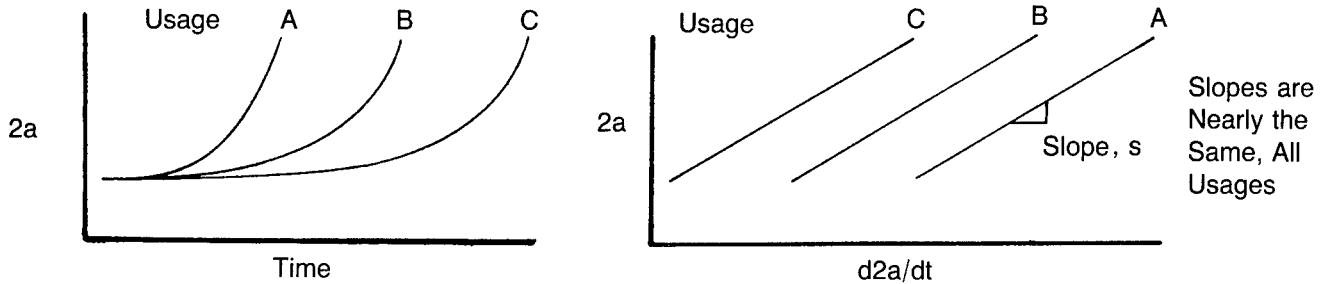
Initially, crack life estimates are predicted on baseline analyses using a forecasted fleet utilization. Transfer functions or life ratios are determined which relate the life remaining at other locations to that calculated for the control point.

The prediction of hours to ERL and safety limits will vary with changes in aircraft utilization and the initial predictions based on a forecasted usage may no longer be valid as illustrated below. Therefore, each significant usage change must be accounted for by assuming a new forecasted usage and then making appropriate revisions to predicted life.

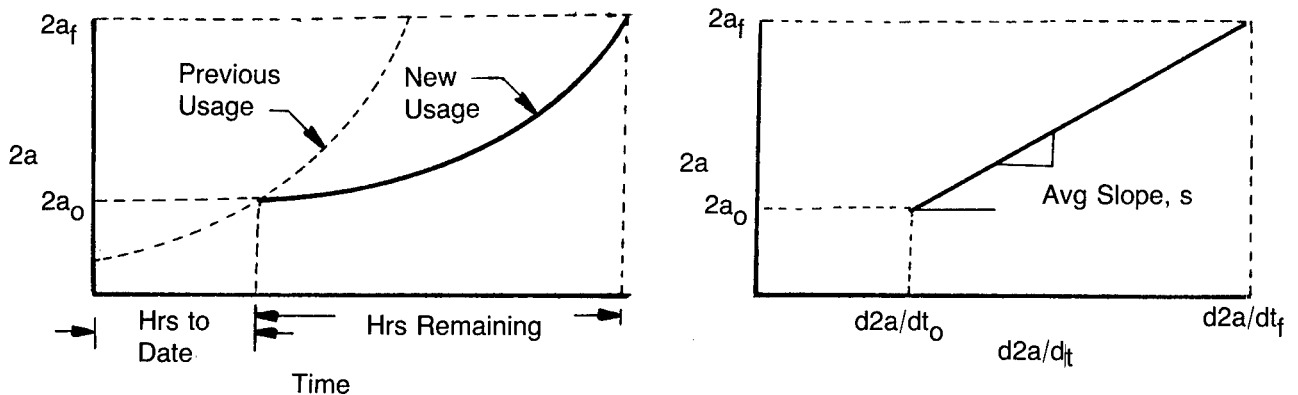


### A Method of Accounting for Usage Changes

Analyses performed during Task 1 of this study showed that a log-linear relationship (straight line on log-log plot) exists between crack length and crack growth rate and that the slopes of these plots were nearly the same for all usages investigated. This phenomenon is illustrated in the sketch below. Using this relationship (slope), which can be derived from analyses or obtained from test data, the predicted time to ERL and safety limits can readily be calculated based on any assumed projected usage.



A method that can be used to predict new times to ERL and safety limit using the values of crack length,  $2a_0$ , and crack growth rate,  $d2a/dt_0$  from the last recording period is depicted in the following illustration.



The plot on the left depicts a change in usage beginning at a crack length,  $2a_0$ . The crack growth rate,  $d2a/dt_0$ , is computed as the ratio of the incremental crack growth for the recording period and the number of hours flown. This rate then accounts for the mix of missions flown during this usage period. The values of  $2a_0$  and  $d2a/dt_0$  correspond to each individual airplane by tail number. Based on the log-linear relationship between crack length and crack growth rate, the slope of the  $2a$  vs  $d2a/dt$  line can be expressed as:

$$\tan\theta = s = \frac{\text{LN}2a - \text{LN}2a_0}{\text{LN}d2a/dt - \text{LN}d2a_0/dt_0} \quad (35)$$

The time remaining to ERL or safety limit can now be calculated by solving Equation 35 for t:

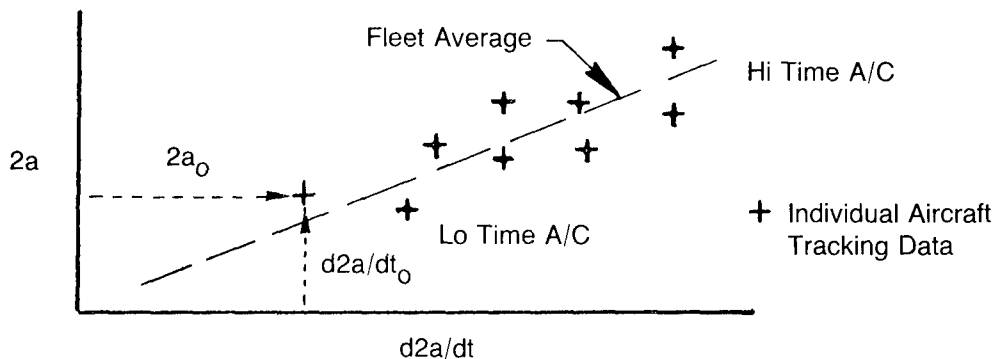
$$t = \frac{(2a_0)^{1/S}}{d2a_0/dt_0} \left[ \frac{S-1}{S} \right] \left[ (2a_f)^{\frac{S-1}{S}} - (2a_0)^{\frac{S-1}{S}} \right] \quad (36)$$

where:

- t = time for crack to grow from  $2a_0$  to  $2a_f$
- $2a_0$  = initial crack length
- $2a_f$  = final crack length
- $d2a_0/dt_0$  = crack growth rate from last period

A similar approach may be used to project time to ERL and safety limits using a fleet average crack growth rate as well as the rates computed for each individual aircraft. For example, the C/KC-135 fleet is comprised of many different Model Designated Series (MDS), each having a specific usage. Each airplane is monitored by MDS using average MDS damage rates from the C/KC-135 Damage Monitoring Program to predict the time to a specified damage limit.

The fleet average crack growth rates for aircraft flying the same missions can be determined by plotting the individual aircraft statistics of  $2a_0$  and  $d2a/dt_0$  as shown in the following illustration. This plot can be generated for



each recording period to examine the variation in usage by tail number. This plot would then be used to predict the time to ERL and safety limits in the same manner as presented previously, except, that the values of  $d2a/dt_0$  for each aircraft would be defined by the fleet average curve (dash line in the illustration).

## SECTION IV

### TASK 3, IMPLEMENTATION OF TRACKING PROGRAM

An Individual Aircraft Tracking (IAT) Program is an essential element of the USAF Structural Integrity Program. The primary objective of the IAT Program is to predict the potential flaw growth in critical areas of the airframe that is keyed to damage growth limits of MIL-A-83444, inspection times and economic repair limits. This requires that the tracking program be fully implemented and maintained to assure economy and flight safety.

The logistics of implementing the tracking programs considered in this study were evaluated by developing a cost model from which relative life cycle costs of each tracking program could be estimated. As a result of performing the studies of Task 1 and 2 and the development of the cost models in Task 3, some technical difficulties were identified. These technical difficulties, costs, accuracy and the present state-of-the-art regarding analysis techniques, data acquisition systems and data processing have been considered in arriving at a recommended tracking program.

#### 4.1 Relative Cost Study

A cost model was developed for the four tracking procedures selected for evaluation in this study. These procedures (Procedures A, B, C and D) were discussed in Section 3.3.

##### Ground Rules

The following ground rules apply to the cost study:

- The transport/bomber fleet to be monitored consist of 500 aircraft
- Each aircraft in the fleet will accumulate 300 flight hours per year at the rate of 25 flight hours and 5 flights per month
- The tracking program will be operational for 15 years
- Both 5 and 10 monitored locations were considered for Procedures A, B and D, and 1 and 5 locations were considered for Procedure C (MSR)

##### Cost Items

Table 14 identifies the costs considered in the relative cost study. Those cost items which impact each tracking procedure are indicated by "X" in this table. Costs were identified as being either nonrecurring or recurring. Nonrecurring costs included the initial investment costs of hardware and installation and the development of the tracking analysis methodology and software. Recurring or operating costs included data acquisition and processing, equipment maintenance and the operation of the Individual Aircraft Tracking (IAT) Computer Program.

##### Assumptions

In order to perform the relative cost study, assumptions had to be made concerning costs of engineering and technician manhours, number of pilot logs processed per month, MSR hardware, installation and data processing,

TABLE 14  
RELATIVE COST STUDY, COSTS CONSIDERED

	<u>Cost Item</u>	<u>Tracking Procedure</u>			
		<u>A</u>	<u>B</u>	<u>C</u>	<u>D</u>
Nonrecurring	Program Development				
	- Develop Analysis Method .....	X	X	X	X
	- Define Economic, Fracture and Inspection Data .....	X	X	X	X
	- Define Pilot Log Data .....	X	X	X	X
	- Parametric Study (Stresses) .....	X	X	—	—
	- Stress Exceedance Tables .....	—	X	—	—
	- Crack Growth Analyses .....	X	—	—	—
	- Crack Growth Rate Tables .....	X	—	—	—
	- MSR Hardware .....	—	—	X	—
	- Crack Growth Gages .....	—	—	—	X
- Instrumentation .....	—	—	X	X	
- Develop IAT Program .....	X	X	X	X	
Recurring	Data Acquisition				
	- Fill Out Pilot Log .....	X	X	X	X
	- MSR Tape Replacement .....	—	—	X	—
	- MSR Tapes .....	—	—	X	—
	- Crack Growth Gage Readings .....	—	—	—	X
	- Maintenance .....	—	—	X	X
Recurring	Data Processing				
	- Pilot Log Review & Editing .....	X	X	X	X
	- Keypunching .....	X	X	X	X
- Automation (MSR) .....	—	—	X	—	
Recurring	Individual Aircraft Tracking				
- Processed Data into IAT Program .....	X	X	X	X	

crack growth gage hardware, installation and costs of reading the gages, maintenance, and development of computer programs and operation of the programs. The assumptions made for these items are as follows:

- \$40/hour engineering  
\$20/hour technicians, computing analysis, keypunch operators and Air Force support
- 2500 pilot logs processed per month, one technician full time, 20 percent processed for MSR and crack gage programs
- MSR hardware
  - \$800/MSR assembly
  - \$178/cassette assembly
  - \$50/tape replacement
- Strain data processing, \$25/100 hours\*
- MSR installation, 3.5 hours/recorder
- MSR tape replacement, 5 minutes/MSR\*
- Crack gage hardware, \$69/gage

\*Air Force activities

- Crack gage readings, 30 minutes/gage read quarterly\*
- Crack gage installation, 3.0 hours/gage
- Maintenance, MSR and crack gage, 3 percent of hardware and installation\*
- Computer costs based on Boeing facilities costs\*

The items which may be considered to be Air Force activities are indicated.

### Results

The results of the relative cost study are presented in Table 15. The dollar summary shown in this figure allows comparison between nonrecurring and recurring costs and between the costs of data acquisition, data processing and the IAT computer runs. For each procedure the number of monitoring locations (control points) considered in determining program costs is indicated. Also noted are the costs to run the IAT computer programs for both a cycle-by-cycle and a blocks of cycles crack growth procedure. A detailed itemized cost summary for the items shown in Table 14 for each procedure is shown in Appendix D. The relative costs are shown in Table 16 based on the selection of Procedure A (costs for ten monitoring locations) as the baseline tracking procedure.

TABLE 15  
RELATIVE COST STUDY, DOLLAR SUMMARY

Tracking Procedure	Number of Locations	Cost Item – Dollars				Total Cost Summary, Dollars
		Nonrecurring	Recurring			
		Program Development	Data Acquisition	Data Processing	IAT Program Runs	
A	5	520,000	Neg.	1,080,000	33,800	1,633,800
A	10	624,000	Neg.	1,080,000	45,000	1,749,000
B	5	499,600	Neg.	1,080,000	(1) 51,800 (2) 213,800	1,631,400 1,793,400
B	10	563,600	Neg.	1,080,000	(1) 81,000 (2) 405,000	1,724,600 2,048,600
C	1	519,400	1,747,900	778,000	(1) 41,400 (2) 170,600	3,086,700 3,215,900
C	5	2,259,400	8,739,500	3,028,500	(1) 155,500 (2) 641,500	14,182,900 14,668,900
D	5	392,500	1,509,800	216,000	2,400	2,210,700
D	10	720,200	3,019,700	216,000	3,600	3,959,500

- (1) Flight-By-Flight Crack Growth, Blocks of Cycles  
(2) Cycle-By-Cycle Crack Growth

TABLE 16  
RELATIVE COSTS

Tracking Procedure	No. Locations Monitored	Relative Cost
A	5	.93
A Baseline	10	1.00
B	5	(1) .93 (2) 1.03
B	10	(1) .99 (2) 1.17
C	1	(1) 1.75 (2) 1.84
C	5	(1) 8.05 (2) 8.39
D	5	1.21
D	10	2.26

- (1) Flight-By-Flight Crack Growth, Blocks of Cycles  
(2) Cycle-By-Cycle Crack Growth

These results show that Procedures A and B are the lower cost methods of tracking pilot log; data processing being the major cost item. The costs of Procedures A and B were about the same. Hardware costs and data acquisition and processing costs make Procedure C the most costly system. Procedure C costs are greatly dependent on the number of MSR recorders per aircraft. Data acquisition (gage readings) contributed most to the costs of Procedure D. The relative costs show that, even though the cycle-by-cycle crack growth methods were much more costly than using a blocks of cycles method (Table 15), the cycle-by-cycle crack growth costs were insignificant when the total program costs were considered.

It may be noted that in any cost study some costs are not identified or considered and these costs may be significant to such a study. One such item that was not considered in this cost study was with regard to inspections. The less accurate tracking system will probably use more conservative inspection/modification actions than the more accurate system. Costs associated with these actions were not included. Also, all testing associated with the selection of a crack growth model (Procedures A, B and C) was considered to be completed as part of previous analyses (DADTA studies).

#### 4.2 Technical Difficulties

Technical difficulties are inherent in each of the tracking procedures studied. These difficulties are dependent on the type of data acquisition device, logistics of fleet implementation and analysis method associated with the tracking procedure.

Procedures A, B and C require that analysis methods be developed that will account for crack retardation as verified by tests. The variability in fleet usage will influence the analysis method since the degree of retardation is sensitive to variations and spectrum content.

The tracking procedures which rely on the pilot log as the primary source of data acquisition, must depend on proper training and motivation to assure that reliable usage parameter data is obtained. A history of acquiring pilot log data for existing damage monitoring programs, i.e. on the B-52 and C/KC-135, shows that the percent of recoverable information varies significantly from one fleet to another.

Procedure C is dependent on acquiring a very high percentage of usable strain recorded data. This requires, of course, that the recorders be properly installed and maintained. The recorded data must be processed using a reliable means to convert the recorded strain trace from the tape into absolute stress values. Both manual and automated data processing techniques must be employed to assure efficient and accurate data reduction.

Procedure D uses the crack growth gage concept which requires that both analyses and testing be used to determine the relationship between gage and structure crack length. At present, based on information/data now available, it appears that the crack growth gage is sensitive to spectrum content making correlation between gage and structure crack growth difficult. This was verified by tests conducted with crack growth gages as part of this contract. To obtain reliable data, it is imperative, as with the MSR installation, that the gages be installed and read by qualified personnel.

### **4.3 Optimum Tracking Scheme**

The selection of an optimum tracking procedure for a particular fleet of airplanes must give consideration to the current state-of-the-art with respect to crack growth analysis techniques and data acquisition and reduction systems. In addition, trade-offs between required accuracy and total systems costs must be thoroughly evaluated.

Of the four procedures studied under this procurement, only Procedure D, which employs a crack growth gage as the primary data acquisition system, is considered to be beyond the state-of-the-art. Even though this concept has many potentially attractive features, consideration of the procedure as a viable tracking procedure must await further gage development.

Procedures A, B and C are all considered to be acceptable methods of tracking crack growth in transport/bomber aircraft. Procedure C, using an MSR for data acquisition, would in all probability provide the most accurate stress history data. However, this system is unproven in actual fleet service and is the most expensive of the systems investigated (up to eight times more expensive than Procedure A or B). Unforeseen data collection or reduction problems could result in loss of vital usage information if this system were the only system in use on a given fleet.

Procedures A and B, which use the pilot's log form for data acquisition, rely upon the L/ESS Program for the original load history update data. Since all fleet aircraft are not instrumented in the L/ESS Program, the acquired data has to be viewed as an average for the fleet. This, of course, makes life prediction on individual aircraft less accurate than that provided by a working MSR system. However, the state-of-the-art of crack growth analyses being what it is today does not necessarily warrant the most accurate (and expensive) load history data.

Procedure B is estimated to be slightly more expensive than Procedure A and would be chosen over A in cases where fleet usage indicated a more definitive representation of load sequence was required.

In view of the discussion above, it would appear at this time either Procedure A or B would be a prudent choice for crack growth tracking along with a few fleet airplanes, possibly 10 to 20 percent, being instrumented with MSR gages. In this way, experience could be gained with MSR data acquisition and reduction on a smaller scale before committing the entire fleet to the more expensive approach. This scheme would also allow comparisons of crack growth estimates by Procedures A or B and Procedure C which could give an indication as to whether or not the MSR data was actually necessary.

## SECTION V CONCLUSIONS

The following general conclusions are drawn from the results of this study:

- The Wheeler Retardation Model is an acceptable analysis tool for investigating the effects of changes in airplane usage on crack growth
- Airplane gross weight and altitude are the primary usage parameters affecting crack growth on transport/bomber aircraft. The effects of speed changes were small for flights covering the same distance
- The use of pilot log forms and parametric crack growth rate tables or stress exceedance tables (Procedure A or B) is a reasonable approach to crack growth tracking at the present time
- The use of mechanical strain recorders on approximately 10 to 20 percent of the fleet aircraft should be considered.
- The crack growth gage concept has great potential as a future tracking system. However, because of dependence of the correlation between gage and structure crack growth on spectrum content, additional development is needed before the crack growth gage can be considered a viable data acquisition device.

## **APPENDIX A RELATED PARAMETRIC ANALYSES DATA**

This appendix presents (1) the mission segment stress spectra used in the parametric study to predict mission segment crack growth and crack growth rates and (2) the crack growth curves for all of the flight conditions studied for three structural analysis locations. These data are discussed in Section 2.7.

### 1. Mission Segment Stress Spectra

The mission segment stress spectra used in the parametric study were derived using two computer programs; a PSD stress/damage program and a stress sequence generator program. These programs and analysis methods were discussed in Section 2.2. Each mission segment spectrum was defined in a Lo-Hi-Lo sequence for a constant mean stress level. The spectrum for each flight condition was defined for a 1.0 hour flight duration except climbs and touch-and-go's. These were defined using the climb time to 30,000 feet and the average time to complete one touch-and-go-around (0.13 hour).

Tables A-1, A-2 and A-3 present a listing of all of the mission segment spectra generated. These tables present these data for the wing, body and fin analysis locations, respectively. Each table shows the maximum stress, minimum stress, R ratio and the number of cycles. For the wing and body climb spectra, the maximum flight stress equaled or exceeded in 10, 100 and 200 flights is shown.

### 2. Mission Segment Crack Growth Curves

Mission segment crack growth was determined using the Wheeler Retardation Model with a shaping exponent,  $m$ , of 0.90. The crack growth determined for each flight segment for the wing, body and fin analysis locations are shown in Figures A-1, A-2 and A-3, respectively. These data were used to determine the mission segment crack growth rates presented in Section 2.7.7.

TABLE A-1  
MISSION SEGMENT STRESS SPECTRA  
WING ANALYSIS LOCATION

<u>STRESS NUMBER</u>	<u>MAXIMUM STRESS KSI</u>	<u>MINIMUM STRESS KSI</u>	<u>R</u>	<u>NUMBER OF CYCLES</u>
CLIMB, T.O. 297 KIPS, WING				
1	26.04	-12.23	-0.47	1
2	22.08	18.25	0.83	38
3	23.35	16.93	0.73	7
4	24.63	15.70	0.64	2
5	25.90	14.43	0.56	1
6	24.63	15.70	0.64	1
7	23.35	16.93	0.73	6
8	22.08	18.25	0.83	38
FMAX EQUALLED OR EXCEEDED IN 10 FLIGHTS = 28.64 KSI				
FMAX EQUALLED OR EXCEEDED IN 100 FLIGHTS = 31.52 KSI				
FMAX EQUALLED OR EXCEEDED IN 200 FLIGHTS = 32.41 KSI				
CLIMB, T.O. 260 KIPS, WING				
1	21.42	-12.23	-0.57	1
2	18.66	14.84	0.80	23
3	19.94	13.56	0.68	4
4	21.21	12.29	0.58	1
5	19.94	13.56	0.68	4
6	18.66	14.84	0.80	25
FMAX EQUALLED OR EXCEEDED IN 10 FLIGHTS = 23.69 KSI				
FMAX EQUALLED OR EXCEEDED IN 100 FLIGHTS = 26.30 KSI				
FMAX EQUALLED OR EXCEEDED IN 200 FLIGHTS = 27.16 KSI				
CLIMB, T.O. 230 KIPS, WING				
1	18.17	-12.23	-0.67	1
2	15.99	12.17	0.76	15
3	17.27	10.89	0.63	2
4	18.54	9.62	0.52	1
5	17.27	10.89	0.63	2
6	15.99	12.17	0.76	14
FMAX EQUALLED OR EXCEEDED IN 10 FLIGHTS = 20.35 KSI				
FMAX EQUALLED OR EXCEEDED IN 100 FLIGHTS = 23.32 KSI				
FMAX EQUALLED OR EXCEEDED IN 200 FLIGHTS = 24.45 KSI				
CLIMB, T.O. 200 KIPS, WING				
1	15.42	-12.23	-0.79	1
2	13.53	9.71	0.72	13
3	14.81	8.43	0.57	3
4	13.53	9.71	0.72	12
FMAX EQUALLED OR EXCEEDED IN 10 FLIGHTS = 17.82 KSI				
FMAX EQUALLED OR EXCEEDED IN 100 FLIGHTS = 21.02 KSI				
FMAX EQUALLED OR EXCEEDED IN 200 FLIGHTS = 22.06 KSI				
CLIMB, T.O. 170 KIPS, WING				
1	12.48	-11.39	-0.91	1
2	11.25	7.43	0.66	8
3	12.53	6.15	0.49	1
4	11.25	7.43	0.66	8
FMAX EQUALLED OR EXCEEDED IN 10 FLIGHTS = 14.35 KSI				
FMAX EQUALLED OR EXCEEDED IN 100 FLIGHTS = 16.77 KSI				
FMAX EQUALLED OR EXCEEDED IN 200 FLIGHTS = 17.55 KSI				

TABLE A-1 (CONT'D)  
MISSION SEGMENT STRESS SPECTRA  
WING ANALYSIS LOCATION

<u>STRESS NUMBER</u>	<u>MAXIMUM STRESS</u> KSI	<u>MINIMUM STRESS</u> KSI	<u>R</u>	<u>NUMBER OF CYCLES</u>
LOW LEVEL, 260 KIPS, WING				
1	18.76	14.94	0.80	226
2	20.04	13.66	0.68	45
3	21.31	12.39	0.58	9
4	22.59	11.11	0.49	2
5	23.86	9.84	0.41	1
6	22.59	11.11	0.49	2
7	21.31	12.39	0.58	9
8	20.04	13.66	0.68	45
9	18.76	14.94	0.80	225
LOW LEVEL, 240 KIPS, WING				
1	17.25	13.43	0.78	215
2	18.53	12.15	0.66	40
3	19.80	10.88	0.55	8
4	21.08	9.60	0.46	2
5	22.35	8.33	0.37	1
6	21.08	9.60	0.46	2
7	19.80	10.88	0.55	8
8	18.53	12.15	0.66	39
9	17.25	13.43	0.78	214
LOW LEVEL, 220 KIPS, WING				
1	15.33	11.50	0.75	198
2	16.60	10.23	0.62	33
3	17.88	8.95	0.50	6
4	19.15	7.68	0.40	2
5	20.43	6.40	0.31	1
6	19.15	7.68	0.40	1
7	17.88	8.95	0.50	6
8	16.60	10.23	0.62	32
9	15.33	11.50	0.75	197
LOW LEVEL, 200 KIPS, WING				
1	13.41	9.58	0.71	178
2	14.68	8.31	0.57	27
3	15.96	7.03	0.44	5
4	17.23	5.76	0.33	2
5	15.96	7.03	0.44	4
6	14.68	8.31	0.57	26
7	13.41	9.58	0.71	178
LOW LEVEL, 180 KIPS, WING				
1	11.55	7.73	0.67	165
2	12.83	6.45	0.50	23
3	14.10	5.18	0.37	4
4	15.38	3.90	0.25	1
5	14.10	5.18	0.37	3
6	12.83	6.45	0.50	22
7	11.55	7.73	0.67	164
CRUISE, 5,000 FT., 297 KIPS, WING				
1	22.38	18.56	0.83	74
2	23.66	17.28	0.73	14
3	24.93	16.01	0.64	3
4	26.21	14.73	0.56	1
5	24.93	16.01	0.64	3

TABLE A-1 (CONT'D)  
MISSION SEGMENT STRESS SPECTRA  
WING ANALYSIS LOCATION

<u>STRESS NUMBER</u>	<u>MAXIMUM STRESS</u> KSI	<u>MINIMUM STRESS</u> KSI	<u>R</u>	<u>NUMBER OF CYCLES</u>
6	23.66	17.28	0.73	13
7	22.38	18.56	0.83	74
CRUISE, 5,000 FT., 280 KIPS, WING				
1	20.84	17.01	0.82	70
2	22.11	15.74	0.71	12
3	23.39	14.46	0.62	2
4	24.66	13.19	0.53	1
5	23.39	14.46	0.62	2
6	22.11	15.74	0.71	12
7	20.84	17.01	0.82	70
CRUISE, 5,000 FT., 260 KIPS, WING				
1	18.85	15.03	0.80	66
2	20.13	13.75	0.68	10
3	21.40	12.48	0.58	2
4	22.68	11.20	0.49	1
5	21.40	12.48	0.58	1
6	20.13	13.75	0.68	10
7	18.85	15.03	0.80	65
CRUISE, 5,000 FT., 240 KIPS, WING				
1	17.34	13.52	0.78	62
2	18.62	12.24	0.66	9
3	19.89	10.97	0.55	2
4	21.17	9.69	0.46	1
5	19.89	10.97	0.55	1
6	18.62	12.24	0.66	8
7	17.34	13.52	0.78	61
CRUISE, 5,000 FT., 220 KIPS, WING				
1	15.42	11.59	0.75	55
2	16.69	10.32	0.62	7
3	17.97	9.04	0.50	2
4	16.69	10.32	0.62	6
5	15.42	11.59	0.75	54
CRUISE, 5,000 FT., 200 KIPS, WING				
1	13.47	9.65	0.72	48
2	14.75	8.37	0.57	5
3	16.02	7.10	0.44	1
4	14.75	8.37	0.57	4
5	13.47	9.65	0.72	47
CRUISE, 5,000 FT., 180 KIPS, WING				
1	11.64	7.82	0.67	41
2	12.92	6.54	0.51	4
3	14.19	5.27	0.37	1
4	12.92	6.54	0.51	3
5	11.64	7.82	0.67	41
CRUISE, 5,000 FT., 160 KIPS, WING				
1	10.46	6.64	0.63	37
2	11.74	5.36	0.46	3
3	13.01	4.09	0.31	1
4	11.74	5.36	0.46	3
5	10.46	6.64	0.63	37

TABLE A-1 (CONT'D)  
MISSION SEGMENT STRESS SPECTRA  
WING ANALYSIS LOCATION

<u>STRESS NUMBER</u>	<u>MAXIMUM STRESS</u> KSI	<u>MINIMUM STRESS</u> KSI	<u>R</u>	<u>NUMBER OF CYCLES</u>
CRUISE, 5,000 FT., 140 KIPS, WING				
1	10.78	6.96	0.65	36
2	12.06	5.68	0.47	3
3	13.33	4.41	0.33	1
4	12.06	5.68	0.47	2
5	10.78	6.96	0.65	36
CRUISE, 10,000 FT., 297 KIPS, WING				
1	22.49	18.67	0.83	34
2	23.77	17.39	0.73	5
3	25.04	16.12	0.64	2
4	23.77	17.39	0.73	5
5	22.49	18.67	0.83	34
CRUISE, 10,000 FT., 280 KIPS, WING				
1	20.95	17.12	0.82	32
2	22.22	15.85	0.71	4
3	23.50	14.57	0.62	2
4	22.22	15.85	0.71	4
5	20.95	17.12	0.82	32
CRUISE, 10,000 FT., 260 KIPS, WING				
1	18.96	15.14	0.80	31
2	20.24	13.86	0.68	4
3	21.51	12.59	0.59	1
4	20.24	13.86	0.68	3
5	18.96	15.14	0.80	31
CRUISE, 10,000 FT., 240 KIPS, WING				
1	17.45	13.63	0.78	30
2	18.73	12.35	0.66	4
3	20.00	11.08	0.55	1
4	18.73	12.35	0.66	3
5	17.45	13.63	0.78	29
CRUISE, 10,000 FT., 220 KIPS, WING				
1	15.52	11.70	0.75	27
2	16.80	10.42	0.62	3
3	18.07	9.15	0.51	1
4	16.80	10.42	0.62	3
5	15.52	11.70	0.75	27
CRUISE, 10,000 FT., 200 KIPS, WING				
1	13.58	9.75	0.72	25
2	14.85	8.48	0.57	3
3	16.13	7.20	0.45	1
4	14.85	8.48	0.57	2
5	13.58	9.75	0.72	24
CRUISE, 10,000 FT., 180 KIPS, WING				
1	11.75	7.93	0.67	22
2	13.03	6.65	0.51	2
3	14.30	5.38	0.38	1
4	13.03	6.65	0.51	2
5	11.75	7.93	0.67	22

TABLE A-1 (CONT'D)  
MISSION SEGMENT STRESS SPECTRA  
WING ANALYSIS LOCATION

<u>STRESS NUMBER</u>	<u>MAXIMUM STRESS</u> KSI	<u>MINIMUM STRESS</u> KSI	<u>R</u>	<u>NUMBER OF CYCLES</u>
CRUISE, 10,000 FT., 160 KIPS, WING				
1	10.57	6.75	0.64	20
2	11.85	5.47	0.46	3
3	10.57	6.75	0.64	19
CRUISE, 10,000 FT., 140 KIPS, WING				
1	10.89	7.06	0.65	19
2	12.16	5.79	0.48	2
3	10.89	7.06	0.65	18
CRUISE, 30,000 FT., 297 KIPS, WING				
1	23.41	19.59	0.84	14
2	24.69	18.31	0.74	3
3	23.41	19.59	0.84	14
CRUISE, 30,000 FT., 280 KIPS, WING				
1	21.88	18.06	0.83	13
2	23.16	16.78	0.72	3
3	21.88	18.06	0.83	13
CRUISE, 30,000 FT., 260 KIPS, WING				
1	19.91	16.09	0.81	12
2	21.19	14.81	0.70	2
3	19.91	16.09	0.81	12
CRUISE, 30,000 FT., 240 KIPS, WING				
1	18.42	14.59	0.79	11
2	19.69	13.32	0.68	2
3	18.42	14.59	0.79	11
CRUISE, 30,000 FT., 220 KIPS, WING				
1	16.50	12.68	0.77	10
2	17.78	11.40	0.64	1
3	16.50	12.68	0.77	9
CRUISE, 30,000 FT., 200 KIPS, WING				
1	14.58	10.75	0.74	9
2	15.85	9.48	0.60	1
3	14.58	10.75	0.74	8
CRUISE, 30,000 FT., 180 KIPS, WING				
1	12.76	8.94	0.70	8
2	14.04	7.66	0.55	1
3	12.76	8.94	0.70	7
CRUISE, 30,000 FT., 160 KIPS, WING				
1	11.59	7.77	0.67	7
2	12.87	6.49	0.50	1
3	11.59	7.77	0.67	6
CRUISE, 30,000 FT., 140 KIPS, WING				
1	11.85	8.03	0.68	6
2	13.13	6.75	0.51	1
3	11.85	8.03	0.68	6

TABLE A-1 (CONT'D)  
MISSION SEGMENT STRESS SPECTRA  
WING ANALYSIS LOCATION

<u>STRESS NUMBER</u>	<u>MAXIMUM STRESS</u> KSI	<u>MINIMUM STRESS</u> KSI	<u>R</u>	<u>NUMBER OF CYCLES</u>
REFUEL, 280 KIPS, WING				
1	21.88	18.06	0.83	179
2	23.16	16.78	0.72	21
3	24.43	15.51	0.63	3
4	25.71	14.23	0.55	1
5	24.43	15.51	0.63	3
6	23.16	16.78	0.72	20
7	21.88	18.06	0.83	178
REFUEL, 220 KIPS, WING				
1	16.50	12.68	0.77	121
2	17.78	11.40	0.64	8
3	16.50	12.68	0.77	120
REFUEL, 160 KIPS, WING				
1	11.59	7.77	0.67	7
2	12.87	6.49	0.50	1
3	11.59	7.77	0.67	6
TOUCH AND GO, 200 KIPS, WING				
1	15.23	-0.20	-0.01	1
2	12.43	8.60	0.69	28
3	13.70	7.33	0.53	5
4	14.98	6.05	0.40	1
5	13.70	7.33	0.53	4
6	12.43	8.60	0.69	28
TOUCH AND GO, 180 KIPS, WING				
1	14.58	-1.26	-0.09	1
2	12.64	8.82	0.70	23
3	13.92	7.54	0.54	3
4	15.19	6.27	0.41	1
5	13.92	7.54	0.54	2
6	12.64	8.82	0.70	22
TOUCH AND GO, 160 KIPS, WING				
1	12.97	-1.73	-0.13	1
2	11.29	7.46	0.66	19
3	12.56	6.19	0.49	3
4	11.29	7.46	0.66	19
TOUCH AND GO, 140 KIPS, WING				
1	11.38	-1.55	-0.14	1
2	10.36	6.54	0.63	16
3	11.64	5.26	0.45	2
4	10.36	6.54	0.63	15
PATTERN, 200 KIPS, WING				
1	12.43	8.60	0.69	216
2	13.70	7.33	0.53	33
3	14.98	6.05	0.40	5
4	16.25	4.78	0.29	2
5	14.98	6.05	0.40	5
6	13.70	7.33	0.53	33
7	12.43	8.60	0.69	215

TABLE A-1 (CONCLUDED)  
MISSION SEGMENT STRESS SPECTRA  
WING ANALYSIS LOCATION

<u>STRESS NUMBER</u>	<u>MAXIMUM STRESS KSI</u>	<u>MINIMUM STRESS KSI</u>	<u>R</u>	<u>NUMBER OF CYCLES</u>
PATTERN, 180 KIPS, WING				
1	12.64	8.82	0.70	173
2	13.92	7.54	0.54	19
3	15.19	6.27	0.41	2
4	16.47	4.99	0.30	1
5	15.19	6.27	0.41	2
6	13.92	7.54	0.54	18
7	12.64	8.82	0.70	172
PATTERN, 160 KIPS, WING				
1	11.29	7.46	0.66	146
2	12.56	6.19	0.49	13
3	13.84	4.91	0.35	2
4	12.56	6.19	0.49	12
5	11.29	7.46	0.66	145
PATTERN, 140 KIPS, WING				
1	10.36	6.54	0.63	119
2	11.64	5.26	0.45	8
3	12.91	3.99	0.31	1
4	11.64	5.26	0.45	8
5	10.36	6.54	0.63	119

TABLE A-2  
MISSION SEGMENT STRESS SPECTRA  
BODY ANALYSIS LOCATION

<u>STRESS NUMBER</u>	<u>MAXIMUM STRESS</u> KSI	<u>MINIMUM STRESS</u> KSI	<u>R</u>	<u>NUMBER OF CYCLES</u>
CLIMB, T.O. 297 KIPS, BODY				
1	13.62	8.50	0.46	1
2	15.09	11.27	0.75	39
3	16.37	9.99	0.61	5
4	17.64	8.72	0.49	2
5	16.37	9.99	0.61	4
6	15.09	11.27	0.75	39
FMAX EQUALLED OR EXCEEDED IN 10 FLIGHTS = 20.41 KSI				
FMAX EQUALLED OR EXCEEDED IN 100 FLIGHTS = 22.45 KSI				
FMAX EQUALLED OR EXCEEDED IN 200 FLIGHTS = 23.06 KSI				
CLIMB, T.O. 260 KIPS BODY				
1	16.23	6.56	0.40	1
2	13.02	9.20	0.71	26
3	14.30	7.92	0.55	3
4	15.57	6.65	0.43	1
5	14.30	7.92	0.55	2
6	13.02	9.20	0.71	26
FMAX EQUALLED OR EXCEEDED IN 10 FLIGHTS = 17.82 KSI				
FMAX EQUALLED OR EXCEEDED IN 100 FLIGHTS = 19.77 KSI				
FMAX EQUALLED OR EXCEEDED IN 200 FLIGHTS = 20.38 KSI				
CLIMB, T.O. 230 KIPS, BODY				
1	14.66	5.84	0.40	1
2	11.91	8.09	0.68	15
3	13.19	6.81	0.52	3
4	11.91	8.09	0.68	15
FMAX EQUALLED OR EXCEEDED IN 10 FLIGHTS = 16.22 KSI				
FMAX EQUALLED OR EXCEEDED IN 100 FLIGHTS = 18.13 KSI				
FMAX EQUALLED OR EXCEEDED IN 200 FLIGHTS = 18.70 KSI				
CLIMB, T.O. 200 KIPS, BODY				
1	13.95	5.09	0.37	1
2	11.17	7.34	0.66	13
3	12.44	6.07	0.49	2
4	11.17	7.34	0.66	12
FMAX EQUALLED OR EXCEEDED IN 10 FLIGHTS = 15.36 KSI				
FMAX EQUALLED OR EXCEEDED IN 100 FLIGHTS = 17.17 KSI				
FMAX EQUALLED OR EXCEEDED IN 200 FLIGHTS = 17.74 KSI				
CLIMB, T.O. 170 KIPS, BODY				
1	13.11	4.75	0.36	1
2	10.56	6.73	0.64	8
3	11.83	5.46	0.46	1
4	10.56	6.73	0.64	8
FMAX EQUALLED OR EXCEEDED IN 10 FLIGHTS = 14.32 KSI				
FMAX EQUALLED OR EXCEEDED IN 100 FLIGHTS = 15.94 KSI				
FMAX EQUALLED OR EXCEEDED IN 200 FLIGHTS = 16.50 KSI				

TABLE A-2 (CONT'D)  
MISSION SEGMENT STRESS SPECTRA  
BODY ANALYSIS LOCATION

<u>STRESS NUMBER</u>	<u>MAXIMUM STRESS</u> KSI	<u>MINIMUM STRESS</u> KSI	<u>R</u>	<u>NUMBER OF CYCLES</u>
LOW LEVEL, 260 KIPS, BODY				
1	13.10	9.28	0.71	273
2	14.38	8.00	0.56	32
3	15.65	6.73	0.43	5
4	16.93	5.45	0.32	2
5	15.65	6.73	0.43	4
6	14.38	8.00	0.56	31
7	13.10	9.28	0.71	272
LOW LEVEL, 240 KIPS, BODY				
1	12.67	8.84	0.70	268
2	13.94	7.57	0.54	31
3	15.22	6.29	0.41	5
4	16.49	5.02	0.30	2
5	15.22	6.29	0.41	4
6	13.94	7.57	0.54	31
7	12.67	8.84	0.70	267
LOW LEVEL, 220 KIPS, BODY				
1	11.62	7.80	0.67	252
2	12.90	6.52	0.51	28
3	14.17	5.25	0.37	4
4	15.45	3.97	0.26	1
5	14.17	5.25	0.37	4
6	12.90	6.52	0.51	28
7	11.62	7.80	0.67	252
LOW LEVEL, 200 KIPS, BODY				
1	10.30	6.47	0.63	236
2	11.57	5.20	0.45	25
3	12.85	3.92	0.31	4
4	14.12	2.65	0.19	1
5	12.85	3.92	0.31	3
6	11.57	5.20	0.45	25
7	10.30	6.47	0.63	235
LOW LEVEL, 180 KIPS, BODY				
1	9.19	5.36	0.58	218
2	10.46	4.09	0.39	22
3	11.74	2.81	0.24	3
4	13.01	1.54	0.12	1
5	11.74	2.81	0.24	3
6	10.46	4.09	0.39	22
7	9.19	5.36	0.58	218
CRUISE, 5,000 FT., 297 KIPS, BODY				
1	15.48	11.65	0.75	62
2	16.75	10.38	0.62	5
3	18.03	9.10	0.50	1
4	16.75	10.38	0.62	4
5	15.48	11.65	0.75	61
CRUISE, 5,000 FT., 280 KIPS, BODY				
1	14.92	11.09	0.74	60
2	16.19	9.82	0.61	5
3	17.47	8.54	0.49	1
4	16.19	9.82	0.61	4

TABLE A-2 (CONT'D)  
MISSION SEGMENT STRESS SPECTRA  
BODY ANALYSIS LOCATION

<u>STRESS NUMBER</u>	<u>MAXIMUM STRESS KSI</u>	<u>MINIMUM STRESS KSI</u>	<u>R</u>	<u>NUMBER OF CYCLES</u>
5	14.92	11.09	0.74	59
CRUISE, 5,000 FT., 260 KIPS, BODY				
1	14.26	10.43	0.73	58
2	15.53	9.16	0.59	5
3	16.81	7.88	0.47	1
4	15.53	9.16	0.59	4
5	14.26	10.43	0.73	58
CRUISE, 5,000 FT., 240 KIPS, BODY				
1	13.82	9.99	0.72	57
2	15.09	8.72	0.58	5
3	16.37	7.44	0.45	1
4	15.09	8.72	0.58	4
5	13.82	9.99	0.72	56
CRUISE, 5,000 FT., 220 KIPS, BODY				
1	12.76	8.94	0.70	52
2	14.04	7.66	0.55	4
3	15.31	6.39	0.42	1
4	14.04	7.66	0.55	4
5	12.76	8.94	0.70	51
CRUISE, 5,000 FT., 200 KIPS, BODY				
1	11.43	7.60	0.67	47
2	12.70	6.33	0.50	4
3	13.98	5.05	0.36	1
4	12.70	6.33	0.50	3
5	11.43	7.60	0.67	47
CRUISE, 5,000 FT., 180 KIPS, BODY				
1	10.31	6.49	0.63	43
2	11.59	5.21	0.45	3
3	12.86	3.94	0.31	1
4	11.59	5.21	0.45	3
5	10.31	6.49	0.63	42
CRUISE, 5,000 FT., 160 KIPS, BODY				
1	9.81	5.99	0.61	38
2	11.09	4.71	0.42	3
3	12.36	3.44	0.28	1
4	11.09	4.71	0.42	2
5	9.81	5.99	0.61	37
CRUISE, 5,000 FT., 140 KIPS, BODY				
1	10.21	6.38	0.63	33
2	11.48	5.11	0.44	2
3	12.76	3.83	0.30	1
4	11.48	5.11	0.44	2
5	10.21	6.38	0.63	33
CRUISE, 10,000 FT., 297 KIPS, BODY				
1	16.50	12.67	0.77	29
2	17.77	11.40	0.64	2
3	19.05	10.12	0.53	1
4	17.77	11.40	0.64	2
5	16.50	12.67	0.77	28

TABLE A-2 (CONT'D)  
MISSION SEGMENT STRESS SPECTRA  
BODY ANALYSIS LOCATION

<u>STRESS NUMBER</u>	<u>MAXIMUM STRESS</u> KSI	<u>MINIMUM STRESS</u> KSI	<u>R</u>	<u>NUMBER OF CYCLES</u>
CRUISE, 10,000 FT., 280 KIPS, BODY				
1	15.92	12.10	0.76	28
2	17.20	10.82	0.63	2
3	18.47	9.55	0.52	1
4	17.20	10.82	0.63	2
5	15.92	12.10	0.76	28
CRUISE, 10,000 FT., 260 KIPS, BODY				
1	15.26	11.44	0.75	28
2	16.54	10.16	0.61	2
3	17.81	8.89	0.50	1
4	16.54	10.16	0.61	2
5	15.26	11.44	0.75	27
CRUISE, 10,000 FT., 240 KIPS, BODY				
1	14.82	10.99	0.74	27
2	16.09	9.72	0.60	2
3	17.37	8.44	0.49	1
4	16.09	9.72	0.60	2
5	14.82	10.99	0.74	27
CRUISE, 10,000 FT., 220 KIPS, BODY				
1	13.75	9.93	0.72	25
2	15.03	8.65	0.58	2
3	16.30	7.38	0.45	1
4	15.03	8.65	0.58	1
5	13.75	9.93	0.72	25
CRUISE, 10,000 FT., 200 KIPS, BODY				
1	12.40	8.58	0.69	23
2	13.68	7.30	0.53	3
3	12.40	8.58	0.69	23
CRUISE, 10,000 FT., 180 KIPS, BODY				
1	11.28	7.46	0.66	21
2	12.56	6.18	0.49	3
3	11.28	7.46	0.66	20
CRUISE, 10,000 FT., 160 KIPS, BODY				
1	10.77	6.95	0.64	18
2	12.05	5.67	0.47	2
3	10.77	6.95	0.64	18
CRUISE, 10,000 FT., 140 KIPS, BODY				
1	11.16	7.34	0.65	16
2	12.44	6.06	0.49	2
3	11.16	7.34	0.66	15
CRUISE, 30,000 FT., 297 KIPS, BODY				
1	19.01	15.19	0.80	9
2	20.29	13.91	0.69	1
3	19.01	15.19	0.80	8
CRUISE, 30,000 FT., 280 KIPS, BODY				
1	18.40	14.57	0.79	8
2	19.67	13.30	0.68	1
3	18.40	14.57	0.79	8

TABLE A-2 (CONT'D)  
MISSION SEGMENT STRESS SPECTRA  
BODY ANALYSIS LOCATION

<u>STRESS NUMBER</u>	<u>MAXIMUM STRESS</u> KSI	<u>MINIMUM STRESS</u> KSI	<u>R</u>	<u>NUMBER OF CYCLES</u>
CRUISE, 30,000 FT., 260 KIPS, BODY				
1	17.67	13.85	0.78	8
2	18.95	12.57	0.66	1
3	17.67	13.85	0.78	8
CRUISE, 30,000 FT., 240 KIPS, BODY				
1	17.19	13.36	0.78	8
2	18.46	12.09	0.65	1
3	17.19	13.36	0.78	7
CRUISE, 30,000 FT., 220 KIPS, BODY				
1	16.08	12.25	0.76	7
2	17.35	10.98	0.63	1
3	16.08	12.25	0.76	7
CRUISE, 30,000 FT., 200 KIPS, BODY				
1	14.68	10.85	0.74	7
2	15.95	9.58	0.60	1
3	14.68	10.85	0.74	6
CRUISE, 30,000 FT., 180 KIPS, BODY				
1	13.51	9.69	0.72	6
2	14.79	8.41	0.57	1
3	13.51	9.69	0.72	5
CRUISE, 30,000 FT., 160 KIPS, BODY				
1	12.96	9.13	0.70	10
CRUISE, 30,000 FT., 140 KIPS, BODY				
1	13.29	9.47	0.71	8
REFUEL, 280 KIPS, BODY				
1	18.40	14.57	0.79	25
2	19.67	13.30	0.68	1
3	18.40	14.57	0.79	25
REFUEL, 220 KIPS, BODY				
1	16.08	12.25	0.76	11
REFUEL, 160 KIPS, BODY				
1	12.96	9.13	0.70	10
TOUCH AND GO, 200 KIPS, BODY				
1	13.20	5.93	0.45	1
2	11.53	7.71	0.67	31
3	12.81	6.43	0.50	3
4	14.08	5.16	0.37	1
5	12.81	6.43	0.50	3
6	11.53	7.71	0.67	31
TOUCH AND GO, 180 KIPS, BODY				
1	11.66	4.91	0.42	1
2	9.95	6.13	0.62	27
3	11.23	4.85	0.43	4
4	9.95	6.13	0.62	26

TABLE A-2 (CONCLUDED)  
MISSION SEGMENT STRESS SPECTRA  
BODY ANALYSIS LOCATION

<u>STRESS NUMBER</u>	<u>MAXIMUM STRESS</u> KSI	<u>MINIMUM STRESS</u> KSI	<u>R</u>	<u>NUMBER OF CYCLES</u>
TOUCH AND GO, 160 KIPS, BODY				
1	10.77	4.53	0.42	1
2	9.43	5.61	0.59	22
3	10.71	4.33	0.40	3
4	9.43	5.61	0.59	21
TOUCH AND GO, 140 KIPS, BODY				
1	10.58	4.70	0.44	1
2	9.53	5.71	0.60	17
3	10.81	4.43	0.41	2
4	9.53	5.71	0.60	17
PATTERN, 200 KIPS, BODY				
1	11.53	7.71	0.67	239
2	12.81	6.43	0.50	22
3	14.08	5.16	0.37	4
4	12.81	6.43	0.50	21
5	11.53	7.71	0.67	239
PATTERN, 180 KIPS, BODY				
1	9.95	6.13	0.62	202
2	11.23	4.85	0.43	16
3	12.50	3.58	0.29	3
4	11.23	4.85	0.43	15
5	9.95	6.13	0.62	202
PATTERN, 160 KIPS, BODY				
1	9.43	5.61	0.59	167
2	10.71	4.33	0.40	11
3	11.98	3.06	0.26	1
4	10.71	4.33	0.40	10
5	9.43	5.61	0.59	166
PATTERN, 140 KIPS, BODY				
1	9.53	5.71	0.60	133
2	10.81	4.43	0.41	7
3	12.08	3.16	0.26	1
4	10.81	4.43	0.41	6
5	9.53	5.71	0.60	132

TABLE A-3  
MISSION SEGMENT STRESS SPECTRA  
FIN ANALYSIS LOCATION

<u>STRESS NUMBER</u>	<u>MAXIMUM STRESS</u> KSI	<u>MINIMUM STRESS</u> KSI	<u>R</u>	<u>NUMBER OF CYCLES</u>
CLIMB, T.O. 297 KIPS, FIN				
1	1.91	-1.91	-1.00	114
2	3.19	-3.19	-1.00	33
3	4.46	-4.46	-1.00	12
4	5.74	-5.74	-1.00	5
5	7.01	-7.01	-1.00	2
6	8.29	-8.29	-1.00	2
7	7.01	-7.01	-1.00	2
8	5.74	-5.74	-1.00	4
9	4.46	-4.46	-1.00	11
10	3.19	-3.19	-1.00	32
11	1.91	-1.91	-1.00	113
CLIMB, T.O. 260 KIPS FIN				
1	1.91	-1.91	-1.00	86
2	3.19	-3.19	-1.00	24
3	4.46	-4.46	-1.00	8
4	5.74	-5.74	-1.00	3
5	7.01	-7.01	-1.00	1
6	8.29	-8.29	-1.00	1
7	7.01	-7.01	-1.00	1
8	5.74	-5.74	-1.00	3
9	4.46	-4.46	-1.00	7
10	3.19	-3.19	-1.00	23
11	1.91	-1.91	-1.00	86
CLIMB, T.O. 230 KIPS, FIN				
1	1.91	-1.91	-1.00	53
2	3.19	-3.19	-1.00	15
3	4.46	-4.46	-1.00	5
4	5.74	-5.74	-1.00	3
5	4.46	-4.46	-1.00	4
6	3.19	-3.19	-1.00	14
7	1.91	-1.91	-1.00	53
CLIMB, T.O. 200 KIPS, FIN				
1	1.91	-1.91	-1.00	52
2	3.19	-3.19	-1.00	13
3	4.46	-4.46	-1.00	4
4	5.74	-5.74	-1.00	3
5	4.46	-4.46	-1.00	4
6	3.19	-3.19	-1.00	13
7	1.91	-1.91	-1.00	52
CLIMB, T.O. 170 KIPS, FIN				
1	1.91	-1.91	-1.00	39
2	3.19	-3.19	-1.00	10
3	4.46	-4.46	-1.00	3
4	5.74	-5.74	-1.00	2
5	4.46	-4.46	-1.00	2
6	3.19	-3.19	-1.00	9
7	1.91	-1.91	-1.00	39
LOW LEVEL, 260 KIPS, FIN				
1	1.91	-1.91	-1.00	538
2	3.19	-3.19	-1.00	208
3	4.46	-4.46	-1.00	82

TABLE A-3 (CONT'D)  
MISSION SEGMENT STRESS SPECTRA  
FIN ANALYSIS LOCATION

<u>STRESS NUMBER</u>	<u>MAXIMUM STRESS</u> KSI	<u>MINIMUM STRESS</u> KSI	<u>R</u>	<u>NUMBER OF CYCLES</u>
4	5.74	-5.74	-1.00	33
5	7.01	-7.01	-1.00	13
6	8.29	-8.29	-1.00	6
7	9.56	-9.56	-1.00	3
8	10.84	-10.84	-1.00	1
9	12.11	-12.11	-1.00	1
10	10.84	-10.84	-1.00	1
11	9.56	-9.56	-1.00	2
12	8.29	-8.29	-1.00	5
13	7.01	-7.01	-1.00	13
14	5.74	-5.74	-1.00	32
15	4.46	-4.46	-1.00	81
16	3.19	-3.19	-1.00	208
17	1.91	-1.91	-1.00	538
LOW LEVEL, 240 KIPS, FIN				
1	1.91	-1.91	-1.00	539
2	3.19	-3.19	-1.00	208
3	4.46	-4.46	-1.00	82
4	5.74	-5.74	-1.00	33
5	7.01	-7.01	-1.00	13
6	8.29	-8.29	-1.00	6
7	9.56	-9.56	-1.00	3
8	10.84	-10.84	-1.00	1
9	12.11	-12.11	-1.00	1
10	10.84	-10.84	-1.00	1
11	9.56	-9.56	-1.00	2
12	8.29	-8.29	-1.00	5
13	7.01	-7.01	-1.00	13
14	5.74	-5.74	-1.00	32
15	4.46	-4.46	-1.00	81
16	3.19	-3.19	-1.00	208
17	1.91	-1.91	-1.00	538
LOW LEVEL, 220 KIPS, FIN				
1	1.91	-1.91	-1.00	544
2	3.19	-3.19	-1.00	208
3	4.46	-4.46	-1.00	80
4	5.74	-5.74	-1.00	32
5	7.01	-7.01	-1.00	13
6	8.29	-8.29	-1.00	6
7	9.56	-9.56	-1.00	3
8	10.84	-10.84	-1.00	1
9	12.11	-12.11	-1.00	1
10	10.84	-10.84	-1.00	1
11	9.56	-9.56	-1.00	2
12	8.29	-8.29	-1.00	5
13	7.01	-7.01	-1.00	12
14	5.74	-5.74	-1.00	31
15	4.46	-4.46	-1.00	80
16	3.19	-3.19	-1.00	207
17	1.91	-1.91	-1.00	543
LOW LEVEL, 200 KIPS, FIN				
1	1.91	-1.91	-1.00	549
2	3.19	-3.19	-1.00	207
3	4.46	-4.46	-1.00	79
4	5.74	-5.74	-1.00	31

TABLE A-3 (CONT'D)  
MISSION SEGMENT STRESS SPECTRA  
FIN ANALYSIS LOCATION

<u>STRESS NUMBER</u>	<u>MAXIMUM STRESS</u> KSI	<u>MINIMUM STRESS</u> KSI	<u>R</u>	<u>NUMBER OF CYCLES</u>
5	7.01	-7.01	-1.00	12
6	8.29	-8.29	-1.00	5
7	9.56	-9.56	-1.00	2
8	10.84	-10.84	-1.00	1
9	12.11	-12.11	-1.00	1
10	10.84	-10.84	-1.00	1
11	9.56	-9.56	-1.00	2
12	8.29	-8.29	-1.00	5
13	7.01	-7.01	-1.00	12
14	5.74	-5.74	-1.00	30
15	4.46	-4.46	-1.00	78
16	3.19	-3.19	-1.00	206
17	1.91	-1.91	-1.00	549
LOW LEVEL, 180 KIPS, FIN				
1	1.91	-1.91	-1.00	554
2	3.19	-3.19	-1.00	205
3	4.46	-4.46	-1.00	77
4	5.74	-5.74	-1.00	30
5	7.01	-7.01	-1.00	12
6	8.29	-8.29	-1.00	5
7	9.56	-9.56	-1.00	2
8	10.84	-10.84	-1.00	1
9	12.11	-12.11	-1.00	1
10	10.84	-10.84	-1.00	1
11	9.56	-9.56	-1.00	2
12	8.29	-8.29	-1.00	4
13	7.01	-7.01	-1.00	11
14	5.74	-5.74	-1.00	29
15	4.46	-4.46	-1.00	76
16	3.19	-3.19	-1.00	204
17	1.91	-1.91	-1.00	553
CRUISE, 5,000 FT., 297 KIPS, FIN				
1	1.91	-1.91	-1.00	174
2	3.19	-3.19	-1.00	51
3	4.46	-4.46	-1.00	15
4	5.74	-5.74	-1.00	5
5	7.01	-7.01	-1.00	2
6	8.29	-8.29	-1.00	1
7	9.56	-9.56	-1.00	1
8	7.01	-7.01	-1.00	2
9	5.74	-5.74	-1.00	5
10	4.46	-4.46	-1.00	15
11	3.19	-3.19	-1.00	50
12	1.91	-1.91	-1.00	174
CRUISE, 5,000 FT., 280 KIPS, FIN				
1	1.91	-1.91	-1.00	174
2	3.19	-3.19	-1.00	51
3	4.46	-4.46	-1.00	15
4	5.74	-5.74	-1.00	5
5	7.01	-7.01	-1.00	2
6	8.29	-8.29	-1.00	1
7	9.56	-9.56	-1.00	1
8	7.01	-7.01	-1.00	2
9	5.74	-5.74	-1.00	5
10	4.46	-4.46	-1.00	15

TABLE A-3 (CONT'D)  
MISSION SEGMENT STRESS SPECTRA  
FIN ANALYSIS LOCATION

<u>STRESS NUMBER</u>	<u>MAXIMUM STRESS</u> KSI	<u>MINIMUM STRESS</u> KSI	<u>R</u>	<u>NUMBER OF CYCLES</u>
11	3.19	-3.19	-1.00	50
12	1.91	-1.91	-1.00	174
CRUISE, 5,000 FT., 260 KIPS, FIN				
1	1.91	-1.91	-1.00	174
2	3.19	-3.19	-1.00	51
3	4.46	-4.46	-1.00	15
4	5.74	-5.74	-1.00	5
5	7.01	-7.01	-1.00	2
6	8.29	-8.29	-1.00	1
7	9.56	-9.56	-1.00	1
8	7.01	-7.01	-1.00	2
9	5.74	-5.74	-1.00	5
10	4.46	-4.46	-1.00	15
11	3.19	-3.19	-1.00	50
12	1.91	-1.91	-1.00	174
CRUISE, 5,000 FT., 240 KIPS, FIN				
1	1.91	-1.91	-1.00	175
2	3.19	-3.19	-1.00	51
3	4.46	-4.46	-1.00	15
4	5.74	-5.74	-1.00	5
5	7.01	-7.01	-1.00	2
6	8.29	-8.29	-1.00	1
7	9.56	-9.56	-1.00	1
8	7.01	-7.01	-1.00	2
9	5.74	-5.74	-1.00	5
10	4.46	-4.46	-1.00	15
11	3.19	-3.19	-1.00	50
12	1.91	-1.91	-1.00	174
CRUISE, 5,000 FT., 220 KIPS, FIN				
1	1.91	-1.91	-1.00	175
2	3.19	-3.19	-1.00	50
3	4.46	-4.46	-1.00	15
4	5.74	-5.74	-1.00	5
5	7.01	-7.01	-1.00	2
6	8.29	-8.29	-1.00	1
7	9.56	-9.56	-1.00	1
8	7.01	-7.01	-1.00	1
9	5.74	-5.74	-1.00	4
10	4.46	-4.46	-1.00	15
11	3.19	-3.19	-1.00	50
12	1.91	-1.91	-1.00	175
CRUISE, 5,000 FT., 200 KIPS, FIN				
1	1.91	-1.91	-1.00	176
2	3.19	-3.19	-1.00	49
3	4.46	-4.46	-1.00	15
4	5.74	-5.74	-1.00	5
5	7.01	-7.01	-1.00	2
6	8.29	-8.29	-1.00	1
7	9.56	-9.56	-1.00	1
8	7.01	-7.01	-1.00	1
9	5.74	-5.74	-1.00	4
10	4.46	-4.46	-1.00	14
11	3.19	-3.19	-1.00	49
12	1.91	-1.91	-1.00	175

TABLE A-3 (CONT'D)  
MISSION SEGMENT STRESS SPECTRA  
FIN ANALYSIS LOCATION

<u>STRESS NUMBER</u>	<u>MAXIMUM STRESS KSI</u>	<u>MINIMUM STRESS KSI</u>	<u>R</u>	<u>NUMBER OF CYCLES</u>
CRUISE, 5,000 FT., 180 KIPS, FIN				
1	1.91	-1.91	-1.00	176
2	3.19	-3.19	-1.00	48
3	4.46	-4.46	-1.00	14
4	5.74	-5.74	-1.00	5
5	7.01	-7.01	-1.00	2
6	8.29	-8.29	-1.00	1
7	9.56	-9.56	-1.00	1
8	7.01	-7.01	-1.00	1
9	5.74	-5.74	-1.00	4
10	4.46	-4.46	-1.00	14
11	3.19	-3.19	-1.00	48
12	1.91	-1.91	-1.00	175
CRUISE, 5,000 FT., 160 KIPS, FIN				
1	1.91	-1.91	-1.00	176
2	3.19	-3.19	-1.00	47
3	4.46	-4.46	-1.00	14
4	5.74	-5.74	-1.00	4
5	7.01	-7.01	-1.00	2
6	8.29	-8.29	-1.00	1
7	9.56	-9.56	-1.00	1
8	7.01	-7.01	-1.00	1
9	5.74	-5.74	-1.00	4
10	4.46	-4.46	-1.00	13
11	3.19	-3.19	-1.00	47
12	1.91	-1.91	-1.00	175
CRUISE, 5,000 FT., 140 KIPS, FIN				
1	1.91	-1.91	-1.00	175
2	3.19	-3.19	-1.00	46
3	4.46	-4.46	-1.00	13
4	5.74	-5.74	-1.00	4
5	7.01	-7.01	-1.00	2
6	8.29	-8.29	-1.00	1
7	9.56	-9.56	-1.00	1
8	7.01	-7.01	-1.00	1
9	5.74	-5.74	-1.00	4
10	4.46	-4.46	-1.00	13
11	3.19	-3.19	-1.00	46
12	1.91	-1.91	-1.00	175
CRUISE, 10,000 FT., 297 KIPS, FIN				
1	1.91	-1.91	-1.00	109
2	3.19	-3.19	-1.00	27
3	4.46	-4.46	-1.00	7
4	5.74	-5.74	-1.00	2
5	7.01	-7.01	-1.00	1
6	8.29	-8.29	-1.00	1
7	5.74	-5.74	-1.00	2
8	4.46	-4.46	-1.00	7
9	3.19	-3.19	-1.00	27
10	1.91	-1.91	-1.00	108

TABLE A-3 (CONT'D)  
MISSION SEGMENT STRESS SPECTRA  
FIN ANALYSIS LOCATION

<u>STRESS NUMBER</u>	<u>MAXIMUM STRESS</u> KSI	<u>MINIMUM STRESS</u> KSI	<u>R</u>	<u>NUMBER OF CYCLES</u>
CRUISE, 10,000 FT., 280 KIPS, FIN				
1	1.91	-1.91	-1.00	109
2	3.19	-3.19	-1.00	27
3	4.46	-4.46	-1.00	7
4	5.74	-5.74	-1.00	2
5	7.01	-7.01	-1.00	1
6	8.29	-8.29	-1.00	1
7	5.74	-5.74	-1.00	2
8	4.46	-4.46	-1.00	7
9	3.19	-3.19	-1.00	27
10	1.91	-1.91	-1.00	108
CRUISE, 10,000 FT., 260 KIPS, FIN				
1	1.91	-1.91	-1.00	109
2	3.19	-3.19	-1.00	27
3	4.46	-4.46	-1.00	7
4	5.74	-5.74	-1.00	2
5	7.01	-7.01	-1.00	1
6	8.29	-8.29	-1.00	1
7	5.74	-5.74	-1.00	2
8	4.46	-4.46	-1.00	7
9	3.19	-3.19	-1.00	27
10	1.91	-1.91	-1.00	108
CRUISE, 10,000 FT., 240 KIPS, FIN				
1	1.91	-1.91	-1.00	109
2	3.19	-3.19	-1.00	27
3	4.46	-4.46	-1.00	7
4	5.74	-5.74	-1.00	2
5	7.01	-7.01	-1.00	1
6	8.29	-8.29	-1.00	1
7	5.74	-5.74	-1.00	2
8	4.46	-4.46	-1.00	7
9	3.19	-3.19	-1.00	27
10	1.91	-1.91	-1.00	108
CRUISE, 10,000 FT., 220 KIPS, FIN				
1	1.91	-1.91	-1.00	109
2	3.19	-3.19	-1.00	27
3	4.46	-4.46	-1.00	7
4	5.74	-5.74	-1.00	2
5	7.01	-7.01	-1.00	1
6	8.29	-8.29	-1.00	1
7	5.74	-5.74	-1.00	2
8	4.46	-4.46	-1.00	7
9	3.19	-3.19	-1.00	26
10	1.91	-1.91	-1.00	108
CRUISE, 10,000 FT., 200 KIPS, FIN				
1	1.91	-1.91	-1.00	109
2	3.19	-3.19	-1.00	26
3	4.46	-4.46	-1.00	7
4	5.74	-5.74	-1.00	2
5	7.01	-7.01	-1.00	1
6	8.29	-8.29	-1.00	1
7	5.74	-5.74	-1.00	2
8	4.46	-4.46	-1.00	6

TABLE A-3 (CONT'D)  
MISSION SEGMENT STRESS SPECTRA  
FIN ANALYSIS LOCATION

<u>STRESS NUMBER</u>	<u>MAXIMUM STRESS</u> KSI	<u>MINIMUM STRESS</u> KSI	<u>R</u>	<u>NUMBER OF CYCLES</u>
9	3.19	-3.19	-1.00	26
10	1.91	-1.91	-1.00	108
CRUISE, 10,000 FT., 180 KIPS, FIN				
1	1.91	-1.91	-1.00	109
2	3.19	-3.19	-1.00	26
3	4.46	-4.46	-1.00	7
4	5.74	-5.74	-1.00	2
5	7.01	-7.01	-1.00	1
6	8.29	-8.29	-1.00	1
7	5.74	-5.74	-1.00	2
8	4.46	-4.46	-1.00	6
9	3.19	-3.19	-1.00	25
10	1.91	-1.91	-1.00	103
CRUISE, 10,000 FT., 160 KIPS, FIN				
1	1.91	-1.91	-1.00	108
2	3.19	-3.19	-1.00	25
3	4.46	-4.46	-1.00	6
4	5.74	-5.74	-1.00	2
5	7.01	-7.01	-1.00	1
6	8.29	-8.29	-1.00	1
7	5.74	-5.74	-1.00	1
8	4.46	-4.46	-1.00	6
9	3.19	-3.19	-1.00	24
10	1.91	-1.91	-1.00	107
CRUISE, 10,000 FT., 140 KIPS, FIN				
1	1.91	-1.91	-1.00	107
2	3.19	-3.19	-1.00	24
3	4.46	-4.46	-1.00	6
4	5.74	-5.74	-1.00	2
5	7.01	-7.01	-1.00	1
6	5.74	-5.74	-1.00	1
7	4.46	-4.46	-1.00	6
8	3.19	-3.19	-1.00	24
9	1.91	-1.91	-1.00	107
CRUISE, 30,000 FT., 297 KIPS, FIN				
1	1.91	-1.91	-1.00	50
2	3.19	-3.19	-1.00	9
3	4.46	-4.46	-1.00	2
4	5.74	-5.74	-1.00	1
5	4.46	-4.46	-1.00	1
6	3.19	-3.19	-1.00	8
7	1.91	-1.91	-1.00	50
CRUISE, 30,000 FT., 280 KIPS, FIN				
1	1.91	-1.91	-1.00	50
2	3.19	-3.19	-1.00	9
3	4.46	-4.46	-1.00	2
4	5.74	-5.74	-1.00	1
5	4.46	-4.46	-1.00	1
6	3.19	-3.19	-1.00	8
7	1.91	-1.91	-1.00	50

TABLE A-3 (CONT'D)  
MISSION SEGMENT STRESS SPECTRA  
FIN ANALYSIS LOCATION

<u>STRESS NUMBER</u>	<u>MAXIMUM STRESS</u> KSI	<u>MINIMUM STRESS</u> KSI	<u>R</u>	<u>NUMBER OF CYCLES</u>
CRUISE, 30,000 FT., 260 KIPS, FIN				
1	1.91	-1.91	-1.00	51
2	3.19	-3.19	-1.00	9
3	4.46	-4.46	-1.00	2
4	5.74	-5.74	-1.00	1
5	4.46	-4.46	-1.00	1
6	3.19	-3.19	-1.00	9
7	1.91	-1.91	-1.00	50
CRUISE, 30,000 FT., 240 KIPS, FIN				
1	1.91	-1.91	-1.00	51
2	3.19	-3.19	-1.00	9
3	4.46	-4.46	-1.00	2
4	5.74	-5.74	-1.00	1
5	4.46	-4.46	-1.00	1
6	3.19	-3.19	-1.00	9
7	1.91	-1.91	-1.00	50
CRUISE, 30,000 FT., 220 KIPS, FIN				
1	1.91	-1.91	-1.00	50
2	3.19	-3.19	-1.00	9
3	4.46	-4.46	-1.00	2
4	5.74	-5.74	-1.00	1
5	4.46	-4.46	-1.00	1
6	3.19	-3.19	-1.00	8
7	1.91	-1.91	-1.00	50
CRUISE, 30,000 FT., 200 KIPS, FIN				
1	1.91	-1.91	-1.00	50
2	3.19	-3.19	-1.00	9
3	4.46	-4.46	-1.00	2
4	5.74	-5.74	-1.00	1
5	4.46	-4.46	-1.00	1
6	3.19	-3.19	-1.00	8
7	1.91	-1.91	-1.00	49
CRUISE, 30,000 FT., 180 KIPS, FIN				
1	1.91	-1.91	-1.00	49
2	3.19	-3.19	-1.00	8
3	4.46	-4.46	-1.00	2
4	5.74	-5.74	-1.00	1
5	4.46	-4.46	-1.00	1
6	3.19	-3.19	-1.00	8
7	1.91	-1.91	-1.00	49
CRUISE, 30,000 FT., 160 KIPS, FIN				
1	1.91	-1.91	-1.00	49
2	3.19	-3.19	-1.00	8
3	4.46	-4.46	-1.00	2
4	5.74	-5.74	-1.00	1
5	4.46	-4.46	-1.00	1
6	3.19	-3.19	-1.00	8
7	1.91	-1.91	-1.00	48

TABLE A-3 (CONT'D)  
MISSION SEGMENT STRESS SPECTRA  
FIN ANALYSIS LOCATION

<u>STRESS NUMBER</u>	<u>MAXIMUM STRESS</u> KSI	<u>MINIMUM STRESS</u> KSI	<u>R</u>	<u>NUMBER OF CYCLES</u>
CRUISE, 30,000 FT., 140 KIPS, FIN				
1	1.91	-1.91	-1.00	48
2	3.19	-3.19	-1.00	8
3	4.46	-4.46	-1.00	2
4	5.74	-5.74	-1.00	1
5	4.46	-4.46	-1.00	1
6	3.19	-3.19	-1.00	7
7	1.91	-1.91	-1.00	47
REFUEL, 280 KIPS, FIN				
1	1.91	-1.91	-1.00	50
2	3.19	-3.19	-1.00	9
3	4.46	-4.46	-1.00	2
4	5.74	-5.74	-1.00	1
5	4.46	-4.46	-1.00	1
6	3.19	-3.19	-1.00	8
7	1.91	-1.91	-1.00	50
REFUEL, 220 KIPS, FIN				
1	1.91	-1.91	-1.00	50
2	3.19	-3.19	-1.00	9
3	4.46	-4.46	-1.00	2
4	5.74	-5.74	-1.00	1
5	4.46	-4.46	-1.00	1
6	3.19	-3.19	-1.00	8
7	1.91	-1.91	-1.00	50
REFUEL, 160 KIPS, FIN				
1	1.91	-1.91	-1.00	49
2	3.19	-3.19	-1.00	8
3	4.46	-4.46	-1.00	2
4	5.74	-5.74	-1.00	1
5	4.46	-4.46	-1.00	1
6	3.19	-3.19	-1.00	8
7	1.91	-1.91	-1.00	48
TOUCH AND GO, 200 KIPS, FIN				
1	1.91	-1.91	-1.00	82
2	3.19	-3.19	-1.00	29
3	4.46	-4.46	-1.00	10
4	5.74	-5.74	-1.00	4
5	7.01	-7.01	-1.00	2
6	8.29	-8.29	-1.00	1
7	7.01	-7.01	-1.00	1
8	5.74	-5.74	-1.00	3
9	4.46	-4.46	-1.00	10
10	3.19	-3.19	-1.00	29
11	1.91	-1.91	-1.00	81
TOUCH AND GO, 180 KIPS, FIN				
1	1.91	-1.91	-1.00	79
2	3.19	-3.19	-1.00	26
3	4.46	-4.46	-1.00	9
4	5.74	-5.74	-1.00	3
5	7.01	-7.01	-1.00	1
6	8.29	-8.29	-1.00	1
7	7.01	-7.01	-1.00	1

TABLE A-3 (CONT'D)  
MISSION SEGMENT STRESS SPECTRA  
FIN ANALYSIS LOCATION

<u>STRESS NUMBER</u>	<u>MAXIMUM STRESS</u> KSI	<u>MINIMUM STRESS</u> KSI	<u>R</u>	<u>NUMBER OF CYCLES</u>
8	5.74	-5.74	-1.00	3
9	4.46	-4.46	-1.00	8
10	3.19	-3.19	-1.00	26
11	1.91	-1.91	-1.00	79
TOUCH AND GO, 160 KIPS, FIN				
1	1.91	-1.91	-1.00	76
2	3.19	-3.19	-1.00	24
3	4.46	-4.46	-1.00	7
4	5.74	-5.74	-1.00	2
5	7.01	-7.01	-1.00	1
6	5.74	-5.74	-1.00	2
7	4.46	-4.46	-1.00	7
8	3.19	-3.19	-1.00	23
9	1.91	-1.91	-1.00	76
TOUCH AND GO, 140 KIPS, FIN				
1	1.91	-1.91	-1.00	73
2	3.19	-3.19	-1.00	21
3	4.46	-4.46	-1.00	6
4	5.74	-5.74	-1.00	2
5	7.01	-7.01	-1.00	1
6	5.74	-5.74	-1.00	1
7	4.46	-4.46	-1.00	5
8	3.19	-3.19	-1.00	20
9	1.91	-1.91	-1.00	72
PATTERN, 200 KIPS, FIN				
1	1.91	-1.91	-1.00	626
2	3.19	-3.19	-1.00	221
3	4.46	-4.46	-1.00	79
4	5.74	-5.74	-1.00	28
5	7.01	-7.01	-1.00	10
6	8.29	-8.29	-1.00	4
7	9.56	-9.56	-1.00	2
8	10.84	-10.84	-1.00	1
9	9.56	-9.56	-1.00	1
10	8.29	-8.29	-1.00	3
11	7.01	-7.01	-1.00	10
12	5.74	-5.74	-1.00	28
13	4.46	-4.46	-1.00	78
14	3.19	-3.19	-1.00	221
15	1.91	-1.91	-1.00	625
PATTERN, 180 KIPS, FIN				
1	1.91	-1.91	-1.00	608
2	3.19	-3.19	-1.00	201
3	4.46	-4.46	-1.00	67
4	5.74	-5.74	-1.00	23
5	7.01	-7.01	-1.00	8
6	8.29	-8.29	-1.00	3
7	9.56	-9.56	-1.00	1
8	10.84	-10.84	-1.00	1
9	9.56	-9.56	-1.00	1
10	8.29	-8.29	-1.00	2
11	7.01	-7.01	-1.00	7
12	5.74	-5.74	-1.00	22
13	4.46	-4.46	-1.00	67

TABLE A-3 (CONCLUDED)  
MISSION SEGMENT STRESS SPECTRA  
FIN ANALYSIS LOCATION

<u>STRESS NUMBER</u>	<u>MAXIMUM STRESS KSI</u>	<u>MINIMUM STRESS KSI</u>	<u>R</u>	<u>NUMBER OF CYCLES</u>
14	3.19	-3.19	-1.00	200
15	1.91	-1.91	-1.00	607
PATTERN, 160 KIPS, FIN				
1	1.91	-1.91	-1.00	585
2	3.19	-3.19	-1.00	179
3	4.46	-4.46	-1.00	55
4	5.74	-5.74	-1.00	17
5	7.01	-7.01	-1.00	6
6	8.29	-8.29	-1.00	2
7	9.56	-9.56	-1.00	1
8	8.29	-8.29	-1.00	2
9	7.01	-7.01	-1.00	5
10	5.74	-5.74	-1.00	17
11	4.46	-4.46	-1.00	55
12	3.19	-3.19	-1.00	179
13	1.91	-1.91	-1.00	584
PATTERN, 140 KIPS, FIN				
1	1.91	-1.91	-1.00	557
2	3.19	-3.19	-1.00	156
3	4.46	-4.46	-1.00	44
4	5.74	-5.74	-1.00	13
5	7.01	-7.01	-1.00	4
6	8.29	-8.29	-1.00	1
7	9.56	-9.56	-1.00	1
8	8.29	-8.29	-1.00	1
9	7.01	-7.01	-1.00	3
10	5.74	-5.74	-1.00	12
11	4.46	-4.46	-1.00	44
12	3.19	-3.19	-1.00	156
13	1.91	-1.91	-1.00	557

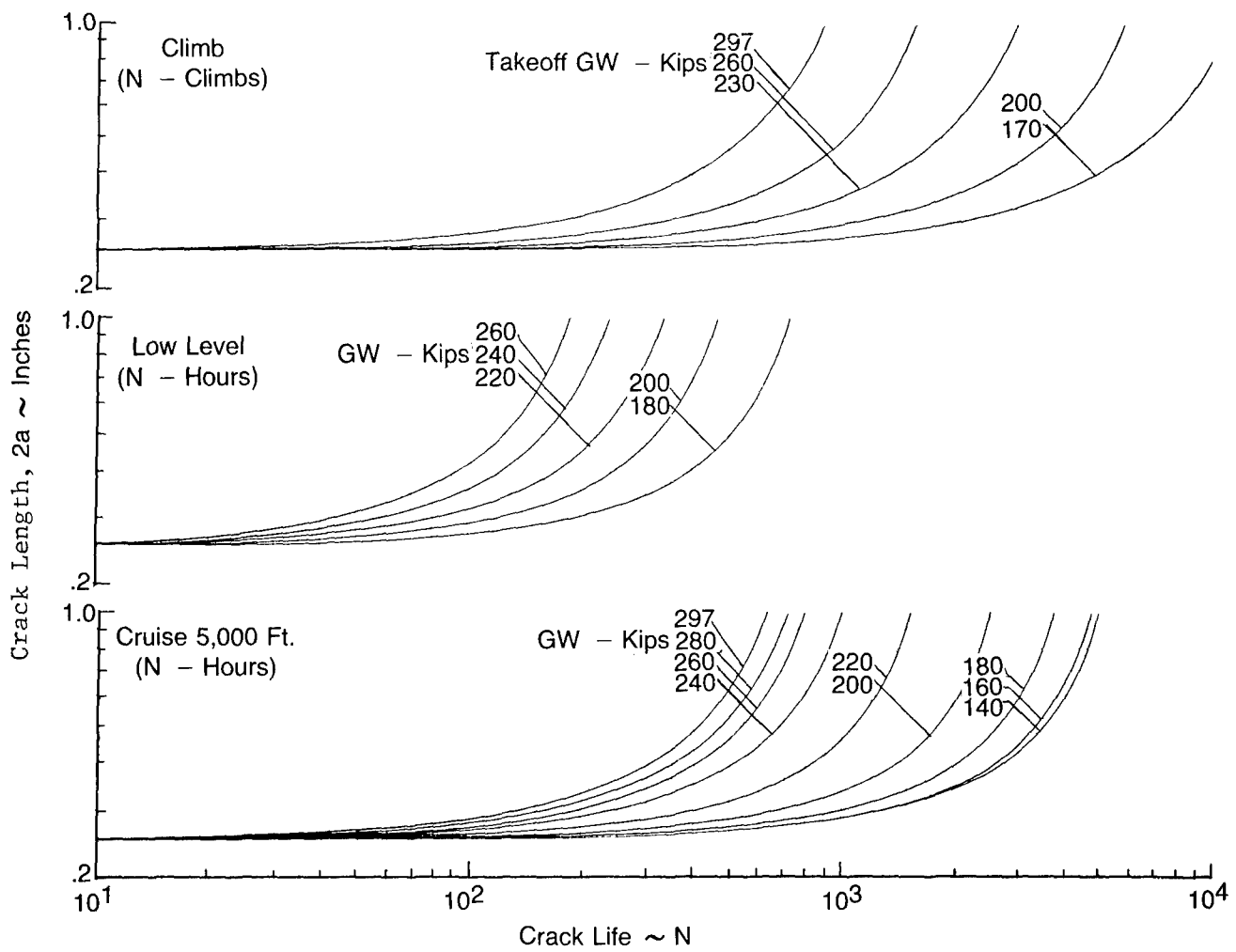


Figure A-1. Mission Segment Crack Growth Climb, Low Level, Cruise 5000 Ft, Wing

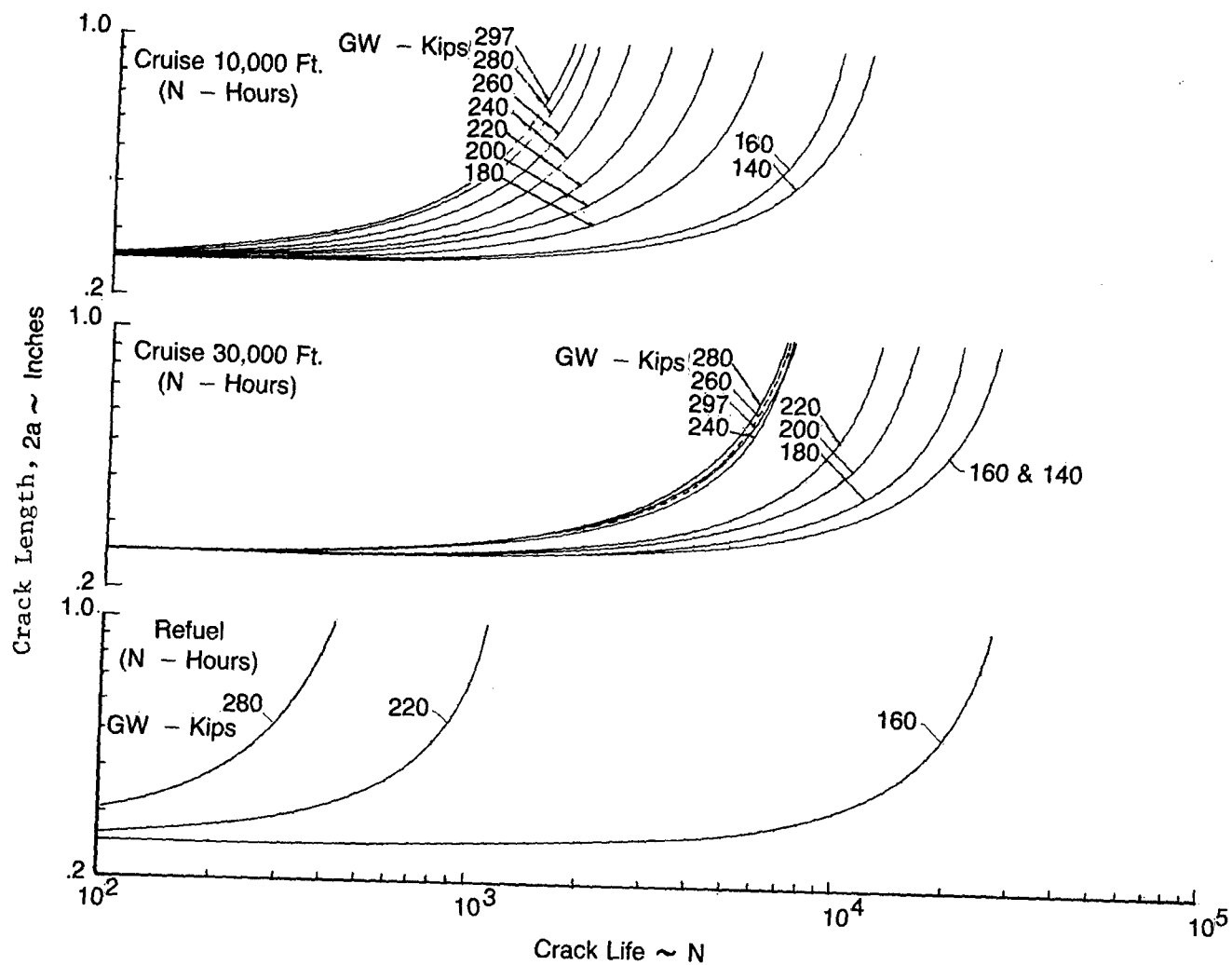


Figure A-1. Mission Segment Crack Growth Cruise 10,000 Ft and 30,000 Ft, Refuel, Wing (Cont'd)

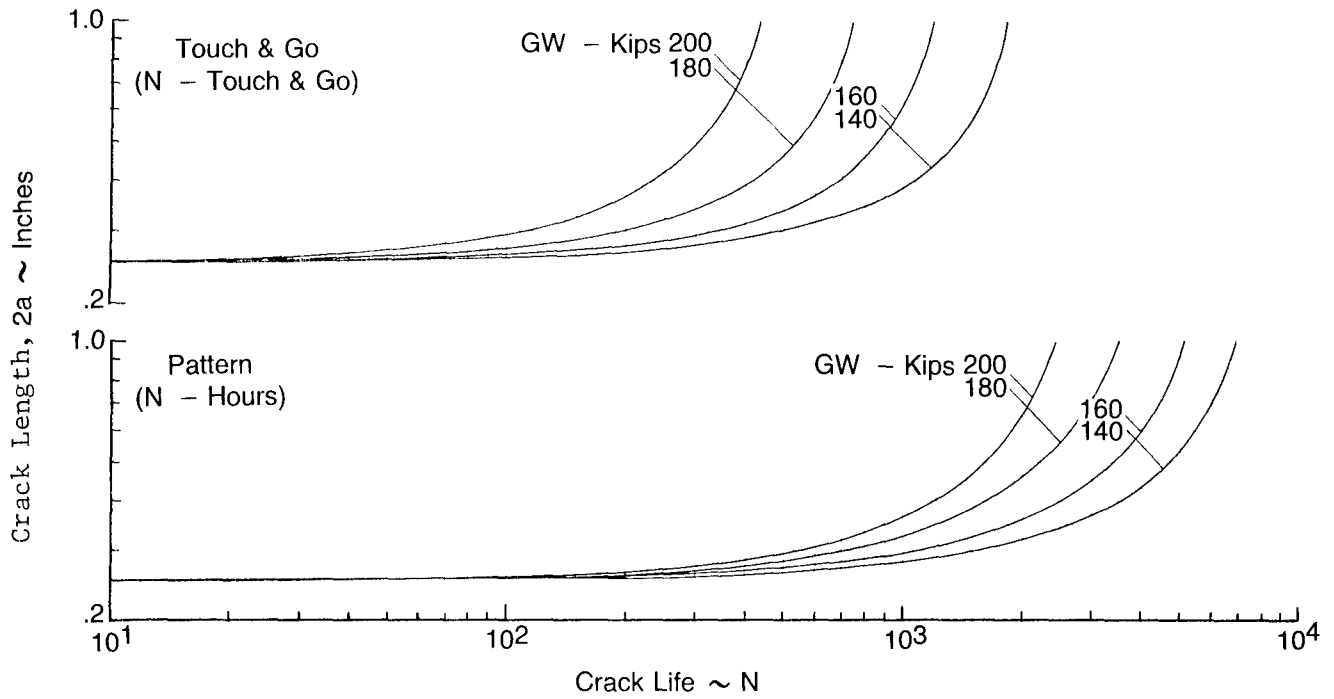


Figure A-1. (Concluded) Mission Segment Crack Growth Touch & Go, Pattern, Wing

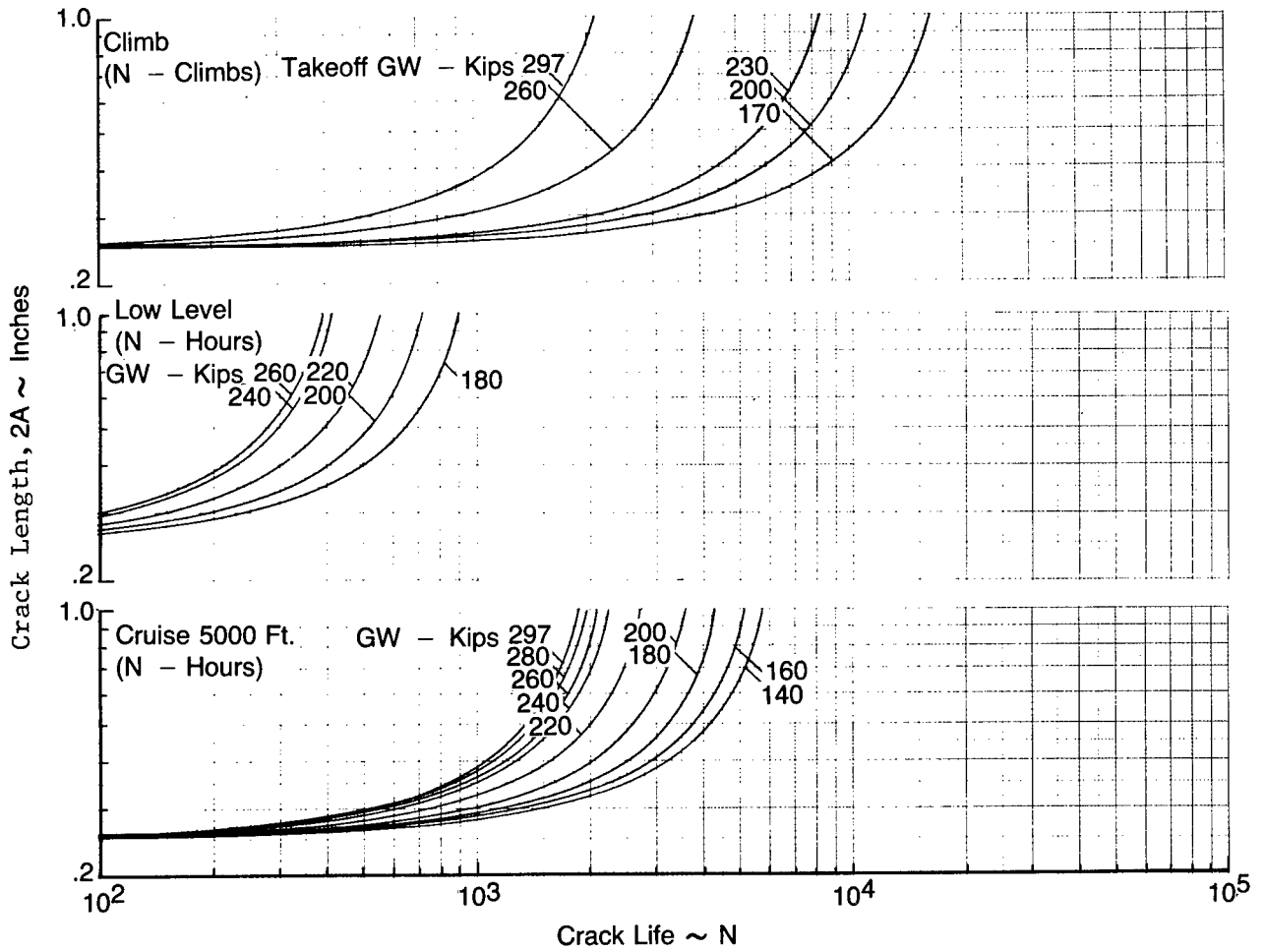


Figure A-2. Mission Segment Crack Growth Climb, Low Level, Cruise 5000 Ft., Body

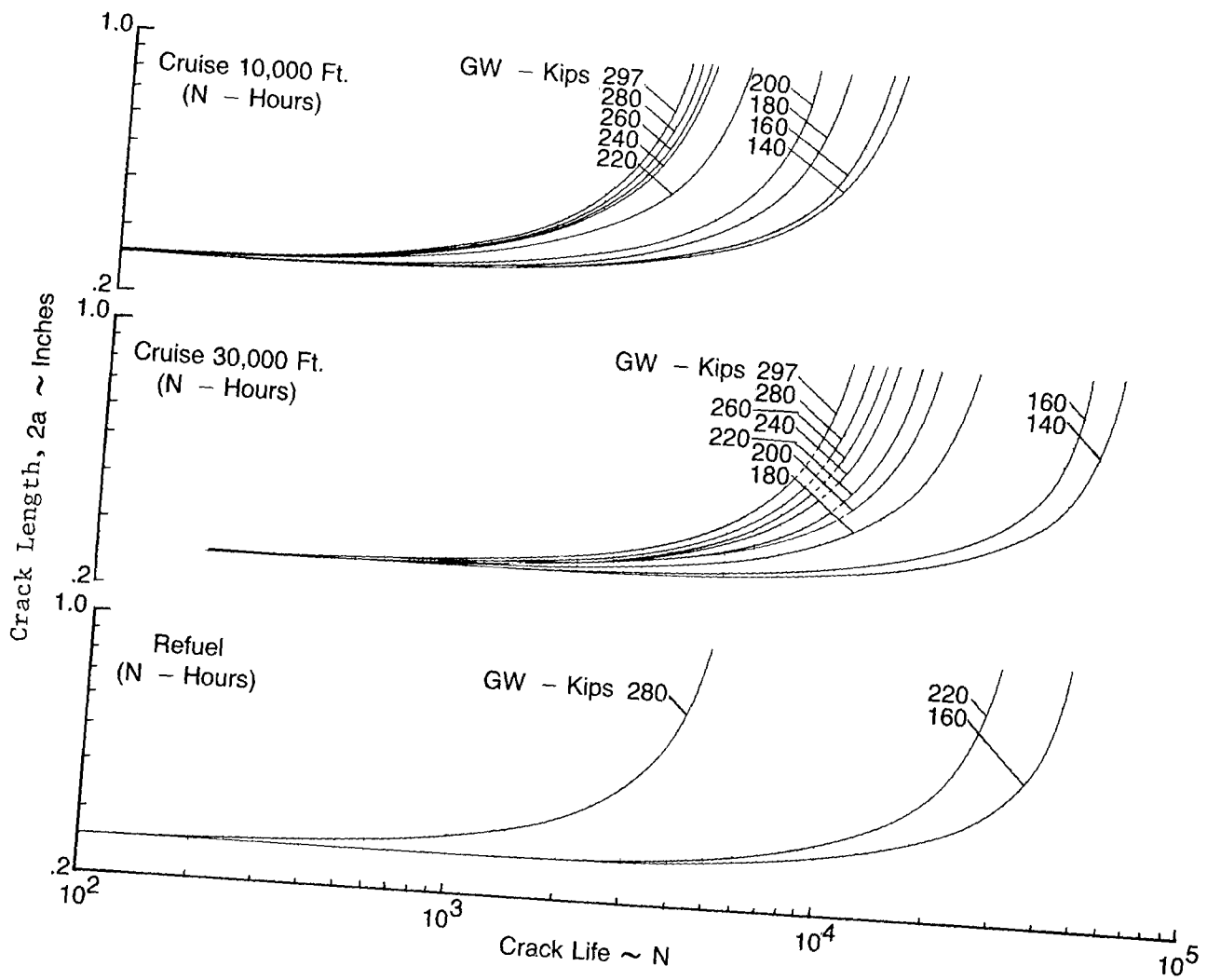


Figure A-2. Mission Segment Crack Growth Cruise 10,000 Ft and 30,000 Ft, Refuel, Body (Cont'd)

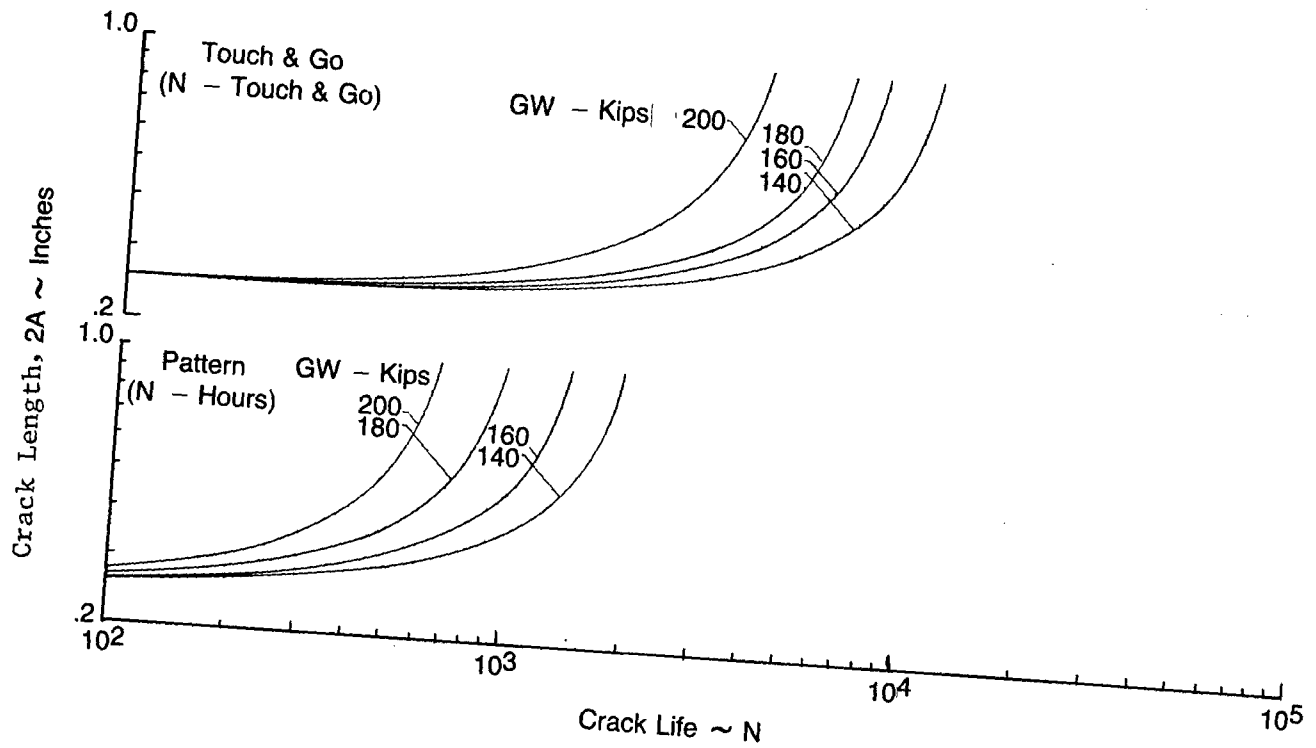


Figure A-2. (Concluded) Mission Segment Crack Growth Touch & Go, Pattern, Body

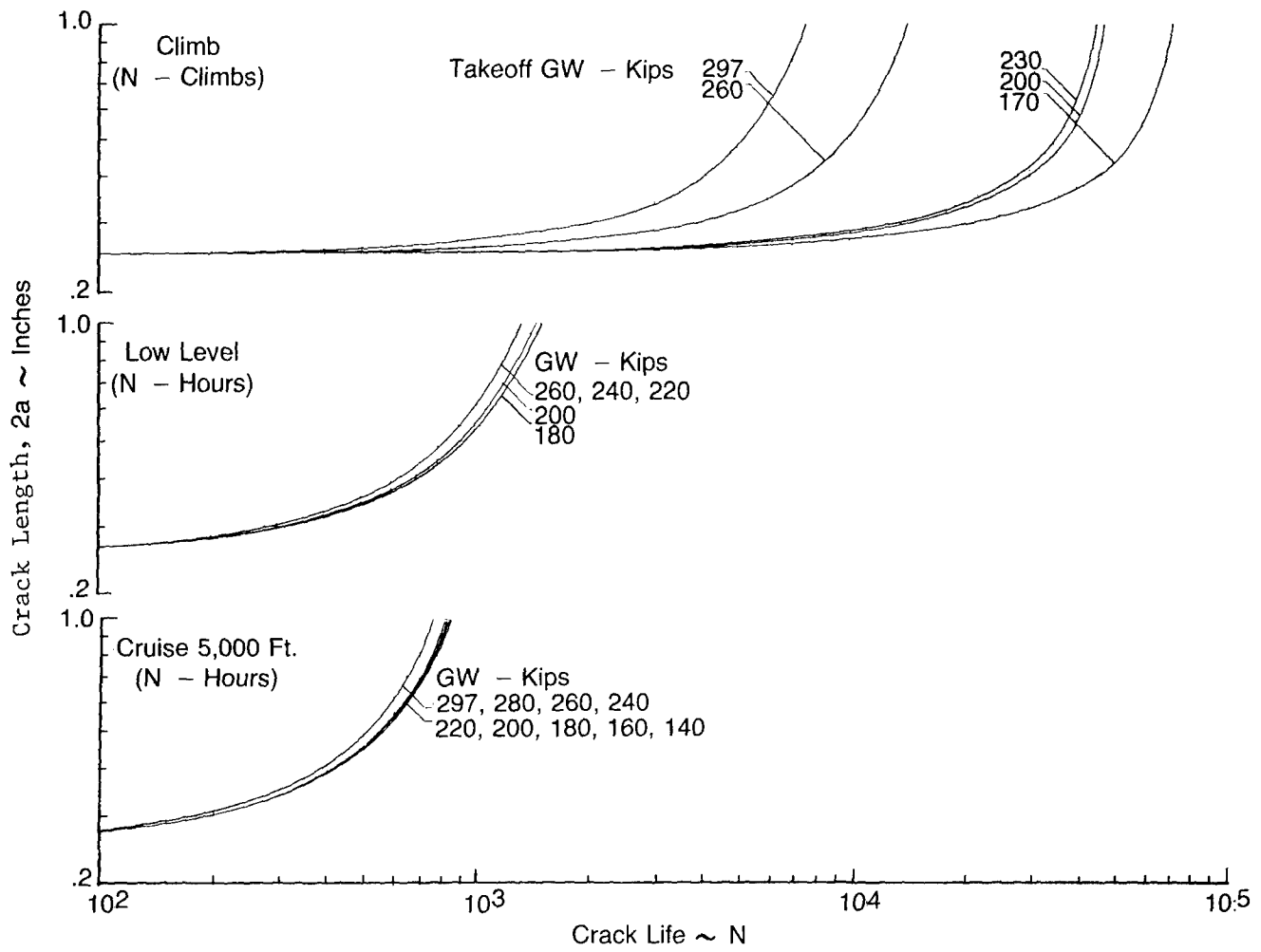


Figure A-3. Mission Segment Crack Growth Climb, Low Level, Cruise 5000 Ft, Fin

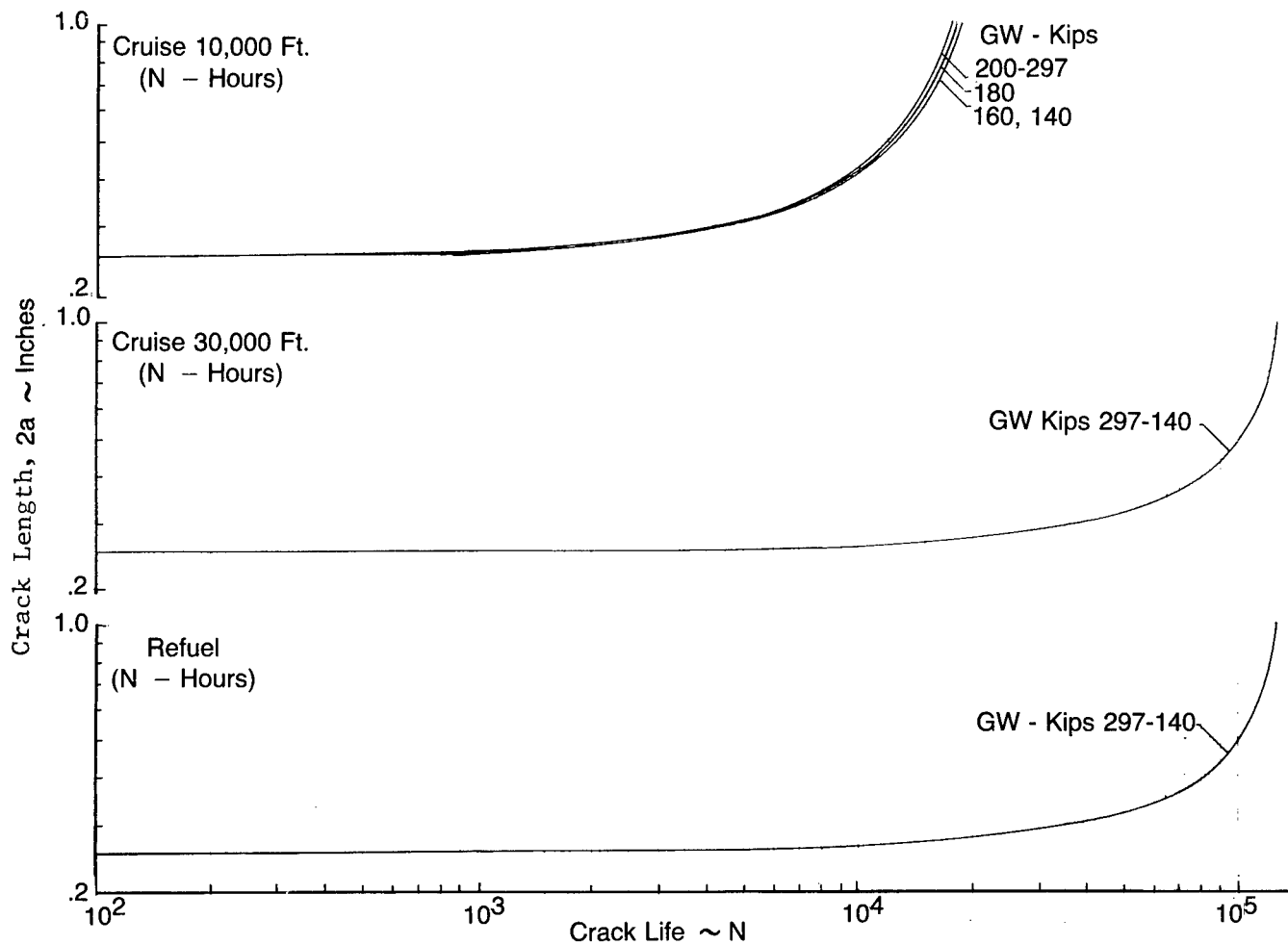


Figure A-3. Mission Segment Crack Growth Cruise 10,000 Ft and 30,000 Ft, Refuel, Fin (Cont'd)

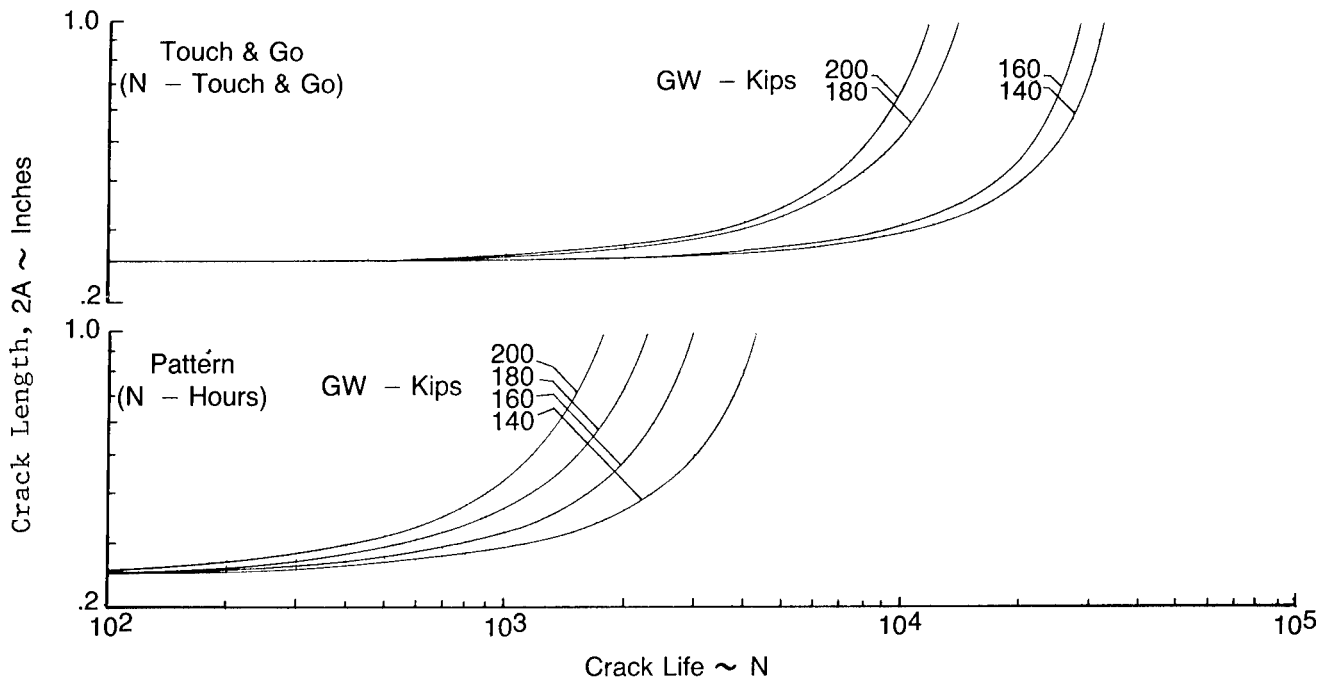


Figure A-3. (Concluded) Mission Segment Crack Growth Touch and Go, Pattern, Fin

## **APPENDIX B RELATED VARIABILITY ANALYSIS DATA**

This appendix presents (1) the mission spectra used in the variability study and (2) the crack growth curves for each of the missions evaluated for the three structural analysis locations. These data are discussed in Section 2.8.

### 1. Mission Stress Spectra

The mission stress spectra were derived from the mission segment stress exceedance data generated from the PSD stress/damage program. The sequence generator program was used to assemble these data in sequence with the appropriate mission segment flight durations included. The programs and analysis methods used were discussed in Section 2.2.

Tables B-1, B-2 and B-3 present a listing of the variable mission spectra generated for the wing, body and fin analysis locations, respectively. The mission profile associated with each spectrum is shown in Section 2.8, Figure 32. Each table shows the maximum stress, minimum stress, R ratio and the number of cycles. For the wing and body spectra, the maximum stress equaled or exceeded in 10, 100 and 200 flights is shown.

### 2. Mission Crack Growth Curves

Mission crack growth was determined using the Wheeler Retardation Model with a shaping exponent,  $m$ , or 0.90. Figures B-1 through B-6 show the crack growth for the wing, body and fin analysis locations based on life in flights and flight hours, respectively.

TABLE B-1  
VARIABLE MISSION STRESS SPECTRA  
WING ANALYSIS LOCATION

<u>STRESS NUMBER</u>	<u>MAXIMUM STRESS</u> KSI	<u>MINIMUM STRESS</u> KSI	<u>R</u>	<u>NUMBER OF CYCLES</u>
VARIABLE MISSION NO. 1A, WING				
1	26.04	-12.23	-0.47	1
2	22.09	18.26	0.83	34
3	23.36	16.99	0.73	7
4	24.64	15.71	0.64	2
5	25.91	14.44	0.56	1
6	24.64	15.71	0.64	1
7	23.36	16.99	0.73	6
8	22.09	18.26	0.83	34
9	21.88	18.06	0.83	7
10	23.16	16.78	0.72	1
11	21.88	18.06	0.83	6
12	19.91	16.09	0.81	17
13	21.19	14.81	0.70	3
14	19.91	16.09	0.81	16
15	18.42	14.59	0.79	16
16	19.69	13.32	0.68	3
17	18.42	14.59	0.79	16
18	16.50	12.68	0.77	15
19	17.78	11.40	0.64	2
20	16.50	12.68	0.77	15
21	14.58	10.75	0.74	9
22	15.85	9.48	0.60	1
23	14.58	10.75	0.74	8

FMAX EQUALLED OR EXCEEDED IN 10 FLIGHTS = 28.64 KSI  
 FMAX EQUALLED OR EXCEEDED IN 100 FLIGHTS = 31.52 KSI  
 FMAX EQUALLED OR EXCEEDED IN 200 FLIGHTS = 32.41 KSI

VARIABLE MISSION NO. 2A, WING				
1	26.04	-12.23	-0.47	1
2	22.09	18.26	0.83	34
3	23.36	16.99	0.73	7
4	24.64	15.71	0.64	2
5	25.91	14.44	0.56	1
6	24.64	15.71	0.64	1
7	23.36	16.99	0.73	6
8	22.09	18.26	0.83	34
9	21.88	18.06	0.83	7
10	23.16	16.78	0.72	1
11	21.88	18.06	0.83	6
12	21.88	18.06	0.83	89
13	23.16	16.78	0.72	10
14	24.43	15.51	0.63	3
15	23.16	16.78	0.72	10
16	21.88	18.06	0.83	89
17	21.88	18.06	0.83	17
18	23.16	16.78	0.72	2
19	24.43	15.51	0.63	1
20	23.16	16.78	0.72	1
21	21.88	18.06	0.83	17
22	19.91	16.09	0.81	17
23	21.19	14.81	0.70	3
24	19.91	16.09	0.81	16
25	18.42	14.59	0.79	16
26	19.69	13.32	0.68	3
27	18.42	14.59	0.79	16

TABLE B-1 (CONT'D)  
 VARIABLE MISSION STRESS SPECTRA  
 WING ANALYSIS LOCATION

<u>STRESS NUMBER</u>	<u>MAXIMUM STRESS</u> KSI	<u>MINIMUM STRESS</u> KSI	<u>R</u>	<u>NUMBER OF CYCLES</u>
FMAX EQUALLED OR EXCEEDED IN 10 FLIGHTS = 28.64 KSI				
FMAX EQUALLED OR EXCEEDED IN 100 FLIGHTS = 31.52 KSI				
FMAX EQUALLED OR EXCEEDED IN 200 FLIGHTS = 32.41 KSI				
VARIABLE MISSION NO. 3A, WING				
1	26.04	-12.23	-0.47	1
2	22.09	18.26	0.83	34
3	23.36	16.99	0.73	7
4	24.64	15.71	0.64	2
5	25.91	14.44	0.56	1
6	24.64	15.71	0.64	1
7	23.36	16.99	0.73	6
8	22.09	18.26	0.83	34
9	21.88	18.06	0.83	7
10	23.16	16.78	0.72	1
11	21.88	18.06	0.83	6
12	18.76	14.94	0.80	226
13	20.04	13.66	0.68	45
14	21.31	12.39	0.58	9
15	22.59	11.11	0.49	2
16	23.86	9.84	0.41	1
17	22.59	11.11	0.49	2
18	21.31	12.39	0.58	9
19	20.04	13.66	0.68	45
20	18.76	14.94	0.80	225
21	17.25	13.43	0.78	215
22	18.53	12.15	0.66	40
23	19.80	10.88	0.55	8
24	21.08	9.60	0.46	2
25	22.35	8.33	0.37	1
26	21.08	9.60	0.46	2
27	19.80	10.88	0.55	8
28	18.53	12.15	0.66	39
29	17.25	13.43	0.78	214
30	16.50	12.68	0.77	15
31	17.78	11.40	0.64	2
32	16.50	12.68	0.77	15
33	14.58	10.75	0.74	9
34	15.85	9.48	0.60	1
35	14.58	10.75	0.74	8
FMAX EQUALLED OR EXCEEDED IN 10 FLIGHTS = 28.64 KSI				
FMAX EQUALLED OR EXCEEDED IN 100 FLIGHTS = 31.52 KSI				
FMAX EQUALLED OR EXCEEDED IN 200 FLIGHTS = 32.41 KSI				
VARIABLE MISSION NO. 4A, WING				
1	26.04	-12.23	-0.47	1
2	22.09	18.26	0.83	34
3	23.36	16.99	0.73	7
4	24.64	15.71	0.64	2
5	25.91	14.44	0.56	1
6	24.64	15.71	0.64	1
7	23.36	16.99	0.73	6
8	22.09	18.26	0.83	34
9	21.88	18.06	0.83	7
10	23.16	16.78	0.72	1
11	21.88	18.06	0.83	6

TABLE B-1 (CONT'D)  
 VARIABLE MISSION STRESS SPECTRA  
 WING ANALYSIS LOCATION

<u>STRESS NUMBER</u>	<u>MAXIMUM STRESS</u> KSI	<u>MINIMUM STRESS</u> KSI	<u>R</u>	<u>NUMBER OF CYCLES</u>
12	19.91	16.09	0.81	17
13	21.19	14.81	0.70	3
14	19.91	16.09	0.81	16
15	18.42	14.59	0.79	16
16	19.69	13.32	0.68	3
17	18.42	14.59	0.79	16
18	16.50	12.68	0.77	15
19	17.78	11.40	0.64	2
20	16.50	12.68	0.77	15
21	15.23	-0.20	-0.01	1
22	12.43	8.60	0.69	28
23	13.70	7.33	0.53	5
24	14.98	6.05	0.40	1
25	13.70	7.33	0.53	4
26	12.43	8.60	0.69	28
27	15.23	-0.20	-0.01	1
28	12.43	8.60	0.69	28
29	13.70	7.33	0.53	5
30	14.98	6.05	0.40	1
31	13.70	7.33	0.53	4
32	12.43	8.60	0.69	28
33	15.23	-0.20	-0.01	1
34	12.43	8.60	0.69	28
35	13.70	7.33	0.53	5
36	14.98	6.05	0.40	1
37	13.70	7.33	0.53	4
38	12.43	8.60	0.69	28

FMAX EQUALLED OR EXCEEDED IN 10 FLIGHTS = 28.64 KSI  
 FMAX EQUALLED OR EXCEEDED IN 100 FLIGHTS = 31.52 KSI  
 FMAX EQUALLED OR EXCEEDED IN 200 FLIGHTS = 32.41 KSI

VARIABLE MISSION NO. 1B, WING

1	18.17	-12.23	-0.67	1
2	15.96	12.14	0.76	13
3	17.24	10.86	0.63	2
4	18.51	9.59	0.52	1
5	17.24	10.86	0.63	2
6	15.96	12.14	0.76	13
7	16.50	12.68	0.77	8
8	17.78	11.40	0.64	1
9	16.50	12.68	0.77	8
10	14.58	10.75	0.74	14
11	15.85	9.48	0.60	2
12	14.58	10.75	0.74	14
13	12.76	8.94	0.70	13
14	14.04	7.66	0.55	2
15	12.76	8.94	0.70	13

FMAX EQUALLED OR EXCEEDED IN 10 FLIGHTS = 20.35 KSI  
 FMAX EQUALLED OR EXCEEDED IN 100 FLIGHTS = 23.32 KSI  
 FMAX EQUALLED OR EXCEEDED IN 200 FLIGHTS = 24.45 KSI

VARIABLE MISSION NO. 2B, WING

1	18.17	-12.23	-0.67	1
2	15.96	12.14	0.76	13
3	17.24	10.86	0.63	2
4	18.51	9.59	0.52	1

TABLE B-1 (CONT'D)  
 VARIABLE MISSION STRESS SPECTRA  
 WING ANALYSIS LOCATION

<u>STRESS NUMBER</u>	<u>MAXIMUM STRESS</u> KSI	<u>MINIMUM STRESS</u> KSI	<u>R</u>	<u>NUMBER OF CYCLES</u>
5	17.24	10.86	0.63	2
6	15.96	12.14	0.76	13
7	16.50	12.68	0.77	8
8	17.78	11.40	0.64	1
9	16.50	12.68	0.77	8
10	16.50	12.68	0.77	61
11	17.78	11.40	0.64	4
12	16.50	12.68	0.77	60
13	16.50	12.68	0.77	15
14	17.78	11.40	0.64	2
15	16.50	12.68	0.77	15
16	14.58	10.75	0.74	9
17	15.85	9.48	0.60	1
18	14.58	10.75	0.74	8

FMAX EQUALLED OR EXCEEDED IN 10 FLIGHTS = 20.35 KSI  
 FMAX EQUALLED OR EXCEEDED IN 100 FLIGHTS = 23.32 KSI  
 FMAX EQUALLED OR EXCEEDED IN 200 FLIGHTS = 24.45 KSI

VARIABLE MISSION NO. 3B, WING

1	18.17	-12.23	-0.67	1
2	15.96	12.14	0.76	13
3	17.24	10.86	0.63	2
4	18.51	9.59	0.52	1
5	17.24	10.86	0.63	2
6	15.96	12.14	0.76	13
7	16.50	12.68	0.77	8
8	17.78	11.40	0.64	1
9	16.50	12.68	0.77	8
10	13.41	9.58	0.71	178
11	14.68	8.31	0.57	27
12	15.96	7.03	0.44	5
13	17.23	5.76	0.33	2
14	15.96	7.03	0.44	4
15	14.68	8.31	0.57	26
16	13.41	9.58	0.71	178
17	11.55	7.73	0.67	165
18	12.83	6.45	0.50	23
19	14.10	5.18	0.37	4
20	15.38	3.90	0.25	1
21	14.10	5.18	0.37	3
22	12.83	6.45	0.50	22
23	11.55	7.73	0.67	164
24	11.59	7.77	0.67	7
25	12.87	6.49	0.50	1
26	11.59	7.77	0.67	6

FMAX EQUALLED OR EXCEEDED IN 10 FLIGHTS = 20.35 KSI  
 FMAX EQUALLED OR EXCEEDED IN 100 FLIGHTS = 23.32 KSI  
 FMAX EQUALLED OR EXCEEDED IN 200 FLIGHTS = 24.45 KSI

VARIABLE MISSION NO. 4B, WING

1	18.17	-12.23	-0.67	1
2	15.96	12.14	0.76	13
3	17.24	10.86	0.63	2
4	18.51	9.59	0.52	1
5	17.24	10.86	0.63	2
6	15.96	12.14	0.76	13

TABLE B-1 (CONT'D)  
VARIABLE MISSION STRESS SPECTRA  
WING ANALYSIS LOCATION

<u>STRESS NUMBER</u>	<u>MAXIMUM STRESS</u> KSI	<u>MINIMUM STRESS</u> KSI	<u>R</u>	<u>NUMBER OF CYCLES</u>
7	16.50	12.68	0.77	8
8	17.78	11.40	0.64	1
9	16.50	12.68	0.77	8
10	14.58	10.75	0.74	14
11	15.85	9.48	0.60	2
12	14.58	10.75	0.74	14
13	14.58	-1.26	-0.09	1
14	12.64	8.82	0.70	23
15	13.92	7.54	0.54	3
16	15.19	6.27	0.41	1
17	13.92	7.54	0.54	2
18	12.64	8.82	0.70	22
19	14.58	-1.26	-0.09	1
20	12.64	8.82	0.70	23
21	13.92	7.54	0.54	3
22	15.19	6.27	0.41	1
23	13.92	7.54	0.54	2
24	12.64	8.82	0.70	22
25	14.58	-1.26	-0.09	1
26	12.64	8.82	0.70	23
27	13.92	7.54	0.54	3
28	15.19	6.27	0.41	1
29	13.92	7.54	0.54	2
30	12.64	8.82	0.70	22

FMAX EQUALLED OR EXCEEDED IN 10 FLIGHTS = 20.35 KSI  
 FMAX EQUALLED OR EXCEEDED IN 100 FLIGHTS = 23.32 KSI  
 FMAX EQUALLED OR EXCEEDED IN 200 FLIGHTS = 24.45 KSI

VARIABLE MISSION NO. 5B, WING

1	18.17	-12.23	-0.67	1
2	15.96	12.14	0.76	13
3	17.24	10.86	0.63	2
4	18.51	9.59	0.52	1
5	17.24	10.86	0.63	2
6	15.96	12.14	0.76	13
7	16.50	12.68	0.77	8
8	17.78	11.40	0.64	1
9	16.50	12.68	0.77	8
10	12.43	8.60	0.69	216
11	13.70	7.33	0.53	33
12	14.98	6.05	0.40	5
13	16.25	4.78	0.29	1
14	17.53	3.50	0.20	1
15	16.25	4.78	0.29	1
16	14.98	6.05	0.40	5
17	13.70	7.33	0.53	33
18	12.43	8.60	0.69	215
19	14.58	-1.26	-0.09	1
20	12.64	8.82	0.70	23
21	13.92	7.54	0.54	3
22	15.19	6.27	0.41	1
23	13.92	7.54	0.54	2
24	12.64	8.82	0.70	22
25	14.58	-1.26	-0.09	1
26	12.64	8.82	0.70	23
27	13.92	7.54	0.54	3
28	15.19	6.27	0.41	1

TABLE B-1 (CONT'D)  
 VARIABLE MISSION STRESS SPECTRA  
 WING ANALYSIS LOCATION

<u>STRESS NUMBER</u>	<u>MAXIMUM STRESS</u> KSI	<u>MINIMUM STRESS</u> KSI	<u>R</u>	<u>NUMBER OF CYCLES</u>
29	13.92	7.54	0.54	2
30	12.64	8.82	0.70	22
31	14.58	-1.26	-0.09	1
32	12.64	8.82	0.70	23
33	13.92	7.54	0.54	3
34	15.19	6.27	0.41	1
35	13.92	7.54	0.54	2
36	12.64	8.82	0.70	22
37	14.58	-1.26	-0.09	1
38	12.64	8.82	0.70	23
39	13.92	7.54	0.54	3
40	15.19	6.27	0.41	1
41	13.92	7.54	0.54	2
42	12.64	8.82	0.70	22
43	14.58	-1.26	-0.09	1
44	12.64	8.82	0.70	23
45	13.92	7.54	0.54	3
46	15.19	6.27	0.41	1
47	13.92	7.54	0.54	2
48	12.64	8.82	0.70	22
49	14.58	-1.26	-0.09	1
50	12.64	8.82	0.70	23
51	13.92	7.54	0.54	3
52	15.19	6.27	0.41	1
53	13.92	7.54	0.54	2
54	12.64	8.82	0.70	22

FMAX EQUALLED OR EXCEEDED IN 10 FLIGHTS = 20.35 KSI  
 FMAX EQUALLED OR EXCEEDED IN 100 FLIGHTS = 23.32 KSI  
 FMAX EQUALLED OR EXCEEDED IN 200 FLIGHTS = 24.45 KSI

VARIABLE MISSION NO. 5B1, WING

1	18.17	-12.23	-0.67	1
2	15.89	12.06	0.76	9
3	17.16	10.79	0.63	3
4	15.89	12.06	0.76	8
5	15.42	11.59	0.75	63
6	16.69	10.32	0.62	7
7	17.97	9.04	0.50	1
8	19.24	7.77	0.40	1
9	17.97	9.04	0.50	1
10	16.69	10.32	0.62	7
11	15.42	11.59	0.75	62
12	12.43	8.60	0.69	216
13	13.70	7.33	0.53	33
14	14.98	6.05	0.40	5
15	16.25	4.78	0.29	1
16	17.53	3.50	0.20	1
17	16.25	4.78	0.29	1
18	14.98	6.05	0.40	5
19	13.70	7.33	0.53	33
20	12.43	8.60	0.69	215
21	14.58	-1.26	-0.09	1
22	12.64	8.82	0.70	23
23	13.92	7.54	0.54	3
24	15.19	6.27	0.41	1
25	13.92	7.54	0.54	2
26	12.64	8.82	0.70	22

TABLE B-1 (CONT'D)  
 VARIABLE MISSION STRESS SPECTRA  
 WING ANALYSIS LOCATION

<u>STRESS NUMBER</u>	<u>MAXIMUM STRESS</u> KSI	<u>MINIMUM STRESS</u> KSI	<u>R</u>	<u>NUMBER OF CYCLES</u>
27	14.58	-1.26	-0.09	1
28	12.64	8.82	0.70	23
29	13.92	7.54	0.54	3
30	15.19	6.27	0.41	1
31	13.92	7.54	0.54	2
32	12.64	8.82	0.70	22
33	14.58	-1.26	-0.09	1
34	12.64	8.82	0.70	23
35	13.92	7.54	0.54	3
36	15.19	6.27	0.41	1
37	13.92	7.54	0.54	2
38	12.64	8.82	0.70	22
39	14.58	-1.26	-0.09	1
40	12.64	8.82	0.70	23
41	13.92	7.54	0.54	3
42	15.19	6.27	0.41	1
43	13.92	7.54	0.54	2
44	12.64	8.82	0.70	22
45	14.58	-1.26	-0.09	1
46	12.64	8.82	0.70	23
47	13.92	7.54	0.54	3
48	15.19	6.27	0.41	1
49	13.92	7.54	0.54	2
50	12.64	8.82	0.70	22
51	14.58	-1.26	-0.09	1
52	12.64	8.82	0.70	23
53	13.92	7.54	0.54	3
54	15.19	6.27	0.41	1
55	13.92	7.54	0.54	2
56	12.64	8.82	0.70	22

FMAX EQUALLED OR EXCEEDED IN 10 FLIGHTS = 20.35 KSI  
 FMAX EQUALLED OR EXCEEDED IN 100 FLIGHTS = 23.32 KSI  
 FMAX EQUALLED OR EXCEEDED IN 200 FLIGHTS = 24.45 KSI

VARIABLE MISSION NO. 1C, WING

1	12.48	-11.39	-0.91	1
2	11.20	7.37	0.66	8
3	12.47	6.10	0.49	1
4	11.20	7.37	0.66	7
5	11.59	7.77	0.67	9
6	12.87	6.49	0.50	1
7	11.59	7.77	0.67	8
8	11.85	8.03	0.68	12
9	13.13	6.75	0.51	1
10	11.85	8.03	0.68	11

FMAX EQUALLED OR EXCEEDED IN 10 FLIGHTS = 14.35 KSI  
 FMAX EQUALLED OR EXCEEDED IN 100 FLIGHTS = 16.76 KSI  
 FMAX EQUALLED OR EXCEEDED IN 200 FLIGHTS = 17.55 KSI

VARIABLE MISSION NO. 2C, WING

1	12.48	-11.39	-0.91	1
2	11.20	7.37	0.66	8
3	12.47	6.10	0.49	1
4	11.20	7.37	0.66	7
5	11.59	7.77	0.67	9
6	12.87	6.49	0.50	1

TABLE B-1 (CONT'D)  
 VARIABLE MISSION STRESS SPECTRA  
 WING ANALYSIS LOCATION

<u>STRESS NUMBER</u>	<u>MAXIMUM STRESS KSI</u>	<u>MINIMUM STRESS KSI</u>	<u>R</u>	<u>NUMBER OF CYCLES</u>
7	11.59	7.77	0.67	8
8	11.59	7.77	0.67	7
9	11.59	7.77	0.67	7
10	12.87	6.49	0.50	1
11	11.59	7.77	0.67	6

FMAX EQUALLED OR EXCEEDED IN 10 FLIGHTS = 14.35 KSI  
 FMAX EQUALLED OR EXCEEDED IN 100 FLIGHTS = 16.76 KSI  
 FMAX EQUALLED OR EXCEEDED IN 200 FLIGHTS = 17.55 KSI

VARIABLE MISSION NO. 4C, WING

1	12.48	-11.39	-0.91	1
2	11.20	7.37	0.66	8
3	12.47	6.10	0.49	1
4	11.20	7.37	0.66	7
5	11.59	7.77	0.67	9
6	12.87	6.49	0.50	1
7	11.59	7.77	0.67	8
8	11.85	8.03	0.68	6
9	13.13	6.75	0.51	1
10	11.85	8.03	0.68	6
11	11.38	-1.55	-0.14	1
12	10.36	6.54	0.63	16
13	11.64	5.26	0.45	2
14	10.36	6.54	0.63	15
15	11.38	-1.55	-0.14	1
16	10.36	6.54	0.63	16
17	11.64	5.26	0.45	2
18	10.36	6.54	0.63	15
19	11.38	-1.55	-0.14	1
20	10.36	6.54	0.63	16
21	11.64	5.26	0.45	2
22	10.36	6.54	0.63	15

FMAX EQUALLED OR EXCEEDED IN 10 FLIGHTS = 14.35 KSI  
 FMAX EQUALLED OR EXCEEDED IN 100 FLIGHTS = 16.76 KSI  
 FMAX EQUALLED OR EXCEEDED IN 200 FLIGHTS = 17.55 KSI

VARIABLE MISSION NO. 5C, WING

1	12.48	-11.39	-0.91	1
2	11.20	7.37	0.66	8
3	12.47	6.10	0.49	1
4	11.20	7.37	0.66	7
5	11.59	7.77	0.67	9
6	12.87	6.49	0.50	1
7	11.59	7.77	0.67	8
8	10.36	6.54	0.63	119
9	11.64	5.26	0.45	8
10	12.91	3.99	0.31	1
11	11.64	5.26	0.45	8
12	10.36	6.54	0.63	119
13	11.38	-1.55	-0.14	1
14	10.36	6.54	0.63	16
15	11.64	5.26	0.45	2
16	10.36	6.54	0.63	15
17	11.38	-1.55	-0.14	1
18	10.36	6.54	0.63	16
19	11.64	5.26	0.45	2

TABLE B-1 (CONT'D)  
 VARIABLE MISSION STRESS SPECTRA  
 WING ANALYSIS LOCATION

<u>STRESS NUMBER</u>	<u>MAXIMUM STRESS</u> KSI	<u>MINIMUM STRESS</u> KSI	<u>R</u>	<u>NUMBER OF CYCLES</u>
20	10.36	6.54	0.63	15
21	11.38	-1.55	-0.14	1
22	10.36	6.54	0.63	16
23	11.64	5.26	0.45	2
24	10.36	6.54	0.63	15
25	11.38	-1.55	-0.14	1
26	10.36	6.54	0.63	16
27	11.64	5.26	0.45	2
28	10.36	6.54	0.63	15
29	11.38	-1.55	-0.14	1
30	10.36	6.54	0.63	16
31	11.64	5.26	0.45	2
32	10.36	6.54	0.63	15
33	11.38	-1.55	-0.14	1
34	10.36	6.54	0.63	16
35	11.64	5.26	0.45	2
36	10.36	6.54	0.63	15

FMAX EQUALLED OR EXCEEDED IN 10 FLIGHTS = 14.35 KSI  
 FMAX EQUALLED OR EXCEEDED IN 100 FLIGHTS = 16.76 KSI  
 FMAX EQUALLED OR EXCEEDED IN 200 FLIGHTS = 17.55 KSI

VARIABLE MISSION NO. 5C1, WING

1	12.48	-11.39	-0.91	1
2	10.94	7.12	0.65	5
3	12.22	5.84	0.48	1
4	10.94	7.12	0.65	5
5	10.46	6.64	0.63	50
6	11.74	5.36	0.46	4
7	13.01	4.09	0.31	1
8	11.74	5.36	0.46	4
9	10.46	6.64	0.63	49
10	10.36	6.54	0.63	119
11	11.64	5.26	0.45	8
12	12.91	3.99	0.31	1
13	11.64	5.26	0.45	8
14	10.36	6.54	0.63	119
15	11.38	-1.55	-0.14	1
16	10.36	6.54	0.63	16
17	11.64	5.26	0.45	2
18	10.36	6.54	0.63	15
19	11.38	-1.55	-0.14	1
20	10.36	6.54	0.63	16
21	11.64	5.26	0.45	2
22	10.36	6.54	0.63	15
23	11.38	-1.55	-0.14	1
24	10.36	6.54	0.63	16
25	11.64	5.26	0.45	2
26	10.36	6.54	0.63	15
27	11.38	-1.55	-0.14	1
28	10.36	6.54	0.63	16
29	11.64	5.26	0.45	2
30	10.36	6.54	0.63	15
31	11.38	-1.55	-0.14	1
32	10.36	6.54	0.63	16
33	11.64	5.26	0.45	2
34	10.36	6.54	0.63	15
35	11.38	-1.55	-0.14	1

TABLE B-1 (CONCLUDED)  
 VARIABLE MISSION STRESS SPECTRA  
 WING ANALYSIS LOCATION

<u>STRESS NUMBER</u>	<u>MAXIMUM STRESS KSI</u>	<u>MINIMUM STRESS KSI</u>	<u>R</u>	<u>NUMBER OF CYCLES</u>
36	10.36	6.54	0.63	16
37	11.64	5.26	0.45	2
38	10.36	6.54	0.63	15

FMAX EQUALLED OR EXCEEDED IN 10 FLIGHTS = 14.35 KSI  
 FMAX EQUALLED OR EXCEEDED IN 100 FLIGHTS = 16.76 KSI  
 FMAX EQUALLED OR EXCEEDED IN 200 FLIGHTS = 17.55 KSI

TABLE B-2  
VARIABLE MISSION STRESS SPECTRA  
BODY ANALYSIS LOCATION

<u>STRESS NUMBER</u>	<u>MAXIMUM STRESS</u> KSI	<u>MINIMUM STRESS</u> KSI	<u>R</u>	<u>NUMBER OF CYCLES</u>
VARIABLE MISSION NO. 1A, BODY				
1	18.62	8.50	0.46	1
2	15.01	11.18	0.75	37
3	16.28	9.91	0.61	5
4	17.56	8.63	0.49	2
5	16.28	9.91	0.61	4
6	15.01	11.18	0.75	37
7	18.40	14.57	0.79	8
8	17.67	13.85	0.78	11
9	18.95	12.57	0.66	1
10	17.67	13.85	0.78	10
11	17.19	13.36	0.78	11
12	18.46	12.09	0.65	1
13	17.19	13.36	0.78	11
14	16.08	12.25	0.76	11
15	17.35	10.98	0.63	1
16	16.08	12.25	0.76	11
17	14.68	10.85	0.74	7
18	15.95	9.58	0.60	1
19	14.68	10.85	0.74	6
FMAX EQUALLED OR EXCEEDED IN 10 FLIGHTS = 20.41 KSI				
FMAX EQUALLED OR EXCEEDED IN 100 FLIGHTS = 22.45 KSI				
FMAX EQUALLED OR EXCEEDED IN 200 FLIGHTS = 23.06 KSI				
VARIABLE MISSION NO. 2A, BODY				
1	18.62	8.50	0.46	1
2	15.01	11.18	0.75	37
3	16.28	9.91	0.61	5
4	17.56	8.63	0.49	2
5	16.28	9.91	0.61	4
6	15.01	11.18	0.75	37
7	18.40	14.57	0.79	8
8	18.40	14.57	0.79	25
9	18.40	14.57	0.79	10
10	19.67	13.30	0.68	1
11	18.40	14.57	0.79	10
12	17.67	13.85	0.78	11
13	18.95	12.57	0.66	1
14	17.67	13.85	0.78	10
15	17.19	13.36	0.78	11
16	18.46	12.09	0.65	1
17	17.19	13.36	0.78	11
FMAX EQUALLED OR EXCEEDED IN 10 FLIGHTS = 20.41 KSI				
FMAX EQUALLED OR EXCEEDED IN 100 FLIGHTS = 22.45 KSI				
FMAX EQUALLED OR EXCEEDED IN 200 FLIGHTS = 23.06 KSI				
VARIABLE MISSION NO. 3A, BODY				
1	18.62	8.50	0.46	1
2	15.01	11.18	0.75	37
3	16.28	9.91	0.61	5
4	17.56	8.63	0.49	2
5	16.28	9.91	0.61	4
6	15.01	11.18	0.75	37
7	18.40	14.57	0.79	8
8	13.10	9.28	0.71	273

TABLE B-2 (CONT'D)  
 VARIABLE MISSION STRESS SPECTRA  
 BODY ANALYSIS LOCATION

<u>STRESS NUMBER</u>	<u>MAXIMUM STRESS</u> KSI	<u>MINIMUM STRESS</u> KSI	<u>R</u>	<u>NUMBER OF CYCLES</u>
9	14.38	8.00	0.56	32
10	15.65	6.73	0.43	5
11	16.93	5.45	0.32	2
12	15.65	6.73	0.43	4
13	14.38	8.00	0.56	31
14	13.10	9.28	0.71	272
15	12.67	8.84	0.70	268
16	13.94	7.57	0.54	31
17	15.22	6.29	0.41	5
18	16.49	5.02	0.30	2
19	15.22	6.29	0.41	4
20	13.94	7.57	0.54	31
21	12.67	8.84	0.70	267
22	16.08	12.25	0.76	11
23	17.35	10.98	0.63	1
24	16.08	12.25	0.76	11
25	14.68	10.85	0.74	7
26	15.95	9.58	0.60	1
27	14.68	10.85	0.74	6

FMAX EQUALLED OR EXCEEDED IN 10 FLIGHTS = 20.41 KSI  
 FMAX EQUALLED OR EXCEEDED IN 100 FLIGHTS = 22.45 KSI  
 FMAX EQUALLED OR EXCEEDED IN 200 FLIGHTS = 23.06 KSI

VARIABLE MISSION NO. 4A, BODY

1	18.62	8.50	0.46	1
2	15.01	11.18	0.75	37
3	16.28	9.91	0.61	5
4	17.56	8.63	0.49	2
5	16.28	9.91	0.61	4
6	15.01	11.18	0.75	37
7	18.40	14.57	0.79	8
8	17.67	13.85	0.78	11
9	18.95	12.57	0.66	1
10	17.67	13.85	0.78	10
11	17.19	13.36	0.78	11
12	18.46	12.09	0.65	1
13	17.19	13.36	0.78	11
14	16.08	12.25	0.76	11
15	17.35	10.98	0.63	1
16	16.08	12.25	0.76	11
17	13.20	5.93	0.45	1
18	11.53	7.71	0.67	31
19	12.81	6.43	0.50	3
20	14.08	5.16	0.37	1
21	12.81	6.43	0.50	3
22	11.53	7.71	0.67	31
23	13.20	5.93	0.45	1
24	11.53	7.71	0.67	31
25	12.81	6.43	0.50	3
26	14.08	5.16	0.37	1
27	12.81	6.43	0.50	3
28	11.53	7.71	0.67	31
29	13.20	5.93	0.45	1
30	11.53	7.71	0.67	31
31	12.81	6.43	0.50	3
32	14.08	5.16	0.37	1
33	12.81	6.43	0.50	3

TABLE B-2 (CONT'D)  
 VARIABLE MISSION STRESS SPECTRA  
 BODY ANALYSIS LOCATION

<u>STRESS NUMBER</u>	<u>MAXIMUM STRESS</u> KSI	<u>MINIMUM STRESS</u> KSI	<u>R</u>	<u>NUMBER OF CYCLES</u>
34	11.53	7.71	0.67	31
FMAX EQUALLED OR EXCEEDED IN 10 FLIGHTS = 20.41 KSI				
FMAX EQUALLED OR EXCEEDED IN 100 FLIGHTS = 22.45 KSI				
FMAX EQUALLED OR EXCEEDED IN 200 FLIGHTS = 23.06 KSI				
VARIABLE MISSION NO. 1B, BODY				
1	14.66	5.84	0.40	1
2	11.78	7.95	0.68	14
3	13.05	6.68	0.51	3
4	11.78	7.95	0.68	14
5	16.08	12.25	0.76	6
6	17.35	10.98	0.63	1
7	16.08	12.25	0.76	6
8	14.68	10.85	0.74	11
9	15.95	9.58	0.60	1
10	14.68	10.85	0.74	10
11	13.51	9.69	0.72	10
12	14.79	8.41	0.57	1
13	13.51	9.69	0.72	10
FMAX EQUALLED OR EXCEEDED IN 10 FLIGHTS = 16.22 KSI				
FMAX EQUALLED OR EXCEEDED IN 100 FLIGHTS = 18.13 KSI				
FMAX EQUALLED OR EXCEEDED IN 200 FLIGHTS = 18.70 KSI				
VARIABLE MISSION NO. 2B, BODY				
1	14.66	5.84	0.40	1
2	11.78	7.95	0.68	14
3	13.05	6.68	0.51	3
4	11.78	7.95	0.68	14
5	16.08	12.25	0.76	6
6	17.35	10.98	0.63	1
7	16.08	12.25	0.76	6
8	16.08	12.25	0.76	7
9	16.08	12.25	0.76	11
10	17.35	10.98	0.63	1
11	16.08	12.25	0.76	11
12	14.68	10.85	0.74	7
13	15.95	9.58	0.60	1
14	14.68	10.85	0.74	6
FMAX EQUALLED OR EXCEEDED IN 10 FLIGHTS = 16.22 KSI				
FMAX EQUALLED OR EXCEEDED IN 100 FLIGHTS = 18.13 KSI				
FMAX EQUALLED OR EXCEEDED IN 200 FLIGHTS = 18.70 KSI				
VARIABLE MISSION NO. 3B, BODY				
1	14.66	5.84	0.40	1
2	11.78	7.95	0.68	14
3	13.05	6.68	0.51	3
4	11.78	7.95	0.68	14
5	16.08	12.25	0.76	6
6	17.35	10.98	0.63	1
7	16.08	12.25	0.76	6
8	12.96	9.13	0.70	10
9	10.30	6.47	0.63	236
10	11.57	5.20	0.45	25
11	12.85	3.92	0.31	4
12	14.12	2.65	0.19	1

TABLE B-2 (CONT'D)  
 VARIABLE MISSION STRESS SPECTRA  
 BODY ANALYSIS LOCATION

<u>STRESS NUMBER</u>	<u>MAXIMUM STRESS</u> KSI	<u>MINIMUM STRESS</u> KSI	<u>R</u>	<u>NUMBER OF CYCLES</u>
13	12.85	3.92	0.31	3
14	11.57	5.20	0.45	25
15	10.30	6.47	0.63	235
16	9.19	5.36	0.58	218
17	10.46	4.09	0.39	22
18	11.74	2.81	0.24	3
19	13.01	1.54	0.12	1
20	11.74	2.81	0.24	3
21	10.46	4.09	0.39	22
22	9.19	5.36	0.53	218

FMAX EQUALLED OR EXCEEDED IN 10 FLIGHTS = 16.22 KSI  
 FMAX EQUALLED OR EXCEEDED IN 100 FLIGHTS = 18.13 KSI  
 FMAX EQUALLED OR EXCEEDED IN 200 FLIGHTS = 18.70 KSI

VARIABLE MISSION NO. 4B, BODY

1	14.66	5.84	0.40	1
2	11.78	7.95	0.68	14
3	13.05	6.68	0.51	3
4	11.78	7.95	0.68	14
5	16.08	12.25	0.76	6
6	17.35	10.98	0.63	1
7	16.08	12.25	0.76	6
8	14.68	10.85	0.74	11
9	15.95	9.58	0.60	1
10	14.68	10.85	0.74	10
11	11.66	4.91	0.42	1
12	9.95	6.13	0.62	27
13	11.23	4.85	0.43	4
14	9.95	6.13	0.62	26
15	11.66	4.91	0.42	1
16	9.95	6.13	0.62	27
17	11.23	4.85	0.43	4
18	9.95	6.13	0.62	26
19	11.66	4.91	0.42	1
20	9.95	6.13	0.62	27
21	11.23	4.85	0.43	4
22	9.95	6.13	0.62	26

FMAX EQUALLED OR EXCEEDED IN 10 FLIGHTS = 16.22 KSI  
 FMAX EQUALLED OR EXCEEDED IN 100 FLIGHTS = 18.13 KSI  
 FMAX EQUALLED OR EXCEEDED IN 200 FLIGHTS = 18.70 KSI

VARIABLE MISSION NO. 5B, BODY

1	14.66	5.84	0.40	1
2	11.78	7.95	0.68	14
3	13.05	6.68	0.51	3
4	11.78	7.95	0.68	14
5	16.08	12.25	0.76	6
6	17.35	10.98	0.63	1
7	16.08	12.25	0.76	6
8	11.53	7.71	0.67	239
9	12.81	6.43	0.50	22
10	14.08	5.16	0.37	4
11	12.81	6.43	0.50	21
12	11.53	7.71	0.67	239
13	11.66	4.91	0.42	1
14	9.95	6.13	0.62	27

TABLE B-2 (CONT'D)  
 VARIABLE MISSION STRESS SPECTRA  
 BODY ANALYSIS LOCATION

<u>STRESS NUMBER</u>	<u>MAXIMUM STRESS</u> KSI	<u>MINIMUM STRESS</u> KSI	<u>R</u>	<u>NUMBER OF CYCLES</u>
15	11.23	4.85	0.43	4
16	9.95	6.13	0.62	26
17	11.66	4.91	0.42	1
18	9.95	6.13	0.62	27
19	11.23	4.85	0.43	4
20	9.95	6.13	0.62	26
21	11.66	4.91	0.42	1
22	9.95	6.13	0.62	27
23	11.23	4.85	0.43	4
24	9.95	6.13	0.62	26
25	11.66	4.91	0.42	1
26	9.95	6.13	0.62	27
27	11.23	4.85	0.43	4
28	9.95	6.13	0.62	26
29	11.66	4.91	0.42	1
30	9.95	6.13	0.62	27
31	11.23	4.85	0.43	4
32	9.95	6.13	0.62	26
33	11.66	4.91	0.42	1
34	9.95	6.13	0.62	27
35	11.23	4.85	0.43	4
36	9.95	6.13	0.62	26

FMAX EQUALLED OR EXCEEDED IN 10 FLIGHTS = 16.22 KSI  
 FMAX EQUALLED OR EXCEEDED IN 100 FLIGHTS = 18.13 KSI  
 FMAX EQUALLED OR EXCEEDED IN 200 FLIGHTS = 18.70 KSI

VARIABLE MISSION NO. 5B1, BODY

1	14.66	5.84	0.40	1
2	11.11	7.29	0.66	10
3	12.39	6.01	0.49	2
4	11.11	7.29	0.66	10
5	12.76	8.94	0.70	59
6	14.04	7.66	0.55	5
7	15.31	6.39	0.42	1
8	14.04	7.66	0.55	4
9	12.76	8.94	0.70	59
10	11.53	7.71	0.67	239
11	12.81	6.43	0.50	22
12	14.08	5.16	0.37	4
13	12.81	6.43	0.50	21
14	11.53	7.71	0.67	239
15	11.66	4.91	0.42	1
16	9.95	6.13	0.62	27
17	11.23	4.85	0.43	4
18	9.95	6.13	0.62	26
19	11.66	4.91	0.42	1
20	9.95	6.13	0.62	27
21	11.23	4.85	0.43	4
22	9.95	6.13	0.62	26
23	11.66	4.91	0.42	1
24	9.95	6.13	0.62	27
25	11.23	4.85	0.43	4
26	9.95	6.13	0.62	26
27	11.66	4.91	0.42	1
28	9.95	6.13	0.62	27
29	11.23	4.85	0.43	4
30	9.95	6.13	0.62	26

TABLE B-2 (CONT'D)  
 VARIABLE MISSION STRESS SPECTRA  
 BODY ANALYSIS LOCATION

<u>STRESS NUMBER</u>	<u>MAXIMUM STRESS</u> KSI	<u>MINIMUM STRESS</u> KSI	<u>R</u>	<u>NUMBER OF CYCLES</u>
31	11.66	4.91	0.42	1
32	9.95	6.13	0.62	27
33	11.23	4.85	0.43	4
34	9.95	6.13	0.62	26
35	11.66	4.91	0.42	1
36	9.95	6.13	0.62	27
37	11.23	4.85	0.43	4
38	9.95	6.13	0.62	26
FMAX EQUALLED OR EXCEEDED IN 10 FLIGHTS = 16.22 KSI				
FMAX EQUALLED OR EXCEEDED IN 100 FLIGHTS = 18.13 KSI				
FMAX EQUALLED OR EXCEEDED IN 200 FLIGHTS = 18.70 KSI				
VARIABLE MISSION NO. 1C, BODY				
1	13.11	4.75	0.36	1
2	10.45	6.63	0.63	8
3	11.73	5.35	0.46	1
4	10.45	6.63	0.63	8
5	12.96	9.13	0.70	6
6	14.23	7.86	0.55	1
7	12.96	9.13	0.70	6
8	13.29	9.47	0.71	8
9	14.57	8.19	0.56	1
10	13.29	9.47	0.71	8
FMAX EQUALLED OR EXCEEDED IN 10 FLIGHTS = 14.32 KSI				
FMAX EQUALLED OR EXCEEDED IN 100 FLIGHTS = 15.94 KSI				
FMAX EQUALLED OR EXCEEDED IN 200 FLIGHTS = 16.50 KSI				
VARIABLE MISSION NO. 2C, BODY				
1	13.11	4.75	0.36	1
2	10.45	6.63	0.63	8
3	11.73	5.35	0.46	1
4	10.45	6.63	0.63	8
5	12.96	9.13	0.70	6
6	14.23	7.86	0.55	1
7	12.96	9.13	0.70	6
8	12.96	9.13	0.70	5
9	12.96	9.13	0.70	10
FMAX EQUALLED OR EXCEEDED IN 10 FLIGHTS = 14.32 KSI				
FMAX EQUALLED OR EXCEEDED IN 100 FLIGHTS = 15.94 KSI				
FMAX EQUALLED OR EXCEEDED IN 200 FLIGHTS = 16.50 KSI				
VARIABLE MISSION NO. 4C, BODY				
1	13.11	4.75	0.36	1
2	10.45	6.63	0.63	8
3	11.73	5.35	0.46	1
4	10.45	6.63	0.63	8
5	12.96	9.13	0.70	6
6	14.23	7.86	0.55	1
7	12.96	9.13	0.70	6
8	13.29	9.47	0.71	8
9	10.58	4.70	0.44	1
10	9.53	5.71	0.60	17
11	10.81	4.43	0.41	2
12	9.53	5.71	0.60	17
13	10.58	4.70	0.44	1

TABLE B-2 (CONT'D)  
 VARIABLE MISSION STRESS SPECTRA  
 BODY ANALYSIS LOCATION

<u>STRESS NUMBER</u>	<u>MAXIMUM STRESS</u> KSI	<u>MINIMUM STRESS</u> KSI	<u>R</u>	<u>NUMBER OF CYCLES</u>
14	9.53	5.71	0.60	17
15	10.81	4.43	0.41	2
16	9.53	5.71	0.60	17
17	10.58	4.70	0.44	1
18	9.53	5.71	0.60	17
19	10.81	4.43	0.41	2
20	9.53	5.71	0.60	17

FMAX EQUALLED OR EXCEEDED IN 10 FLIGHTS = 14.32 KSI  
 FMAX EQUALLED OR EXCEEDED IN 100 FLIGHTS = 15.94 KSI  
 FMAX EQUALLED OR EXCEEDED IN 200 FLIGHTS = 16.50 KSI

VARIABLE MISSION NO. 5C, BODY

1	13.11	4.75	0.36	1
2	10.45	6.63	0.63	8
3	11.73	5.35	0.46	1
4	10.45	6.63	0.63	8
5	12.96	9.13	0.70	6
6	14.23	7.86	0.55	1
7	12.96	9.13	0.70	6
8	9.53	5.71	0.60	133
9	10.81	4.43	0.41	7
10	12.08	3.16	0.26	1
11	10.81	4.43	0.41	6
12	9.53	5.71	0.60	132
13	10.58	4.70	0.44	1
14	9.53	5.71	0.60	17
15	10.81	4.43	0.41	2
16	9.53	5.71	0.60	17
17	10.58	4.70	0.44	1
18	9.53	5.71	0.60	17
19	10.81	4.43	0.41	2
20	9.53	5.71	0.60	17
21	10.58	4.70	0.44	1
22	9.53	5.71	0.60	17
23	10.81	4.43	0.41	2
24	9.53	5.71	0.60	17
25	10.58	4.70	0.44	1
26	9.53	5.71	0.60	17
27	10.81	4.43	0.41	2
28	9.53	5.71	0.60	17
29	10.58	4.70	0.44	1
30	9.53	5.71	0.60	17
31	10.81	4.43	0.41	2
32	9.53	5.71	0.60	17
33	10.58	4.70	0.44	1
34	9.53	5.71	0.60	17
35	10.81	4.43	0.41	2
36	9.53	5.71	0.60	17

FMAX EQUALLED OR EXCEEDED IN 10 FLIGHTS = 14.32 KSI  
 FMAX EQUALLED OR EXCEEDED IN 100 FLIGHTS = 15.94 KSI  
 FMAX EQUALLED OR EXCEEDED IN 200 FLIGHTS = 16.50 KSI

VARIABLE MISSION NO. 5C1, BODY

1	13.11	4.75	0.36	1
2	9.66	5.83	0.60	6
3	10.93	4.56	0.42	1

TABLE B-2 (CONCLUDED)  
 VARIABLE MISSION STRESS SPECTRA  
 BODY ANALYSIS LOCATION

<u>STRESS NUMBER</u>	<u>MAXIMUM STRESS</u> KSI	<u>MINIMUM STRESS</u> KSI	<u>R</u>	<u>NUMBER OF CYCLES</u>
4	9.66	5.83	0.60	5
5	9.81	5.99	0.61	50
6	11.09	4.71	0.42	4
7	12.36	3.44	0.28	1
8	11.09	4.71	0.42	3
9	9.81	5.99	0.61	50
10	9.53	5.71	0.60	133
11	10.81	4.43	0.41	7
12	12.08	3.16	0.26	1
13	10.81	4.43	0.41	6
14	9.53	5.71	0.60	132
15	10.53	4.70	0.44	1
16	9.53	5.71	0.60	17
17	10.81	4.43	0.41	2
18	9.53	5.71	0.60	17
19	10.53	4.70	0.44	1
20	9.53	5.71	0.60	17
21	10.81	4.43	0.41	2
22	9.53	5.71	0.60	17
23	10.58	4.70	0.44	1
24	9.53	5.71	0.60	17
25	10.81	4.43	0.41	2
26	9.53	5.71	0.60	17
27	10.58	4.70	0.44	1
28	9.53	5.71	0.60	17
29	10.81	4.43	0.41	2
30	9.53	5.71	0.60	17
31	10.58	4.70	0.44	1
32	9.53	5.71	0.60	17
33	10.81	4.43	0.41	2
34	9.53	5.71	0.60	17
35	10.58	4.70	0.44	1
36	9.53	5.71	0.60	17
37	10.81	4.43	0.41	2
38	9.53	5.71	0.60	17

FMAX EQUALLED OR EXCEEDED IN 10 FLIGHTS = 14.32 KSI  
 FMAX EQUALLED OR EXCEEDED IN 100 FLIGHTS = 15.94 KSI  
 FMAX EQUALLED OR EXCEEDED IN 200 FLIGHTS = 16.50 KSI

TABLE B-3  
VARIABLE MISSION STRESS SPECTRA  
FIN ANALYSIS LOCATION

<u>STRESS NUMBER</u>	<u>MAXIMUM STRESS</u> KSI	<u>MINIMUM STRESS</u> KSI	<u>R</u>	<u>NUMBER OF CYCLES</u>
VARIABLE MISSION NO. 1A, FIN				
1	1.91	-1.91	-1.00	96
2	3.19	-3.19	-1.00	30
3	4.46	-4.46	-1.00	11
4	5.74	-5.74	-1.00	5
5	7.01	-7.01	-1.00	2
6	8.29	-8.29	-1.00	1
7	9.56	-9.56	-1.00	1
8	8.29	-8.29	-1.00	1
9	7.01	-7.01	-1.00	2
10	5.74	-5.74	-1.00	4
11	4.46	-4.46	-1.00	11
12	3.19	-3.19	-1.00	30
13	1.91	-1.91	-1.00	96
14	1.91	-1.91	-1.00	26
15	3.19	-3.19	-1.00	5
16	4.46	-4.46	-1.00	2
17	3.19	-3.19	-1.00	4
18	1.91	-1.91	-1.00	25
19	1.91	-1.91	-1.00	69
20	3.19	-3.19	-1.00	12
21	4.46	-4.46	-1.00	3
22	5.74	-5.74	-1.00	1
23	4.46	-4.46	-1.00	2
24	3.19	-3.19	-1.00	12
25	1.91	-1.91	-1.00	68
26	1.91	-1.91	-1.00	73
27	3.19	-3.19	-1.00	13
28	4.46	-4.46	-1.00	3
29	5.74	-5.74	-1.00	1
30	4.46	-4.46	-1.00	2
31	3.19	-3.19	-1.00	12
32	1.91	-1.91	-1.00	73
33	1.91	-1.91	-1.00	78
34	3.19	-3.19	-1.00	14
35	4.46	-4.46	-1.00	3
36	5.74	-5.74	-1.00	1
37	4.46	-4.46	-1.00	2
38	3.19	-3.19	-1.00	13
39	1.91	-1.91	-1.00	77
40	1.91	-1.91	-1.00	50
41	3.19	-3.19	-1.00	9
42	4.46	-4.46	-1.00	2
43	5.74	-5.74	-1.00	1
44	4.46	-4.46	-1.00	1
45	3.19	-3.19	-1.00	8
46	1.91	-1.91	-1.00	49
VARIABLE MISSION NO. 2A, FIN				
1	1.91	-1.91	-1.00	96
2	3.19	-3.19	-1.00	30
3	4.46	-4.46	-1.00	11
4	5.74	-5.74	-1.00	5
5	7.01	-7.01	-1.00	2
6	8.29	-8.29	-1.00	1
7	9.56	-9.56	-1.00	1
8	8.29	-8.29	-1.00	1

TABLE B-3 (CONT'D)  
 VARIABLE MISSION STRESS SPECTRA  
 FIN ANALYSIS LOCATION

<u>STRESS NUMBER</u>	<u>MAXIMUM STRESS</u> KSI	<u>MINIMUM STRESS</u> KSI	<u>R</u>	<u>NUMBER OF CYCLES</u>
9	7.01	-7.01	-1.00	2
10	5.74	-5.74	-1.00	4
11	4.46	-4.46	-1.00	11
12	3.19	-3.19	-1.00	30
13	1.91	-1.91	-1.00	96
14	1.91	-1.91	-1.00	26
15	3.19	-3.19	-1.00	5
16	4.46	-4.46	-1.00	2
17	3.19	-3.19	-1.00	4
18	1.91	-1.91	-1.00	25
19	1.91	-1.91	-1.00	25
20	3.19	-3.19	-1.00	5
21	4.46	-4.46	-1.00	2
22	3.19	-3.19	-1.00	4
23	1.91	-1.91	-1.00	25
24	1.91	-1.91	-1.00	64
25	3.19	-3.19	-1.00	11
26	4.46	-4.46	-1.00	2
27	5.74	-5.74	-1.00	1
28	4.46	-4.46	-1.00	2
29	3.19	-3.19	-1.00	11
30	1.91	-1.91	-1.00	63
31	1.91	-1.91	-1.00	69
32	3.19	-3.19	-1.00	12
33	4.46	-4.46	-1.00	3
34	5.74	-5.74	-1.00	1
35	4.46	-4.46	-1.00	2
36	3.19	-3.19	-1.00	12
37	1.91	-1.91	-1.00	68
38	1.91	-1.91	-1.00	73
39	3.19	-3.19	-1.00	13
40	4.46	-4.46	-1.00	3
41	5.74	-5.74	-1.00	1
42	4.46	-4.46	-1.00	2
43	3.19	-3.19	-1.00	12
44	1.91	-1.91	-1.00	73
VARIABLE MISSION NO. 3A, FIN				
1	1.91	-1.91	-1.00	96
2	3.19	-3.19	-1.00	30
3	4.46	-4.46	-1.00	11
4	5.74	-5.74	-1.00	5
5	7.01	-7.01	-1.00	2
6	8.29	-8.29	-1.00	1
7	9.56	-9.56	-1.00	1
8	8.29	-8.29	-1.00	1
9	7.01	-7.01	-1.00	2
10	5.74	-5.74	-1.00	4
11	4.46	-4.46	-1.00	11
12	3.19	-3.19	-1.00	30
13	1.91	-1.91	-1.00	96
14	1.91	-1.91	-1.00	26
15	3.19	-3.19	-1.00	5
16	4.46	-4.46	-1.00	2
17	3.19	-3.19	-1.00	4
18	1.91	-1.91	-1.00	25
19	1.91	-1.91	-1.00	538
20	3.19	-3.19	-1.00	208

TABLE B-3 (CONT'D)  
 VARIABLE MISSION STRESS SPECTRA  
 FIN ANALYSIS LOCATION

<u>STRESS NUMBER</u>	<u>MAXIMUM STRESS</u> KSI	<u>MINIMUM STRESS</u> KSI	<u>R</u>	<u>NUMBER OF CYCLES</u>
21	4.46	-4.46	-1.00	82
22	5.74	-5.74	-1.00	33
23	7.01	-7.01	-1.00	13
24	8.29	-8.29	-1.00	6
25	9.56	-9.56	-1.00	3
26	10.84	-10.84	-1.00	1
27	12.11	-12.11	-1.00	1
28	10.84	-10.84	-1.00	1
29	9.56	-9.56	-1.00	2
30	8.29	-8.29	-1.00	5
31	7.01	-7.01	-1.00	13
32	5.74	-5.74	-1.00	32
33	4.46	-4.46	-1.00	81
34	3.19	-3.19	-1.00	208
35	1.91	-1.91	-1.00	538
36	1.91	-1.91	-1.00	539
37	3.19	-3.19	-1.00	208
38	4.46	-4.46	-1.00	82
39	5.74	-5.74	-1.00	33
40	7.01	-7.01	-1.00	13
41	8.29	-8.29	-1.00	6
42	9.56	-9.56	-1.00	3
43	10.84	-10.84	-1.00	1
44	12.11	-12.11	-1.00	1
45	10.84	-10.84	-1.00	1
46	9.56	-9.56	-1.00	2
47	8.29	-8.29	-1.00	5
48	7.01	-7.01	-1.00	13
49	5.74	-5.74	-1.00	32
50	4.46	-4.46	-1.00	81
51	3.19	-3.19	-1.00	208
52	1.91	-1.91	-1.00	538
53	1.91	-1.91	-1.00	78
54	3.19	-3.19	-1.00	14
55	4.46	-4.46	-1.00	3
56	5.74	-5.74	-1.00	1
57	4.46	-4.46	-1.00	2
58	3.19	-3.19	-1.00	13
59	1.91	-1.91	-1.00	77
60	1.91	-1.91	-1.00	50
61	3.19	-3.19	-1.00	9
62	4.46	-4.46	-1.00	2
63	5.74	-5.74	-1.00	1
64	4.46	-4.46	-1.00	1
65	3.19	-3.19	-1.00	8
66	1.91	-1.91	-1.00	49
VARIABLE MISSION NO. 4A, FIN				
1	1.91	-1.91	-1.00	96
2	3.19	-3.19	-1.00	30
3	4.46	-4.46	-1.00	11
4	5.74	-5.74	-1.00	5
5	7.01	-7.01	-1.00	2
6	8.29	-8.29	-1.00	1
7	9.56	-9.56	-1.00	1
8	8.29	-8.29	-1.00	1
9	7.01	-7.01	-1.00	2
10	5.74	-5.74	-1.00	4

TABLE B-3 (CONT'D)  
 VARIABLE MISSION STRESS SPECTRA  
 FIN ANALYSIS LOCATION

<u>STRESS NUMBER</u>	<u>MAXIMUM STRESS KSI</u>	<u>MINIMUM STRESS KSI</u>	<u>R</u>	<u>NUMBER OF CYCLES</u>
11	4.46	-4.46	-1.00	11
12	3.19	-3.19	-1.00	30
13	1.91	-1.91	-1.00	96
14	1.91	-1.91	-1.00	26
15	3.19	-3.19	-1.00	5
16	4.46	-4.46	-1.00	2
17	3.19	-3.19	-1.00	4
18	1.91	-1.91	-1.00	25
19	1.91	-1.91	-1.00	69
20	3.19	-3.19	-1.00	12
21	4.46	-4.46	-1.00	3
22	5.74	-5.74	-1.00	1
23	4.46	-4.46	-1.00	2
24	3.19	-3.19	-1.00	12
25	1.91	-1.91	-1.00	68
26	1.91	-1.91	-1.00	73
27	3.19	-3.19	-1.00	13
28	4.46	-4.46	-1.00	3
29	5.74	-5.74	-1.00	1
30	4.46	-4.46	-1.00	2
31	3.19	-3.19	-1.00	12
32	1.91	-1.91	-1.00	73
33	1.91	-1.91	-1.00	78
34	3.19	-3.19	-1.00	14
35	4.46	-4.46	-1.00	3
36	5.74	-5.74	-1.00	1
37	4.46	-4.46	-1.00	2
38	3.19	-3.19	-1.00	13
39	1.91	-1.91	-1.00	77
40	1.91	-1.91	-1.00	82
41	3.19	-3.19	-1.00	29
42	4.46	-4.46	-1.00	10
43	5.74	-5.74	-1.00	4
44	7.01	-7.01	-1.00	2
45	8.29	-8.29	-1.00	1
46	7.01	-7.01	-1.00	1
47	5.74	-5.74	-1.00	3
48	4.46	-4.46	-1.00	10
49	3.19	-3.19	-1.00	29
50	1.91	-1.91	-1.00	81
51	1.91	-1.91	-1.00	82
52	3.19	-3.19	-1.00	29
53	4.46	-4.46	-1.00	10
54	5.74	-5.74	-1.00	4
55	7.01	-7.01	-1.00	2
56	8.29	-8.29	-1.00	1
57	7.01	-7.01	-1.00	1
58	5.74	-5.74	-1.00	3
59	4.46	-4.46	-1.00	10
60	3.19	-3.19	-1.00	29
61	1.91	-1.91	-1.00	81
62	1.91	-1.91	-1.00	82
63	3.19	-3.19	-1.00	29
64	4.46	-4.46	-1.00	10
65	5.74	-5.74	-1.00	4
66	7.01	-7.01	-1.00	2
67	8.29	-8.29	-1.00	1
68	7.01	-7.01	-1.00	1

TABLE B-3 (CONT'D)  
 VARIABLE MISSION STRESS SPECTRA  
 FIN ANALYSIS LOCATION

<u>STRESS NUMBER</u>	<u>MAXIMUM STRESS</u> KSI	<u>MINIMUM STRESS</u> KSI	<u>R</u>	<u>NUMBER OF CYCLES</u>
69	5.74	-5.74	-1.00	3
70	4.46	-4.46	-1.00	10
71	3.19	-3.19	-1.00	29
72	1.91	-1.91	-1.00	81
VARIABLE MISSION NO. 1B, FIN				
1	1.91	-1.91	-1.00	44
2	3.19	-3.19	-1.00	13
3	4.46	-4.46	-1.00	5
4	5.74	-5.74	-1.00	2
5	7.01	-7.01	-1.00	1
6	5.74	-5.74	-1.00	1
7	4.46	-4.46	-1.00	4
8	3.19	-3.19	-1.00	13
9	1.91	-1.91	-1.00	43
10	1.91	-1.91	-1.00	43
11	3.19	-3.19	-1.00	8
12	4.46	-4.46	-1.00	2
13	5.74	-5.74	-1.00	1
14	4.46	-4.46	-1.00	1
15	3.19	-3.19	-1.00	7
16	1.91	-1.91	-1.00	42
17	1.91	-1.91	-1.00	82
18	3.19	-3.19	-1.00	14
19	4.46	-4.46	-1.00	3
20	5.74	-5.74	-1.00	1
21	4.46	-4.46	-1.00	2
22	3.19	-3.19	-1.00	13
23	1.91	-1.91	-1.00	81
24	1.91	-1.91	-1.00	85
25	3.19	-3.19	-1.00	14
26	4.46	-4.46	-1.00	3
27	5.74	-5.74	-1.00	1
28	4.46	-4.46	-1.00	2
29	3.19	-3.19	-1.00	14
30	1.91	-1.91	-1.00	84
VARIABLE MISSION NO. 2B, FIN				
1	1.91	-1.91	-1.00	44
2	3.19	-3.19	-1.00	13
3	4.46	-4.46	-1.00	5
4	5.74	-5.74	-1.00	2
5	7.01	-7.01	-1.00	1
6	5.74	-5.74	-1.00	1
7	4.46	-4.46	-1.00	4
8	3.19	-3.19	-1.00	13
9	1.91	-1.91	-1.00	43
10	1.91	-1.91	-1.00	43
11	3.19	-3.19	-1.00	8
12	4.46	-4.46	-1.00	2
13	5.74	-5.74	-1.00	1
14	4.46	-4.46	-1.00	1
15	3.19	-3.19	-1.00	7
16	1.91	-1.91	-1.00	42
17	1.91	-1.91	-1.00	25
18	3.19	-3.19	-1.00	5
19	4.46	-4.46	-1.00	2
20	3.19	-3.19	-1.00	4

TABLE B-3 (CONT'D)  
 VARIABLE MISSION STRESS SPECTRA  
 FIN ANALYSIS LOCATION

<u>STRESS NUMBER</u>	<u>MAXIMUM STRESS</u> KSI	<u>MINIMUM STRESS</u> KSI	<u>R</u>	<u>NUMBER OF CYCLES</u>
21	1.91	-1.91	-1.00	25
22	1.91	-1.91	-1.00	78
23	3.19	-3.19	-1.00	14
24	4.46	-4.46	-1.00	3
25	5.74	-5.74	-1.00	1
26	4.46	-4.46	-1.00	2
27	3.19	-3.19	-1.00	13
28	1.91	-1.91	-1.00	77
29	1.91	-1.91	-1.00	50
30	3.19	-3.19	-1.00	9
31	4.46	-4.46	-1.00	2
32	5.74	-5.74	-1.00	1
33	4.46	-4.46	-1.00	1
34	3.19	-3.19	-1.00	8
35	1.91	-1.91	-1.00	49
VARIABLE MISSION NO. 3B, FIN				
1	1.91	-1.91	-1.00	44
2	3.19	-3.19	-1.00	13
3	4.46	-4.46	-1.00	5
4	5.74	-5.74	-1.00	2
5	7.01	-7.01	-1.00	1
6	5.74	-5.74	-1.00	1
7	4.46	-4.46	-1.00	4
8	3.19	-3.19	-1.00	13
9	1.91	-1.91	-1.00	43
10	1.91	-1.91	-1.00	43
11	3.19	-3.19	-1.00	8
12	4.46	-4.46	-1.00	2
13	5.74	-5.74	-1.00	1
14	4.46	-4.46	-1.00	1
15	3.19	-3.19	-1.00	7
16	1.91	-1.91	-1.00	42
17	1.91	-1.91	-1.00	549
18	3.19	-3.19	-1.00	207
19	4.46	-4.46	-1.00	79
20	5.74	-5.74	-1.00	31
21	7.01	-7.01	-1.00	12
22	8.29	-8.29	-1.00	5
23	9.56	-9.56	-1.00	2
24	10.84	-10.84	-1.00	1
25	12.11	-12.11	-1.00	1
26	10.84	-10.84	-1.00	1
27	9.56	-9.56	-1.00	2
28	8.29	-8.29	-1.00	5
29	7.01	-7.01	-1.00	12
30	5.74	-5.74	-1.00	30
31	4.46	-4.46	-1.00	78
32	3.19	-3.19	-1.00	206
33	1.91	-1.91	-1.00	549
34	1.91	-1.91	-1.00	554
35	3.19	-3.19	-1.00	205
36	4.46	-4.46	-1.00	77
37	5.74	-5.74	-1.00	30
38	7.01	-7.01	-1.00	12
39	8.29	-8.29	-1.00	5
40	9.56	-9.56	-1.00	2
41	10.84	-10.84	-1.00	1

TABLE B-3 (CONT'D)  
 VARIABLE MISSION STRESS SPECTRA  
 FIN ANALYSIS LOCATION

<u>STRESS NUMBER</u>	<u>MAXIMUM STRESS</u> KSI	<u>MINIMUM STRESS</u> KSI	<u>R</u>	<u>NUMBER OF CYCLES</u>
42	12.11	-12.11	-1.00	1
43	10.84	-10.84	-1.00	1
44	9.56	-9.56	-1.00	2
45	8.29	-8.29	-1.00	4
46	7.01	-7.01	-1.00	11
47	5.74	-5.74	-1.00	29
48	4.46	-4.46	-1.00	76
49	3.19	-3.19	-1.00	204
50	1.91	-1.91	-1.00	553
51	1.91	-1.91	-1.00	49
52	3.19	-3.19	-1.00	8
53	4.46	-4.46	-1.00	2
54	5.74	-5.74	-1.00	1
55	4.46	-4.46	-1.00	1
56	3.19	-3.19	-1.00	8
57	1.91	-1.91	-1.00	48
VARIABLE MISSION NO. 4B, FIN				
1	1.91	-1.91	-1.00	44
2	3.19	-3.19	-1.00	13
3	4.46	-4.46	-1.00	5
4	5.74	-5.74	-1.00	2
5	7.01	-7.01	-1.00	1
6	5.74	-5.74	-1.00	1
7	4.46	-4.46	-1.00	4
8	3.19	-3.19	-1.00	13
9	1.91	-1.91	-1.00	43
10	1.91	-1.91	-1.00	43
11	3.19	-3.19	-1.00	8
12	4.46	-4.46	-1.00	2
13	5.74	-5.74	-1.00	1
14	4.46	-4.46	-1.00	1
15	3.19	-3.19	-1.00	7
16	1.91	-1.91	-1.00	42
17	1.91	-1.91	-1.00	82
18	3.19	-3.19	-1.00	14
19	4.46	-4.46	-1.00	3
20	5.74	-5.74	-1.00	1
21	4.46	-4.46	-1.00	2
22	3.19	-3.19	-1.00	13
23	1.91	-1.91	-1.00	81
24	1.91	-1.91	-1.00	79
25	3.19	-3.19	-1.00	26
26	4.46	-4.46	-1.00	9
27	5.74	-5.74	-1.00	3
28	7.01	-7.01	-1.00	1
29	8.29	-8.29	-1.00	1
30	7.01	-7.01	-1.00	1
31	5.74	-5.74	-1.00	3
32	4.46	-4.46	-1.00	8
33	3.19	-3.19	-1.00	26
34	1.91	-1.91	-1.00	79
35	1.91	-1.91	-1.00	79
36	3.19	-3.19	-1.00	26
37	4.46	-4.46	-1.00	9
38	5.74	-5.74	-1.00	3
39	7.01	-7.01	-1.00	1
40	8.29	-8.29	-1.00	1

TABLE B-3 (CONT'D)  
 VARIABLE MISSION STRESS SPECTRA  
 FIN ANALYSIS LOCATION

<u>STRESS NUMBER</u>	<u>MAXIMUM STRESS</u> KSI	<u>MINIMUM STRESS</u> KSI	<u>R</u>	<u>NUMBER OF CYCLES</u>
41	7.01	-7.01	-1.00	1
42	5.74	-5.74	-1.00	3
43	4.46	-4.46	-1.00	8
44	3.19	-3.19	-1.00	26
45	1.91	-1.91	-1.00	79
46	1.91	-1.91	-1.00	79
47	3.19	-3.19	-1.00	26
48	4.46	-4.46	-1.00	9
49	5.74	-5.74	-1.00	3
50	7.01	-7.01	-1.00	1
51	8.29	-8.29	-1.00	1
52	7.01	-7.01	-1.00	1
53	5.74	-5.74	-1.00	3
54	4.46	-4.46	-1.00	8
55	3.19	-3.19	-1.00	26
56	1.91	-1.91	-1.00	79
VARIABLE MISSION NO. 5B, FIN				
1	1.91	-1.91	-1.00	44
2	3.19	-3.19	-1.00	13
3	4.46	-4.46	-1.00	5
4	5.74	-5.74	-1.00	2
5	7.01	-7.01	-1.00	1
6	5.74	-5.74	-1.00	1
7	4.46	-4.46	-1.00	4
8	3.19	-3.19	-1.00	13
9	1.91	-1.91	-1.00	43
10	1.91	-1.91	-1.00	43
11	3.19	-3.19	-1.00	8
12	4.46	-4.46	-1.00	2
13	5.74	-5.74	-1.00	1
14	4.46	-4.46	-1.00	1
15	3.19	-3.19	-1.00	7
16	1.91	-1.91	-1.00	42
17	1.91	-1.91	-1.00	626
18	3.19	-3.19	-1.00	221
19	4.46	-4.46	-1.00	79
20	5.74	-5.74	-1.00	28
21	7.01	-7.01	-1.00	10
22	8.29	-8.29	-1.00	4
23	9.56	-9.56	-1.00	2
24	10.84	-10.84	-1.00	1
25	9.56	-9.56	-1.00	1
26	8.29	-8.29	-1.00	3
27	7.01	-7.01	-1.00	10
28	5.74	-5.74	-1.00	28
29	4.46	-4.46	-1.00	78
30	3.19	-3.19	-1.00	221
31	1.91	-1.91	-1.00	625
32	1.91	-1.91	-1.00	79
33	3.19	-3.19	-1.00	26
34	4.46	-4.46	-1.00	9
35	5.74	-5.74	-1.00	3
36	7.01	-7.01	-1.00	1
37	8.29	-8.29	-1.00	1
38	7.01	-7.01	-1.00	1
39	5.74	-5.74	-1.00	3
40	4.46	-4.46	-1.00	8

TABLE B-3 (CONT'D)  
 VARIABLE MISSION STRESS SPECTRA  
 FIN ANALYSIS LOCATION

<u>STRESS NUMBER</u>	<u>MAXIMUM STRESS</u> KSI	<u>MINIMUM STRESS</u> KSI	<u>R</u>	<u>NUMBER OF CYCLES</u>
41	3.19	-3.19	-1.00	26
42	1.91	-1.91	-1.00	79
43	1.91	-1.91	-1.00	79
44	3.19	-3.19	-1.00	26
45	4.46	-4.46	-1.00	9
46	5.74	-5.74	-1.00	3
47	7.01	-7.01	-1.00	1
48	8.29	-8.29	-1.00	1
49	7.01	-7.01	-1.00	1
50	5.74	-5.74	-1.00	3
51	4.46	-4.46	-1.00	8
52	3.19	-3.19	-1.00	26
53	1.91	-1.91	-1.00	79
54	1.91	-1.91	-1.00	79
55	3.19	-3.19	-1.00	26
56	4.46	-4.46	-1.00	9
57	5.74	-5.74	-1.00	3
58	7.01	-7.01	-1.00	1
59	8.29	-8.29	-1.00	1
60	7.01	-7.01	-1.00	1
61	5.74	-5.74	-1.00	3
62	4.46	-4.46	-1.00	8
63	3.19	-3.19	-1.00	26
64	1.91	-1.91	-1.00	79
65	1.91	-1.91	-1.00	79
66	3.19	-3.19	-1.00	26
67	4.46	-4.46	-1.00	9
68	5.74	-5.74	-1.00	3
69	7.01	-7.01	-1.00	1
70	8.29	-8.29	-1.00	1
71	7.01	-7.01	-1.00	1
72	5.74	-5.74	-1.00	3
73	4.46	-4.46	-1.00	8
74	3.19	-3.19	-1.00	26
75	1.91	-1.91	-1.00	79
76	1.91	-1.91	-1.00	79
77	3.19	-3.19	-1.00	26
78	4.46	-4.46	-1.00	9
79	5.74	-5.74	-1.00	3
80	7.01	-7.01	-1.00	1
81	8.29	-8.29	-1.00	1
82	7.01	-7.01	-1.00	1
83	5.74	-5.74	-1.00	3
84	4.46	-4.46	-1.00	8
85	3.19	-3.19	-1.00	26
86	1.91	-1.91	-1.00	79
87	1.91	-1.91	-1.00	79
88	3.19	-3.19	-1.00	26
89	4.46	-4.46	-1.00	9
90	5.74	-5.74	-1.00	3
91	7.01	-7.01	-1.00	1
92	8.29	-8.29	-1.00	1
93	7.01	-7.01	-1.00	1
94	5.74	-5.74	-1.00	3
95	4.46	-4.46	-1.00	8
96	3.19	-3.19	-1.00	26
97	1.91	-1.91	-1.00	79

TABLE B-3 (CONT'D)  
 VARIABLE MISSION STRESS SPECTRA  
 FIN ANALYSIS LOCATION

<u>STRESS NUMBER</u>	<u>MAXIMUM STRESS</u> KSI	<u>MINIMUM STRESS</u> KSI	<u>R</u>	<u>NUMBER OF CYCLES</u>
VARIABLE MISSION NO. 5B1, FIN				
1	1.91	-1.91	-1.00	24
2	3.19	-3.19	-1.00	9
3	4.46	-4.46	-1.00	4
4	5.74	-5.74	-1.00	2
5	7.01	-7.01	-1.00	1
6	5.74	-5.74	-1.00	1
7	4.46	-4.46	-1.00	3
8	3.19	-3.19	-1.00	9
9	1.91	-1.91	-1.00	24
10	1.91	-1.91	-1.00	200
11	3.19	-3.19	-1.00	57
12	4.46	-4.46	-1.00	17
13	5.74	-5.74	-1.00	6
14	7.01	-7.01	-1.00	2
15	8.29	-8.29	-1.00	1
16	9.56	-9.56	-1.00	1
17	8.29	-8.29	-1.00	1
18	7.01	-7.01	-1.00	2
19	5.74	-5.74	-1.00	5
20	4.46	-4.46	-1.00	17
21	3.19	-3.19	-1.00	57
22	1.91	-1.91	-1.00	200
23	1.91	-1.91	-1.00	626
24	3.19	-3.19	-1.00	221
25	4.46	-4.46	-1.00	79
26	5.74	-5.74	-1.00	28
27	7.01	-7.01	-1.00	10
28	8.29	-8.29	-1.00	4
29	9.56	-9.56	-1.00	2
30	10.84	-10.84	-1.00	1
31	9.56	-9.56	-1.00	1
32	8.29	-8.29	-1.00	3
33	7.01	-7.01	-1.00	10
34	5.74	-5.74	-1.00	28
35	4.46	-4.46	-1.00	78
36	3.19	-3.19	-1.00	221
37	1.91	-1.91	-1.00	625
38	1.91	-1.91	-1.00	79
39	3.19	-3.19	-1.00	26
40	4.46	-4.46	-1.00	9
41	5.74	-5.74	-1.00	3
42	7.01	-7.01	-1.00	1
43	8.29	-8.29	-1.00	1
44	7.01	-7.01	-1.00	1
45	5.74	-5.74	-1.00	3
46	4.46	-4.46	-1.00	8
47	3.19	-3.19	-1.00	26
48	1.91	-1.91	-1.00	79
49	1.91	-1.91	-1.00	79
50	3.19	-3.19	-1.00	26
51	4.46	-4.46	-1.00	9
52	5.74	-5.74	-1.00	3
53	7.01	-7.01	-1.00	1
54	8.29	-8.29	-1.00	1
55	7.01	-7.01	-1.00	1
56	5.74	-5.74	-1.00	3

TABLE B-3 (CONT'D)  
 VARIABLE MISSION STRESS SPECTRA  
 FIN ANALYSIS LOCATION

<u>STRESS NUMBER</u>	<u>MAXIMUM STRESS</u> KSI	<u>MINIMUM STRESS</u> KSI	<u>R</u>	<u>NUMBER OF CYCLES</u>
57	4.46	-4.46	-1.00	8
58	3.19	-3.19	-1.00	26
59	1.91	-1.91	-1.00	79
60	1.91	-1.91	-1.00	79
61	3.19	-3.19	-1.00	26
62	4.46	-4.46	-1.00	9
63	5.74	-5.74	-1.00	3
64	7.01	-7.01	-1.00	1
65	8.29	-8.29	-1.00	1
66	7.01	-7.01	-1.00	1
67	5.74	-5.74	-1.00	3
68	4.46	-4.46	-1.00	8
69	3.19	-3.19	-1.00	26
70	1.91	-1.91	-1.00	79
71	1.91	-1.91	-1.00	79
72	3.19	-3.19	-1.00	26
73	4.46	-4.46	-1.00	9
74	5.74	-5.74	-1.00	3
75	7.01	-7.01	-1.00	1
76	8.29	-8.29	-1.00	1
77	7.01	-7.01	-1.00	1
78	5.74	-5.74	-1.00	3
79	4.46	-4.46	-1.00	8
80	3.19	-3.19	-1.00	26
81	1.91	-1.91	-1.00	79
82	1.91	-1.91	-1.00	79
83	3.19	-3.19	-1.00	26
84	4.46	-4.46	-1.00	9
85	5.74	-5.74	-1.00	3
86	7.01	-7.01	-1.00	1
87	8.29	-8.29	-1.00	1
88	7.01	-7.01	-1.00	1
89	5.74	-5.74	-1.00	3
90	4.46	-4.46	-1.00	8
91	3.19	-3.19	-1.00	26
92	1.91	-1.91	-1.00	79
93	1.91	-1.91	-1.00	79
94	3.19	-3.19	-1.00	26
95	4.46	-4.46	-1.00	9
96	5.74	-5.74	-1.00	3
97	7.01	-7.01	-1.00	1
98	8.29	-8.29	-1.00	1
99	7.01	-7.01	-1.00	1
100	5.74	-5.74	-1.00	3
101	4.46	-4.46	-1.00	8
102	3.19	-3.19	-1.00	26
103	1.91	-1.91	-1.00	79
VARIABLE MISSION NO. 1C, FIN				
1	1.91	-1.91	-1.00	34
2	3.19	-3.19	-1.00	9
3	4.46	-4.46	-1.00	3
4	5.74	-5.74	-1.00	1
5	7.01	-7.01	-1.00	1
6	5.74	-5.74	-1.00	1
7	4.46	-4.46	-1.00	2
8	3.19	-3.19	-1.00	9
9	1.91	-1.91	-1.00	34

TABLE B-3 (CONT'D)  
 VARIABLE MISSION STRESS SPECTRA  
 FIN ANALYSIS LOCATION

<u>STRESS NUMBER</u>	<u>MAXIMUM STRESS</u> KSI	<u>MINIMUM STRESS</u> KSI	<u>R</u>	<u>NUMBER OF CYCLES</u>
10	1.91	-1.91	-1.00	61
11	3.19	-3.19	-1.00	10
12	4.46	-4.46	-1.00	2
13	5.74	-5.74	-1.00	1
14	4.46	-4.46	-1.00	2
15	3.19	-3.19	-1.00	10
16	1.91	-1.91	-1.00	61
17	1.91	-1.91	-1.00	89
18	3.19	-3.19	-1.00	14
19	4.46	-4.46	-1.00	3
20	5.74	-5.74	-1.00	1
21	4.46	-4.46	-1.00	2
22	3.19	-3.19	-1.00	14
23	1.91	-1.91	-1.00	88
VARIABLE MISSION NO. 2C, FIN				
1	1.91	-1.91	-1.00	34
2	3.19	-3.19	-1.00	9
3	4.46	-4.46	-1.00	3
4	5.74	-5.74	-1.00	1
5	7.01	-7.01	-1.00	1
6	5.74	-5.74	-1.00	1
7	4.46	-4.46	-1.00	2
8	3.19	-3.19	-1.00	9
9	1.91	-1.91	-1.00	34
10	1.91	-1.91	-1.00	61
11	3.19	-3.19	-1.00	10
12	4.46	-4.46	-1.00	2
13	5.74	-5.74	-1.00	1
14	4.46	-4.46	-1.00	2
15	3.19	-3.19	-1.00	10
16	1.91	-1.91	-1.00	61
17	1.91	-1.91	-1.00	24
18	3.19	-3.19	-1.00	4
19	4.46	-4.46	-1.00	1
20	3.19	-3.19	-1.00	4
21	1.91	-1.91	-1.00	24
22	1.91	-1.91	-1.00	49
23	3.19	-3.19	-1.00	8
24	4.46	-4.46	-1.00	2
25	5.74	-5.74	-1.00	1
26	4.46	-4.46	-1.00	1
27	3.19	-3.19	-1.00	8
28	1.91	-1.91	-1.00	48
VARIABLE MISSION NO. 4C, FIN				
1	1.91	-1.91	-1.00	34
2	3.19	-3.19	-1.00	9
3	4.46	-4.46	-1.00	3
4	5.74	-5.74	-1.00	1
5	7.01	-7.01	-1.00	1
6	5.74	-5.74	-1.00	1
7	4.46	-4.46	-1.00	2
8	3.19	-3.19	-1.00	9
9	1.91	-1.91	-1.00	34
10	1.91	-1.91	-1.00	61
11	3.19	-3.19	-1.00	10
12	4.46	-4.46	-1.00	2

TABLE B-3 (CONT'D)  
 VARIABLE MISSION STRESS SPECTRA  
 FIN ANALYSIS LOCATION

<u>STRESS NUMBER</u>	<u>MAXIMUM STRESS</u> KSI	<u>MINIMUM STRESS</u> KSI	<u>R</u>	<u>NUMBER OF CYCLES</u>
13	5.74	-5.74	-1.00	1
14	4.46	-4.46	-1.00	2
15	3.19	-3.19	-1.00	10
16	1.91	-1.91	-1.00	61
17	1.91	-1.91	-1.00	48
18	3.19	-3.19	-1.00	8
19	4.46	-4.46	-1.00	2
20	5.74	-5.74	-1.00	1
21	4.46	-4.46	-1.00	1
22	3.19	-3.19	-1.00	7
23	1.91	-1.91	-1.00	47
24	1.91	-1.91	-1.00	73
25	3.19	-3.19	-1.00	21
26	4.46	-4.46	-1.00	6
27	5.74	-5.74	-1.00	2
28	7.01	-7.01	-1.00	1
29	5.74	-5.74	-1.00	1
30	4.46	-4.46	-1.00	5
31	3.19	-3.19	-1.00	20
32	1.91	-1.91	-1.00	72
33	1.91	-1.91	-1.00	73
34	3.19	-3.19	-1.00	21
35	4.46	-4.46	-1.00	6
36	5.74	-5.74	-1.00	2
37	7.01	-7.01	-1.00	1
38	5.74	-5.74	-1.00	1
39	4.46	-4.46	-1.00	5
40	3.19	-3.19	-1.00	20
41	1.91	-1.91	-1.00	72
42	1.91	-1.91	-1.00	73
43	3.19	-3.19	-1.00	21
44	4.46	-4.46	-1.00	6
45	5.74	-5.74	-1.00	2
46	7.01	-7.01	-1.00	1
47	5.74	-5.74	-1.00	1
48	4.46	-4.46	-1.00	5
49	3.19	-3.19	-1.00	20
50	1.91	-1.91	-1.00	72
VARIABLE MISSION NO. 5C, FIN				
1	1.91	-1.91	-1.00	34
2	3.19	-3.19	-1.00	9
3	4.46	-4.46	-1.00	3
4	5.74	-5.74	-1.00	1
5	7.01	-7.01	-1.00	1
6	5.74	-5.74	-1.00	1
7	4.46	-4.46	-1.00	2
8	3.19	-3.19	-1.00	9
9	1.91	-1.91	-1.00	34
10	1.91	-1.91	-1.00	61
11	3.19	-3.19	-1.00	10
12	4.46	-4.46	-1.00	2
13	5.74	-5.74	-1.00	1
14	4.46	-4.46	-1.00	2
15	3.19	-3.19	-1.00	10
16	1.91	-1.91	-1.00	61
17	1.91	-1.91	-1.00	557
18	3.19	-3.19	-1.00	156

TABLE B-3 (CONT'D)  
 VARIABLE MISSION STRESS SPECTRA  
 FIN ANALYSIS LOCATION

<u>STRESS NUMBER</u>	<u>MAXIMUM STRESS</u> KSI	<u>MINIMUM STRESS</u> KSI	<u>R</u>	<u>NUMBER OF CYCLES</u>
19	4.46	-4.46	-1.00	44
20	5.74	-5.74	-1.00	13
21	7.01	-7.01	-1.00	4
22	8.29	-8.29	-1.00	1
23	9.56	-9.56	-1.00	1
24	8.29	-8.29	-1.00	1
25	7.01	-7.01	-1.00	3
26	5.74	-5.74	-1.00	12
27	4.46	-4.46	-1.00	44
28	3.19	-3.19	-1.00	156
29	1.91	-1.91	-1.00	557
30	1.91	-1.91	-1.00	73
31	3.19	-3.19	-1.00	21
32	4.46	-4.46	-1.00	6
33	5.74	-5.74	-1.00	2
34	7.01	-7.01	-1.00	1
35	5.74	-5.74	-1.00	1
36	4.46	-4.46	-1.00	5
37	3.19	-3.19	-1.00	20
38	1.91	-1.91	-1.00	72
39	1.91	-1.91	-1.00	73
40	3.19	-3.19	-1.00	21
41	4.46	-4.46	-1.00	6
42	5.74	-5.74	-1.00	2
43	7.01	-7.01	-1.00	1
44	5.74	-5.74	-1.00	1
45	4.46	-4.46	-1.00	5
46	3.19	-3.19	-1.00	20
47	1.91	-1.91	-1.00	72
48	1.91	-1.91	-1.00	73
49	3.19	-3.19	-1.00	21
50	4.46	-4.46	-1.00	6
51	5.74	-5.74	-1.00	2
52	7.01	-7.01	-1.00	1
53	5.74	-5.74	-1.00	1
54	4.46	-4.46	-1.00	5
55	3.19	-3.19	-1.00	20
56	1.91	-1.91	-1.00	72
57	1.91	-1.91	-1.00	73
58	3.19	-3.19	-1.00	21
59	4.46	-4.46	-1.00	6
60	5.74	-5.74	-1.00	2
61	7.01	-7.01	-1.00	1
62	5.74	-5.74	-1.00	1
63	4.46	-4.46	-1.00	5
64	3.19	-3.19	-1.00	20
65	1.91	-1.91	-1.00	72
66	1.91	-1.91	-1.00	73
67	3.19	-3.19	-1.00	21
68	4.46	-4.46	-1.00	6
69	5.74	-5.74	-1.00	2
70	7.01	-7.01	-1.00	1
71	5.74	-5.74	-1.00	1
72	4.46	-4.46	-1.00	5
73	3.19	-3.19	-1.00	20
74	1.91	-1.91	-1.00	72
75	1.91	-1.91	-1.00	73
76	3.19	-3.19	-1.00	21

TABLE B-3 (CONT'D)  
 VARIABLE MISSION STRESS SPECTRA  
 FIN ANALYSIS LOCATION

<u>STRESS NUMBER</u>	<u>MAXIMUM STRESS KSI</u>	<u>MINIMUM STRESS KSI</u>	<u>R</u>	<u>NUMBER OF CYCLES</u>
77	4.46	-4.46	-1.00	6
78	5.74	-5.74	-1.00	2
79	7.01	-7.01	-1.00	1
80	5.74	-5.74	-1.00	1
81	4.46	-4.46	-1.00	5
82	3.19	-3.19	-1.00	20
83	1.91	-1.91	-1.00	72
VARIABLE MISSION NO. 5C1, FIN				
1	1.91	-1.91	-1.00	19
2	3.19	-3.19	-1.00	6
3	4.46	-4.46	-1.00	2
4	5.74	-5.74	-1.00	1
5	7.01	-7.01	-1.00	1
6	4.46	-4.46	-1.00	2
7	3.19	-3.19	-1.00	6
8	1.91	-1.91	-1.00	19
9	1.91	-1.91	-1.00	235
10	3.19	-3.19	-1.00	63
11	4.46	-4.46	-1.00	18
12	5.74	-5.74	-1.00	6
13	7.01	-7.01	-1.00	2
14	8.29	-8.29	-1.00	1
15	9.56	-9.56	-1.00	1
16	8.29	-8.29	-1.00	1
17	7.01	-7.01	-1.00	2
18	5.74	-5.74	-1.00	5
19	4.46	-4.46	-1.00	18
20	3.19	-3.19	-1.00	63
21	1.91	-1.91	-1.00	234
22	1.91	-1.91	-1.00	557
23	3.19	-3.19	-1.00	156
24	4.46	-4.46	-1.00	44
25	5.74	-5.74	-1.00	13
26	7.01	-7.01	-1.00	4
27	8.29	-8.29	-1.00	1
28	9.56	-9.56	-1.00	1
29	8.29	-8.29	-1.00	1
30	7.01	-7.01	-1.00	3
31	5.74	-5.74	-1.00	12
32	4.46	-4.46	-1.00	44
33	3.19	-3.19	-1.00	156
34	1.91	-1.91	-1.00	557
35	1.91	-1.91	-1.00	73
36	3.19	-3.19	-1.00	21
37	4.46	-4.46	-1.00	6
38	5.74	-5.74	-1.00	2
39	7.01	-7.01	-1.00	1
40	5.74	-5.74	-1.00	1
41	4.46	-4.46	-1.00	5
42	3.19	-3.19	-1.00	20
43	1.91	-1.91	-1.00	72
44	1.91	-1.91	-1.00	73
45	3.19	-3.19	-1.00	21
46	4.46	-4.46	-1.00	6
47	5.74	-5.74	-1.00	2
48	7.01	-7.01	-1.00	1
49	5.74	-5.74	-1.00	1

TABLE B-3 (CONCLUDED)  
 VARIABLE MISSION STRESS SPECTRA  
 FIN ANALYSIS LOCATION

<u>STRESS NUMBER</u>	<u>MAXIMUM STRESS KSI</u>	<u>MINIMUM STRESS KSI</u>	<u>R</u>	<u>NUMBER OF CYCLES</u>
50	4.46	-4.46	-1.00	5
51	3.19	-3.19	-1.00	20
52	1.91	-1.91	-1.00	72
53	1.91	-1.91	-1.00	73
54	3.19	-3.19	-1.00	21
55	4.46	-4.46	-1.00	6
56	5.74	-5.74	-1.00	2
57	7.01	-7.01	-1.00	1
58	5.74	-5.74	-1.00	1
59	4.46	-4.46	-1.00	5
60	3.19	-3.19	-1.00	20
61	1.91	-1.91	-1.00	72
62	1.91	-1.91	-1.00	73
63	3.19	-3.19	-1.00	21
64	4.46	-4.46	-1.00	6
65	5.74	-5.74	-1.00	2
66	7.01	-7.01	-1.00	1
67	5.74	-5.74	-1.00	1
68	4.46	-4.46	-1.00	5
69	3.19	-3.19	-1.00	20
70	1.91	-1.91	-1.00	72
71	1.91	-1.91	-1.00	73
72	3.19	-3.19	-1.00	21
73	4.46	-4.46	-1.00	6
74	5.74	-5.74	-1.00	2
75	7.01	-7.01	-1.00	1
76	5.74	-5.74	-1.00	1
77	4.46	-4.46	-1.00	5
78	3.19	-3.19	-1.00	20
79	1.91	-1.91	-1.00	72
80	1.91	-1.91	-1.00	73
81	3.19	-3.19	-1.00	21
82	4.46	-4.46	-1.00	6
83	5.74	-5.74	-1.00	2
84	7.01	-7.01	-1.00	1
85	5.74	-5.74	-1.00	1
86	4.46	-4.46	-1.00	5
87	3.19	-3.19	-1.00	20
88	1.91	-1.91	-1.00	72

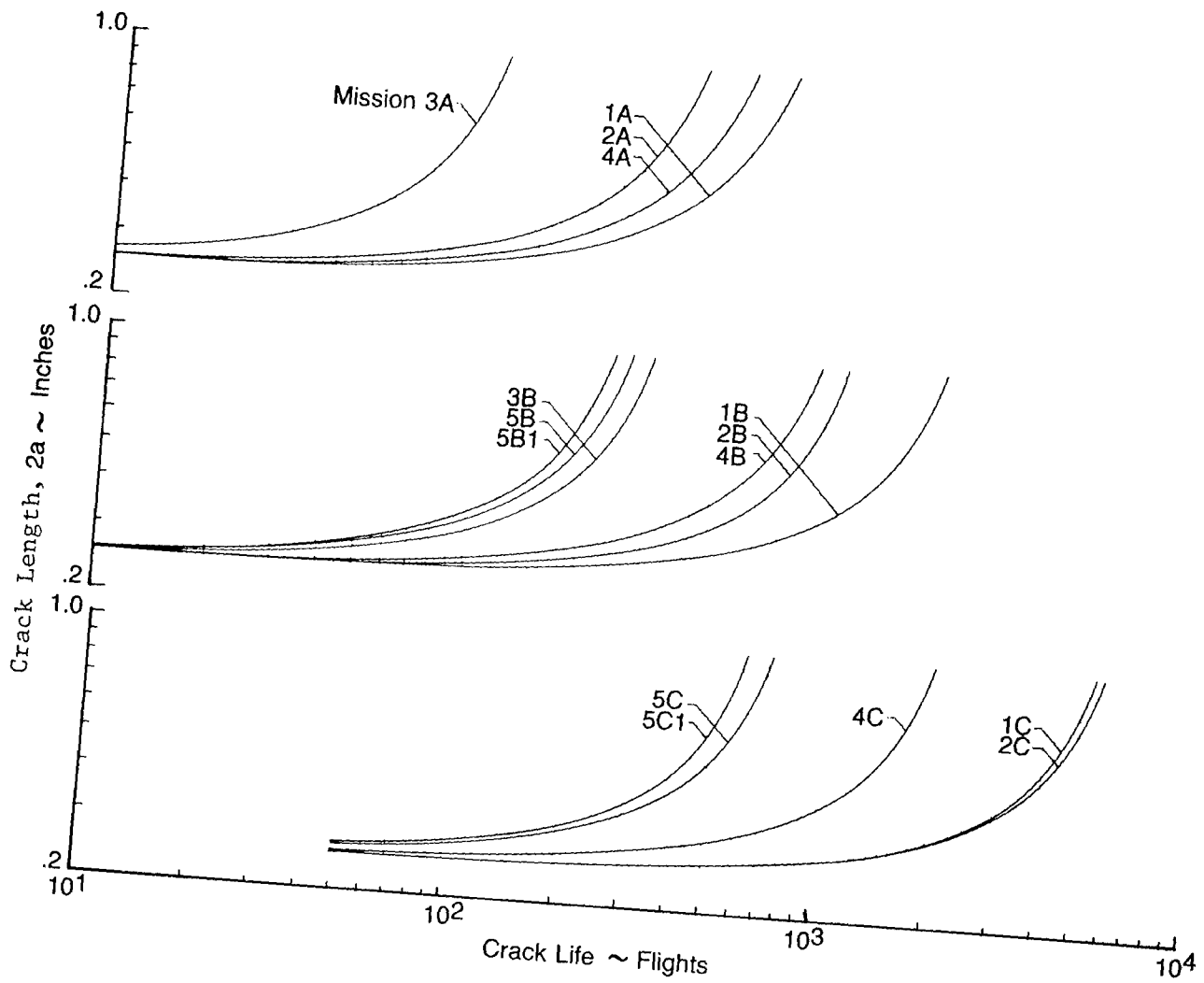


Figure B-1. Mission Crack Growth (Life in Flights), Wing

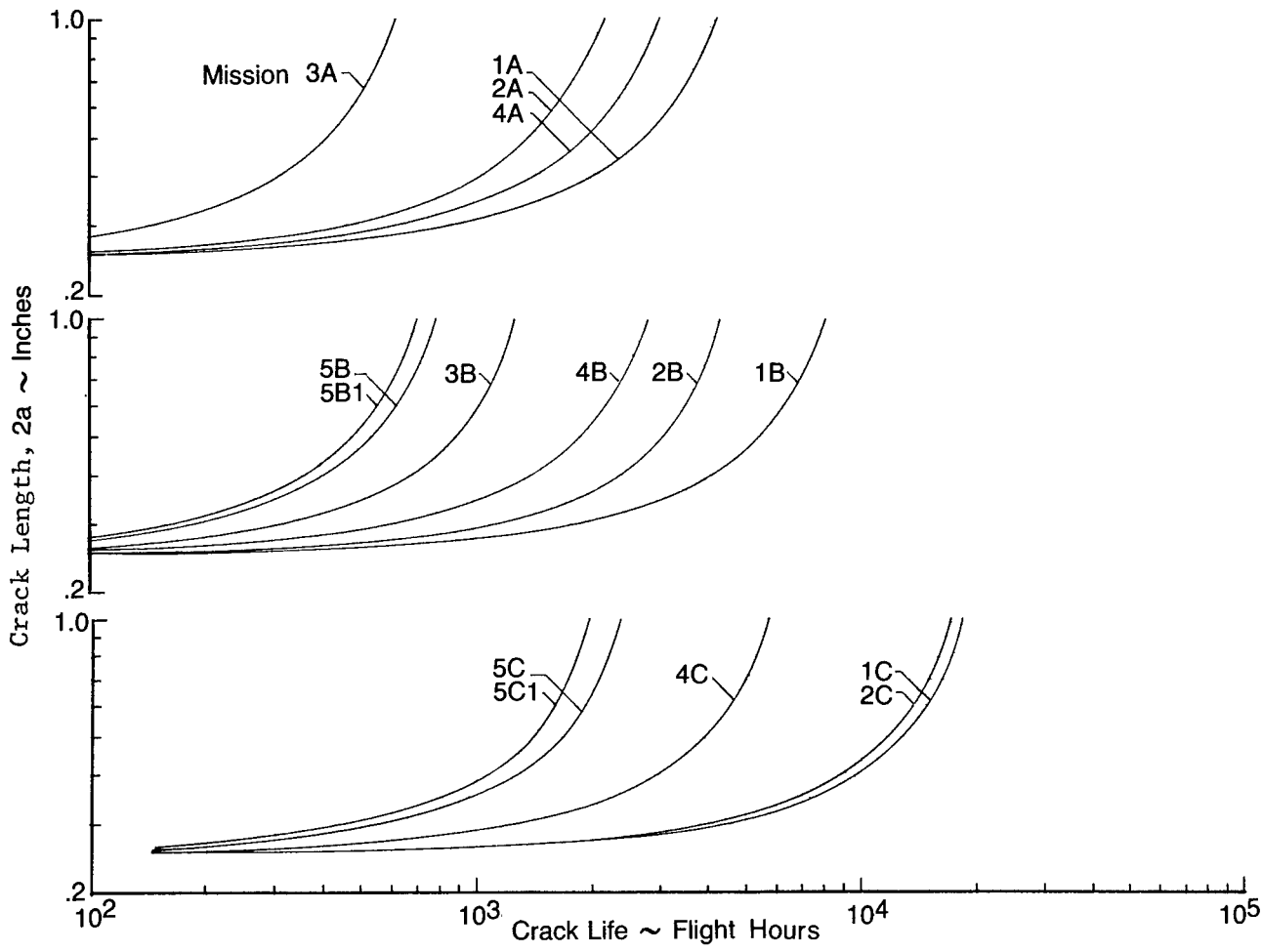


Figure B-2. Mission Crack Growth (Life in Hours), Wing

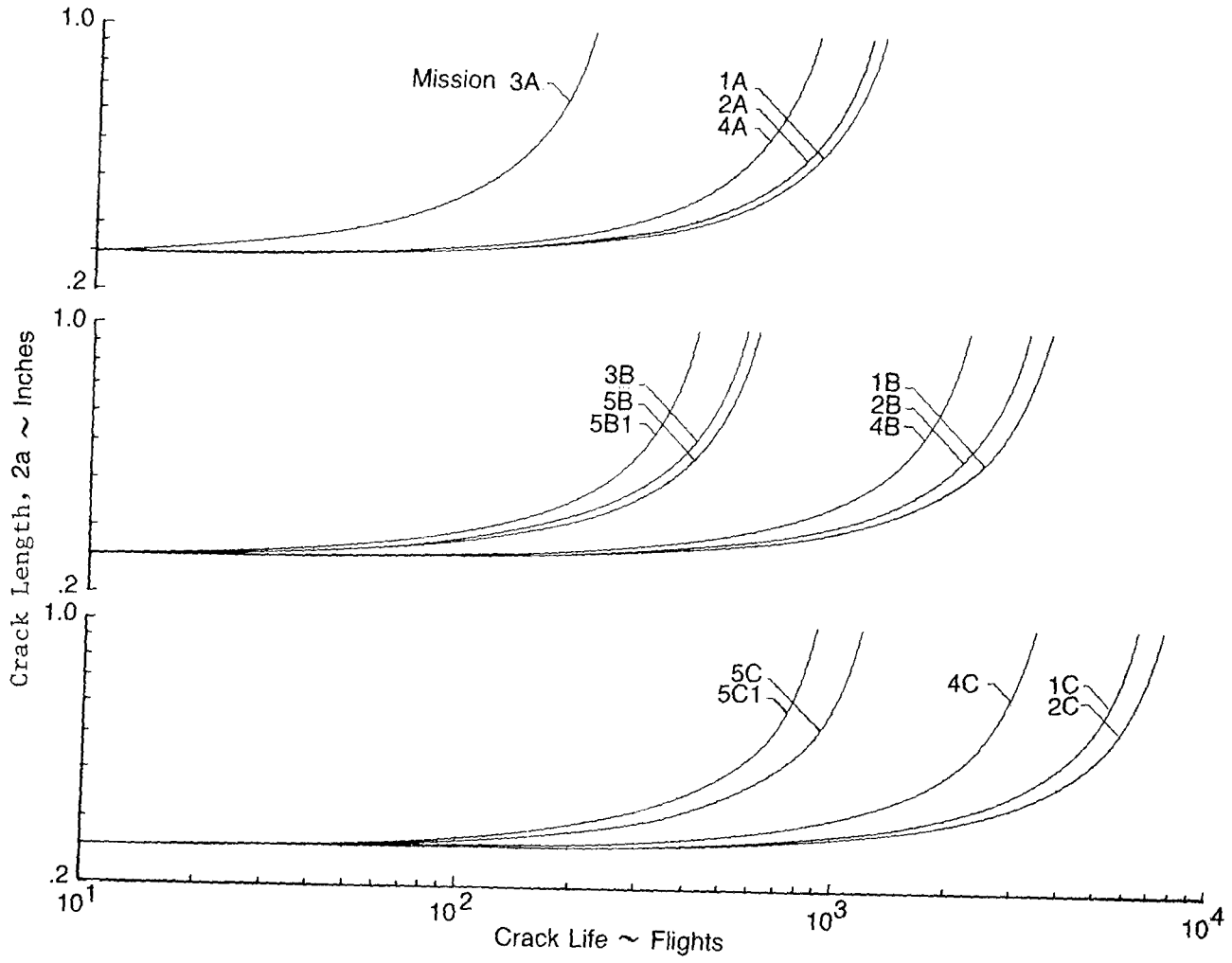


Figure B-3. Mission Crack Growth (Life in Flights), Body

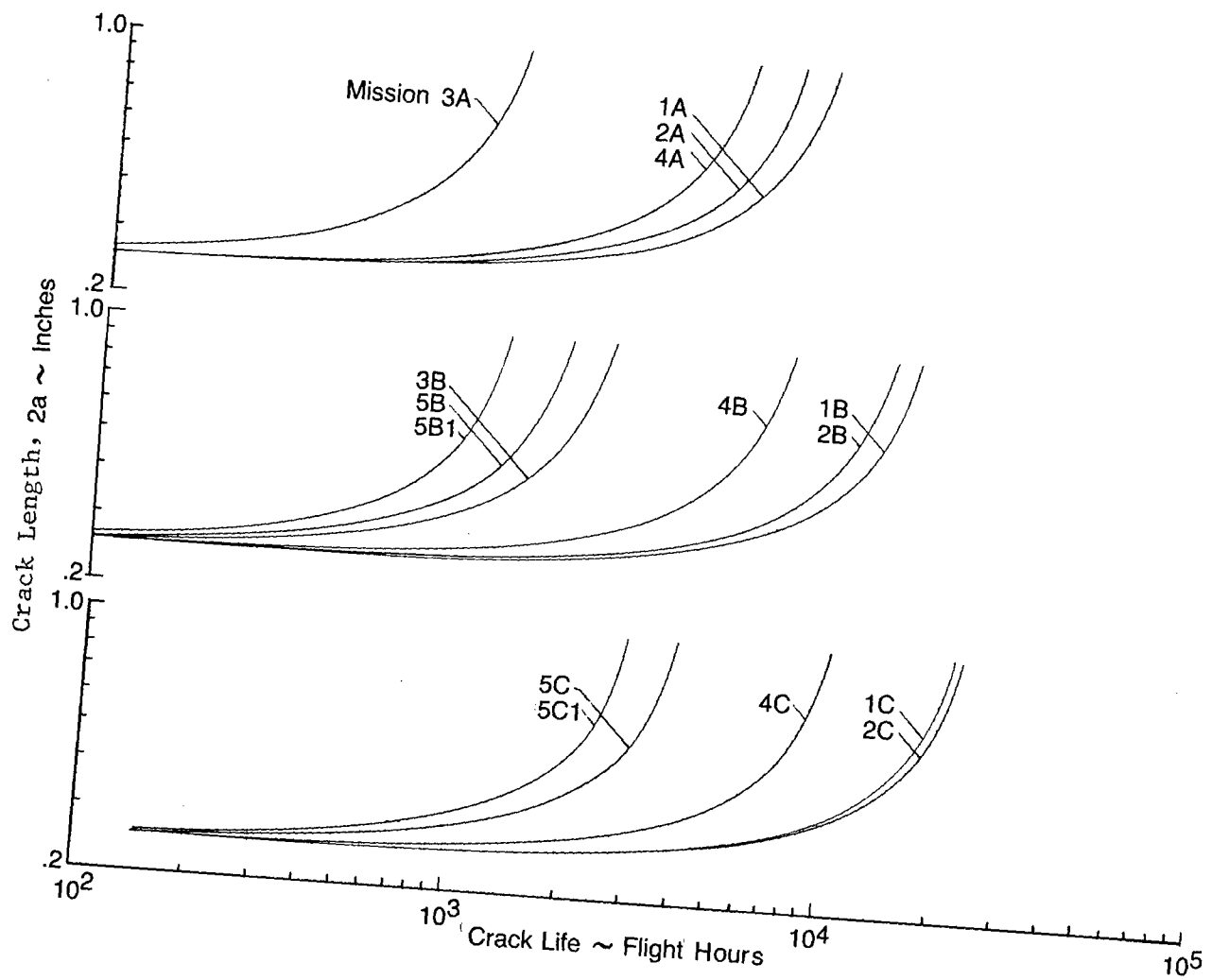


Figure B-4. Mission Crack Growth (Life in Hours), Body

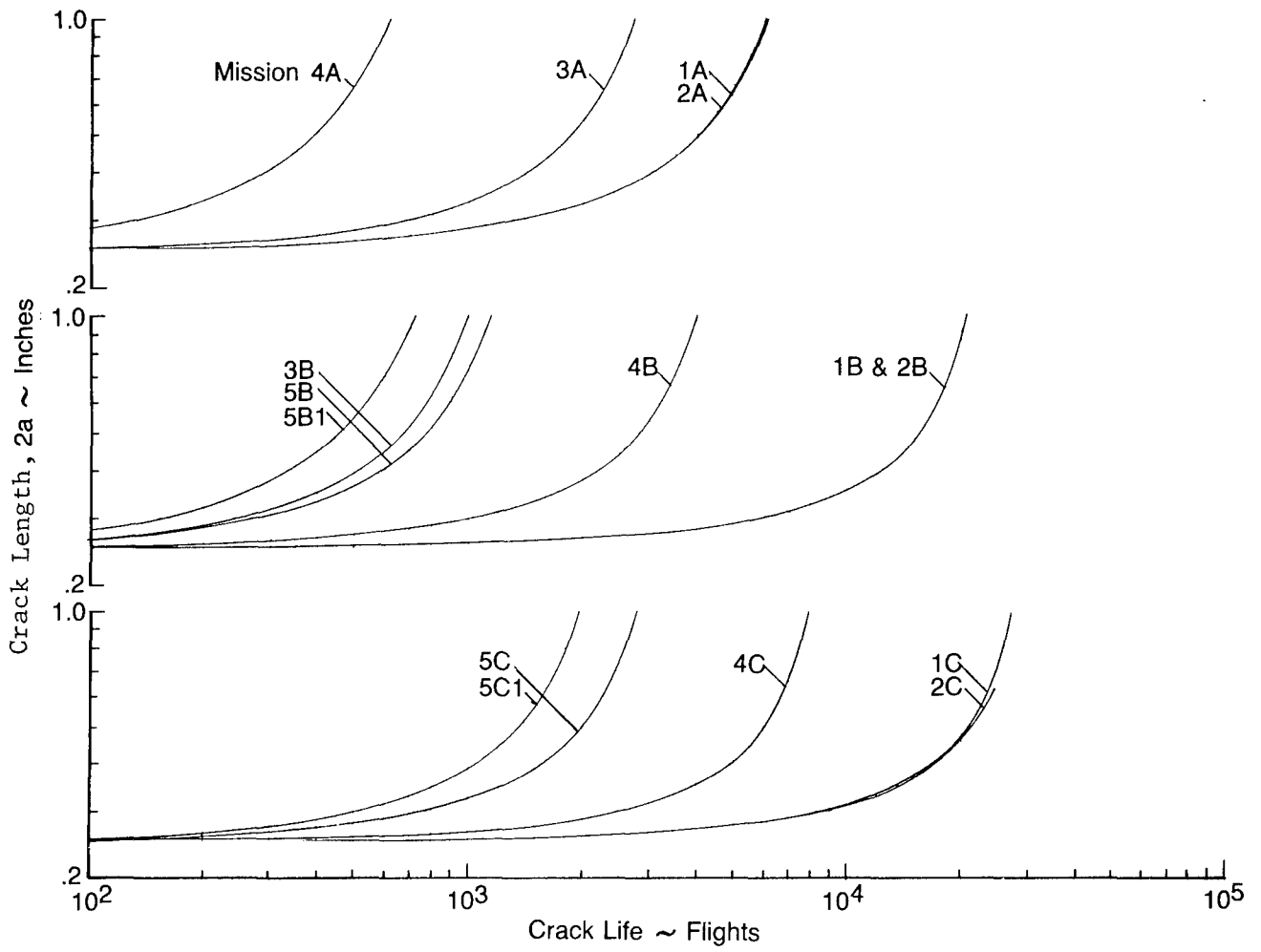


Figure B-5. Mission Crack Growth (Life in Flights), Fin

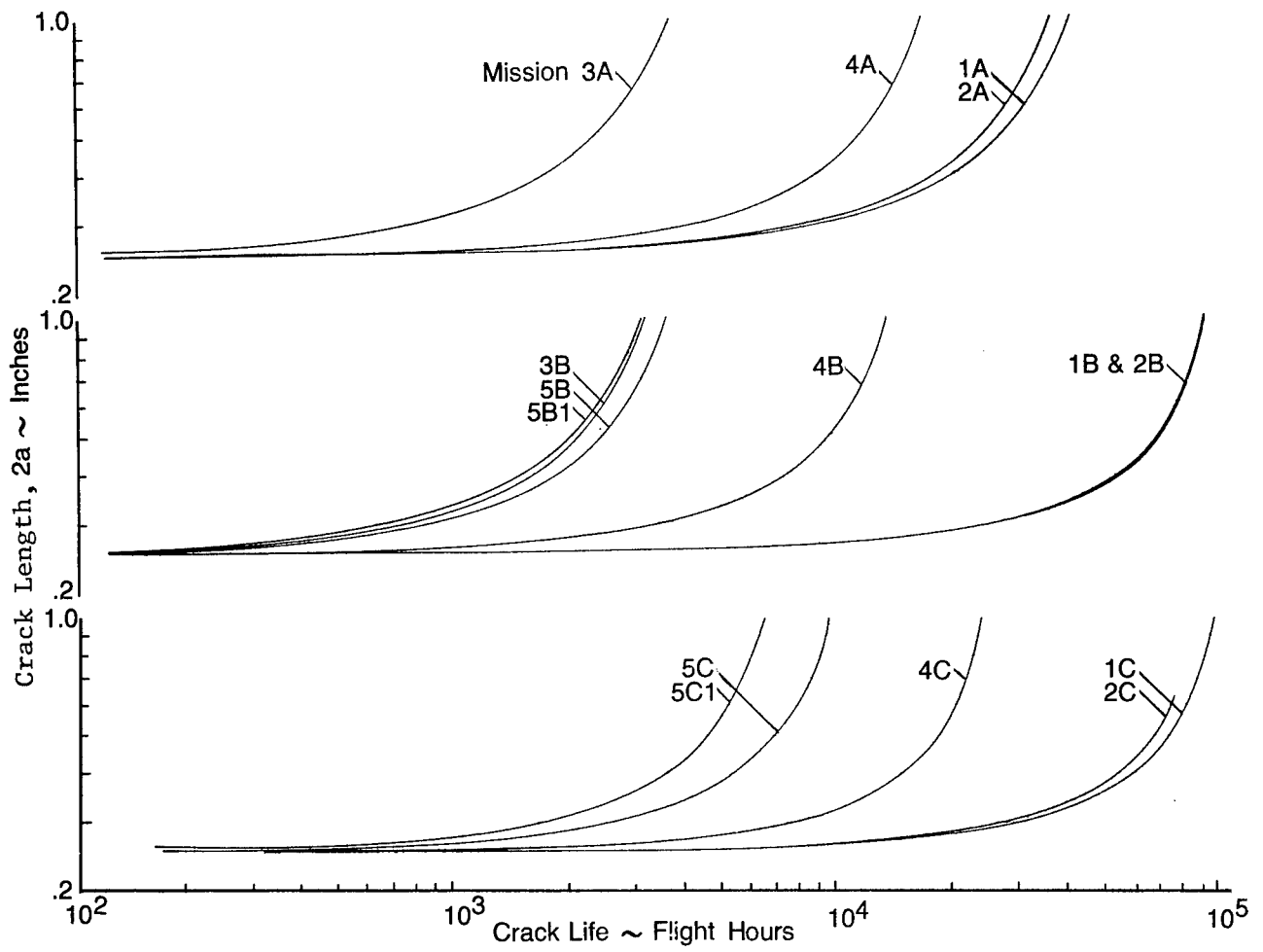


Figure B-6. Mission Crack Growth (Life in Hours), Fin

**APPENDIX C**  
**RELATED TEST DATA**

This appendix presents (1) a sketch of the mission profile and stress spectrum for each of the variable missions selected for experimental verification testing and (2) mission crack growth data used in the determination of the Wheeler shaping exponents,  $m$ .

1. Mission Profiles and Test Spectra

Several mission spectra derived as part of the variability study, Section 2.8, were selected for verification testing. The mission profiles and stress spectra selected for testing are shown in Figures C-1 through C-9. The sketch of each stress spectrum is representative of the magnitude and order of applied stresses.

2. Mission Crack Growth Data and the Determination of  $m$  Values

The Wheeler shaping exponent,  $m$ , was determined for each variable mission and mission segment spectra that was subjected to experimental verification testing. These values were determined by trial and error until the best match between predicted and test was obtained. The values of  $m$  were determined by matching crack growth from 0.25 to 0.35 inch. Figures C-10 through C-14 show a comparison of the predicted crack growth using the derived values of  $m$  with the verification test results.

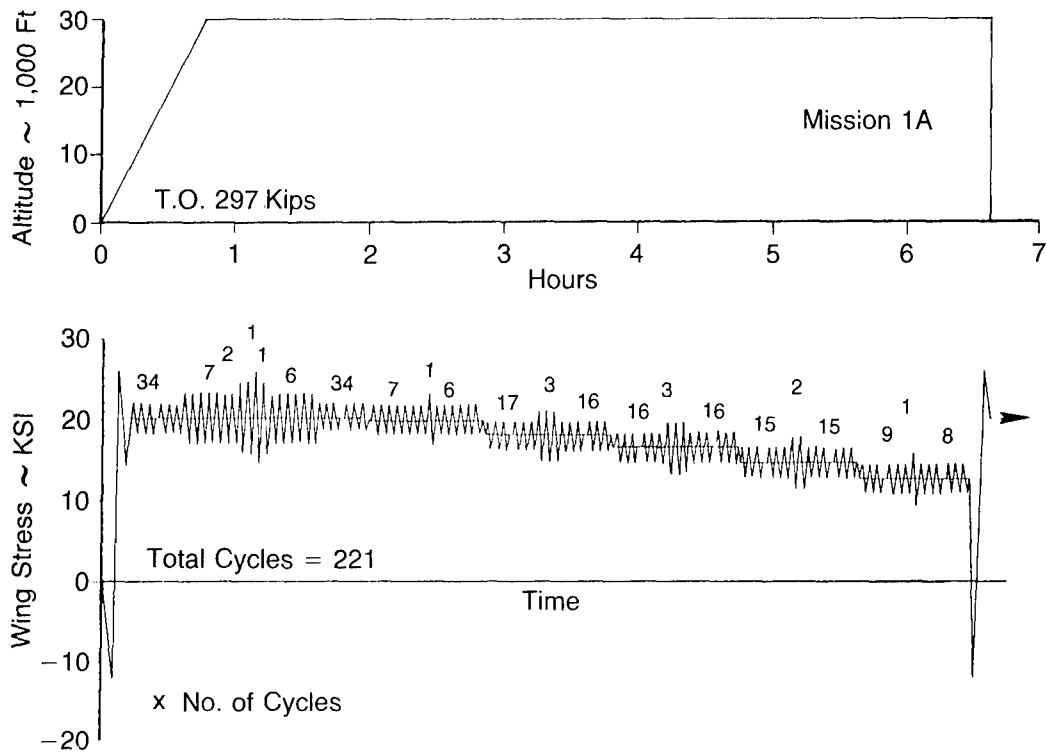


Figure C-1. Mission Profile and Test Spectrum, Mission 1A

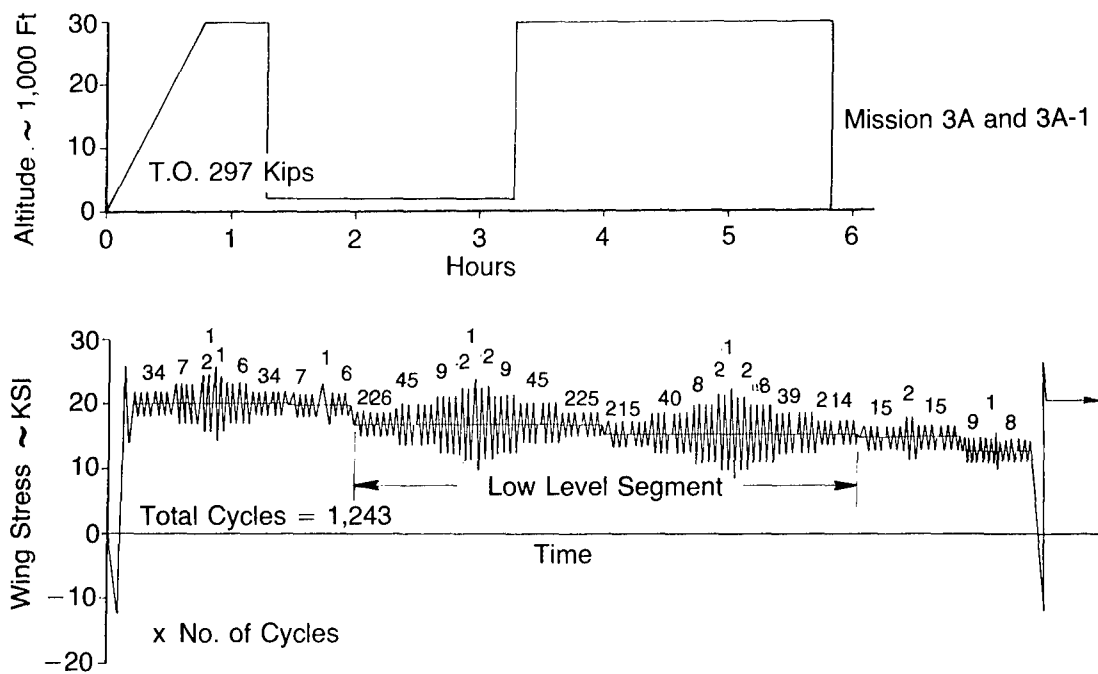


Figure C-2. Mission Profile and Test Spectrum, Mission 3A

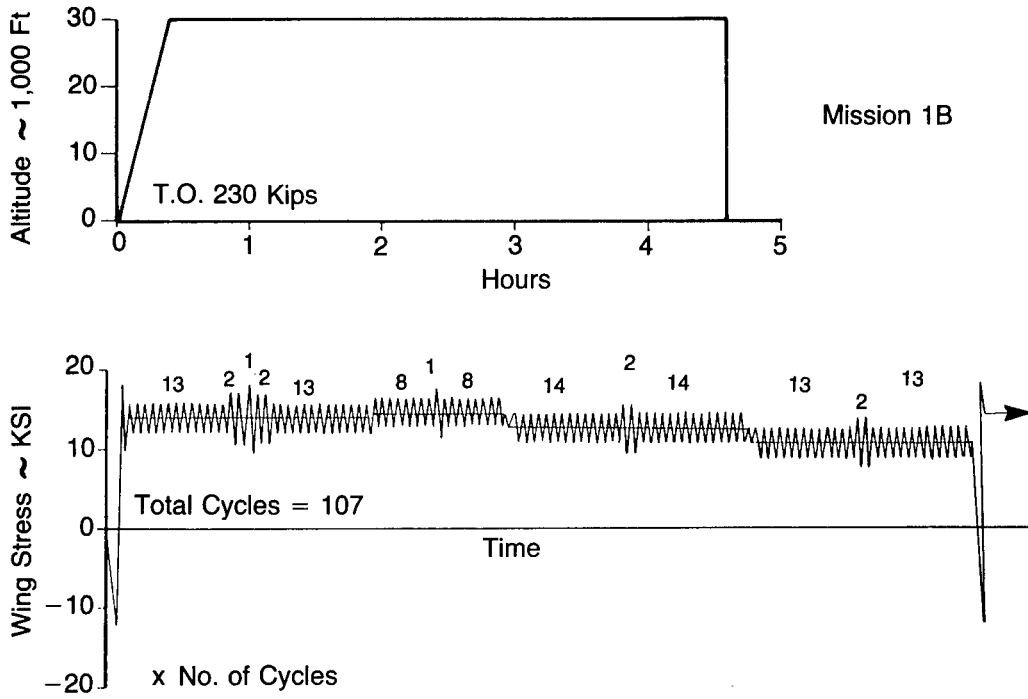


Figure C-3. Mission Profile and Test Spectrum, Mission 1B

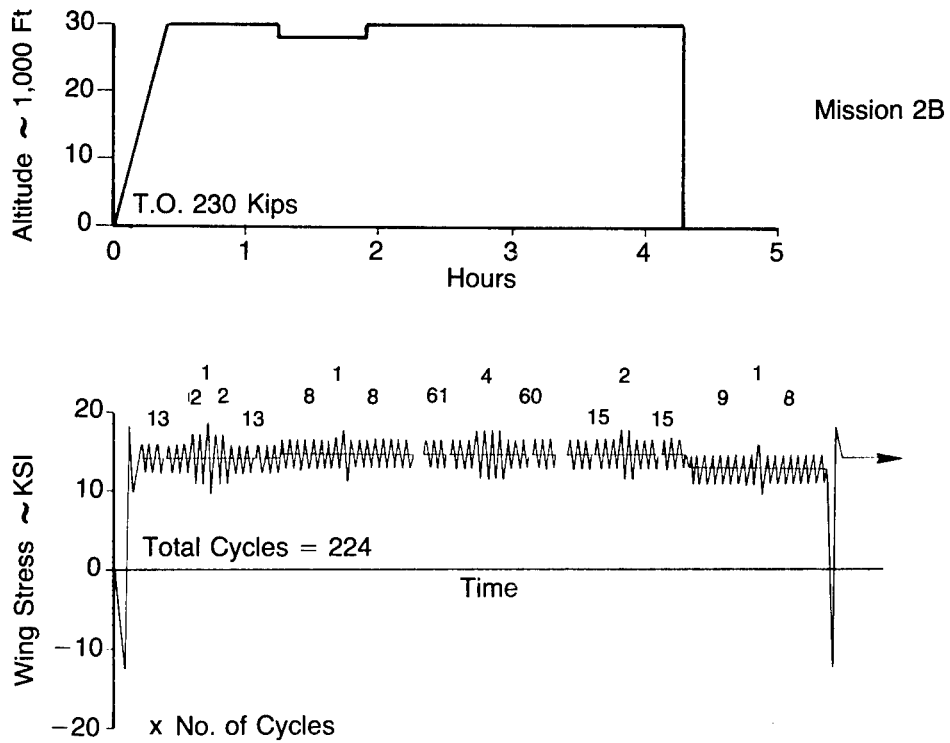


Figure C-4. Mission Profile and Test Spectrum, Mission 2B

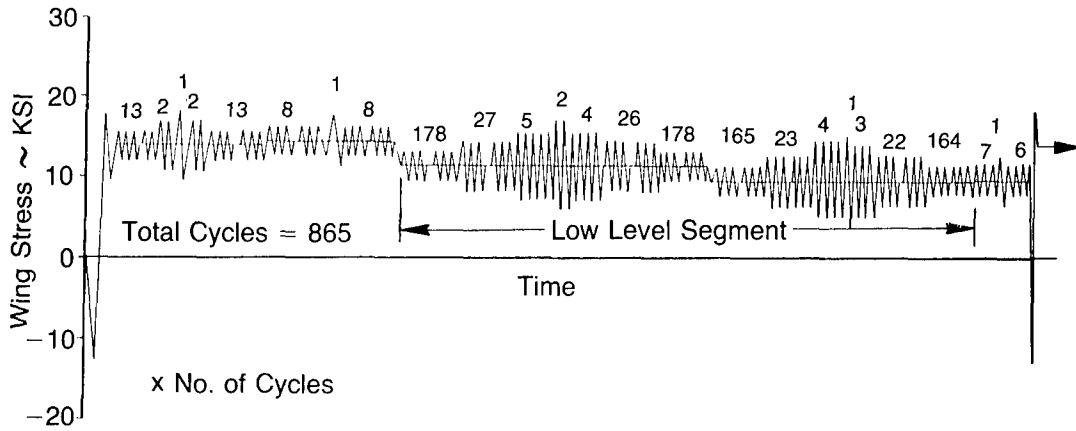
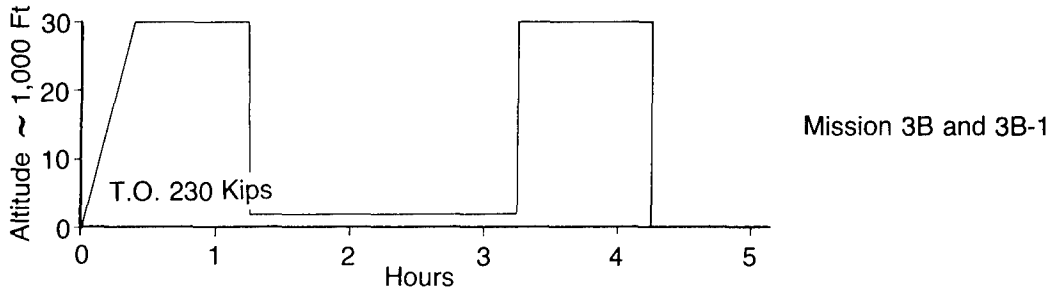


Figure C-5. Mission Profile and Test Spectrum, Mission 3B

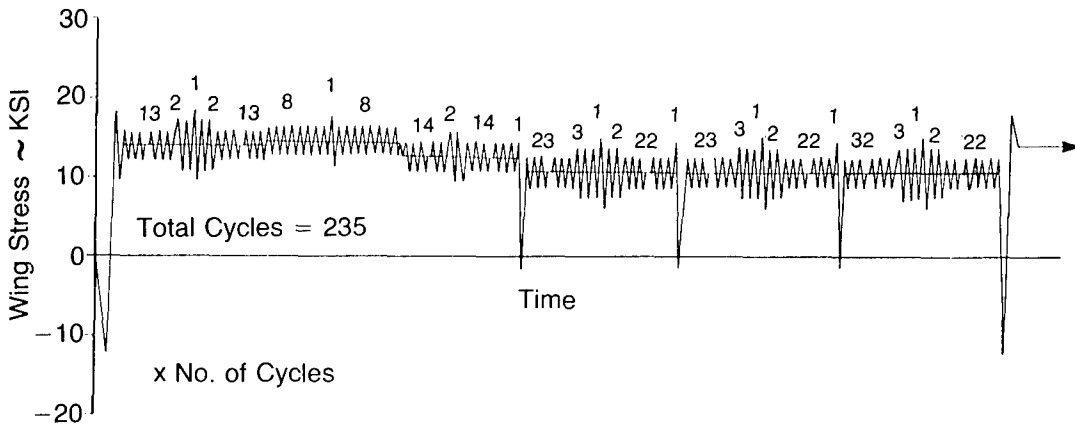
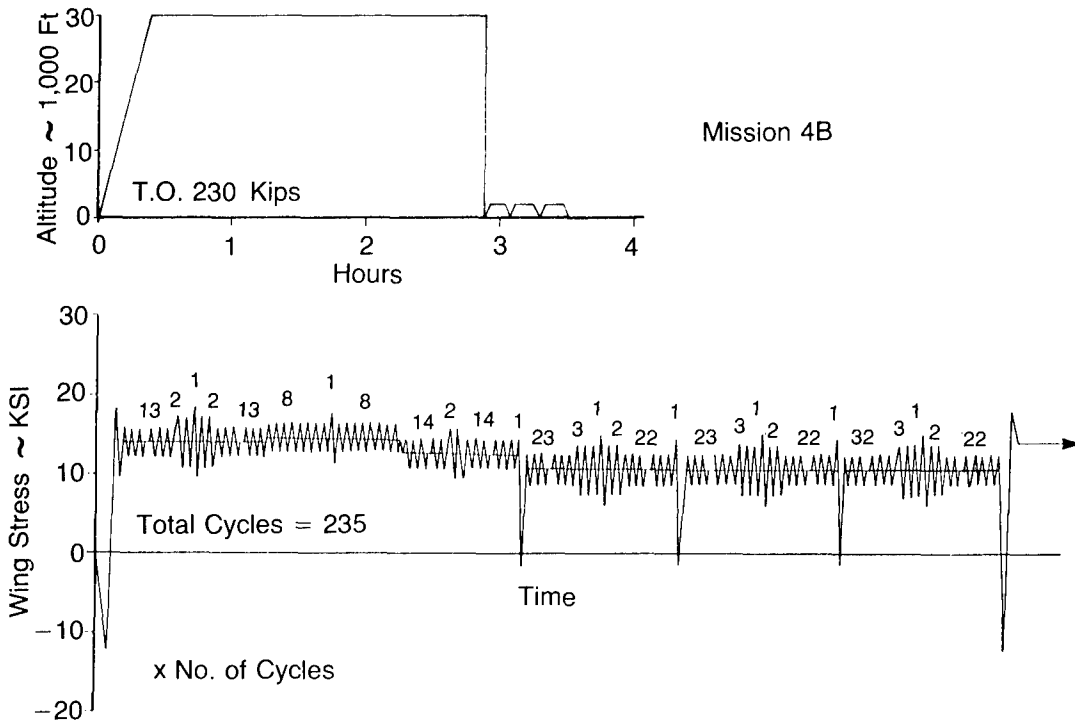


Figure C-6. Mission Profile and Test Spectrum, Mission 4B

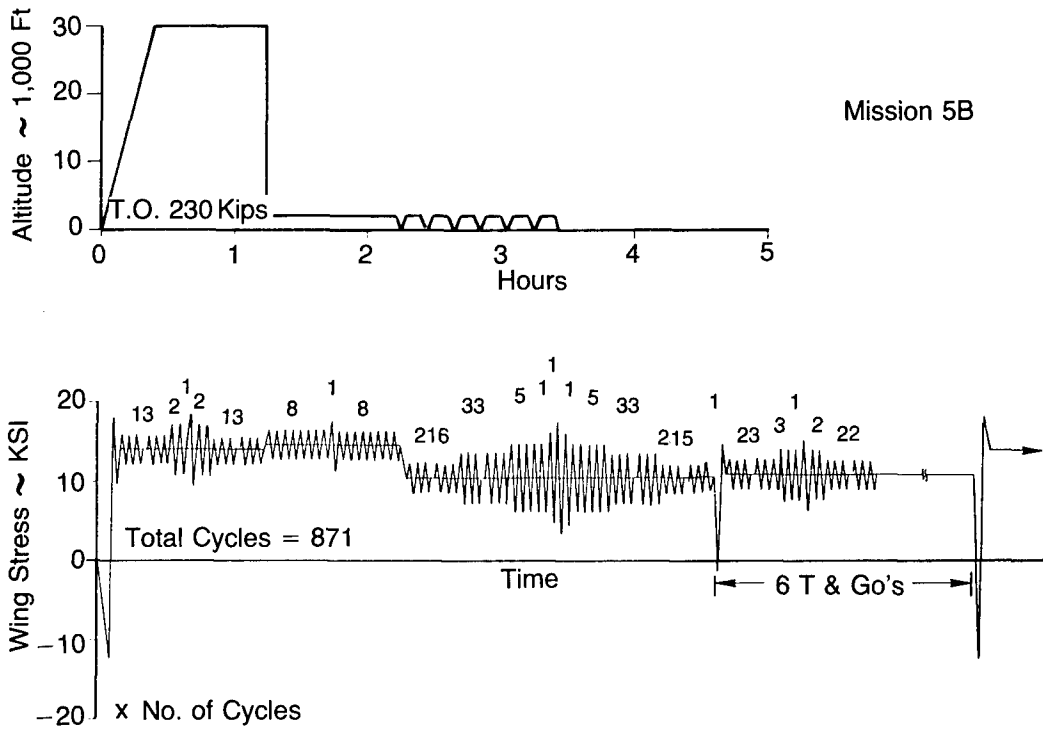


Figure C-7. Mission Profile and Test Spectrum, Mission 5B

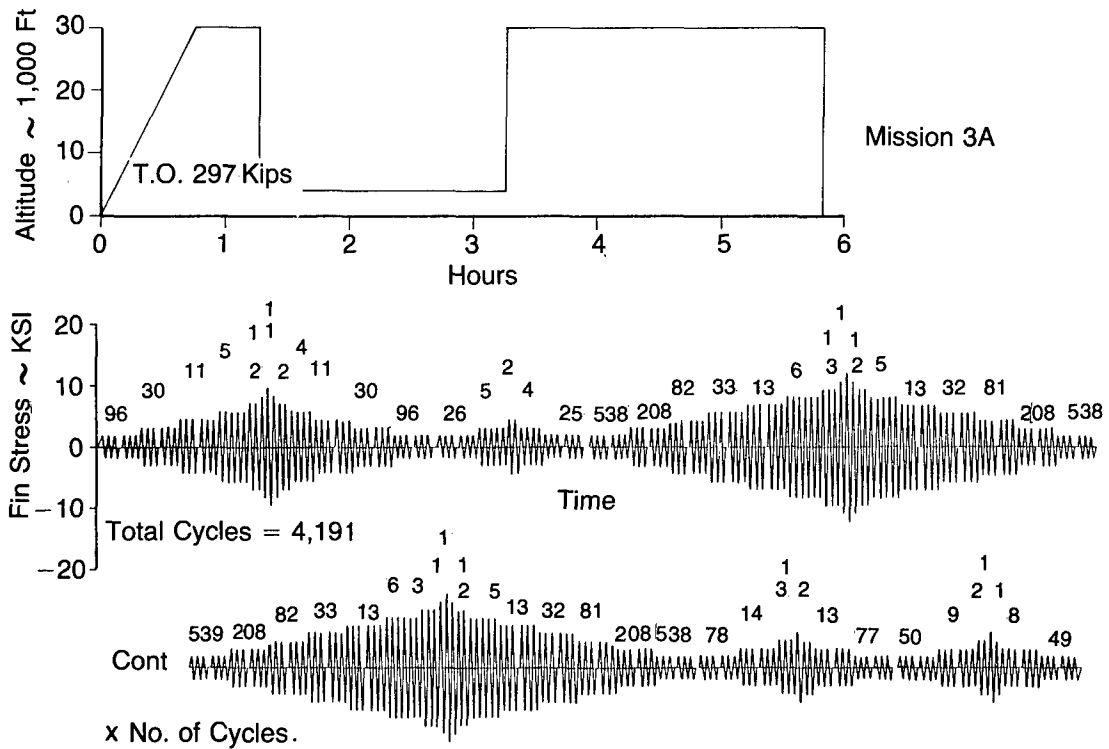


Figure C-8. Mission Profile and Test Spectrum, Mission 3A

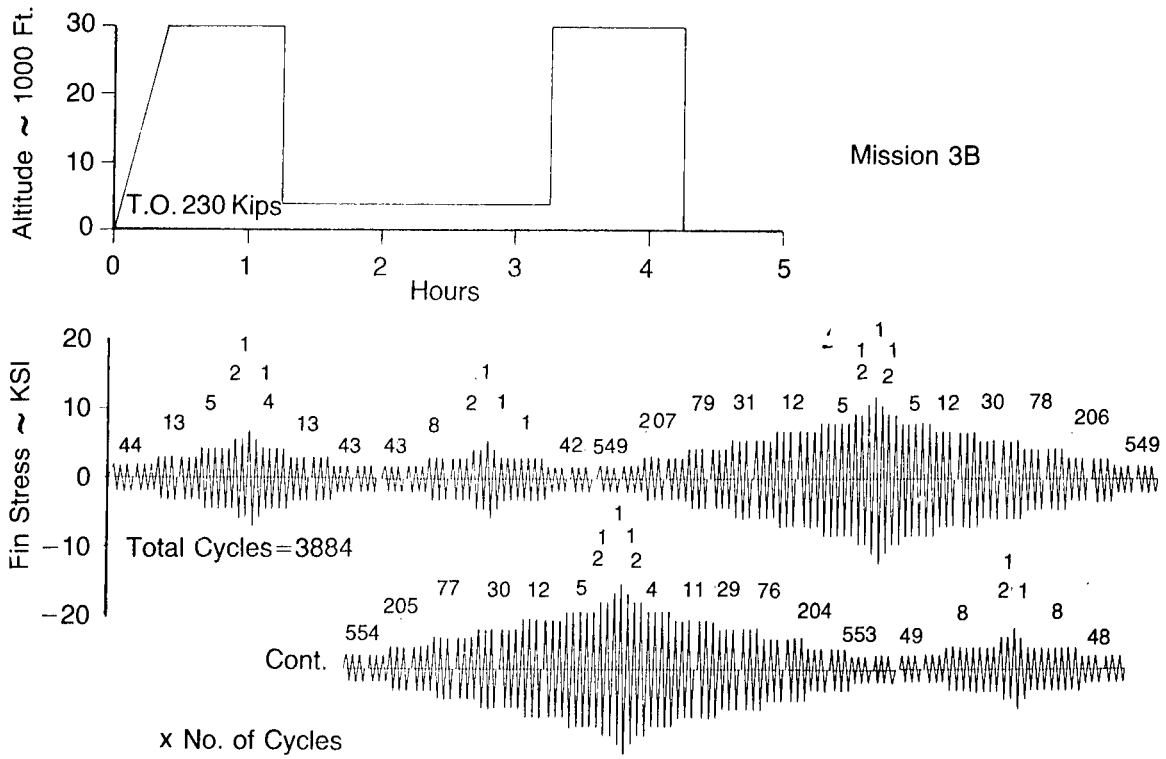


Figure C-9. Mission Profile and Stress Spectrum Mission 3B

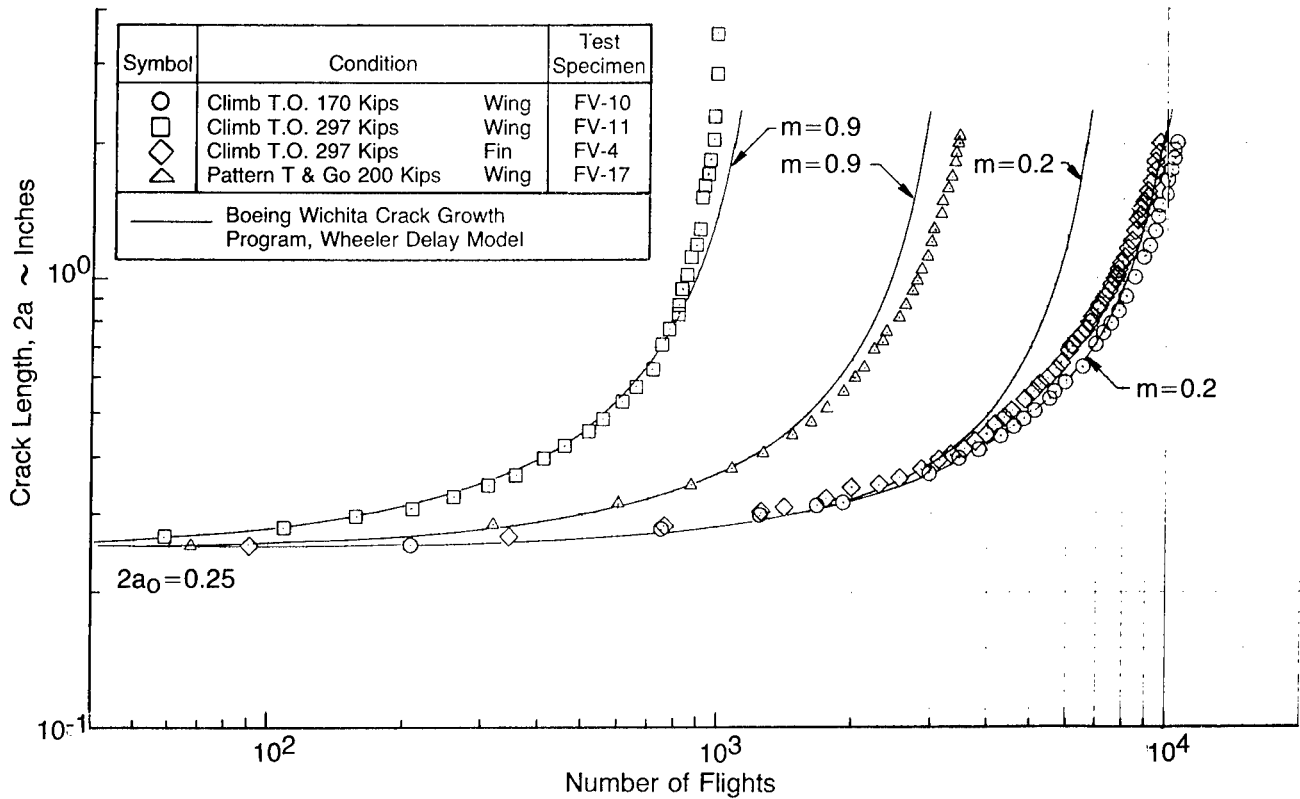


Figure C-10. Mission Segment Crack Growth Determination of m Values

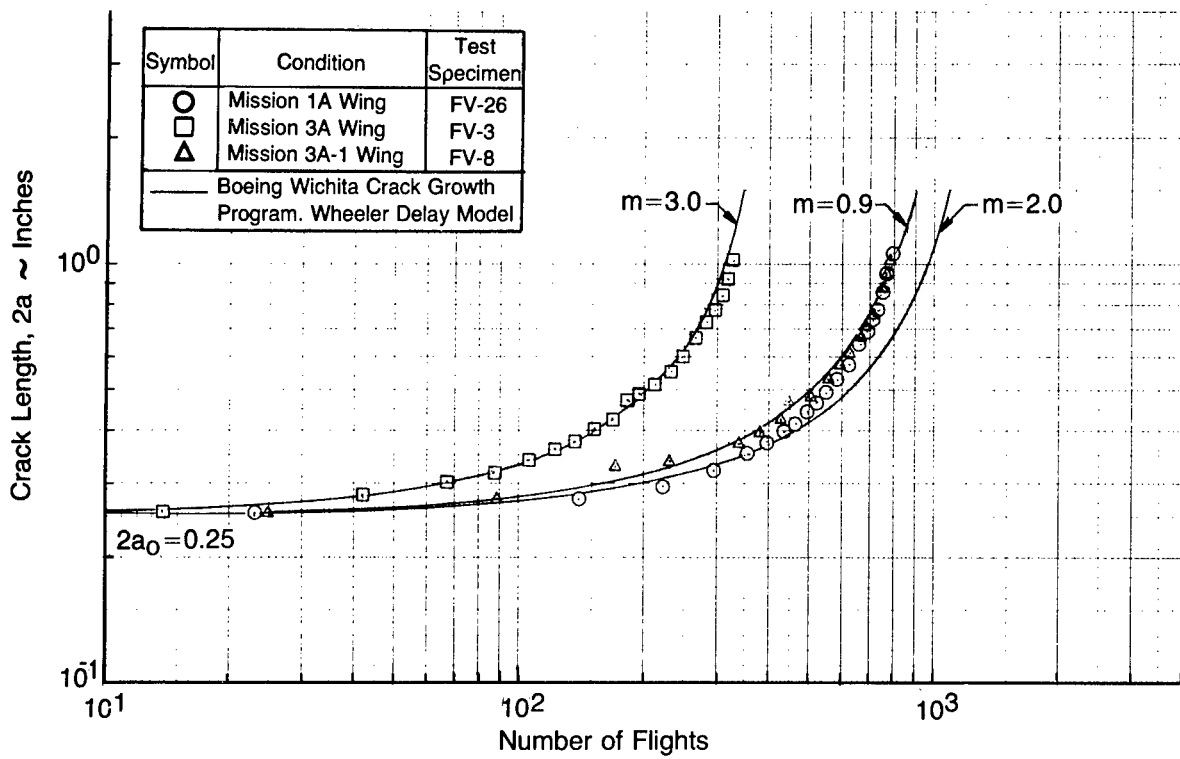


Figure C-11. Mission Crack Growth Determination of  $m$  Values Wing Spectra 1A, 3A, 3A-1

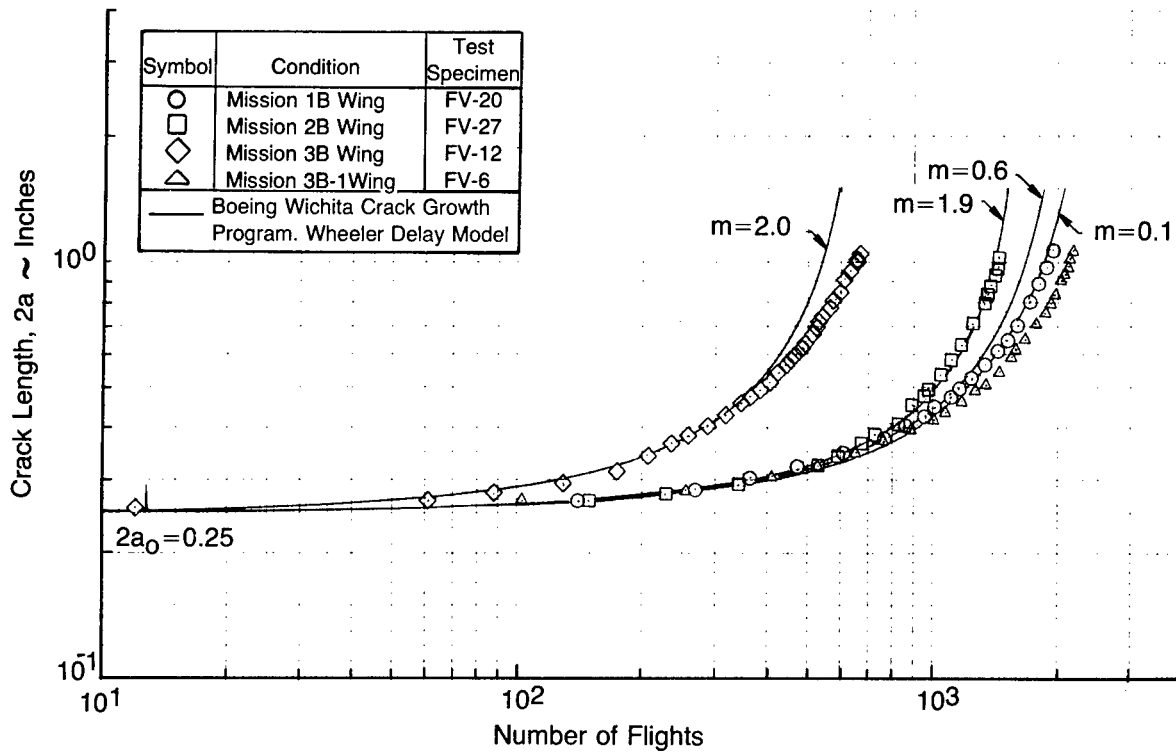


Figure C-12. Mission Crack Growth Determination of  $m$  Values Wing Spectra 1B, 2B, 3B, 3B-1

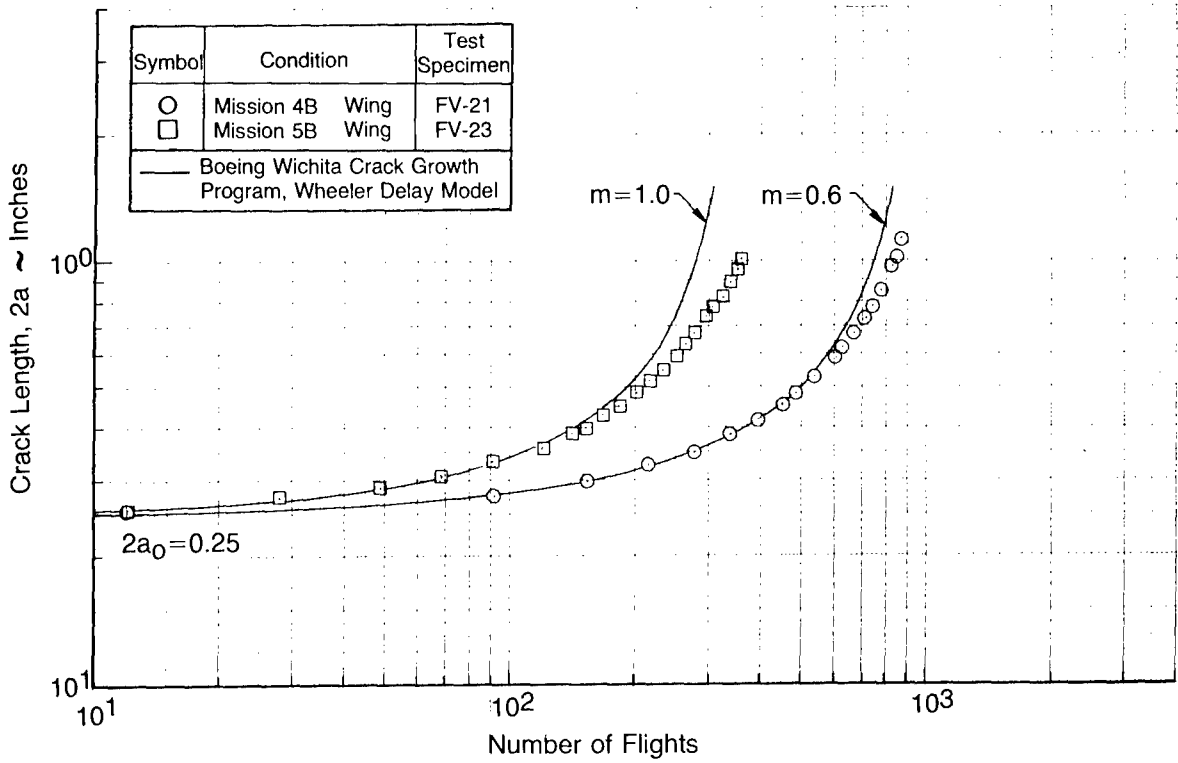


Figure C-13. Mission Crack Growth Determination of  $m$  Values Wing Spectra 4B, 5B

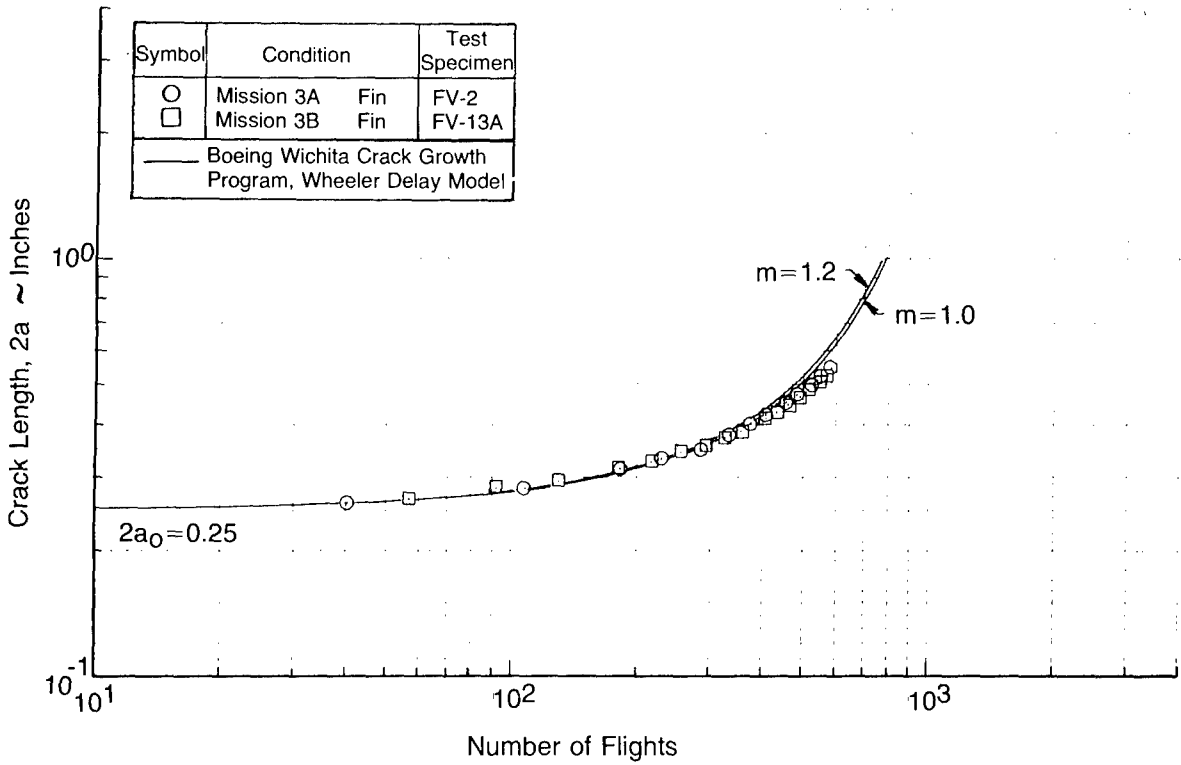


Figure C-14. Mission Crack Growth Determination of  $m$  Values Fin Spectra 3A, 3B

## **APPENDIX D**

### **RELATED COST STUDY DATA**

This appendix shows the manhour and/or cost estimates for each item considered in the relative cost study of Tracking Procedures A, B, C and D. Tables D-1 through D-4 show these estimates for nonrecurring costs of program development and recurring costs of data acquisition, data processing and running the IAT Computer Program. The cost study was discussed in Section 4.1.

TABLE D-1  
RELATIVE COST STUDY  
PROCEDURE A - ITEMIZED COSTS

COST ITEM	TRACKING PROCEDURE A		
	<u>Manhours</u>	<u>Cost</u>	
↑ NONRECURRING ↓	Program Development		
	Develop Analysis Method	280	11,200
	Define Economic, Fracture and Inspection Data	280	11,200
	Define Pilot Log Data	80	3,200
	Parametric Study (Stresses)	9,000/10,500	360,000/420,000
	Stress Exceedance Tables	-	-
	Crack Growth Analyses	1,000/2,000	40,000/80,000
	Crack Growth Rate Tables	400/500	16,000/20,000
	MSR Hardware	-	-
	Crack Growth Gages	-	-
	Instrumentation	-	-
	Develop IAT Program	2,080	62,400
	CRUs	8,000	16,000
		520,000/624,000	
↑ RECURRING ↓	Data Acquisition		
	Fill Out Pilot Log	Neg	Neg
	MSR Tape Replacement	-	-
	MSR Tapes	-	-
	Crack Growth Gage Readings	-	-
	Maintenance	-	-
			Neg
	Data Processing		
	Pilot Log Review and Editing	35,100	702,000
	Keypunching	18,000	360,000
Automation (MSR)	-	-	
CRUs	9,000	18,000	
		1,080,000	
Individual Aircraft Tracking			
Processed Data Into IAT Program (CRUs)	16,920/22,500	33,840/45,000	
		1,633,840/1,749,000	

Note: CRU - Computing Resources Units  
 XX/XX - 5 Locations/10 Locations

TABLE D-2  
RELATIVE COST STUDY  
PROCEDURE B – ITEMIZED COSTS

COST ITEM	TRACKING PROCEDURE B	
	Manhours	Cost
<div style="display: flex; align-items: center;"> <div style="writing-mode: vertical-rl; transform: rotate(180deg); border-left: 1px solid black; border-right: 1px solid black; padding: 0 5px;">NONRECURRING</div> <div style="margin-left: 10px;"> <p>Program Development</p> <p>Develop Analysis Method</p> <p>Define Economic, Fracture and Inspection Data</p> <p>Define Pilot Log Data</p> <p>Parametric Study (Stresses)</p> <p>Stress Exceedance Tables</p> <p>Crack Growth Analyses</p> <p>Crack Growth Rate Tables</p> <p>MSR Hardware</p> <p>Crack Growth Gages</p> <p>Instrumentation</p> <p>Develop IAT Program</p> <p>CRUs</p> </div> </div>		
	280	11,200
	280	11,200
	80	3,200
	9,000/10,500	360,000/420,000
	400/500	16,000/20,000
	-	-
	-	-
	-	-
	-	-
	2,600	78,000
	10,000	20,000
		499,600/563,600
<div style="display: flex; align-items: center;"> <div style="writing-mode: vertical-rl; transform: rotate(180deg); border-left: 1px solid black; border-right: 1px solid black; padding: 0 5px;">RECURRING</div> <div style="margin-left: 10px;"> <p>Data Acquisition</p> <p>Fill Out Pilot Log</p> <p>MSR Tape Replacement</p> <p>MSR Tapes</p> <p>Crack Growth Gage Readings</p> <p>Maintenance</p> </div> </div>	Neg	Neg
	-	-
	-	-
	-	-
	-	-
		Neg
<div style="display: flex; align-items: center;"> <div style="writing-mode: vertical-rl; transform: rotate(180deg); border-left: 1px solid black; border-right: 1px solid black; padding: 0 5px;">RECURRING</div> <div style="margin-left: 10px;"> <p>Data Processing</p> <p>Pilot Log Review and Editing</p> <p>Keypunching</p> <p>Automation (MSR)</p> <p>CRUs</p> </div> </div>	35,100	702,000
	18,000	360,000
	-	-
	9,000	18,000
		1,080,000
<div style="display: flex; align-items: center;"> <div style="writing-mode: vertical-rl; transform: rotate(180deg); border-left: 1px solid black; border-right: 1px solid black; padding: 0 5px;">RECURRING</div> <div style="margin-left: 10px;"> <p>Individual Aircraft Tracking</p> <p>Processed Data Into IAT Program (CRUs)</p> <p>CRUs (Cycle-by-Cycle Crack Growth)</p> </div> </div>	25,920/40,500	51,840/81,000
		1,631,440/1,724,600
	106,920/202,500	213,840/405,000
	1,793,440/2,048,600	

Note: CRU – Computing Resources Units  
XX/XX – 5 Locations/10 Locations

TABLE D-3  
RELATIVE COST STUDY  
PROCEDURE C – ITEMIZED COSTS

COST ITEM	TRACKING PROCEDURE C		
	Manhours	Cost	
<div style="display: flex; align-items: center;"> <div style="writing-mode: vertical-rl; transform: rotate(180deg); border: 1px solid black; padding: 5px; margin-right: 5px;">NONRECURRING</div> <div style="border-left: 1px solid black; border-right: 1px solid black; padding: 5px; margin-right: 5px;"> <div style="text-align: center;">↑</div> <div style="text-align: center;">↓</div> </div> </div> Program Development			
	Develop Analysis Method	280	11,200
	Define Economic, Fracture and Inspection Data	280	11,200
	Define Pilot Log Data	80	3,200
	Parametric Study (Stresses)	-	-
	Stress Exceedance Tables	-	-
	Crack Growth Analyses	-	-
	Crack Growth Rate Tables	-	-
	MSR Hardware	-	400,000/2,000,000
	Crack Growth Gages	-	-
	Instrumentation	1,750/8,750	35,000/175,000
	Develop IAT Program	1,560	46,800
	CRUs	6,000	12,000
		519,400 /2,259,400	
<div style="display: flex; align-items: center;"> <div style="writing-mode: vertical-rl; transform: rotate(180deg); border: 1px solid black; padding: 5px; margin-right: 5px;">RECURRING</div> <div style="border-left: 1px solid black; border-right: 1px solid black; padding: 5px; margin-right: 5px;"> <div style="text-align: center;">↑</div> <div style="text-align: center;">↓</div> </div> </div> Data Acquisition			
	Fill Out Pilot Log	Neg	Neg
	MSR Tape Replacement	2,500/12,500	50,000/250,000
	MSR Tapes	-	1,678,000/8,390,000
	Crack Growth Gage Readings	-	-
	Maintenance	128/640	19,000/99,500
		1,747,900/8,739,500	
<div style="display: flex; align-items: center;"> <div style="writing-mode: vertical-rl; transform: rotate(180deg); border: 1px solid black; padding: 5px; margin-right: 5px;">RECURRING</div> <div style="border-left: 1px solid black; border-right: 1px solid black; padding: 5px; margin-right: 5px;"> <div style="text-align: center;">↑</div> <div style="text-align: center;">↓</div> </div> </div> Data Processing			
	Pilot Log Review and Editing	7,020	140,400
	Key punching	3,600	72,000
	Automation (MSR)	-	562,000/2,812,500
	CRUs	1,800	3,600
		778,000/3,028,500	
<div style="display: flex; align-items: center;"> <div style="writing-mode: vertical-rl; transform: rotate(180deg); border: 1px solid black; padding: 5px; margin-right: 5px;">RECURRING</div> <div style="border-left: 1px solid black; border-right: 1px solid black; padding: 5px; margin-right: 5px;"> <div style="text-align: center;">↑</div> <div style="text-align: center;">↓</div> </div> </div> Individual Aircraft Tracking			
	Processed Data Into IAT Program (CRUs)	20,700/77,760	41,400/155,520
	CRUs (Cycle-by-Cycle Crack Growth)	85,320/320,760	170,640/641,520
		3,215,940/14,668,920	

Note: CRU – Computing Resources Units  
XX/XX – 1 Location/ 5 Locations

TABLE D-4  
RELATIVE COST STUDY  
PROCEDURE D - ITEMIZED COSTS

COST ITEM	TRACKING PROCEDURE D		
	Manhours	Cost	
<div style="display: flex; align-items: center;"> <div style="writing-mode: vertical-rl; transform: rotate(180deg); border: 1px solid black; padding: 5px; margin-right: 5px;">NONRECURRING</div> <div style="border-left: 1px solid black; border-right: 1px solid black; padding: 0 10px;"> <div style="text-align: center;">↑</div> <div style="text-align: center;">↓</div> </div> </div> Program Development			
	Develop Analysis Method	280	11,200
	Define Economic, Fracture and Inspection Data	280	11,200
	Define Pilot Log Data	80	3,200
	Parametric Study (Stresses)	-	-
	Stress Exceedance Tables	-	-
	Crack Growth Analyses	-	-
	Crack Growth Rate Tables	-	-
	MSR Hardware	-	-
	Crack Growth Gages	-	172,700/345,400
	Instrumentation	7,750/15,500	155,000/310,000
	Develop IAT Program	1,040	31,200
CRUs	4,000	8,000	
		392,500/720,200	
<div style="display: flex; align-items: center;"> <div style="writing-mode: vertical-rl; transform: rotate(180deg); border: 1px solid black; padding: 5px; margin-right: 5px;">RECURRING</div> <div style="border-left: 1px solid black; border-right: 1px solid black; padding: 0 10px;"> <div style="text-align: center;">↑</div> <div style="text-align: center;">↓</div> </div> </div> Data Acquisition			
	Fill Out Pilot Log	Neg	Neg
	MSR Tape Replacement	-	-
	MSR Tapes	-	-
	Crack Growth Gage Readings	75,000/150,000	1,500,000/3,000,000
	Maintenance	233/466	9,840/19,680
		1,509,840/3,019,680	
<div style="display: flex; align-items: center;"> <div style="writing-mode: vertical-rl; transform: rotate(180deg); border: 1px solid black; padding: 5px; margin-right: 5px;">RECURRING</div> <div style="border-left: 1px solid black; border-right: 1px solid black; padding: 0 10px;"> <div style="text-align: center;">↑</div> <div style="text-align: center;">↓</div> </div> </div> Data Processing			
	Pilot Log Review and Editing	7,020	140,400
	Keypunching	3,600	72,000
	Automation (MSR)	-	-
CRUs	1,800	3,600	
		3,600	
<div style="display: flex; align-items: center;"> <div style="writing-mode: vertical-rl; transform: rotate(180deg); border: 1px solid black; padding: 5px; margin-right: 5px;">RECURRING</div> <div style="border-left: 1px solid black; border-right: 1px solid black; padding: 0 10px;"> <div style="text-align: center;">↑</div> <div style="text-align: center;">↓</div> </div> </div> Individual Aircraft Tracking			
	Processed Data Into IAT Program (CRUs)	1,200/1,800	2,400/3,600
		2,120,700/3,959,500	

Note: CRU - Computing Resources Units  
XX/XX - 5 Locations/10 Locations

## REFERENCES

1. ZLP911, "Power Spectral Density (PSD) Stress/Damage Computer Program", Boeing Wichita Company.
2. Military Specification MIL-A-008861A, "Airplane Strength and Rigidity, Flight Loads", 31 March 1971.
3. West, Blaine S., "WC-135B and C-135A/B Aircraft Flight Loads Program", UDRI TR 68-10, University of Dayton, February 1968.
4. Schwartz, Robert B., "C-135 A/B Aircraft Flight Loads Program", UDRI TR 66-105, University of Dayton, June 1966.
5. "Stress Sequence Generator Program ZSS921, Program Documentation and Users Guide", Boeing Document D3-11039-1, Boeing Wichita Company, June 1976.
6. Wheeler, O. E., "Crack Propagation under Spectrum Loading", FZM-5602, General Dynamics, Fort Worth Division, June 1970.
7. Willenborg, J. D., Engle, R. M. and Wood, H. A., "A Crack Growth Retardation Model Using an Effective Stress Concept", AFFDL-TM-FBR-71-1, Air Force Flight Dynamics Laboratory, January, 1971.
8. Gallagher, J. P., "A Generalized Development of Yield Zone Models", AFFDL-TM-FBR-74-28, Air Force Flight Dynamics Laboratory, January 1974.
9. ZSS926, "Boeing Wichita Crack Growth Program", Boeing Wichita Company.
10. "Test Plan-Influence of Fleet Variability on Crack Growth Tracking Procedures for Transport/Bomber Aircraft", Boeing Document D3-11039-2, Boeing Wichita Company, November 1976.
11. Pinckert, R. E., "Damage Tolerance Assessment of F-4 Aircraft", MCAIR 76-015, McDonnell Aircraft Company, September 1976.
12. W. Pacquette, G. Johnson, "F-16 Tracking Program," General Dynamics, paper presented at Force Management, ASIP/ASIMIS Meeting at Wright-Patterson AFB, October 1978.
13. "Crack Gage Test Results – Influence of Fleet Variability on Crack Growth Tracking Procedures for Transport/Bomber Aircraft", Boeing Document T3-1816-1, Boeing Wichita Company, December 1978.